Analysis of the Mutational Landscape of Marginal Zone B-Cell Lymphomas by High Throughput Sequencing Techniques

---

Inauguraldissertation

zur

Erlangung der Würde eines Doktors der Philosophie

vorgelegt der

Philosophisch-Naturwissenschaftlichen Fakultät

der Universität Basel

von

Visar Vela

Basel, 2021

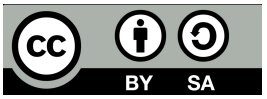

Genehmigt von der Philosophisch-Naturwissenschaftlichen Fakultät
auf Antrag von

Prof. Dr. Alexandar Tzankov

Prof. Dr. Gerhard M. Christofori

Prof. Dr. Davide Rossi

Basel, den 21. September, 2021

Prof. Dr. Marcel Mayor
Dekan

Ich widme diese Arbeit meinen Eltern und meiner Schwester

Ju falënderoj për gjithçka që keni bërë për mua !

TABLE OF CONTENTS

SUMMARY

Marginal zone lymphoma (MZL) is a rare tumor that accounts for only 7%-8% of all lymphoid neoplasms; however, the incidence rate has increased in recent years.[1] The median age at disease onset is 60 years, with a 5-year overall survival (OS) rate of 85%. Depending on the MZL subtype, different treatment options are available. New personalized therapy is a promising approach to increase the effectiveness of anti-tumor treatments in MZL lymphomas. However, the heterogeneity of MZL subtypes makes it challenging to have a single treatment approach for patients with MZL. These challenges are also due to an unexplored genetic landscape and a lack of understanding of the molecular pathogenesis of MZL tumor development.

In my doctoral thesis, I characterized the genetic landscape of two marginal zone lymphoma subtypes in two independent patient cohorts. The first cohort consisted of 34 patients with ocular adnexal marginal zone lymphomas (OMZL) and the second comprised 28 patients with primary pulmonary marginal zone lymphomas (PMZL). We used a customized high-throughput sequencing gene panel covering 146 genes to study the most common nucleotide-level alterations in both study cohorts. In OMZL, we frequently saw mutations in genes related to the nuclear factor kappa-light-chain-enhancer of activated B cells (NF-κB) pathway like *TNFAIP3* were; on the other hand, in PMZL, we detected higher frequencies of chromatin modifier-encoding gene mutations, like *KMT2D*. We compared the mutational profiles with other lymphomas as well as lymphoproliferative and reactive lesions from the same anatomic region. We detected a different mutational composition of pulmonary diffuse large B-cell lymphoma (DLBCL) compared to PMZL, suggesting that there is no transformation from PMZL to DLBCL. Further, we found recurrent *PTEN* mutations in reactive lesions, these might play an important role in diagnostics. In addition, we performed pathway analyses of the three main affected pathways, namely chromatin modifiers, the NF-κB pathway and the NOTCH pathway, to identify cluster patterns. We did not find any association between *Chlamydia spp.* infections and OMZL in the Basel cohort. Furthermore, we studied genetic evolution patterns in relapsing OMZL. To get a complete picture of the

mutational landscape across all MZL, we performed a comparative meta-analysis of reported genetic variants in various MZL subtypes.

1. INTRODUCTION

1.1 Development of B-cells

The human immune system reacts to foreign pathogens in two different manners. First, pathogens induce a fast but a non-specific innate immune response by preformed immune cells such as macrophages and neutrophils with germ-line encoded receptors. By contrast, the second is a slower but more specific adaptive immune response. Here, B-lymphocytes are referred to as "B-cells", and T-lymphocytes ("T-cells") fight the invading pathogens.[2]

B-cells originate from the bone marrow, where they derive from hematopoietic stem cells (HSCs) (Figure 1). B-cells detect antigens by their B-cell receptor (BCR), a membrane-bound immunoglobulin (Ig). The diverse repertoire of BCR is generated during B-cell development, a process that involves interaction with bone marrow stromal cells as well as cytokines. The first phase of B-cell development takes place in the fetal liver and bone marrow. Afterwards, the maturation continues in secondary lymphoid organs such as the spleen, lymph nodes, and mucosa-associated lymphoid tissue (MALT). B-cell development results in either memory B-cells or antigen-specific plasma cells.[3]

B-cell development starts when HSCs in the fetal liver differentiate to form **progenitor cells**.[3] HSCs migrate to the bone marrow, a dynamic microenvironment that provides a niche where the primary site of B-cell development occurs.[4]

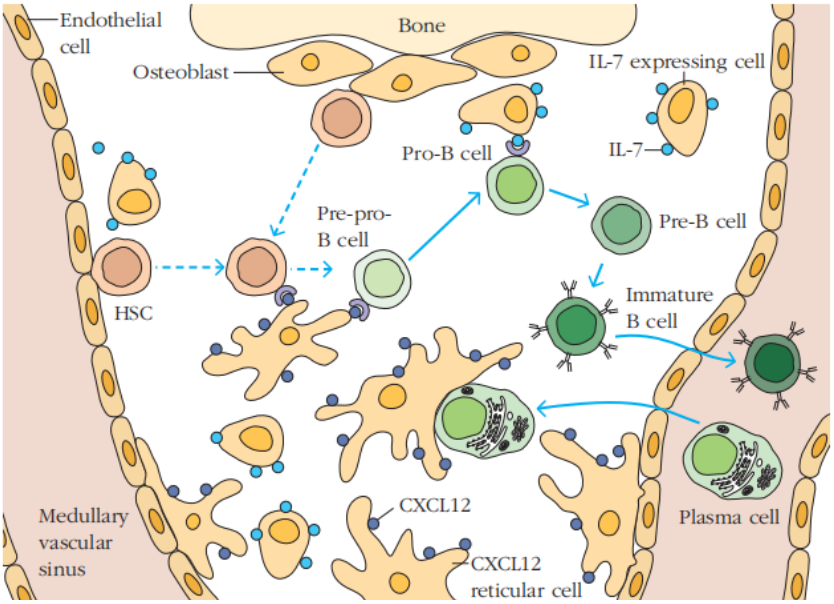

Figure 1. Interactions between haematopoietic stem cells (HSCs) and B-cell progenitors in the bone marrow. HSCs enter the bone marrow from the blood (left) and start to develop close to the osteoblasts (top). Progenitor cells seek contact with CXCL12-expressing stromal cells (purple) to mature into pre-pro B-cells. Then, the cells locate and receive signals from IL-7-producing stromal cells (blue) to proceed to the pro-B-cell stage. After completing differentiation, the pre-B-cells become immature B-cells and leave the bone marrow. Image from ref.[3]

The first stage of development is the **pre-pro B-cell stage.** During this stage, pre-pro B-cells show elevated expression of *CD45R* and early B cell factor (*EBF1).*[5] Stromal cells supply these developing B-cells with CXCL12 chemokine signals for further development.[4] The transcription factors *EBF1* and *E2A* bind to the Ig heavy chain (*IGH*) gene. Together they promote accessibility of the D-J_H locus in preparation for the first immunoglobulin (Ig) gene recombination. Expression of *EBF1* is necessary to initiate the expression of *CD79A* and *CD79B*, which bind non-covalently to the Ig heavy chain forming the B-cell receptor (BCR) complex.[6]

The great diversity of Ig allows each antibody to bind to a specific antigen. This antibody repertoire is generated by multiple mechanisms of gene rearrangements, recombination, hypermutation, etc. D to J_H Ig gene recombination starts in the early **pro-B-cell stage**.[3] Pro-B-cells migrate in the bone marrow along a chemo gradient towards interleukin (IL)-7-secreting stromal cells, as pro-B-cells require signaling from the IL-7 cytokine (Figure 2).[4] The binding of IL-7 to its receptors stimulates the activation of the signal transducer and

activator of transcription 5 (*STAT5)* transcription factor, causing the upregulation c-myc (*MYC*) and n-myc (*MYCN*) and stimulation of cell proliferation.[3] When D to J_H recombination is completed, the preparation for V to D-J_H joining begins with the help of the *PAX5* transcription factor.

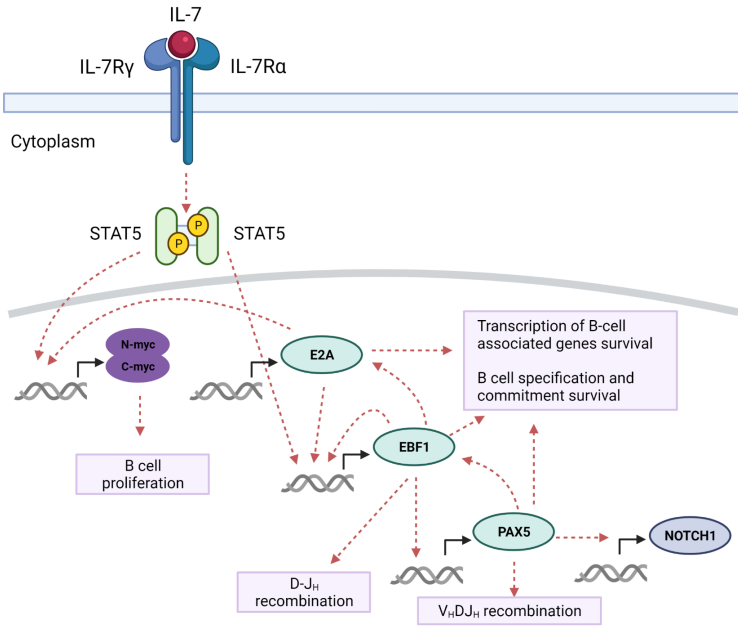

Figure 2. Transcription factors in early B-cell development. As interleukin (IL)-7 binds to its receptor, activation of transcription factor *STAT5* is stimulated. This process activates the *N-myc* and *C-myc* proteins and stimulates B-cell proliferation. In addition, signal transducer and activator of transcription 5 (STAT5), together with E2A, promotes the expression of early B cell factor 1 (*EBF1*), which induces the expression of paired box 5 (*PAX5*). These actions activate genes that lead to B cell lineage specification. Adapted from ref.[3]

At the beginning of the early **pre-B-cell** stage, the V_H to D-J_H Ig gene recombination ends. In this stage, the pre-B-cell receptor (pre-BCR), composed of the rearranged heavy chain with the VpreB and λ5 surrogate light chain components, starts to be expressed.[3] Pre-BCR signaling recombination activating genes 1 and 2 (*RAG1* and *RAG2*, respectively), which encode enzymes, to prevent further *IGH* rearrangements.[7] Failure to express a pre-BCR will cause the cell to undergo apoptosis, which is the first checkpoint of B-cell development. Progress through this checkpoint leads to proliferation.[8]

After several rounds of proliferation, pre-B-cells lose their pre-BCR receptor. Then, re-expression of *RAG1* and *RAG2* initiates the light chain gene rearrangement. These steps

mark the entry into the late pre-B-cell stage.[9] Successful rearrangement of light chain genes leads to the expression of the IgM receptor on the cell surface, characteristic of the beginning of the **immature B-cell stage**. Cells without successful light chain Ig gene rearrangement are blocked at the second checkpoint of B-cell development and undergo apoptosis.[8]

Immature B-cells display a functional IgM on their cell membrane. They migrate to the spleen to complete their maturation. Upon encountering antigens, these cells re-express *RAG1* and *RAG2* genes and modify their light chain genes.[7] If no functional BCR is expressed on the cell surface, the cells undergo apoptosis. Immature B-cells are categorized into two subtypes of **transitional B-cells, T1 and T2** (Figure 3). These cells leave the bone marrow as T1 B-cells, enter the spleen through the central arteriole, and get deposited in the marginal sinuses.[10,11] T1 B-cells mature into T2 B-cells to enter the B-cell follicles and recirculate, or enter the marginal zone and develop into marginal zone B-cells.[12]

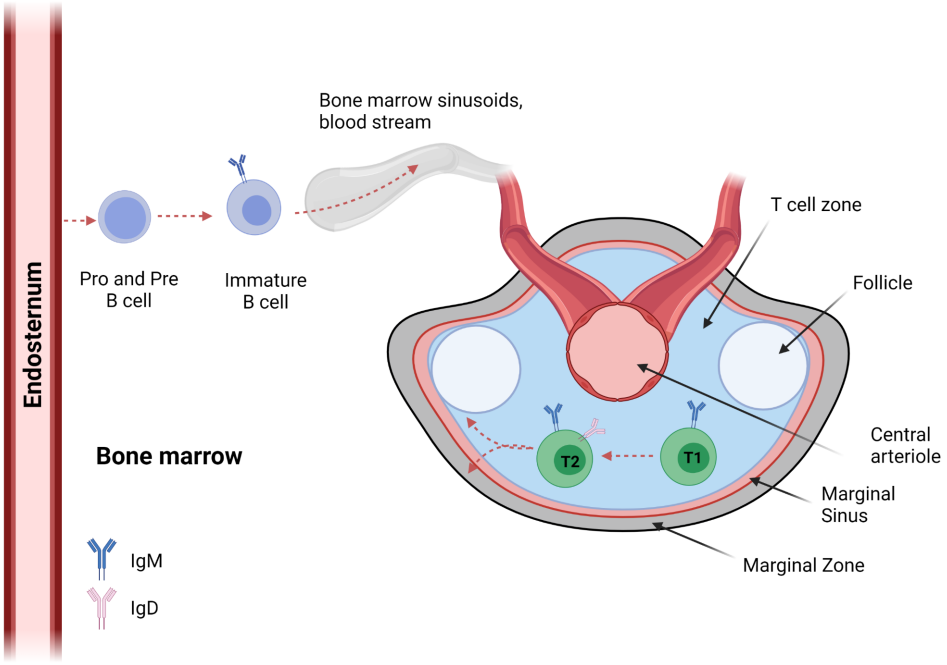

Figure 3. Movement of immature T1 and T2 transitional B-cells. Immature T1 B-cells leave the bone marrow, go to the bloodstream and enter the spleen via the marginal sinuses. They percolate to the T-cell zones and differentiate to T2 transitional B-cells. Some T2 transitional B-cells develop into marginal zone cells. Adapted from ref.[3]

1.1.1 Structural organization and rearrangement of *Ig* genes

Antibodies have a Y-shaped structure composed of four polypeptide chains: two identical **light (L) chains**, and two identical **heavy (H) chains** (Figure 4). Located at the tips are the complementarity-determining regions where antigens (epitopes) are bound.[3]

There are two types of light chains, the kappa (κ) chain and the lambda (λ) chain. In addition, there are five different main antibody classes or isotypes, defined by their heavy chain constant regions, which affect the antibody effector functions. Antibodies with a mu (μ) heavy chain isotype belong to the IgM class; antibodies with delta (δ), gamma (γ), epsilon (ε), and alpha (α) heavy chain belong to the IgD, IgG, IgE, and IgA classes, respectively. The γ, δ, and α heavy chains are 330 amino acid residues long, while μ and ε heavy chains are 440 amino acid residues long. In addition, IgM and IgE antibodies are 20% heavier than IgA, IgD, and IgG antibodies. The α and γ heavy chains are further classified into sub-isotypes α1 and α2, and γ1, γ2, γ3, and γ4; these sub-isotypes encode subclasses of respective antibodies: IgA1, IgA2, and IgG1, IgG2, IgG3, and IgG4.[3]

The heavy and light chains of the Ig gene are composed of two domains. First is the **variable (V) domain**, where the amino acid sequence diversely varies widely among antibodies. The second region is the **constant (C) domain**, where the amino acid sequences are less variable.[13] The V domain of the light chain is encoded by two gene segments, the **variable (V) gene segment,** and the **joining (J) gene segment**, while individual exons encode the C domain. In the case of the V domain of the heavy chain, a third gene segment, **diversity (D)**, is required. DNA recombination in the B-lymphocyte precursors brings these gene segments together to create a complete variable region gene.[3]

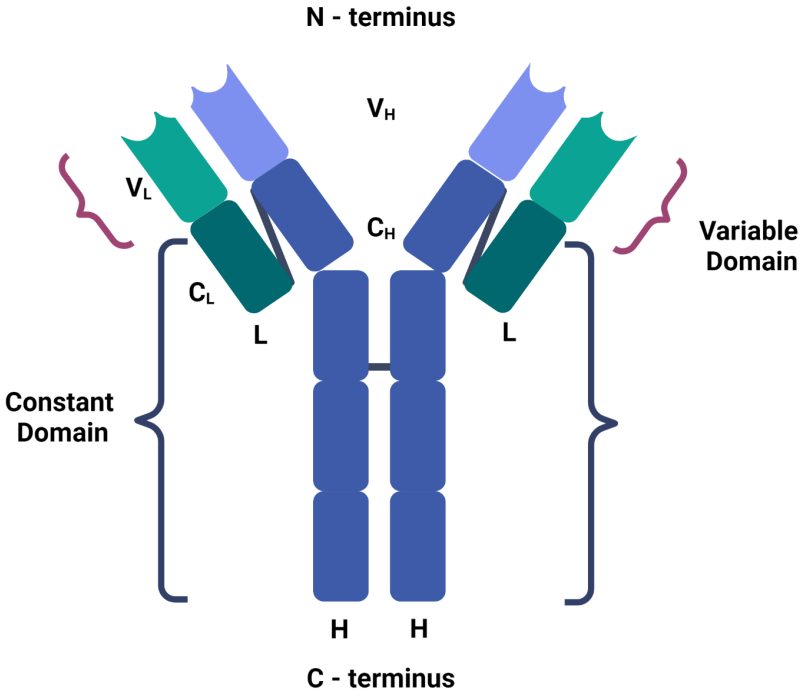

Figure 4. Schematic antibody structure. The general structure of the Ig gene molecule showing the four polypeptide chains linked by disulfide bonds and the two domains. Adapted from ref.[13]

V(D)J recombination involves bringing together V_L and J_L, or V_H, D, and J_H gene segments to produce an intact Ig gene with complete heavy and light chain genes.[3] The entire mechanism is initiated by recombination activating genes 1 and 2 (*RAG1* and *RAG2*) by introducing a DNA double-strand break (DSB). The recombination signal sequences (RSS) direct the process by serving as the site of DNA cleavage and rearranging gene segments.[14] The RSS comprises conserved heptamer and nonamer sequences, together with a spacer of either 12 or 23 base pairs (12-RSS or 23-RSS). The recombinase *RAG1/RAG2* recognizes the RSS and forms a complex following the 12-23 rule of binding. This rule only permits the 12-RSS flanked gene coding segment to join the 23-RSS-flanked gene coding segment to ensure no wasteful recombination (Figure 5).[15] Actions of high-mobility groups 1 and 2 (HMG1, HMG2) proteins facilitate this process.[14] The RAG1/RAG2 protein complex introduces a single-strand nick in the DNA precisely at the 5' junction of the RSS heptamer sequence and the V and J coding segments. Then, the 3′-OH group of the coding sequence ligates to the 5′-phosphate group on the non-coding segment creating a DNA hairpin loop and a blunt signal end.[3] For heavy chains, the D gene segment is first joined with the J segment following the steps above. Then, the joining of the V segment to the D-J complex ensues, completing

the V(D)J recombination. In the case of light chains, only the V-J joining takes place. Signal joints are formed when signal ends are ligated. Next, the hairpin loop is reopened to yield a 3′ overhang, a 5′ overhang, or a blunt end, and all are left open for modifications. Finally, the cut ends of the coding segments are repaired by the components of the DNA repair process called non-homologous end joining (NHEJ) proteins.[3,14]

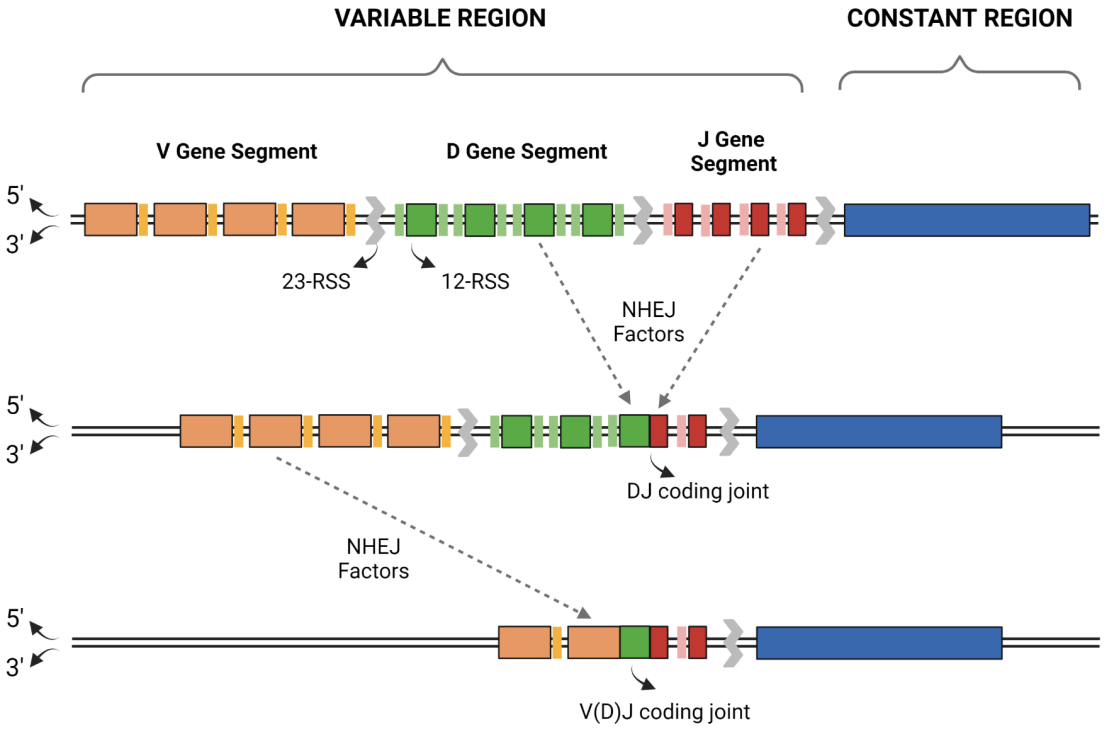

Figure 5. V(D)J recombinations. Joining the D and J gene segments occurs, forming the D-J coding joint, followed by joining the V segment to the D-J complex. In the case of light chains, only the V-J joining takes place. The 12- recombination signal sequence (RSS) is paired with the 23-RSS to avoid unintentional ligation. Adapted from ref.[3]

1.1.2 Isotype switching

The B-cell's Ig production or expression can be changed from one type/class to another due to an infection to improve the capacity to fight off the pathogen. This mechanism is called isotype switching, Ig class switching, or class-switch recombination (CSR). The process entails changing the constant region of the heavy chain (C_H) from μ and δ with γ, ε or α via a DNA recombination event. Thus, there is a change in surface expression from IgM and IgD to IgG, IgE, or IgA.[16]

Isotype switching is deletional, which means that a portion of the coding DNA is removed, and the remaining parts are rejoined. This mechanism occurs within the switch (S) regions, located upstream of the constant domain of the heavy chain gene segments (C_H).[16] Recombination begins when a DNA single-strand DNA break (SSB) is converted into a DSB, initiated by activation-induced cytidine deaminase (AID).[17] Deletion of intermediary DNA ensues between S regions, and unwanted C_H regions are removed and substituted.[18] Then, NHEJ recombines the DSBs.[16]

1.2 Marginal zone

The **spleen** is a secondary lymphoid organ that plays a significant role in the fast immune response to antigens in the bloodstream (Figure 6). Besides blood filtration, the spleen traps antigens and plays an important role the in response to systemic infections.[3] Studies have shown that compromised spleen function leads to high susceptibility to recurrent infections due to a lack of antibody responses.[19]

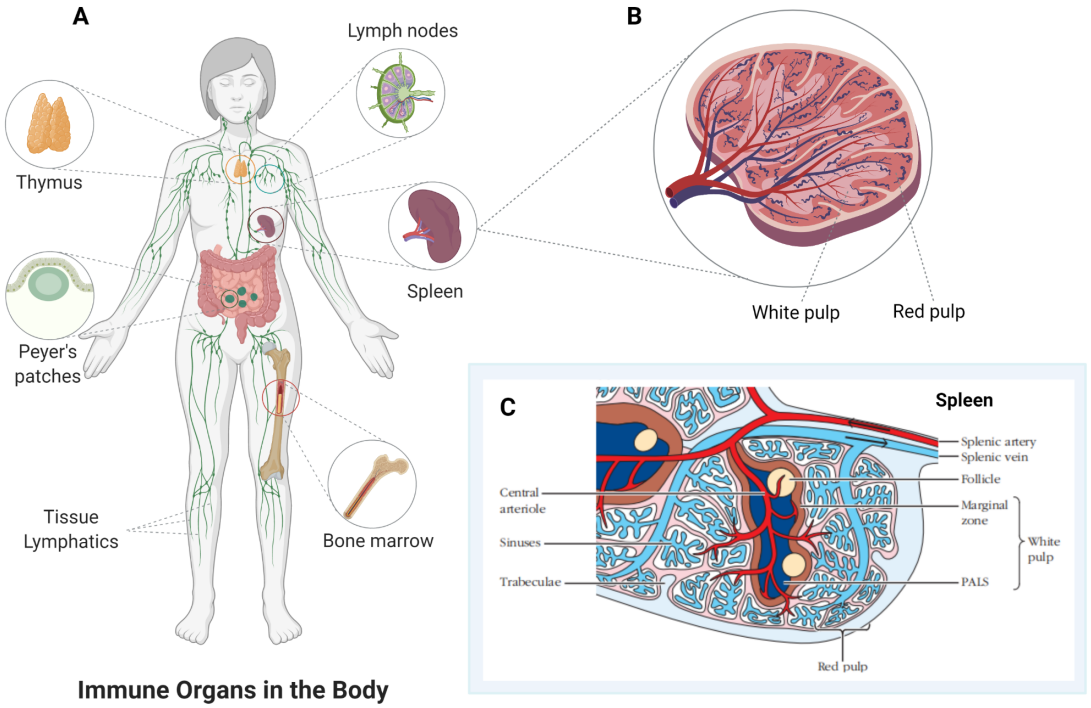

Immune Organs in the Body

Figure 6. Primary and secondary lymphoid organs. A) A diagram showing the different immune organs throughout the body. B) Illustration of the cross-section of the spleen, a secondary lymphoid organ, with red and white pulp. C) A deeper look into the anatomy of the spleen, identifying the significant parts associated with the role of marginal B-cells. Adapted from ref.[3]

The spleen has two main distinct compartments, the **red pulp** and the **white pulp**. The **marginal zone**, a specialized region bordering the white pulp, separating the two compartments, contains specialized macrophages and B-cells that serve as the first line of defense against pathogens in the blood.[3]

The marginal zone is further divided into two compartments, the large inner and the small outer compartments. These are separated by a ring of T-cells and a network of fibroblast-like cells that express alpha-smooth muscle actin (ASM).[20] The B-cell and T-cell area, called the periarteriolar lymphoid sheath (PALS), is surrounded by the marginal sinus, bridging the white and red pulps.[21] In addition, migrating B- and T-cells enter the marginal zone sinuses from the blood and migrate to the follicles and the PALS, respectively.[3]

Besides the spleen, other lymphatic tissues show marginal zones where B-cells are constantly exposed to antigens. These areas include the skin, mucosal surfaces,[22] subepithelial areas of MALT, the subepithelial dome of intestinal Peyer's patches, and the inner wall of the subcapsular sinus of the lymph nodes.[23–26] These areas have a similar composition to the splenic marginal zone and serve as alternative functional niches for marginal zone B-cells.[27]

1.2.1 Marginal zone B-cells

Marginal zone B-cells are characterized by high-level expression of IgM and CD21 and low expression of IgD and CD23.[28] In addition, marginal zone B-cells express other clusters of differentiation markers like CD9 and CD27 that help to distinguish them from follicular B-cells.[19,29]

Different signaling pathways like BCR signaling, canonical nuclear factor kappa-light-chain-enhancer of activated B-cells (NF-κB) signaling downstream of the B cell–activating factor receptor (BAFFR), and signaling through *NOTCH2* on B-cells are essential for marginal zone B-cell development.[12] Uptake of particulate antigens and their transport to the cluster of differentiation 1D (CD1D)-containing endocytic compartments is aided by the BCR.[19] The binding of the αLβ2 and α4β7 integrins to their ligands, intercellular adhesion molecule, and vascular cell adhesion molecule are also essential for the marginal zone B-cells to be retained in their niche.[30]

As the first line of defense, marginal zone B-cells can respond quickly and efficiently to protein and other blood-borne antigen particulates[19] and induce an antigen-specific clonal expansion of T-cells.[31] Marginal zone B-cells encompass both innate and adaptive immune systems due to their preliminary T-cell-independent IgM production ability within a few hours of infection.[19] They also play an important role in priming splenic T-cells.[19]

Upon entering the spleen via the splenic artery, the blood-borne antigens and lymphocytes interact first with the marginal zone B-cells, which generate activated effector B-cells that differentiate into plasma cells to boost IgM and IgG antibody production.[30] Reduced *CD23* levels allow this rapid secretion of antibodies to help trap the antigens, enhance their processing to T-cells or B-cells and develop T-cell-dependent IgG response.[19,32–34] Toll-like receptor (TLR) signaling mediates this immune response. It promotes marginal zone B-cell proliferation, antibody production, and maturation, thereby increasing the expression of major histocompatibility complex (MHC) class II, CD40, and CD86 molecules.[19] Specialized resident marginal zone B-cells, with the help of high CD21 levels, efficiently bind the antigens to the complementary receptors.[3] Then, the trapped antigens, called immune complexes, are transported to the follicular dendritic cells traveling to the PALS, deposited on their surfaces, or processed for direct presentation on the MHC class II molecules to naive CD4+ T-cells.[19,21,31] This action promotes T-cell proliferation, cytokine production, and expression of high levels of *CD86* on the marginal zone B-cell surface.[19]

Older studies suggest that neutrophils aid marginal zone B-cells in antibody secretion.[23] In the absence of infection, these antibodies become part of the general circulation. This innate response provides a collection of antibodies providing a systemic line of defense against pathogens or infectious agents.[3] On the other hand, marginal zone B-cells respond more vigorously and proliferate to various stimuli such as lipopolysaccharide antigens (LPS) and anti-CD40[35] but do not need constant replenishment due to their capacity for self-renewal.[3]

Phospholipid receptors and adhesion molecules enable marginal zone B-cells to interact with other cells in the marginal zone.[3] These other cells include marginal zone macrophages (MZM) that exist at the boundary of the marginal and follicular zones. Upon binding with a pathogen, MZM directly interacts with marginal zone B-cells. These interactions are necessary for the overall structure of the marginal zone and efficient immune response by modulating the MZM function in capturing antigens to avoid severe infection. MZM are scattered in several areas of the marginal zone. These cell types express MARCO, a scavenger receptor of the class A receptor family, and the marker *ER-TR9*.[19] Another significant interaction of marginal zone B-cells is the activation of invariant natural killer T (iNKT) cells to stimulate the release of Interferon-gamma (IFN)-γ and IL-4.[36]

1.3 Marginal zone lymphoma

Marginal zone lymphoma (MZL) is a heterogeneous group of indolent, so–called non-Hodgkin's lymphomas (NHL) originating from mature B-cells of the marginal zone. As discussed, in the previous section, marginal zone B-cells are constantly exposed to antigens and have a reduced threshold for triggering proliferation, which makes them more vulnerable to malignant transformation.[37] MZL may begin with the occurrence of the condition called clonal B-cell lymphocytosis of marginal zone origin (CBL-MZ), where circulating clonal B-cells of marginal zone origin are observed. However, only a fraction of patients with CBL-MZ progress to an overt MZL.[38] The median age of presentation for MZL is 60 years, it affects more females than males, and is in most cases it is indolent, with a 5-year overall survival (OS) rate of 85%.[39]

1.3.1 Classification of MZL

Out of all lymphomas, 7% - 8% are diagnosed as MZL (Figure 7).[40,41] Of these, extranodal marginal zone lymphoma (EMZL) accounts for 70% of the cases, followed by splenic marginal zone lymphoma (SMZL) with approximately 20% and nodal marginal zone lymphoma (NMZL) with roughly less than 10%.[38] Classification of MZL is essential because correct identification of the disease and its subsets would lead to accurate diagnosis and eventually propose the best treatment course.[42] According to the current classification and definition of MZL by the World Health Organization, there are three distinct clinical entities with unique diagnostic criteria, genetic features, clinical course, and treatment or therapy implications (Figure 8).

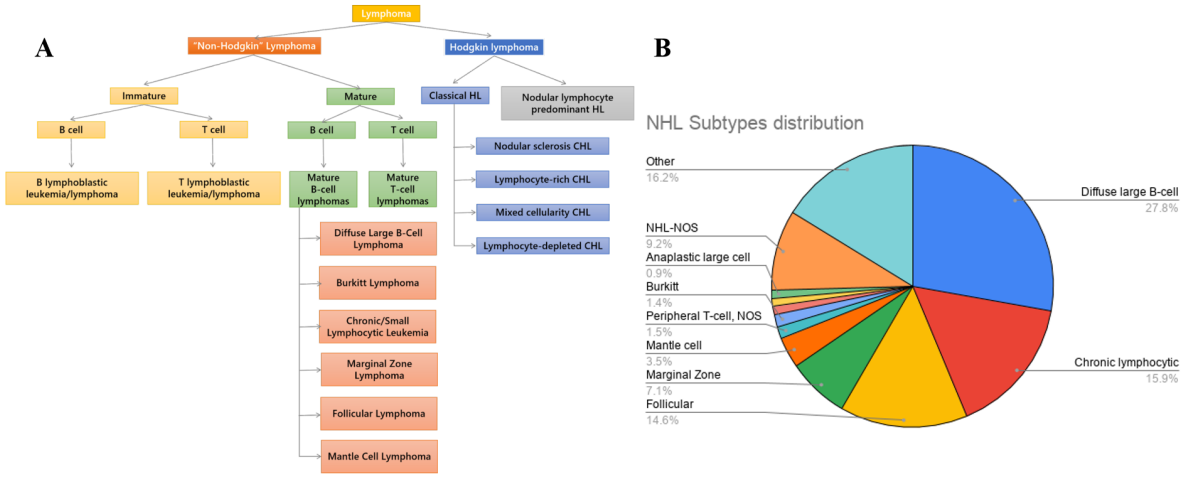

Figure 7. Classification of lymphomas. A.) Marginal zone lymphoma (MZL) is a group of indolent slow-growing so-called non- Hodgkin's mature B-cell lymphomas (NHL), B.) accounting for approximately 7%-8% of all NHL cases. Adapted from ref.[43,44]

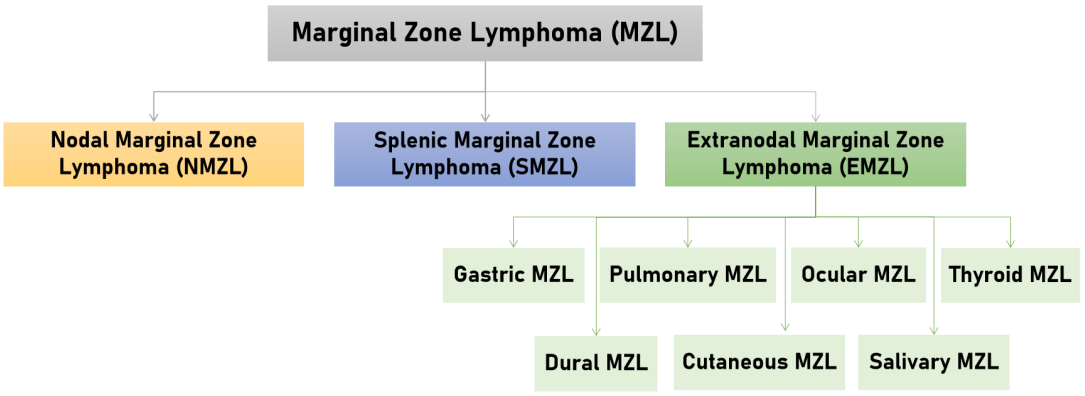

Figure 8. Marginal zone lymphoma (MZL) entities. The World Health Organization has categorized MZL into three types based on specific characteristics. EMZL is further subdivided into different entities based on the organ affected. Adapted from ref.[41]

1.3.1.1 Nodal MZL (NMZL)

NMZL is a primary B-cell lymphoma of the lymph node resembling both EMZL and SMZL without evidence of such. NMZL is located in the peripheral lymph nodes, occasionally infiltrates the bone marrow, and may show peripheral blood involvement. Around 1.5%-1.8% of lymphomas account for NMZL, occurring primarily in adults after 60 years of age. NMZL affects both genders equally, but females with autoimmune disorders have been observed to have a higher incidence. Hepatitis C virus (HCV) infection has been observed in several cases. Most patients present peripheral lymphadenopathy in the head and neck lymph nodes.[41]

1.3.1.2 Splenic MZL (SMZL)

SMZL is a B-cell neoplasm wherein small lymphocytes surrounding the splenic white pulp expand and merge with the marginal zone, infiltrating the red pulp.[41] Being a rare lymphoma, SMZL accounts for less than 2% of all lymphoid neoplasms. It is known to be a disease of the elderly, as almost all patients are over 50 years old, with a median age of 65 years.[45] Females are slightly more predominantly affected by SMZL, where most patients have a stage 4 disease with bone marrow involvement.[46,47] The lymphoma is localized in the spleen, splenic hilar lymph nodes, bone marrow, peripheral blood, and the liver. Patients with SMZL often have splenomegaly with associated symptoms such as anemia and the presence of peripheral blood villous lymphocytes. This type of lymphoma is often associated with HCV infections.[45] In most instances, patients with SMZL experience an indolent progression; however, around 25% of the cases take on a progressive course and cause early death.[48,49]

1.3.1.3 Extranodal MZL (EMZL)

Heterogeneous cell types such as small marginal zone B-cells, small lymphocytes, and other scattered immunoblasts comprise the extranodal marginal zone tissue. These neoplasms are

found in the marginal zones extending to the interfollicular region and the follicles. They also form lymphoepithelial lesions by infiltrating the epithelial tissues[41] and affect the bone marrow in 20% of the cases.[50] EMZL cases are mainly indolent with an 87% overall survival rate, a 98% disease-specific survival rate, and a 76% 10-year recurrence-free rate.[51]

MALT EMZL is further divided into subentities depending on the site of involvement. Roughly around 7%-8%[46,52] of all B-cell lymphomas are attributed to EMZL. EMZLs can arise at any extranodal site and can present either similar or site-specific features. The most common location for EMZL is the gastrointestinal tract, taking accounting for 70% of the cases, followed by the lung with 14%, ocular adnexa (OA) with 12%, thyroid with 4%, but no incidence data for other sites such as dura mater, skin,[53] breasts, and liver is reported. EMZL often remains localized in the tissue of origin but may spread to multiple areas.[37] EMZL involves both male and female adults of around 70 years of age. Females are predominantly affected in the thyroid, salivary glands, and soft tissues. At the same time, male incidence rates are higher for the stomach, small intestine, and skin, whereas lung, ocular, colon, and rectum diseases occur equally in both genders.[54] Variations in MZL incidences are also thought to be influenced by geography. For example, a 1992 study noted a significantly higher number of gastric marginal zone lymphoma (GMZL) patients in Northeast Italy compared with the United Kingdom.[55] In ocular adnexal marginal zone lymphoma (OMZL), a large number of cases have been reported in Japan, Italy, and Korea.[56]

EMZLs can arise at any extranodal site and often begin with chronic inflammation caused by microbial pathogens. Bacterial and viral infections lead to an accumulation of extranodal MALT in the respective organs, which serves as soil for neoplastic outgrowth.[41,53]

GMZL is linked to *Helicobacter pylori* infection. *H. pylori* is a Gram-negative bacterium causing gastric mucosal atrophy and ulceration associated with gastric cancer.[1] Preclinical studies have shown that *H. pylori* affects lymphoma pathogenesis by acting on transformed B-cells and other immune cells.[57,58] The 120-145 kDa peptide, cytotoxin-associated gene A (*CagA*), is secreted by the *H. pylori* and taken up by the epithelial cells.[59] This protein causes *H. pylori* to interact with the gastric mucosa, increasing the risk of gastric cancer pathogenesis and peptic ulcers. CagA is also shown to be present in malignant EMZL.[60–62] *CagA* interacts

with tyrosine phosphatase SHP-2 Ras/MEK/extracellular signal-regulated kinase (ERK) pathway to activate and to cause the proliferation of epithelial cells.[63,64] In addition, CagA upregulates the anti-apoptotic Bcl2 and Bcl-xL proteins, which leads to persistent *H. pylori* infection.[65]

Another pathogen linked with EMZL is the *Chlamydia psittaci*, which is associated with OMZL. Several studies came across *C. psittaci* in tumor tissues through immunohistochemistry and detect bacterial DNA in tumor biopsies by polymerase chain reaction (PCR).[66,67] *C. psittaci* infection is caused by inhaling airborne bacteria and contamination through the feathers and feces of infected birds.[68] However, the correlation of *C. psittaci* and OMZL varies significantly by factors such as geography.

Borrelia burgdorferi causes antigen stimulation that leads to cutaneous MZL (CMZL). This association was first speculated upon observing that acrodermatitis chronica atrophicans, an indication of Lyme disease caused by *B. burgdorferi* infection through tick bites, is linked to skin B-cell lymphomas.[69,70] Similarly to the *C. psittaci* in OMZL, *B. burgdorferi* in CMZL varies greatly depending on geography.

Achromobacter xylosoxidans, a Gram-negative bacterium, is correlated with pulmonary MZL (PMZL). *A. xylosoxidans* is prevalent in MALT lymphoma biopsies (46%) and in patients with cystic fibrosis and with severe lung damage.[71]

Hepatitis C virus (HCV) is associated with all types of MZL, SMZL, NMZL, and EMZL. HCV is transmitted through blood and perinatal transmission.[72,73] In B-cell lymphomas, HCV plays a significant role in binding activated B-lymphocytes to CD81 cell surface receptors, thus stimulating polyclonal proliferation.[74] HCV is prevalent in GMZL (50%), salivary MZL (SAMZL, 47%), CMZL (43%), OMZL (36%), as well as SMZL, and NMZL.[75,76]

Aside from bacterial and viral infections, autoimmune diseases are also linked with EMZL. For example, Sjögren syndrome increases the risk of SAMZL. Lymphoid tissue in the salivary glands is activated by a local chronic antigen associated with Sjögren syndrome. Overexpression of the B-cell–activating factor (BAFF) in conjunction with *CD40/CD40*

ligand (CD40L) and *BCL2* family proteins leads to uncontrolled autoantibody production and reduced apoptosis. This process causes unrestricted B-cell proliferation.[77–79] Hashimoto thyroiditis has been proposed to be related to thyroid MZL (TMZL).[80] This autoimmune disease causes the infiltration of lymphocytes into the lymphoid tissue, which the thyroid gland initially lacks due to the absence of lymph nodes. B-cells then appear in the tissue and differentiate into plasma cells.[80] It is estimated that 0.5% of the cases of Hashimoto thyroiditis develop into TMZL, occurring at a 9-10 year interval.[81]

1.3.1.4 Diagnosis

MZL is diagnosed according to the current classification and definition of the disease set by the World Health Organization.[41] However, it is recommended that an experienced hematopathologist confirms and reviews the diagnosis as other lymphomas and reactive conditions mimic MZLs.[42]

1.3.2 Genetic abnormalities and signaling pathways

Different MZL entities do not exhibit defined phenotypes and diagnostic borders.[82] However, the three MZL entities display recurrent trisomies of chromosomes 3 and 18 and deletions at 6q23.[83] In NMZL, structural alterations include chromosome 1 structural rearrangements involving 1q21 or 1p334, and abnormalities in chromosome 3.[84] In SMZL, a partial deletion of chromosome 7, del(7)(q31), is found exclusively.[85,86] Other abnormalities include 7q32 as well as 9p34, 12q23-24, 18q, 17p, 7q22-36 deletions, 12q gains, trisomies of 3q, and frequent complete 7q loss.[49] EMZL presents gains at 3p, 6p, and 18p.[83] In addition, 20%–30% of EMZL have trisomies of chromosomes 3, 12, and 18. The t(11;18)(q21;q21) translocation that leads to *BIRC3–MALT1* fusion is linked with several EMZL. However, this translocation has not been reported in SMZL and NMZL.[87] Other chromosomal translocations detected in EMZL and the gene fusions involved are listed in Table 1.

Table 1. Common chromosomal translocations and genetic aberrations involved in EMZL.[37,87]

EMZL Entity	Chromosomal Translocation	Genes involved	Prevalence
GMZL	t(11;18)(q21;q21) t(3;14)(p14;q32) t(1;14)(p22;q32) t(14;18)(q32;q21)	*BIRC3-MALT1* *IGH-FOXP1* *IGH-BCL10* *IGH-MALT1*	23% 3% 2% 1%
SAMZL	t(14;18)(q32;q21) t(11;18)(q21;q21) t(1;14)(p22;q32)	*IGH-MALT1* *BIRC3-MALT1* *IGH-BCL10*	6% 2% 1%
OMZL	t(3;14)(p14;q32) t(14;18)(q32;q21) t(11;18)(q21;q21)	*IGH-FOXP1* *IGH-MALT1* *BIRC3-MALT1*	20% 16% 7%
PMZL	t(11;18)(q21;q21) t(1;14)(p22;q32) t(14;18)(q32;q21)	*BIRC3-MALT1* *IGH-BCL10* *IGH-MALT1*	45% 8% 7%
CMZL	t(3;14)(p14;q32) t(14;18)(q32;q21) t(11;18)(q21;q21)	*IGH-FOXP1* *IGH-MALT1* *BIRC3-MALT1*	10% 7% 4%
TMZL	t(3;14)(p14;q32) t(11;18)(q21;q21)	*IGH-FOXP1* *BIRC3-MALT1*	50% 9%

1.3.2.1 NF-κB pathway

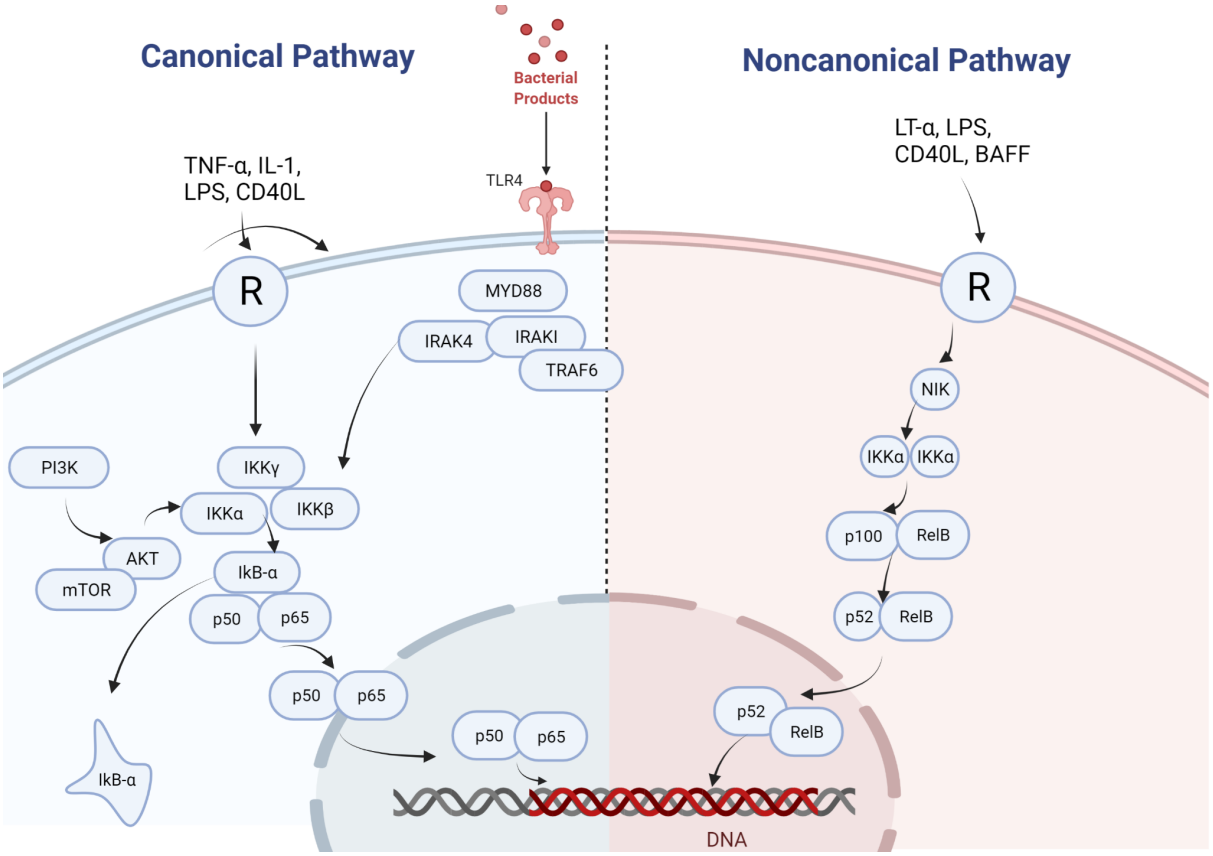

Figure 9. NF-κB signaling pathway. Receptors and signaling molecules that activate both the canonical and non-canonical NF-κB signaling pathways include the toll-like receptors (TLR), tumor necrosis factor receptors (TNFR), interleukin-1 receptor (IL-1R), CD40, initiation of B cell activation factor (BAFFR), and receptor activator for nuclear factor kappa B (RANK). In the canonical NF-κB pathway, NF-κB is inhibited by the IκB by binding it to the p50–p65 heterodimer in the cytoplasm, thus preventing it from entering the nucleus. On the other hand, IKKα is activated in the non-canonical pathway by the upstream kinase NF-κB-inducing kinase (NIK), which promotes the processing of p100 into the active RelB-p52 isoform of NF-κB. This pathway does not rely on IKKβ or IKKγ (NEMO) but only needs IKKα to phosphorylate the p52 precursor, p100. Adapted from ref.[88]

The NF-κB pathway regulates the expression of genes in B-cells related to the development, survival, differentiation, and proliferation of immune cells, making it a key transcription factor.[37] The constitutive activation of this pathway plays a significant role in B-cell transformation and progression of MZL.[89] NF-κB signalling is regulated through the

canonical (classical) and non-canonical (alternative) pathways. Both pathways are regulated by the activation of the IκB kinase (IKK) protein complex. In the canonical NF-κB pathway, the dimers are maintained in the nucleus. A ligand binds to a cell surface receptor such as the tumour necrosis factor receptor (TNFR) or TLR, leading to the recruitment of adaptors such as TNF receptor-associated factor (TRAF) to the cytoplasmic domain of the receptor. These processes engage and activate the IKK complex, enabling the NF-κB dimers to translocate from the cytoplasm to the nucleus, to bind to target genes, and to induce transcription. On the other hand, the non-canonical NF-κB pathway activates the p100/RelB complex during B-cell and T cell development. Only specific receptor signals such as the lymphotoxin B (LTβ), BAFF, and CD40 signalling activate this pathway.[90]

1.3.2.1.1 Aberrations of the canonical NF-κB pathway

One of the genes that negatively regulate the NF-κB pathway include *TNFAIP3* (or *A20*) gene that exerts dual ubiquitin-editing functions.[91] This gene also augments the TNFR, TLR/IL1-R, and BCR signalling pathways that are critical for marginal zone B-cell development.[92] Loss-of-function mutations of *TNFAIP3* that occur in MZL stimulate canonical NF-κB signalling, which reduces apoptosis and cell proliferation.[93,94] *TNFAIP3* knockout in mice leads to inflammation and inability to terminate TLR-dependent NF-κB activation.[95] The *NFKBIE* gene also negatively regulates the NF-κB pathway.[96] Patients bearing mutation in this gene have advanced disease course.[97] The *TBL1XR1* gene is a regulator of the NF-κB pathway and is highly mutated in EMZL.[98] This gene is required for transcriptional activation by various transcription factors,[99] such as NF-κB and JUN, thereby contributing to the NF-κB activity in OMZL. Therefore, mutation in this gene is linked with a poor MZL prognosis.[100,101] Another NF-κB pathway inhibitor is the transcription factor *KLF2*, or Krüppel-like factor 2. KLF2 modulates the recruitment of NF-κB coactivators and plays a significant role in cell differentiation, proliferation, and activation.[102–106] Unmutated *KLF2* is an effective suppressor of NF-κB activation by stimulating other signalling pathways such as TLR, BCR, BAFFR, and TNFR.[107] *KLF2* plays a major role in SMZL and is associated with several other genetic mutations, suggesting potential cell survival, tumorigenesis, and transformation.[108] A large fraction of these mutations are potentially deleterious. They are predicted to disrupt the protein's transcriptional function, affect its nuclear localisation to produce a truncated

protein,[109] and alter gene expression to favour homing of B-cells.[110] The intracellular protein BCL10 promotes apoptosis[111] and is a marker protein in EMZL. Expression of this gene is associated with the pathogenesis and development of lymphoma by playing a key role in chromosomal variation[112] leading to insertion, deletion, and substitution of single nucleotides.[113] *BCL10* mutations activate the NF-κB signalling pathway: they cause abnormal NF-κB nuclear translocation, leading to a loss in its capability to adjust apoptosis, and a gain of carcinogenic abilities. This results in the formation and proliferation of MZL cells.[113,114]

1.3.2.1.2 Aberrations of the non-canonical NF-κB Pathway

Downregulation of the tumor suppressor gene *TRAF3* causes stabilisation of the NF-κB-inducing kinase (NIK) to activate the non-canonical NF-κB pathway.[115] *TRAF3* alterations have been identified in GMZL[116] and SMZL.[117] The gene encoding myeloid differentiation primary response protein 88, or *MYD88*, stimulates TLR signalling, IL-1, and IL-18 receptors to activate NF-κB signaling.[118] The most potent *MYD88* mutation is the L265P variant located in the *MYD88* TIR domain, which can interact with the TIR domains of other receptors during the innate immune response. The L265P variant can coordinate a stable IRAK1–IRAK4 signalling complex, which activates NF-κB. These complex favors tumor-cell survival and is identified as a reason for the high recurrence of *MYD88* mutations in lymphomas, making it an enticing therapeutic target. In addition, *MYD88* mutations can cause Janus activated kinase (JAK)/STAT3 transcriptional responses and promote lymphomagenesis through cooperation with chronic active BCR signalling.[118] *MYD88* mutations have been identified in a variety of mature B-cell tumors by Next-generation sequencing studies. In these indolent B-cell malignancies, *MYD88* mutations occur in 90% of Lymphoplasmacytic lymphoma (LPL) patients and 5% to 10% in MZL patients.[119,120] *TNFRSF14*, a TNFR superfamily member,[121] is prevalently mutated in NMZL and EMZL entities.[98,122] These mutations disrupt lymphoma B-cell and T helper cell interactions via its ligand B- and T-Lymphocyte Attenuator (BTLA), thereby affecting lymphomagenesis.[123] Another genetic mutation with possible diagnostic and pathogenic importance in MZL includes *BRAF*. The majority of these mutations bear the canonical V600E hotspot mutation, and others have damaging mutations like N58II and L597Q.[107] The V600E hotspot mutation activates the

serine/threonine kinase encoded by the *BRAF* gene[124] and represents a therapeutic target for *BRAF* kinase inhibitors.[125,126]

1.3.2.2 NOTCH pathway

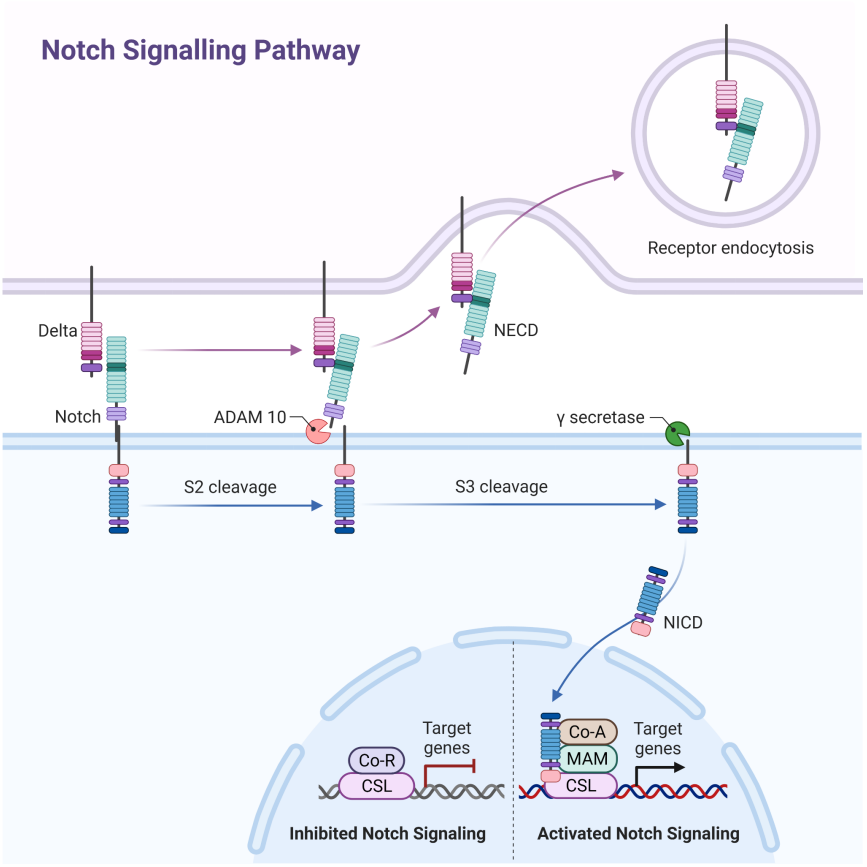

Figure 10. NOTCH signaling pathway.

Notch receptors are single-pass transmembrane proteins composed of functional extracellular (NECD), transmembrane (TM), and intracellular (NICD) domains. Notch receptors undergo proteolytic processing in the ER and Golgi within the signal-receiving cell through S1 cleavage and glycosylation. Then, it is transported to the cell surface membrane. The NECD in the signaling cell binds with the Notch ligands and is expressed by the adjacent cell, inducing the second proteolytic step, S2 cleavage by ADAM metalloproteases. This leads to the endocytosis of the NECD into the ligand-expressing cell, followed by the release of the Notch intracellular domain (NICD). NICD is then freed and migrates into the cell nucleus, where it binds with transcriptional factor CSL, increases CSL dwell time on DNA, and recruits co-factor MAM to initiate the gene transcription. Adapted from ref.[127,128]

NOTCH is a highly conserved signaling pathway that is crucial in various biological processes.[129] Mechanisms in this pathway involve communication between adjacent cells to convey information and genetic instructions.[130] Canonical NOTCH signaling starts with the interaction of the Delta-like or Jagged ligands to the NOTCH protein resulting in a cleavage. This pathway is associated with early development and normal cellular processes. However, another NOTCH signaling pathway called non-canonical NOTCH signaling is associated with immune system activation and pathological conditions such as cancer.[131] The NOTCH pathway is essential for marginal zone B-cell development.[12,132,133] It has been shown that conditional knockout of *NOTCH2* in mice results in the complete absence of marginal zone B-cells,[134] leaving other B-cell subsets unaffected. The NOTCH pathway is mainly targeted by genetic lesions such as mutations of *NOTCH2*, *NOTCH1,* and *SPEN*,[135] which are all relevant for normal marginal zone differentiation.[12,134]

NOTCH2 mutations have been identified in NMZL[136] and SMZL cases.[137] These mutations are located in the exons that encode for the transactivation domain (TAD) or the PEST-rich domain (a C-terminal region rich in proline, glutamate, serine, and threonine), leading to constitutive activation of the NOTCH pathway.[108] Patients harboring the *NOTCH2* mutations are more prone to have adverse outcomes, a shorter relapse-free survival, and the worst patient outcome.[108,138] *NOTCH1* mutations found in the HD and PEST domains also play a role in the oncogenesis of SMZL,[108] and EMZL entities.[139] The *SPEN/MINT* gene suppresses the NOTCH signaling pathway by inhibiting the RBPJ transcription factor; thus, functioning as a negative regulator of B-cell differentiation into marginal zone B-cells,[133,140,141] it is mutated in SMZL.[142]

1.3.2.3 Chromatin modifiers

Epigenetic changes occur in all human cancers and cooperate with genetic alterations to drive the cancer phenotype. These changes include DNA methylation, histone modifiers, chromatin remodelers and other components of chromatin. Epigenetic changes can cause mutation in genes and are frequently observed in genes that modify the epigenome. Epigenetic silencing deregulates the epigenetic machinery at different levels. On one hand we have inappropriate methylation of cytosine (C) in CpG sequencing motives and on the other hand we have

histone post translational modification. The epigenetic functional classification system divides cancer genes into epigenetic modifiers, mediators and modulators. Epigenetic mediators are those genes whose products are the epigenetic modifiers. Mutations of epigenetic modifiers cause genome-wide epigenetic alterations in cancer. Most cancers harbor frequent mutations in genes that encode for components of the epigenetic machinery that affect gene genomic stability. Mutations in DNA methylation are common in haematological malignancies. Disruption of the epigenome results from mutations in chromatin regulators that affect DNA methylation, so that the active or passive process of removing DNA methylation is promoted.[143–146] These mutations may lead to the initiation and progression of cancer. Chromatin remodeling involves modification of chromatin arrangement to open a once condensed state allowing the DNA to be accessed by transcription factors and binding proteins to control gene expression.[147] Genes that encode for chromatin modifiers were found to be mutated in MZL. *KMT2D/MLL2*, an epigenetic regulator and a gene that plays a role in chromatin remodeling and transcriptional regulation, is a commonly mutated gene in MZL,[108,136,139] where the mutations are found along the whole length of the gene.[139] The *CREBBP* gene, a coactivator of several transcription factors[148] involved in chromatin remodeling and transcription factor recognition, is mutated in MZL.[107,108,148] Deletion or inactivation of the *CREBBP* gene causes a loss of the acetyltransferase domain,[142] leading to downregulation of the transcription of MHC class II genes, aiding lymphomagenesis and regulation of apoptosis.[149] Genetic mutations of the epigenetic regulator *TET2* are also prevalent in SMZL,[107] and EMZL.[122] These loss-of-function mutations inactivate the protein resulting in hypermethylated cells.[150] In addition, SMZL samples studied by Martinez et al. harbored mutations of genes involved in this pathway. These genes comprise the histone cluster 1 (*HIST1H1D*, *HIST1H1E*, *HIST1H2BI,* and *HIST1H4H*) that link nucleosomes; the *SMARCA2,* an encoder of the SWI/SNF ATP-dependent chromatin remodeling complex; an

the *CDH2* gene, an essential protein for hematopoiesis and tumor suppression.[151]

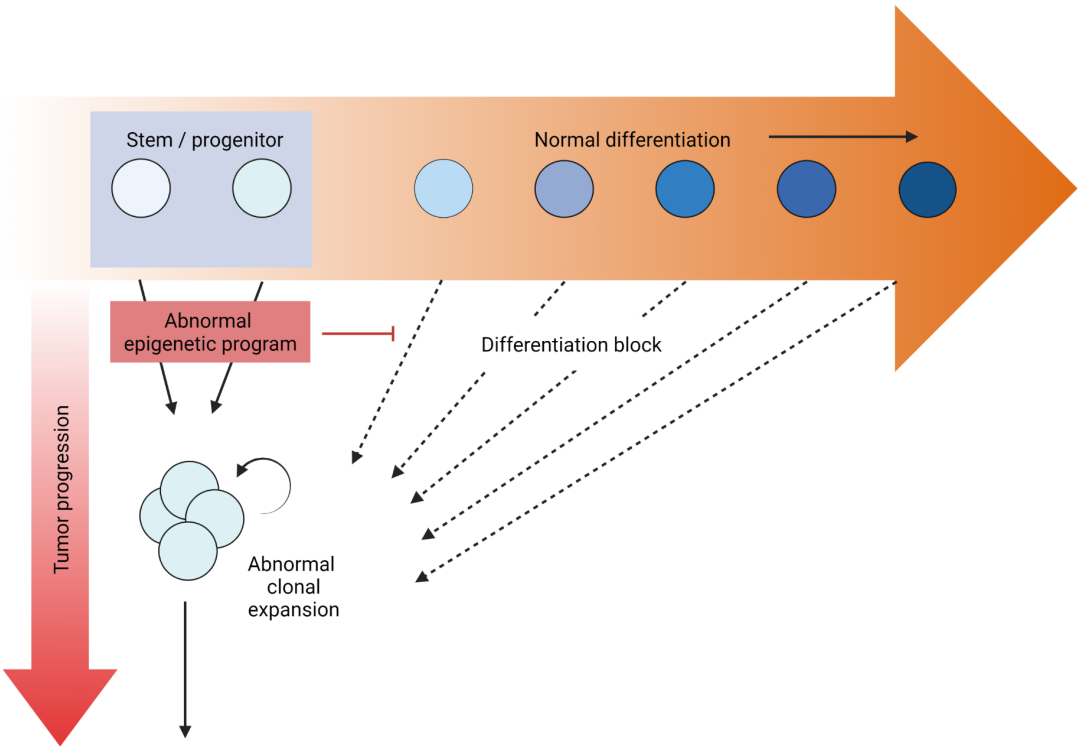

Figure 11. Epigenetic events and tumorigenesis. Tumorigenesis begins with an abnormal clonal expansion caused by the stress of renewing cells. These clones are at risk of further genetic and epigenetic events that stimulate tumor progression. Abnormal epigenetic events play a role in inducing the abnormal clonal expansion from within stem/progenitor cell compartments in adult cell renewal. Chromatin modifiers repress transcription and trigger gene silencing, disrupting normal homeostasis and preventing stem and progenitor cells from differentiating correctly. Adapted from ref.[152]

1.3.3 Treatment

1.3.3.1 NMZL

Currently, there is no specific recommendation for NMZL treatment, but therapy for follicular lymphoma (FL) is applied.[42] Treatment options are surgery, radiotherapy, and chemotherapy. Some of the drugs used include bortezomib, veltuzumab, anti-CD20 antibody, and pegylated IFN and ribavirin.[84] Different combinations are also employed, such as rituximab-bendamustine, rituximab-cyclophosphamide-doxorubicin-vincristine-prednisone (R-CHOP), rituximab-cyclophosphamide-vincristine-prednisone (R-CVP), or rituximab-fludarabine. However, the choice should depend on the patient's fitness and infection risks.[38]

1.3.3.2 SMZL

For SMZL, treatment options include splenectomy, chemotherapy, rituximab alone, or a combination of rituximab and chemotherapy. Rituximab exhibits an 80% overall quick response rate and 40% complete response rate.[42] Other regimens include chlorambucil, cyclophosphamide, fludarabine, and bendamustine.[84]

For HCV-positive cases of both SMZL and NMZL, antiviral therapy with pegylated IFNα used in combination with ribavirin or on its own has been observed to reduce remission.[153] An Italian study noted that anti-HCV therapy is used in HCV-positive patients with indolent B-cell NHL. Patients who achieved the HCV load clearance have exhibited a 77% diagnosis response rate and 85% relapse response rate.[154]

1.3.3.3 EMZL

The first line treatment for GMZL treatment is *H. pylori* eradication therapy involving the use of a proton pump inhibitor with amoxicillin and clarithromycin.[84] 80% of GMZL patients are treated with antibiotics and become healed after therapy. The International Extranodal

Lymphoma Study Group (IELSG) has reported that patients treated with a combination of chlorambucil and rituximab have shown a significantly better 5-year event-free survival.[155]

Patients with *C. psittaci* positive OMZL patients treated with doxycycline yielded a 65% overall response rate and a 5-year progression-free survival (PFS) rate of 68%.[66] In addition, patients with OMZL who experienced a first relapse were treated with clarithromycin and showed a 50% partial response. Clarithromycin shows anti-tumor properties by inducing apoptosis of tumor cells. However, further studies are needed to cement its potential.[1] For CMZL, if the patient is positive for *B. burgdorferi*, treatment with antibiotics such as cephalosporins and tetracyclines is the initial recommendation.[156] For other EMZL entities, combination chemotherapy is also employed. The regimens used include rituximab-chlorambucil and rituximab-bendamustine.[38]

1.3.4 Progression and histological transformation

1.3.4.1 Progression

Around 50%-70% of patients with NMZL are reported to have an overall survival of 5 years, with an indication that the disease is not currently curable.

The median 5-year overall survival of patients with SMZL is 50%.[157–160] At times, these cases may undergo progression to lymph nodes or extranodal sites, with a median time of 3.7 years.[159]

Among the different lymphoma subtypes, the EMZL has a more favorable outcome. EMZL prognosis includes a poor pathological stage (PS), bulky tumor, high levels of lactate dehydrogenase (LDH), β2-microglobulin, and serum albumin; and a large cell component associated with a poor outcome.[161,162] Recurrence of this lymphoma involves different extranodal or nodal sites.[163]

1.3.4.2 Transformation

NMZL is a rare disease; thus, biological processes involved in its transformation remain largely unknown. A study by Qian and colleagues[164] identified a high incidence of del(20q12), with enriched extracellular matrix proteins, growth factor receptor, DNA protein, and signalling protein in transformed MZL compared with non-transformed NMZL.

Around 10% of SMZL cases with recurrent tumors undergo histological transformation to diffuse large B-cell lymphoma (DLBCL). These transformations occur at either the time of diagnosis or progression, with a transformation median time of 12-85 months. Transformations are usually associated with B symptoms, poor performance status, disseminated disease in nodal and extranodal locations, high LDH, and poor outcome, with a median survival of 26 months.[159,165] These transformations are seen in association with p53 inactivation and chromosomal abnormalities.[166]

The overall survival of more than 85%-95% of EMZL cases is at five (5) years. Around 10% of the cases have been reported to undergo a histologic transformation during the late course of the disease and dissemination.[84,161,163,167] This transformation might result from antigenic stimulation, which causes the B-cells to acquire genetic abnormalities and undergo proliferation.[168,169] EMZL with the t(11;18) translocation has a lower risk of transformation to DLBCL. However, GMZL cases possessing the said translocation have more advanced disease, are *H. pylori*-negative, and have a lower response rate to antibiotics.[170–172] On the other hand, those with the t(3;14) translocation are associated with transformation to high-grade tumors.[173,174]

2. AIMS

2.1 To characterize ocular adnexal marginal zone B-cell lymphomas by targeted high-throughput sequencing

Despite multiple high throughput sequencing (HTS) studies, the molecular basis of OMZL is not fully understood. OMZL shows inconsistent results, and the distribution of mutations in reactive lymphoid lesions of this anatomic region has not yet been sufficiently addressed sufficiently. Furthermore, there have been some discrepancies about the infection status in OMZL. Data of cohorts from Italy, South Korea, Germany, and Austria suggest an association between OMZL and infection with *Chlamydia* spp., whereas Japanese and Danish OMZL cohorts were negative for *Chlamydia* spp. Therefore, we aimed to characterize the genetic landscape of OMZL compared with other types of lymphomas and to determine the infectious status of our OMZL cohort. Our study allowed us to compare chromosomal aberrations in OMZL with previous studies, to uncover the most commonly mutated genes in OMZL, to determine the infectious status of OMZL patients in the area of Basel, Switzerland, and to investigate the genetic evolutionary patterns of MZL relapses.

2.2 To uncover the genetic landscape of pulmonary lymphomas

Primary lymphomas of the lung are very rare, accounting for only 0.4% of all lymphomas; PMZL is the most common type. So far, we know that PMZL more commonly displays structural and numeric chromosomal aberrations compared with other EMZL entities. However, little is known about point mutations in primary pulmonary lymphomas. In this study, we aimed to investigate and to characterise the mutational landscape of PMZL at a larger scale. Furthermore, we aimed to compare the most affected signalling pathways in PMZL to our previous OMZL and NMZL studies. HTS allowed us to determine the most commonly mutated genes in PMZL. Finally, we wanted to investigate whether primary pulmonary lymphomas like PMZL have distinct mutational patterns compared with DLBCL and lymphomatoid granulomatosis (LyG) at the same anatomic region.

2.3 To summarize the genetic landscape of splenic, nodal, and extranodal marginal zone lymphomas in the dura mater, salivary gland, thyroid, ocular adnexa, lung, stomach and skin

Because the different MZL entities do not exhibit a disease-defining phenotype, the diagnostic borders between them are blurred. In addition, there is considerable overlap between the genetic mutations across various MZL entities and sub-entities. Consequently, a general overview of the mutational landscape across all MZL subtypes is still unavailable. We aimed to conduct a meta-analysis through a systematic PubMed search for MZL sequencing studies, where reported somatic mutations and identified variants in the different entities are gathered and combined. Genomic information was extracted and uniformed to the GRCh38 genome by applying the LiftOver – UCSC Genome Browser. Annotations were done using the Variant Effect Predictor (VEP) and Annovar. The collated somatic variants were evaluated regarding their potential diagnostic importance. Furthermore, an unbiased analysis of the genomic landscape of MZL derived from whole exome sequencing (WES) and HTS was also done to estimate the overlap of various mutational frequencies of different protein-coding genes. Recognising such mutational distribution patterns may help assign MZL origin in difficult lymphoma cases and possibly pave the way for novel, more tailored treatment concepts.

3. RESULTS

3.1 Mutational landscape of marginal zone B-cell lymphomas of various origin: organotypic alterations and diagnostic potential for assignment of organ origin

Visar Vela, Darius Juskevicius, Stefan Dirnhofer, Thomas Menter, Alexandar Tzankov

-Original Research Article-
Published in *Virchows Archiv*, 2021

Virchows Archiv
https://doi.org/10.1007/s00428-021-03186-3

ORIGINAL ARTICLE

Mutational landscape of marginal zone B-cell lymphomas of various origin: organotypic alterations and diagnostic potential for assignment of organ origin

Visar Vela[1] · Darius Juskevicius[1] · Stefan Dirnhofer[1] · Thomas Menter[1] · Alexandar Tzankov[1]

Received: 12 May 2021 / Revised: 4 August 2021 / Accepted: 11 August 2021

Abstract
This meta-analysis aims to concisely summarize the genetic landscape of splenic, nodal and extranodal marginal zone lymphomas (MZL) in the dura mater, salivary glands, thyroid, ocular adnexa, lung, stomach and skin with respect to somatic variants. A systematic PubMed search for sequencing studies of MZL was executed. All somatic mutations of the organs mentioned above were combined, uniformly annotated, and a dataset containing 25 publications comprising 6016 variants from 1663 patients was created. In splenic MZL, *KLF2* (18%, 103/567) and *NOTCH2* (16%, 118/725) were the most frequently mutated genes. Pulmonary and nodal MZL displayed recurrent mutations in chromatin-modifier-encoding genes, especially *KMT2D* (25%, 13/51, and 20%, 20/98, respectively). In contrast, ocular adnexal, gastric, and dura mater MZL had mutations in genes encoding for NF-κB pathway compounds, in particular *TNFAIP3,* with 39% (113/293), 15% (8/55), and 45% (5/11), respectively. Cutaneous MZL frequently had *FAS* mutations (63%, 24/38), while MZL of the thyroid had a higher prevalence for *TET2* variants (61%, 11/18). Finally, *TBL1XR1* (24%, 14/58) was the most commonly mutated gene in MZL of the salivary glands. Mutations of distinct genes show origin-preferential distribution among nodal and splenic MZL as well as extranodal MZL at/from different anatomic locations. Recognition of such mutational distribution patterns may help assigning MZL origin in difficult cases and possibly pave the way for novel more tailored treatment concepts.

Keywords Marginal zone lymphoma · Meta-analysis · *FAS* · *KLF2* · NF-κB · *TET2*

Introduction

Marginal zone lymphomas (MZL) represent 7–8% [1, 2] of all lymphoid neoplasms. The World Health Organization (WHO) [3] subdivides MZL into three distinct entities: splenic MZL (SMZL), nodal MZL (NMZL), and extranodal MZL (EMZL) [2]. The organs most commonly affected by EMZL are the stomach (70%), followed by the lungs (14%), ocular adnexa (12%), thyroid (4%), and the small intestine (1%) [4], while for salivary glands, dura mater, and cutaneous MZL, no incidence data is available [5]. The median age of MZL presentation is 60 years, with a higher proportion of females affected [6]. MZL are mostly indolent with a 5-year overall survival (OS) rate of 85% [6].

There is evidence that some EMZL are associated with and dependent on chronic antigenic stimulation, either by autoantigens or by foreign pathogens, especially bacteria, that lead to accumulation of secondary mucosa-associated lymphoid tissue (MALT) in respective organs due to chronic inflammation, with this MALT serving as soil for neoplastic outgrowth [5]. Infectious agents that have been found to be associated with EMZL are, e.g., *Helicobacter pylori* and *Helicobacter heilmannii* in the stomach, *Achrombacter xylosoxidans* in the lung, *Chlamydophila psittaci* in the ocular adnexa, and *Borrelia burgdorferi* in the skin. Moreover, autoimmune diseases such as Sjögren syndrome and Hashimoto thyroiditis predispose to the development of EMZL [7] (Suppl. Table 1). There is a useful, practical aspect in this consideration: since most EMZL retain their dependence on the respective antigenic stimulation, they may regress upon removal of the antigen, e.g., by antibiotics or by modulation of T-/B-cell interactions by immunomodulatory drugs, even in disseminated disease [8–10].

Thomas Menter and Alexandar Tzankov contributed equally to this work.

✉ Alexandar Tzankov
alexandar.tzankov@usb.ch

[1] Pathology, Institute of Medical Genetics and Pathology, University Hospital Basel, University of Basel, Schönbeinstrasse 40, 4031 Basel, Switzerland

Published online: 08 September 2021

Compared to other mature small B-cell lymphomas, MZL does not display a disease-defining phenotype. Thus, at occasions, the diagnostic borders among each other, i.e., SMZL, NMZL, and EMZL, as well as within EMZL of various organ origin, and to other small B-cell lymphomas without a defined phenotype are blurred [11, 12].

The pathogenesis of EMZL is linked to several recurrent numerical and structural chromosomal aberrations, i.e., trisomies and chromosomal translocations. Trisomies of chromosomes 3, 12, and 18 are found in 20–30% of EMZL [7]. One of the most common translocations in EMZL, t(11;18)(q21;q21), leads to the fusion of *BIRC3* to *MALT1*. It is tightly linked to EMZL of the lung, and occurs in as much as 45% of cases, followed by the stomach (23%) and the intestine (19%) [7]. Further, this *BIRC3/MALT1* fusion is specific for EMZL, since it is not reported in SMZL or NMZL [7]. On the other hand, partial deletion of the long arm of chromosome 7, del(7)(q31), is found exclusively in SMZL and may even be a biomarker of more aggressive behavior [13, 14]. Another common chromosomal translocation in MZL is t(3;14)(p14;q32) leading to *IGH-FOXP1* rearrangement [7]. Suppl. Table 2 summarizes organotypic chromosomal rearrangements in various MZL.

In the last decade, the genomic landscape of MZL has been extensively studied. With a few exceptions, there seems to be considerable overlap between mutated genes across the various MZL entities and subentities and sites of origin, but this has not yet been integratively analyzed, and being a rare tumor, MZL is still not included in databases such as the International Cancer Genome Consortium (IGGC) and the Cancer Genome Atlas (TGCA).

To address these shortcomings, we performed a meta-analysis of 25 carefully selected PubMed-listed publications reporting on somatic mutations in MZL of various origins, and report here the results of identified variants with consistent and detailed annotation. Whole-genome (WGS), whole exome (WES), targeted high-throughput sequencing (HTS) analysis, and/or Sanger sequencing were read-out methods in these studies.

Materials and methods

Literature search

We performed a literature search in October 2020 using PubMed [15] as the primary source. The keywords used and literature research results are detailed in Supplementary Fig. 1. Only studies explicitly stating that cases included had been reviewed and confirmed by staff pathologists were considered.

Data extraction and annotation

Genomic information was extracted from the supplementary materials of the selected studies and uniformed to the GRCh38-hg38 genome by applying LiftOver - UCSC Genome Browser [15]. The missing information on variants such as genomic location and reference sequence variant effect annotation was obtained with the variant effect predictor (VEP) by Ensemble [15] and Annovar software [16] (Fig. 1).

Meta-analysis of mutated gene frequencies

The number of mutated and unmutated cases was retrieved and the frequencies of mutations per gene was calculated (Suppl. Table 3). Given the main focus or the current study, namely to assess whether somatic nucleotide variants may be of diagnostic importance, a shortlist was generated for mutated genes with a mutational frequency of > 7.5% in at least one entity (Suppl. Table 4).

Due to format incompatibility and insufficient details, the supplementary list of the study by van den Brand et al. [17] was only used for frequency calculation and not further included. Seven patients from the study of Cascione et al. [18] and 14 from the study of Moody et al. [19] were excluded due to unspecified site of origin.

Statistical analysis

All statistical calculations were executed with MS Excel or R statistical packages and Statistical Package of Social Sciences (IBM SPSS version 22.0, Chicago, IL, USA) for Windows. Differences of mutational frequencies between EMZL, NMZL, and SMZL entities, as well as between EMZL subentities, were compared using the two-tailed Fisher's exact test (Suppl. Table 5, Suppl. Fig. 3). The statistical significance threshold was corrected for multiple testing and was set at $p < 0.017$.

Results

Filtering of literature, sequencing techniques, and patient characterization

After removing duplicate entries, 1602 of 3088 manuscripts were considered unique. After selection based on the criteria detailed above, 142 manuscripts remained for further analysis. Next, all manuscripts and their supplementary data were studied to ensure they reported a full list of variants with appropriate sample information and genetic coordinates. At the end, 25 studies were selected; 3 studies implemented WGS comprising 22 cases, 10 studies applied WES in 111 patients, 2 studies applied Sanger sequencing in 185 probands and 23

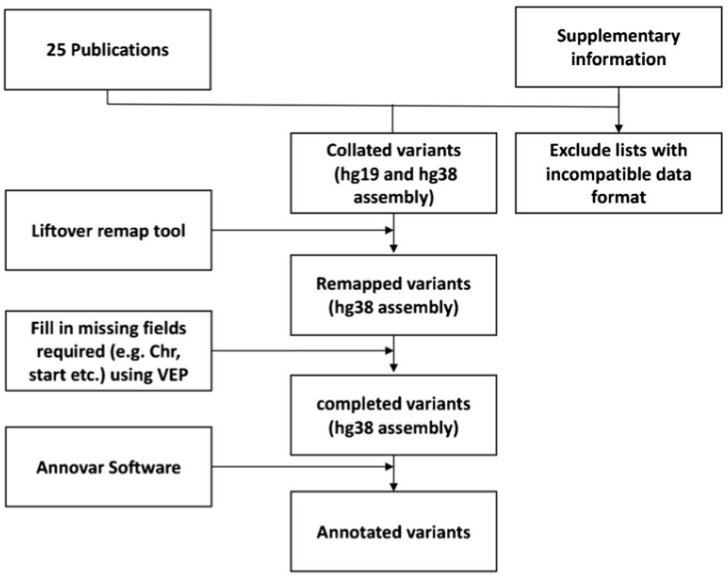

Fig. 1 Flowchart explaining the data set compilation and variant assembling strategy implemented in this study

studies screened 1434 patients utilizing targeted HTS (Suppl. Table 6); several studies utilized a mix of sequencing strategies. Either formalin-fixed paraffin-embedded (FFPE; n = 1327) tissues or/and fresh frozen (FF; n = 478) tissues were examined (Fig. 2, Suppl. Table 7).

Dataset collation and cohort description

Six thousand sixteen variants in 2553 genes of 1663 cases (Fig. 2) were extracted (Suppl. Table 8). With 13 studies, SMZL was the most comprehensively investigated entity and encompassed 58% of cases in the total cohort, whereas dural (DMZL) and cutaneous MZL (CMZL) accounted for only 3% each, and data was extracted from one publication each per these two respective sites/organs of origin (Fig. 2, Suppl. Fig. 1). Most MZL studies applied NGS-based techniques, only 2 studies on SMZL investigated cases by Sanger sequencing (Suppl. Fig. 2). Table 1 summarizes mutation frequencies per site and per case. Mutations numbers ranged between 1.8 and 27 per case being highest in NMZL. In all entities, single nucleotide variants (SNV) were the most common mutational type. Mutational frequencies in MZL of different entities are represented in Figs. 3, 4, and 5. The statistical comparison results of mutational frequencies by Fisher's exact test can be found in the Supplementary Table 5.

Heat-maps for the distribution of the various mutations per entity/organ/site are provided in Supplementary Figs. 4.1–4.7; for NMZL and SMZL, no heat-maps were constructed due to the large amount of cases and mutations found by WGS and WES, which would have rendered meaningful arrangement confusing.

Mutational profile of SMZL

Thirteen SMZL studies [20–32] consistently showed that *KLF2* was the most widely mutated gene (18%, 103/567; rather unique for this sub-entity), followed by *NOTCH2* (16%, 118/724) and *TP53* (12%, 59/493) (Figs. 3, 4, and 5). SMZL showed a higher prevalence of *KLF2* and, to a marginal extent, of *NOTCH2* mutations compared to EMZL (4%, 4/90, p = 5.73E−04, and 9%, 16/169, p = 2.33E−02, respectively). *TP53* was slightly more often mutated in SMZL compared to NMZL (3%, 2/68, p = 2.15E−02) and considerably to EMZL (4%, 11/279, p = 1.26E−04) (Suppl. Table 5, Suppl. Fig. 3A).

Mutational profile of NMZL

In four NMZL studies [17, 20, 21, 33], *KMT2D* was reportedly the most frequently mutated gene (20%, 20/98). Genes that were second most commonly mutated, with a frequency of 10%, include *LRP1B* (5/51), *TET2* (5/51), and *TNFRSF14* (10/98). These were followed by *BRAF* (4/51), *EZH2* (4/51), and *HIST1H1E* (8/98), with a frequency of 8% each (Figs. 3, 4, and 5). *KMT2D* was more commonly mutated in NMZL (20%, 20/98) than in SMZL (7%, 28/404, p = 1.80E−04). *LRP1B* was more frequently mutated in NMZL (10%, 5/51) compared to SMZL (1%, 4/484, p = 6.12E−04). NMZL showed a higher prevalence of *TNFRSF14* mutations (10%, 10/98) compared to SMZL (2%, 6/286, p = 1.55E−03). Moreover, we could demonstrate near exclusivity of *BRAF* (8%, 4/51) mutations in NMZL, which reached statistical significance compared to SMZL (1%, 2/301, p = 4.74E−03).

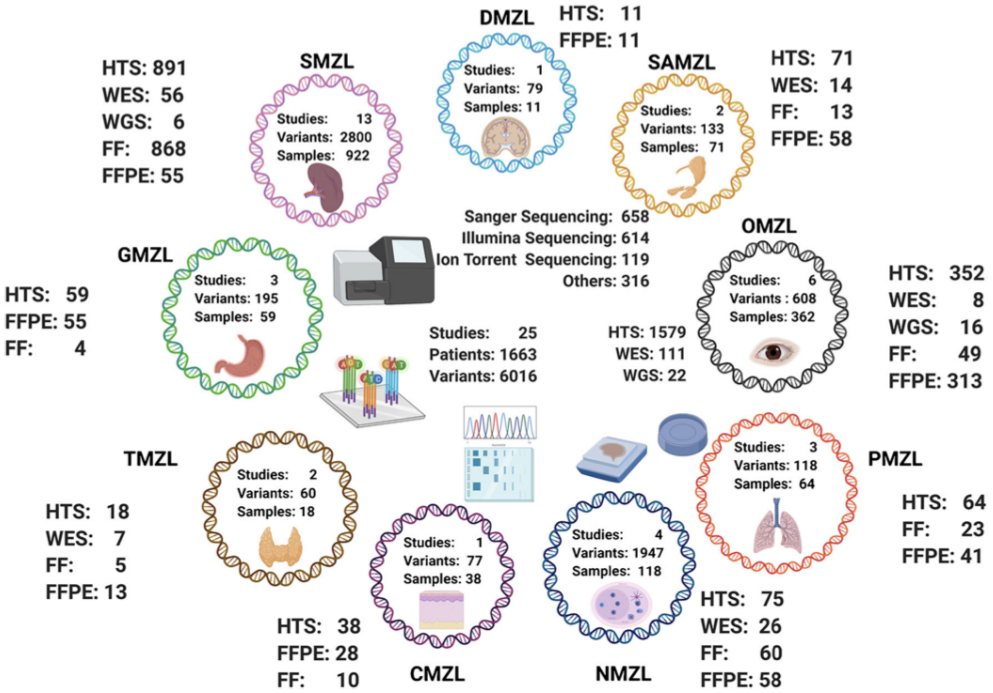

Fig. 2 Total number of samples, variants, tissue type material, and sequencing technology applied on 1663 cases for every target organ/site [whole-genome sequencing (WGS) (n = 22), whole-exome sequencing (WES) (n = 111), Sanger sequencing (n = 185), and high-throughput sequencing (HTS) (n = 1434)]; twenty-one HTS samples are from an unspecified organ of origin; the different types of tissue source, formalin-fixed paraffin-embedded (FFPE) tissue (n = 1327) or fresh frozen (FF) tissue (n = 478), are given for each organ/site

EZH2 mutations also appeared more frequently in NMZL (8%, 4/51) than in SMZL (1%, 2/265, p = 7.12E−03). Lastly, the *HIST1H1E* mutational rate in NMZL (8%, 8/98) exceeded that in SMZL (2%, 3/188, p = 9.35E−03). There was no statistical difference between the mutational profiles of NMZL and EMZL (Suppl. Table 5, Suppl. Fig. 3A).

Mutational profile of EMZL

Due to the differing cohort numbers, mutational rates are more difficult to describe in EMZL. Ten EMZL [18, 19, 33–40] studies extensively looked for *TNFAIP3* and *TBL1XR1* mutations and detected 140/500 and 66/515 mutant cases, respectively. A total of 29 cases with *NOTCH1* mutations was found in 324 samples, while 14 cases with *KMT2C* mutations were identified in 135 studied instances. Only three studies [33–35] explored *FAS* mutations, which were detected in 26/68 patients. Other genes detected in EMZL studies include *PALB2* (2/11), *JAK3* (11/122), *HIST1H1D* (2/23), and *PTEN* (4/47).

TNFAIP3 mutations were considerably more detectable in EMZL (28%, 140/500) compared to NMZL (14%, 12/88, p = 3.63E−03) and SMZL (8%, 52/628, p = 2.21E−18). EMZL displayed a high rate of *TBL1XR1* mutations (13%, 66/515/), which set them apart from SMZL (3%, 7/244, p = 4.51E−06). EMZL displayed a high occurrence of *NOTCH1* mutations, differentiating them from SMZL (5%, 24/529, p = 1.25E−02). *KMT2C* mutations also appeared to be more frequent in EMZL (10%, 14/135) compared to SMZL (1%, 1/90, p = 5.49E−03). *FAS* mutations (38%, 26/68) were more prevalent in EMZL than in SMZL (1%, 4/295, p = 2.01E−17) and NMZL (12%, 8/68, p = 6.23E−04). *PALB2* mutations were nearly exclusive to EMZL (18%, 2/11), reaching statistical significance compared to SMZL (0.4%, 1/265, p = 4.25E−03). *JAK3* was more commonly mutated in EMZL (9%, 11/122) than in SMZL (0.4%, 1/265, p = 1.94E−05). *HIST1H1D* mutations were slightly more commonly observable in (9%, 2/23) in EMZL compared to SMZL (1%, 2/265, p = 3.32E−02), as were *PTEN* mutations in EMZL (9%, 4/47) compared to SMZL (1%, 1/99, p = 3.72E−02) (Suppl. Table 5, Suppl. Fig. 3A).

Comparing mutational frequencies of EMZL occurring in different locations, several important differences could be demonstrated:

Two thyroid MZL (TMZL) studies [18, 19] showed a high prevalence of *TET2* mutations (61%, 11/18), which statistically significantly exceeded that in salivary gland

Table 1 Comparative overview of the mutational landscape of different MZL

MZL type	Number of cases	Frequency of cases with mutations	Mean mutations per case*	Mean mutated genes per case*	Types of mutation	Most frequently mutated genes	Most frequently mutated pathways
DMZL	11	100%	7.2	6.5	Missense 72% Frameshift del/ins 10% Nonsense 8% Intronic/Intergenic 6% Splicing site mutation 3% Nonframeshift del/ins 1%	*TNFAIP3* 45% *NOTCH2* 36% *TLBXR1* 36% *EP300* 18% *KLHL6* 18%	Chromatin modifiers 73% NF-κB 63% NOTCH 45%
OMZL	362	67%	2.5	1.78	Missense 59% Nonsense 18% Frameshift del/ins 15% Splicing site mutation 4% Nonframeshift del/ins 2% Intronic/Intergenic 2%	*TNFAIP3* 39% *KMT2D* 15% *CREBBP* 10% *LRP1B* 10% *MYD88* 10%	NF-κB 64% Chromatin modifiers 34% NOTCH 25%
SAMZL	71	70%	2.7	2.3	Missense 67% Nonframeshift del/ins 17% Nonsense 13% Splicing site mutation 2% Frameshift del/ins 1% Intronic/Intergenic 0%	*TBL1XR1* 24% *GPR34* 16% *NOTCH2* 11% *SPEN* 11% *KMT2C* 11%	NOTCH 44% Chromatin modifiers 32% NF-κB 28%
TMZL	18	83%	4	3.1	Missense 60% Frameshift del/ins 15% Nonsense 12% Splicing site mutation 12% Nonframeshift del/ins 1% Intronic/Intergenic 0%	*TET2* 61% *TNFRSF14* 44% *PIK3CD* 23% *SPEN* 17% *CREBBP* 8%	Chromatin modifiers 73% NF-κB 20% NOTCH 20%
PMZL	64	70%	2.6	2.6	Missense 72% Nonsense 16% Frameshift del/ins 8% Nonframeshift del/ins 2% Splicing site mutation 2% Intronic/Intergenic 0%	*KMT2D* 25% *TNFAIP3* 18% *PRDM1* 12% *NOTCH1* 12% *EP300* 11%	Chromatin modifiers 74% NF-κB 42% NOTCH 30%
GMZL	59	64%	5.1	4.4	Missense 74% Frameshift del/ins 12% Nonsense 8% Splicing site mutation 5% Nonframeshift del/ins 1% Intronic/Intergenic 0%	*NOTCH1* 17% *NF1* 16% *TNFAIP3* 15% *TRAF3* 13% *ATM* 13%	NF-κB 61% Chromatin modifiers 55% NOTCH 42%
NMZL	118	75%	29	27	Missense 75% Nonsense 8% Frameshift del/ins 7% Nonframeshift del/ins 5% Splicing site mutation 4% Intronic/Intergenic 1%	*KMT2D* 20% *TNFAIP3* 14% *CREBBP* 12% *FAS* 12% *KLF2* 12%	Chromatin modifiers 70% NOTCH 53% NF-κB 45%
SMZL	922	53%	5.8	5.9	Missense 77% Frameshift del/ins 10%	*KLF2* 18% *NOTCH2* 16%	NOTCH 53% Chromatin modifiers 43%

Table 1 (continued)

MZL type	Number of cases	Frequency of cases with mutations	Mean mutations per case*	Mean mutated genes per case*	Types of mutation	Most frequently mutated genes	Most frequently mutated pathways
					Nonsense 10%	*TP53* 12%	NF-κB 41%
					Splicing site mutation 2%	*TNFAIP3* 8%	
					Nonframeshift del/ins 1%	*KMT2D* 7%	
					Intronic/Intergenic 0%		
CMZL	38	84%	2.4	1.8	Missense 70%	*FAS* 63%	NOTCH 44%
					Splicing site mutation 13%	*SLAMF1* 24%	NF-κB 6%
					Nonsense 8%	*SPEN* 18%	Chromatin modifiers 6%
					Intronic/Intergenic 5%	*NCOR2* 13%	
					Frameshift del/ins 4%	*CASP10* 11%	
					Nonframeshift del/ins 0%		

*Numbers containing cases both investigated with WGS/WES and targeted sequencing panels

MZL (SAMZL), gastric MZL (GMZL), pulmonary MZL (PMZL), and ocular adnexal MZL (OMZL).

In the two studies with available information on sub-localization of the OMZL (conjunctival versus periorbital) [37, 38], total numbers of mutations in conjunctival OMZL were higher than in periorbital OMZL (median 2 versus 1; mean 2.38 versus 1.56, range 0–9 versus 0–5; $p = 0.028$). *TBL1XR1* mutations were enriched in conjunctival OMZL (8/27 versus 1/17, $p = 4.63E{-}02$ [37]; 7/22 versus 0/12, $p = 0.095$ [38]).

Compared to other MZL, *FAS* (63%, 24/38) was the most frequently mutated gene in CMZL [35] (Figs. 3, 4, and 5). These characteristic *FAS* mutations were substantially linked to CMZL compared to GMZL and DMZL, displaying such mutations in 5% (1/19, $p = 3.58E{-}05$) and 9% (1/11, $p = 1.92E{-}03$) of cases, respectively . Compared to all other MZL, CMZL also showed the highest proportion of splice-site mutations.

A detailed comparison of mutations of EMZL of various sites can be found in the supplementary files.

Preferred activation of the NOTCH pathway and NF-κB pathway by mutations across different MZL entities

Mutations related to the NOTCH pathway, NF-κB signaling pathway and in genes encoding for chromatin modifiers were grouped and analyzed regarding their role in different MZL. We could observe that mutations related to the NOTCH pathway were rather mutually exclusive to mutations of genes playing a role in the NF-κB pathway and to chromatin modifier-encoding genes. In MZL containing sufficient information density (adequate coverage of genes related to these pathways) to address this issue, 140 cases displayed mutations in both the NF-κB and NOTCH pathway, while 553 cases bore mutations exclusively of genes affecting either pathway, and 242 cases were unmutated, suggesting a nonrandom mutual exclusivity ($p = 1E{-}09$). Analyzing the different entities separately, statistically significant differences in that consideration were observable in SMZL ($p = 4E{-}08$) and OMZL ($p = 8E{-}03$), and as a trend in GMZL. Regarding chromatin modifiers, 207 cases displayed mutual mutations in the NOTCH pathway, while 407 cases bore mutations exclusively of genes affecting either cellular process ($p = 1E{-}03$). This applied to SMZL ($p = 1E{-}03$) and OMZL ($p = 7E{-}03$), and as a trend to SAMZL.

Concordance between three NMZL WES studies

An additional aim of our study was to perform an unbiased analysis of the genomic landscape of MZL derived from WES as well as targeted HTS to provide an estimation of the overlap of various mutational frequencies of different protein-coding

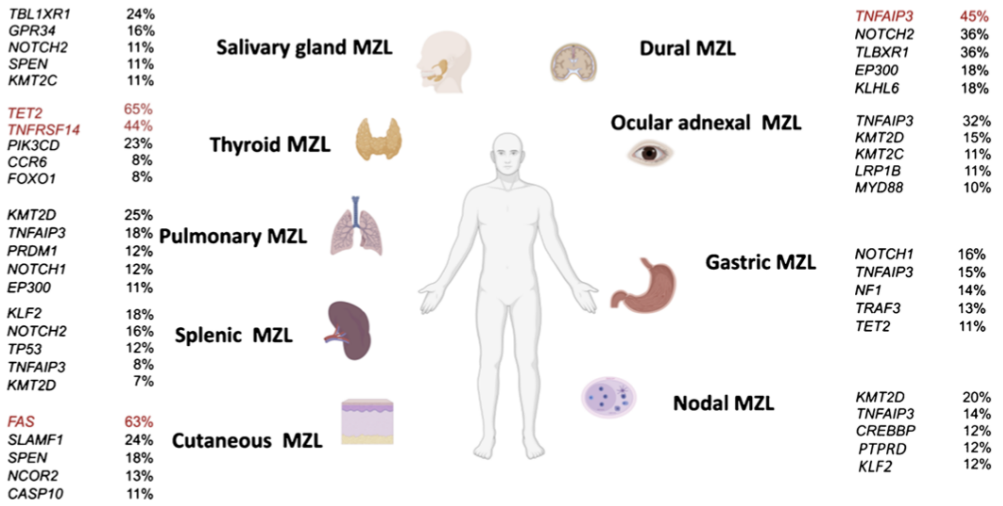

Fig. 3 Mutational frequencies of the five most commonly affected genes per entity; genes with frequencies ≥ 40% are highlighted in red

genes. To examine the concordance between studies, we compared WES data of three NMZL studies (Suppl. Fig. 5) [20, 21, 41]. A total of 34 samples sequenced by WES, accounting for 1593 variants, were included in the final list. Similar to a previous report [42] that addressed this concordance in SMZL, our analysis showed a very limited concordance across all three NMZL studies, with only 11 overlapping genes in all three studies.

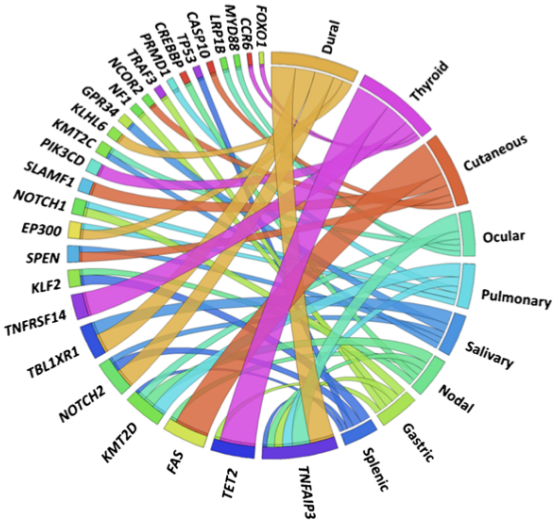

Fig. 4 Circos diagram showing the five most frequently mutated genes per entity at various MZL sites; the width of the migration curves indicates the relative frequency of the respective gene mutations

Discussion

Our knowledge about the genetic landscape of MZL has increased with the application of new sequencing techniques. However, separate study cohorts, usually derived from archives of one institution, are still limited in size and mutational profiles have been obtained applying different methods. As a result, a general overview of the mutational landscape across all MZL subtypes is lacking. We aimed to perform a comparative meta-analysis of reported genetic variants in various MZL subtypes to address the question of site/organ-of-origin-specific differences.

Some entities displayed similar mutational profiles. These comprise OMZL, PMZL, GMZL, and DMZL, which all showed recurrent *TNFAIP3* mutations and high concordant mutational rates in genes encoding for other compounds of the NF-κB pathway; *TNFAIP3* inhibits NF-κB activation by exerting dual ubiquitin-editing functions [43], thus inactivating mutations of *TNFAIP3* provide an advantage to the cells via activating NF-κB-related signaling.

In contrast, some genes were predominantly mutated in distinct MZL of specific organs/sites, including TMZL that showed a high prevalence of *TET2* mutations and CMZL, which demonstrated a predominance of *FAS* mutations. TET2 is involved in epigenetic regulation; like in *TNFAIP3*, *TET2* mutations are generally loss-of-function mutations that result in an inactive protein and, thus, a net general hypermethylated state of the cells [44]. *TET2* mutations are commonly seen in myeloid neoplasms, ranging from myelodysplastic and overlap syndromes to acute myeloid leukemias as well as in T-cell lymphomas [45]. In B-cell lymphomas in general, they are rather uncommon. Therefore, it is notable that *TET2* mutations occurred in 61% of TMZL, in contrast to all other MZL with *TET2* mutation frequencies <

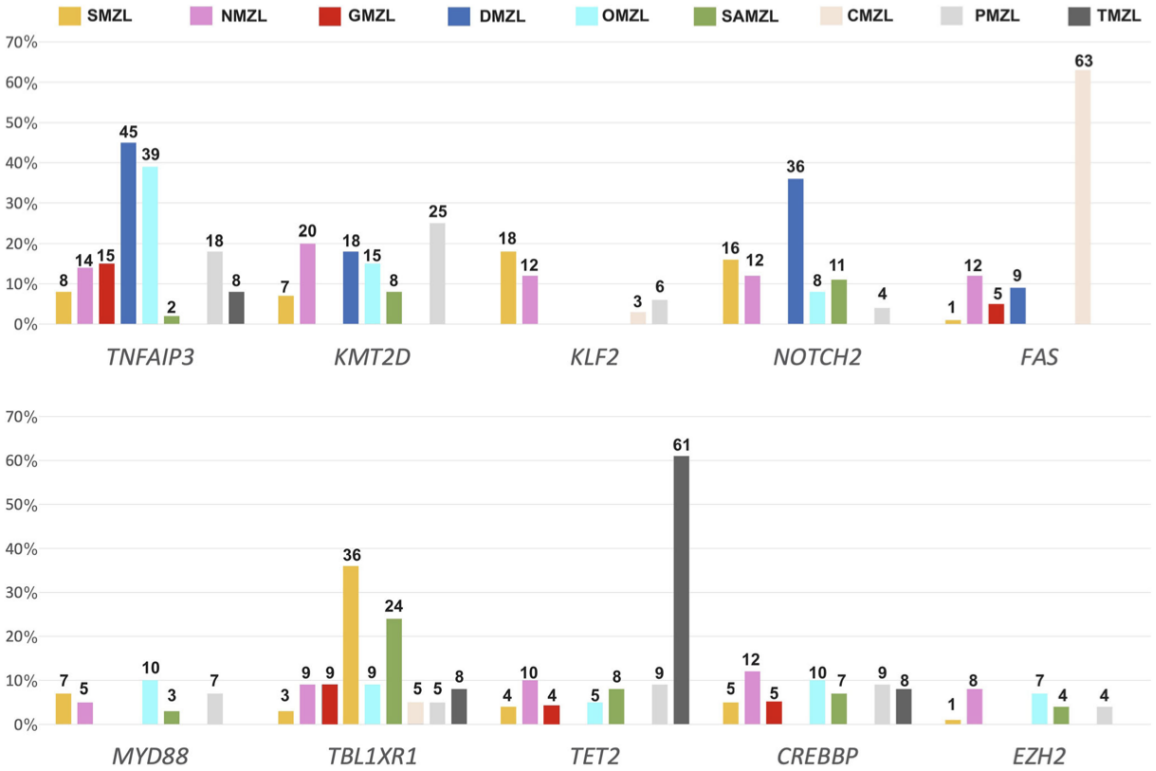

Fig. 5 Barplot showing frequencies of ten selected most differentially mutated genes and their distribution throughout the MZL in different anatomic locations; numbers at the top of the bars indicate %

15% (Fig. 5). Thus, *TET2* mutations can be regarded as rather specific for TMZL and might be of diagnostic help in distinguishing TMZL from other EMZL types of the head and neck.

Another gene primarily mutated in TMZL was *TNFRSF14*. TNFRSF14 is a member of the tumor necrosis factor receptor superfamily and has been described in both follicular lymphomas [46] and diffuse large B-cell lymphomas [47]. It is involved in lymphomagenesis since its inactivating mutations lead to increased B-cell receptor dependent signaling and, via its ligand BTLA, to disrupted interaction of lymphoma B-cells with modulatory T-helper cells [48], thus linking lymphomagenesis to disrupted immune cell crosstalk.

FAS was most frequently mutated in CMZL (63%) (Fig. 5), with predominantly splice-site mutations. FAS belongs to the tumor necrosis factor receptor family and its mutations affect the death domain fostering anti-apoptotic properties leading to disrupted protein function and empowering cancer cells with survival advantages [35, 49]. Indeed, Maurus and colleagues reported that all CMZL patients bearing *FAS* mutations showed at least one cutaneous relapse during 84.5 months, while 50% of patients without *FAS* mutations remained free of disease after therapy [35]. *FAS* splice site mutation render cells insensitive to FAS-mediated apoptotic stimuli [50]. *FAS* mutations were, though rarely, also observed in NMZL and SMZL [20, 21, 32]. Thus, *FAS* mutations can be regarded as rather specific for CMZL and might be of diagnostic help in distinguishing primary CMZL from other EMZL types, and pseudolymphoma of the skin.

There were also some other mutations, which tended to be rather organ/site-specific such as *KLF2* and *TP53* in SMZL, *BRAF* and *PTPRD* in NMZL, *NOTCH1* and *NF1* in GMZL, as well as *TBL1XR1* in MZL of the head and neck region. These mutations could also help to provide a tailored diagnostic and may play a role in distinguishing between entities.

In OMZL, the mutational profile of conjunctival and periorbital cases differs, raising the question whether OMZL of different anatomic sub-sites are, e.g., linked to different etiologies and should generally be further subdivided.

Besides single gene comparisons, we also performed analyses of pathways in order to see whether different types of MZL rely on different intracellular signaling conduits. In the majority of cases, we could show that mutations related to the NOTCH pathway were rather mutually exclusive to mutations in the NF-κB pathway and in chromatin modifier-encoding genes, while the two latter showed overlap. This mutual exclusivity was most prominently seen in SMZL and OMZL,

and to a lesser extent in SAMZL and GMZL. This again underlines the heterogeneity of MZL and might pave the way towards considerations on tailored targeted treatment approaches for distinct subentities.

The comparably low mutation rates in e.g. GMZL or PMZL might be explained by higher rates of translocations in these entities, which activate the NF-κB pathway. Notably, chromosomal translocations may thus play a more important role in molecular differentiation of MZL entities/subentities than nucleotide-level mutations (Suppl. Table 2). Due to methodological restrictions of the last years, mainly the necessity to perform studies based on FISH, which are both labor- and material-intensive, translocations have not been investigated and compared at large scale between different MZL so far, yet older data suggest certain diagnostic potential linked to distinct rearrangements in MZL [51]. The advent of RNA-based sequencing techniques has the potential to overcome these issues in near future [52].

Limited numbers of patients for some entities/subentities and the heterogeneity of the investigated cohorts without consistent clinical data are potential limitations of the present study, along with differences in sequencing strategies and bioinformatic work-up. Also, the nature of the material employed—either FF or FFPE tissue—may have affected the results. Indeed, discrepancies between the results of single observations, especially when comparing WES-based studies, became obvious, as shown in the Venn diagram for NMZL, which revealed a very small overlap (0.7%) of mutated genes found, although considering the large amount of different genes bearing mutations, this was not surprising (Suppl. Fig. 5). In order to tackle these issues, we homogenized the published data using the algorithms provided and normalized data based on reference genome hg38. Regarding the limitations based on the type of material (FFPE vs FF), Pillonel et al. showed for NMZL an excellent linear correlation between results obtained on either material type as it has been also shown for DLBCL [20, 53], suggesting that at least this might not represent a major confounding factor.

Unfortunately, information regarding infectious agents such as *Helicobacter pylori* (GMZL), *Borrelia burgdorferi* (CMZL), or *Chlamydia psittaci* (OMZL) has not been consistently provided to address the interrelations between mutational profiles and infectious etiology with exception of three studies on OMZL, in which all cases were tested negative for *Chlamydia psittaci*. As the authors of these studies stated in their discussions, infection of OMZL by *Chlamydia psittaci* seems to have a very distinct geographic distribution. Similarly, no information on autoimmune diseases, especially in SAMZL and TMZL, had been provided in the studies included to address mutational differences in instances arising in an autoimmune background.

To conclude, our meta-analysis was able to identify some unique characteristics of organ/site-specific MZL subtypes. *FAS* mutations were found to be restricted to CMZL, while *TET2* and *TNFRSF14* mutations were predominantly found in TMZL. In addition, mutations of *KLF2* and *TP53* (SMZL), *BRAF* and *PTPRD* (NMZL), *NOTCH1* and *NF1* (GMZL), and *TBL1XR1* (MZL of the head and neck region) might help in equivocal instances. Furthermore, *TNFAIP3* mutations and mutations affecting the NF-κB pathway in general are commonly found in OMZL, PMZL, GMZL and DMZL. Recognition of such mutational distribution patterns may be of additional help assigning MZL origin in difficult cases and might possibly pave the way for novel tailored treatment concepts.

Supplementary Information The online version contains supplementary material available at https://doi.org/10.1007/s00428-021-03186-3.

Author contribution AT, VV and DJ designed the study. VV, DJ, SD, TM, and AT accrued and analyzed the data. VV and TM wrote the manuscript. All authors critically reviewed the manuscript.

Funding Open Access funding provided by Universität Basel (Universitätsbibliothek Basel).

Data availability All raw data is supplied in the supplementary files.

Code availability Not applicable.

Declarations

Ethics approval was obtained from the local ethics committee (applicable to the previously published own studies on NMZL, OMZL and PMZL). The procedures used in this study adhere to the tenets of the Declaration of Helsinki.

Conflict of interest The authors declare no competing interests.

Consent to participate Not applicable.

Consent for publication Not applicable.

References

1. Joshi M, Sheikh H, Abbi K et al (2012) Marginal zone lymphoma: old, new, targeted, and epigenetic therapies. Ther Adv Hematol 3: 275–290. https://doi.org/10.1177/2040620712453595
2. Swerdlow S, Campo E, Harris N et al (2017) WHO classification of tumours of haematopoietic and lymphoid tissues, 4th edn. IARC Press, Lyon

3. Cogliatti S, Bargetzi M, Bertoni F et al (2016) Supplementum 216: Diagnosis and treatment of marginal zone lymphoma. Swiss Med Wkly 146:w14324. https://doi.org/10.4414/smw.2016.14324
4. Khalil MO, Morton LM, Devesa SS et al (2014) Incidence of marginal zone lymphoma in the United States, 2001–2009 with a focus on primary anatomic site. Br J Haematol 165:67–77. https://doi.org/10.1111/bjh.12730
5. Troppan K, Wenzl K, Neumeister P, Deutsch A (2015, 2015) Molecular pathogenesis of MALT lymphoma. Gastroenterol Res Pract. https://doi.org/10.1155/2015/102656
6. Bertoni F, Coiffier B, Salles G et al (2011) MALT lymphomas: pathogenesis can drive treatment. Oncology 25(1134–1142):1147
7. Schreuder MI, van den Brand M, Hebeda KM et al (2017) Novel developments in the pathogenesis and diagnosis of extranodal marginal zone lymphoma. J Hematop 10:91–107. https://doi.org/10.1007/s12308-017-0302-2
8. Kiesewetter B, Raderer M (2020) Immunomodulatory treatment for mucosa-associated lymphoid tissue lymphoma (MALT lymphoma). Hematol Oncol 38:417–424. https://doi.org/10.1002/hon.2754
9. Defrancesco I, Arcaini L (2018) Overview on the management of non-gastric MALT lymphomas. Best Pract Res Clin Haematol 31:57–64. https://doi.org/10.1016/j.beha.2017.11.001
10. Thieblemont C, Zucca E (2017) Clinical aspects and therapy of gastrointestinal MALT lymphoma. Best Pract Res Clin Haematol 30:109–117. https://doi.org/10.1016/j.beha.2017.01.002
11. van den Brand M, van Krieken JHJM (2013) Recognizing nodal marginal zone lymphoma: recent advances and pitfalls. A systematic review. Haematologica 98:1003–1013. https://doi.org/10.3324/haematol.2012.083386
12. Pileri S, Ponzoni M (2017) Pathology of nodal marginal zone lymphomas. Best Pract Res Clin Haematol 30:50–55. https://doi.org/10.1016/j.beha.2016.11.001
13. Boonstra R, Bosga-Bouwer A, van Imhoff GW et al (2003) Splenic marginal zone lymphomas presenting with splenomegaly and typical immunophenotype are characterized by allelic loss in 7q31–32. Mod Pathol 16:1210–1217. https://doi.org/10.1097/01.MP.0000095895.19756.77
14. Lloret E, Mollejo M, Mateo MS et al (1999) Splenic marginal zone lymphoma with increased number of blasts: An aggressive variant? Hum Pathol 30:1153–1160. https://doi.org/10.1016/S0046-8177(99)90031-X
15. McLaren W, Gil L, Hunt SE et al (2016) The Ensembl variant effect predictor. Genome Biol 17. https://doi.org/10.1186/s13059-016-0974-4
16. Wang K, Li M, Hakonarson H (2010) ANNOVAR: functional annotation of genetic variants from high-throughput sequencing data. Nucleic Acids Res 38:e164. https://doi.org/10.1093/nar/gkq603
17. van den Brand M, Rijntjes J, Hebeda KM et al (2017) Recurrent mutations in genes involved in nuclear factor-κB signalling in nodal marginal zone lymphoma—diagnostic and therapeutic implications. Histopathology 70:174–184. https://doi.org/10.1111/his.13015
18. Cascione L, Rinaldi A, Bruscaggin A et al (2019) Novel insights into the genetics and epigenetics of MALT lymphoma unveiled by next generation sequencing analyses. Haematologica 104:e558–e561. https://doi.org/10.3324/haematol.2018.214957
19. Moody S, Thompson JS, Chuang S-S et al (2018) Novel GPR34 and CCR6 mutation and distinct genetic profiles in MALT lymphomas of different sites. Haematologica 103:1329–1336. https://doi.org/10.3324/haematol.2018.191601
20. Pillonel V, Juskevicius D, Ng CKY et al (2018) High-throughput sequencing of nodal marginal zone lymphomas identifies recurrent BRAF mutations. Leukemia 32:2412–2426. https://doi.org/10.1038/s41375-018-0082-4
21. Spina V, Khiabanian H, Messina M et al (2016) The genetics of nodal marginal zone lymphoma. Blood 128:1362–1373. https://doi.org/10.1182/blood-2016-02-696757
22. Clipson A, Wang M, de Leval L et al (2015) KLF2 mutation is the most frequent somatic change in splenic marginal zone lymphoma and identifies a subset with distinct genotype. Leukemia 29:1177–1185. https://doi.org/10.1038/leu.2014.330
23. Parry M, Rose-Zerilli MJ, Ljungström V et al (2015) Genetics and prognostication in splenic marginal zone lymphoma: revelations from deep sequencing. Clin Cancer Res Off J Am Assoc Cancer Res 21:4174–4183. https://doi.org/10.1158/1078-0432.CCR-14-2759
24. Piva R, Deaglio S, Famà R et al (2015) The Krüppel-like factor 2 transcription factor gene is recurrently mutated in splenic marginal zone lymphoma. Leukemia 29:503–507. https://doi.org/10.1038/leu.2014.294
25. Kiel MJ, Velusamy T, Betz BL et al (2012) Whole-genome sequencing identifies recurrent somatic NOTCH2 mutations in splenic marginal zone lymphoma. J Exp Med 209:1553–1565. https://doi.org/10.1084/jem.20120910
26. Rossi D, Trifonov V, Fangazio M et al (2012) The coding genome of splenic marginal zone lymphoma: activation of NOTCH2 and other pathways regulating marginal zone development. J Exp Med 209:1537–1551. https://doi.org/10.1084/jem.20120904
27. Parry M, Rose-Zerilli MJJ, Gibson J et al (2013) Whole exome sequencing identifies novel recurrently mutated genes in patients with splenic marginal zone lymphoma. PLoS One 8(12):e83244. https://doi.org/10.1371/journal.pone.0083244
28. Campos-Martín Y, Martínez N, Martínez-López A et al (2017) Clinical and diagnostic relevance of NOTCH2-and KLF2-mutations in splenic marginal zone lymphoma. Haematologica 102:e310–e312. https://doi.org/10.3324/haematol.2016.161711
29. Rossi D, Deaglio S, Dominguez-Sola D et al (2011) Alteration of BIRC3 and multiple other NF-κB pathway genes in splenic marginal zone lymphoma. Blood 118:4930–4934. https://doi.org/10.1182/blood-2011-06-359166
30. Peveling-Oberhag J, Wolters F, Döring C et al (2015) Whole exome sequencing of microdissected splenic marginal zone lymphoma: a study to discover novel tumor-specific mutations. BMC Cancer 15:773. https://doi.org/10.1186/s12885-015-1766-z
31. Jallades L, Baseggio L, Sujobert P et al (2017) Exome sequencing identifies recurrent BCOR alterations and the absence of KLF2, TNFAIP3 and MYD88 mutations in splenic diffuse red pulp small B-cell lymphoma. Haematologica 102:1758–1766. https://doi.org/10.3324/haematol.2016.160192
32. Martínez N, Almaraz C, Vaqué JP et al (2014) Whole-exome sequencing in splenic marginal zone lymphoma reveals mutations in genes involved in marginal zone differentiation. Leukemia 28:1334–1340. https://doi.org/10.1038/leu.2013.365
33. Ganapathi KA, Jobanputra V, Iwamoto F et al (2016) The genetic landscape of dural marginal zone lymphomas. Oncotarget 7:43052–43061. https://doi.org/10.18632/oncotarget.9678
34. Hyeon J, Lee B, Shin S-H et al (2018) Targeted deep sequencing of gastric marginal zone lymphoma identified alterations of TRAF3 and TNFAIP3 that were mutually exclusive for MALT1 rearrangement. Mod Pathol 31:1418–1428. https://doi.org/10.1038/s41379-018-0064-0
35. Maurus K, Appenzeller S, Roth S et al (2018) Panel sequencing shows recurrent genetic FAS alterations in primary cutaneous

marginal zone lymphoma. J Invest Dermatol 138:1573–1581. https://doi.org/10.1016/j.jid.2018.02.015
36. Johansson P, Klein-Hitpass L, Grabellus F et al (2016) Recurrent mutations in NF-κB pathway components, KMT2D, and NOTCH1/2 in ocular adnexal MALT-type marginal zone lymphomas. Oncotarget 7:62627–62639. https://doi.org/10.18632/oncotarget.11548
37. Jung H, Yoo HY, Lee SH et al (2017) The mutational landscape of ocular marginal zone lymphoma identifies frequent alterations in TNFAIP3 followed by mutations in TBL1XR1 and CREBBP. Oncotarget 8:17038–17049. https://doi.org/10.18632/oncotarget.14928
38. Vela V, Juskevicius D, Gerlach MM et al (2020) High throughput sequencing reveals high specificity of TNFAIP3 mutations in ocular adnexal marginal zone B-cell lymphomas. Hematol Oncol 38:284–292. https://doi.org/10.1002/hon.2718
39. Johansson P, Klein-Hitpass L, Budeus B et al (2020) Identifying genetic lesions in ocular adnexal extranodal marginal zone lymphomas of the MALT subtype by whole genome, whole exome and targeted sequencing. Cancers (Basel) 12(4):986. https://doi.org/10.3390/cancers12040986
40. Vela V, Juskevicius D, Prince SS et al (2021) Deciphering the genetic landscape of pulmonary lymphomas. Mod Pathol 34:371–379. https://doi.org/10.1038/s41379-020-00660-2
41. Koh J, Jang I, Choi S et al (2020) Discovery of novel recurrent mutations and clinically meaningful subgroups in nodal marginal zone lymphoma. Cancers 12. https://doi.org/10.3390/cancers12061669
42. Jaramillo Oquendo C, Parker H, Oscier D et al (2019) Systematic review of somatic mutations in splenic marginal zone lymphoma.Sci Rep 9(1):10444. https://doi.org/10.1038/s41598-019-46906-1
43. Heyninck K, Beyaert R (2005) A20 inhibits NF-κB activation by dual ubiquitin-editing functions. Trends Biochem Sci 30:1–4. https://doi.org/10.1016/j.tibs.2004.11.001
44. Forbes SA, Beare D, Gunasekaran P et al (2015) COSMIC: exploring the world's knowledge of somatic mutations in human cancer. Nucleic Acids Res 43:D805–D811. https://doi.org/10.1093/nar/gku1075
45. Ko M, Huang Y, Jankowska AM et al (2010) Impaired hydroxylation of 5-methylcytosine in myeloid cancers with mutant TET2. Nature 468:839–843. https://doi.org/10.1038/nature09586
46. Kotsiou E, Okosun J, Besley C et al (2016) TNFRSF14 aberrations in follicular lymphoma increase clinically significant allogeneic T-cell responses. Blood 128:72–81. https://doi.org/10.1182/blood-2015-10-679191
47. Lohr JG, Stojanov P, Lawrence MS et al (2012) Discovery and prioritization of somatic mutations in diffuse large B-cell lymphoma (DLBCL) by whole-exome sequencing. Proc Natl Acad Sci U S A 109:3879–3884. https://doi.org/10.1073/pnas.1121343109
48. Mintz MA, Felce JH, Chou MY et al (2019) The HVEM-BTLA axis restrains T cell help to germinal center b cells and functions as a cell-extrinsic suppressor in lymphomagenesis. Immunity 51:310–323.e7. https://doi.org/10.1016/j.immuni.2019.05.022
49. Zhang J, Manley JL (2013) Misregulation of pre-mRNA alternative splicing in cancer. Cancer Discov 3:1228–1237. https://doi.org/10.1158/2159-8290.CD-13-0253
50. Fisher GH, Rosenberg FJ, Straus SE et al (1995) Dominant interfering Fas gene mutations impair apoptosis in a human autoimmune lymphoproliferative syndrome. Cell 81:935–946. https://doi.org/10.1016/0092-8674(95)90013-6
51. Streubel B, Simonitsch-Klupp I, Müllauer L et al (2004) Variable frequencies of MALT lymphoma-associated genetic aberrations in MALT lymphomas of different sites. Leukemia 18:1722–1726. https://doi.org/10.1038/sj.leu.2403501
52. Crotty R, Hu K, Stevenson K et al (2021) Simultaneous identification of cell of origin, translocations, and hotspot mutations in diffuse large B-cell lymphoma using a single RNA-sequencing assay. Am J Clin Pathol 155:748–754. https://doi.org/10.1093/ajcp/aqaa185
53. Juskevicius D, Lorber T, Gsponer J et al (2016) Distinct genetic evolution patterns of relapsing diffuse large B-cell lymphoma revealed by genome-wide copy number aberration and targeted sequencing analysis. Leukemia 30:2385–2395. https://doi.org/10.1038/leu.2016.135

3.2 High throughput sequencing reveals high specificity of *TNFAIP3* mutations in ocular adnexal marginal zone B-cell lymphomas

Visar Vela, Darius Juskevicius, Magdalena M. Gerlach, Peter Meyer, Anne Graber, Gieri Cathomas, Stefan Dirnhofer, Alexandar Tzankov

-Original Research Article-
Published in *Wiley*, 2020

Received: 30 September 2019 | Revised: 15 January 2020 | Accepted: 24 January 2020
DOI: 10.1002/hon.2718

ORIGINAL RESEARCH ARTICLE

WILEY

High throughput sequencing reveals high specificity of *TNFAIP3* mutations in ocular adnexal marginal zone B-cell lymphomas

Visar Vela[1] | Darius Juskevicius[1] | Magdalena M. Gerlach[1] | Peter Meyer[1,2] | Anne Graber[3] | Gieri Cathomas[3] | Stefan Dirnhofer[1] | Alexandar Tzankov[1]

[1]Institute of Medical Genetics and Pathology, University Hospital Basel, Basel, Switzerland
[2]Eye Clinic, University Hospital Basel, Basel, Switzerland
[3]Cantonal Institute of Pathology, Liestal, Switzerland

Correspondence
Prof Dr med Alexandar Tzankov, Head Histopathology and Autopsy, University Hospital Basel Institute of Medical Genetics and Pathology, Schoenbeinstrasse 40, CH-4031 Basel, Switzerland.
Email: alexandar.tzankov@usb.ch

Funding information
Stiftung zur Krebsbekämpfung Zürich, Grant/Award Number: 460

Peer Review
The peer review history for this article is available at https://publons.com/publon/10.1002/hon.2718.

Abstract

The majority of ocular adnexal (OA) lymphomas (OAL) are extranodal marginal zone lymphomas (MZL). First high throughput sequencing (HTS) studies on OA-MZL showed inconsistent results and the distribution of mutations in reactive lymphoid lesions of this anatomic region has not yet been sufficiently addressed.

We characterized OAL and lymphoid lesions of the OA by targeted HTS. The study included 34 OA-MZL, 11 chronic conjunctivitis, five mature small cell B-cell lymphomas spreading to the OA, five diseases with increase of IgG4+ plasma cells, three Burkitt lymphomas (BL), three diffuse large B-cell lymphomas (DLBCL), three mantle cell lymphomas, three idiopathic orbital inflammations/orbital pseudo tumors (PT), and three OA lymphoid hyperplasia.

All cases were negative for *Chlamydia*. The mutational number was highest in BL and lowest in PT. The most commonly (and exclusively) mutated gene in OA-MZL was *TNFAIP3* (10 of 34 cases). Altogether, 20 out of 34 patients harbored mutually exclusive mutations of either *TNFAIP3*, *BCL10*, *MYD88*, *ATM*, *BRAF*, or *NFKBIE*, or non-exclusive mutations of *IRF8*, *TNFRSF14*, *KLHL6*, and *TBL1XR1*, all encoding for NK-κB pathway compounds or regulators. Thirteen patients (38%) had, to a great part, mutually exclusive mutations of chromatin modifier-encoding genes: *KMT2D*, *CREBBP*, *BCL7A*, *DNMT3A*, *EP300*, or *HIST1H1E*. Only four patients harbored co-occurring mutations of genes encoding for NK-κB compounds and chromatin modifiers. Finally, *PTEN*, *KMT2D*, *PRDM1*, and *HIST1H2BK* mutations were observable in reactive lymphoid lesions too, while such instances were devoid of NF-κB compound mutations and/or mutations of acetyltransferase-encoding genes.

In conclusion, 80% of OA-MZL display mutations of either NK-κB compounds or chromatin modifiers. Lymphoid lesions of the OA bearing NF-κB compound mutations and/or mutations of acetyltransferase-encoding genes highly likely represent lymphomas.

KEYWORDS
BCL10, high throughput sequencing, marginal zone B-cell lymphoma, *MYD88*, NF-κB, ocular adnexa, *TNFAIP3*

1 | INTRODUCTION

Ocular adnexal lymphomas (OAL) are rare.[1] They account for 1% to 2% of all lymphomas and 7% to 8% of extranodal lymphomas,[2] with a rising incidence.[3,4] OAL involve the orbital soft tissues, the eyelids, and conjunctiva or affect the lacrimal gland and lacrimal draining apparatus.[1] The vast majority (more than 95%) of OAL are of B-cell origin, while T-cell lymphomas and Hodgkin lymphomas are rather exceptional.[2] OAL often arise in a background of acquired mucosa-associated lymphoid tissue (MALT) and belong to the extranodal marginal zone lymphomas (EMZL) of MALT (Figure 1).[4] Other common OAL represent follicular (FL) and mantle cell (MCL), diffuse large B-cell (DLBCL) and Burkitt lymphomas (BL), particularly endemic BL.[5]

Secondary orbital involvement can be observed in many types of lymphomas, but most commonly apply to FL.[1] Various conjunctival and idiopathic orbital inflammatory diseases, eg, "orbital pseudo tumors," can clinically and histopathologically mimic OAL.[6]

Until today, the molecular basis of OA-MZL is not fully understood. Chromosomal translocations, found in a small proportion of OA-MZL,[7] are *t*(11;18) leading to *API2-MALT1* fusion, *t*(14;18) - to *IGH-MALT1*, t(3;14) - to *IGH-FOXP1* and *t*(1;14) - to *IGH-BCL10*. Karyotype analyses showed trisomies of chromosomes 3 and 18 and gains of 6p to be recurrent in OA-MZL.[2,7-9] All these chromosomal abnormalities finally lead to net activation of nuclear factor (NF)-κB compounds that enhance proliferation and survival,[8] being gatekeeping to OA-MZL lymphomagenesis.[10] Importantly, the mentioned aberrations are not specific for OA-MZL, and have been documented in reactive conditions from the same anatomic region, too.[11,12]

Sequencing studies showed mutations of *TNFAIP3*, *KMT2D*, *TBL1XR1*, *CREBBP*, *MYD88*, *CDKN2A*, and *NOTCH1/2* to be recurrent in OA-MZL.[8,9,13-15] Importantly, *TNFAIP3* and *BCL10* encode for compounds of the NF-κB signaling pathway. In the case of *TNFAIP3*, encoding for the A20 protein, a negative regulator of NF-κB,[16] its locus at 6q23.3 [17] is also targeted by recurrent deletions or promoter hypermethylations in up to 50% of cases,[15,18] while structural aberrations involving the *BCL10* locus are not characteristic of OA-MZL. Another regulator of NF-κB, namely, *MYD88*, shows a higher mutation frequency in DLBCL of orbital and OA origin than in other locations.[14,18] Data of cohorts from Italy, South Korea, Germany, and Austria suggest association between OA-MZL and infection with *Chlamydia spp*., whereas Japanese and Danish OA-MZL cohorts were negative for *Chlamydia spp*.[11,19-21]

The mutational landscape of OA-MZL is still somewhat controversial. Except for *MYD88*,[8] there are no data on the prognostic value of recurrent point mutations in OA-MZL. Moreover, the genetic landscape of clinically and histologically related, lesions, such as idiopathic orbital inflammations/orbital pseudotumors, IgG4-associtaed lesions, severe chronic conjunctivitis, and other orbital lymphomas, has not been studied on larger collectives, and the practical diagnostic usefulness of gene sequencing approaches considering OAL has not been addressed.

To tackle these challenges, utilizing targeted high throughput sequencing (HTS), we characterized the genetic background of OA-MZL in comparison with other types of lymphomas and reactive lesions occurring in the same anatomic region.

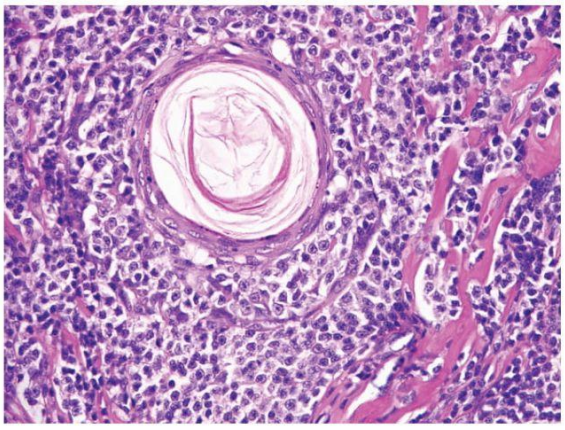

FIGURE 1 Typical histopathologic appearance of an ocular adnexal marginal zone B-cell lymphoma with a lympho-epithelial lesion attacking a squamous epithelium-lined skin appendicular structure in the center of the microphotograph and surrounded by a clear cell lymphoid infiltrate arranged in a targetoid pattern; original magnification 280×, H&E stain

2 | MATERIALS AND METHODS

2.1 | Patients, immunohistochemistry, fluorescence in situ hybridization of the MALT1 locus, *t*(11;14) and IGH PCR analysis, *Chlamydia spp*. PCR, and DNA extraction for HTS and statistics

We kindly refer to the Supplementary information for detailed descriptions of the studied cases and the applied methods (Data S1, Table S1 & S2). PCR for *Chlamydia psittaci* and *Chlamydia trachomatis* using PCR was performed as described[22] with minimal modification of the cycling conditions to increase the sensitivity of the method. Unsupervised clustering analysis to assess whether mutational profiles correlate with the conventional diagnoses was performed exactly as described.[23]

2.2 | Targeted HTS with custom lymphoma panel and data analysis

Targeted HTS was performed with the IonTorrent S5XL instrument and Ion 540 sequencing chips. Target enrichment for library preparation was done with an amplicon-based (AmpliSeq, IonTorrent, Thermo Fisher Scientific, Carlsbad, California) custom lymphoma panel (Table S3), which has been validated and used in earlier studies.[24] All samples including the relapses displayed a mean coverage depth of 1853× (range 690-6818). Information for coverage depth, uniformity,

and mapping quality are summarized in Table S4. The variant caller plug-in v5.10 from the IonTorrent software suite (Thermo Fisher Scientific) with default settings was used to identify mutations. Variants were annotated with ion reporter single sample annotation workflow and dbNSFP database v3.2. Filtering was done according to criteria listed in Table S5. Remaining mutations were manually reviewed, using the IGV viewer to exclude remaining artifacts. Ensemble MetaLR score combining multiple functional prediction and conservation algorithms[13] were used for in silico effect prediction of missense somatic point mutations.

3 | RESULTS

3.1 | Clinical course of OA-MZL patients

A detailed description of the OA-MZL is given in the Supplementary information, Table 1 and Tables S1 and S6. No patient died of lymphoma within the observational period. For 19 patients, only the treatment strategy was known: 16 have been treated by local radiotherapy (36Gy before 2012, applying to nine patients, and 24Gy after 2012, applying to seven patients; in altogether seven patients after unsuccessful application of doxycycline), two by systemic immunochemotherapy (rituximab + chlorambucil + prednisone), and a watchful waiting strategy (after the complete surgical excision) has been chosen in one patient. There were only two relapses in the 16 patients treated by radiotherapy, while all three patients, who were not irradiated, relapsed (Figure S1).

TABLE 1 Studied entities

Entity[a]	N	Median age (range)	M:F
Ocular adnexal marginal zone B-cell lymphomas (MZL)	34	78 (32-97)	18:16
Chronic lymphofollicular conjunctivitis	11	52 (11-87)	8:3
Mature small cell B-cell lymphomas 2 chronic lymphocytic leukemias, 2 lymphoplasmacytic- and 1 follicular lymphomas	5	73 (56-101)	4:1
Diseases with IgG4 increase	5	58 (13-83)	0:5
Other marginal zone B-cell lymphomas	4	68(63-70)	2:2
Orbital lymphoproliferative diseases[b]	3	61 (24-86)	1:2
Idiopathic orbital inflammations/ orbital pseudotumors	3	87(58-87)	2:1
Diffuse large B-cell lymphomas	3	52 (40-84)	2:1
Burkitt lymphomas	3	28 (5-72)	1:2
Mantle cell lymphomas	3	70(61-81)	1:2

[a]All cases *Chlamydia spp*. negative.
[b]Polyclonal follicular hyperplasias with lympho-epithelial lesions, not fulfilling MZL criteria.

Interestingly, three out of 26 patients with sufficient clinical records had a history of a second (most probably unrelated) lymphoid neoplasm, including (a) one 74-year-old male patient who has been suffering from a primary bone lymphoma 20 years prior to the diagnosis of OA-MZL; (b) one 63-year-old female patient who had a history of EMZL of the stomach 10 years before the diagnosis of OA-MZL (at the time of OA-MZL being in complete endoscopic, radiologic, and histopathologic remission in the stomach and presenting with unilateral right conjunctival tumor); and (c) one 58-year-old male patient who developed an IgA+ plasma cell myeloma 6 years after the diagnosis of OA-MZL (the latter being at that time in complete remission).

3.2 | Light chain expression, clonality, MALT1 locus aberrations, and Chlamydia-infection

Out of the 34 OA-MZL, 21 (62%) showed immunoglobulin light chain expression; of these 15 were κ-clonal (two of them tested showed also clonal *IGH* rearrangements), while six were λ-clonal; two additional cases tested showed a clonal *IGH* rearrangement without expression of light chains. Importantly, out of the five OA-MZL without detectable point mutations, four were clonal on light chain testing (two showed also a clonal *IGH* rearrangement) and the one without light chain expression displayed a clonal *IGH* rearrangement. Light chain expressing cases displayed mean 1.8 ± 1.7 (median 1) mutations, while nonexpressing cases had 3.0 ± 2.2 (median 3) mutations ($P^{\text{Mann-Whitney}} = .043$).

Informative FISH results for the *MALT1* locus were obtained in 25 OA-MZL cases. No *MATL1* rearrangements suggesting a *t*(14;18) or *t*(11;18) were detected, but 10 cases (40%) showed *MALT1* gains (ie, greater than or equal to three distinct 18q21 signals). Cases with *MALT1* gains displayed mean 1.7 ± 1.3 (median 2) mutations, while cases with two *MALT1* signals had 2.4 ± 1.7 (median 2.5) mutations ($P^{\text{Mann-Whitney}} = .179$).

All cases except for one DLBCL, for which PCR failed because of technical problems, were negative for *Chlamydia spp*.

3.3 | Mutational landscape of OA-MZL

HTS data (Table S1) are deposited in NCBI SRA (accession number SUB5214285). The most commonly mutated gene of our OA-MZL cohort was *TNFAIP3* (10 of 34, 29%). Mutations of this gene were exclusive to OA-MZL and displayed a statistically significant discriminatory power between OA-MZL and the other studied lymphomas in/of this anatomic region ($P^{\text{Fisher's}} = .008$), which was also corroborated by the unsupervised clustering analysis (Figure S2). Altogether, 22 out of 34 patients (65%) harbored mutations of NF-κB compounds. Mutations of *TNFAIP3*, *BCL10*, *MYD88*, *ATM*, *BRAF* (D594N), or *NFKBIE* (18 patients, 53%) were mutually exclusive (Figure 2). In contrast, mutations of *IRF8*, *TNFRSF14*, and *KLHL6* were not exclusive. Mutations of *TBL1XR1* were mutually exclusive in two patients and promiscuous with other NF-κB compound mutations in four patients.

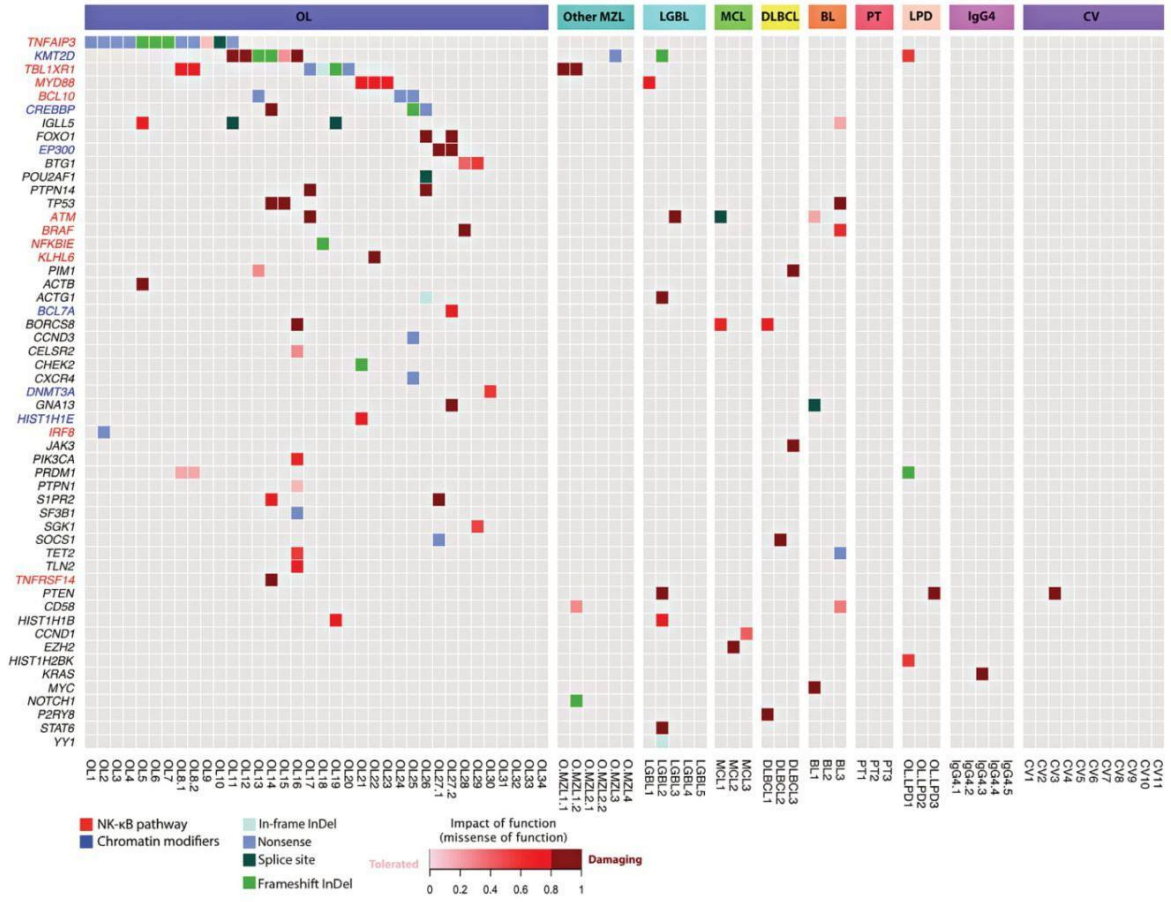

FIGURE 2 Heat map plot of the somatic mutations in the studied entities showing all nonsynonymous mutations detected by targeted high-throughput sequencing. Each column represents a primary tumor grouped according to the assigned subtype; where applicable primaries and relapses are grouped together and designated as, eg, OL8.1 and OL8.2, respectively. Each row represents a gene ordered top-down in decreasing order of detection frequency in ocular adnexal marginal zone B-cell lymphomas (OL). When multiple mutations are present in the same gene, the most damaging mutation is displayed. BL, Burkitt lymphoma; CV, chronic conjunctivitis; DLBCL, diffuse large B-cell lymphoma; LGBL, "low grade" B-cell lymphoma; LPD, lymphoproliferative disease; MCL, mantle cell lymphoma; MZL, marginal zone B-cell lymphoma; PT, pseudotumor

Finally, two patients displayed *MALT1* locus gains without detectable mutations. Interestingly, *BCL10* mutant cases did not display *MALT1* locus gains, which was not the case in other NK-κB compound mutants.

Thirteen patients (38%) had, to a great part, mutually exclusive mutations of genes encoding for chromatin modifiers: *KMT2D*, *CREBBP*, *BCL7A*, *DNMT3A*, *EP300*, and *HIST1H1E*; *KMT2D* and *CREBBP*. Interestingly, only four patients (12%) harbored synchronous mutations of NK-κB compounds and of chromatin modifiers, two in combination with *MYD88* and each one is in combination with *BCL10* and *TNFRSF14* mutations. Thus, 80% of OA-MZL display rather non-overlapping mutations of either NK-κB compounds or chromatin modifiers. There were only three OA-MZL neither harboring mutations nor *MALT1* locus gains, and all three displayed clonal *IGH* rearrangements.

The total number of mutations, presence of greater than or equal to three mutations and mutational status of genes mutated in at least three OA-MZL cases were analyzed with regard to PFS. Only presence of *BCL10* mutations was of possible prognostic importance since all three mutant patients relapsed (median PFS 41 months, 95% CI, 20-62), while there were only two relapses in the 21 wild type instances (median PFS not reached, Figure S3).

3.4 | Mutational profile of OA-MZL in comparison with other lymphomas, lymphoproliferative, and reactive lesions of the same anatomic region

With a median of two mutations/case (mean 2.4, range 0-9), OA-MZL displayed more mutations than reactive lesions and more than other

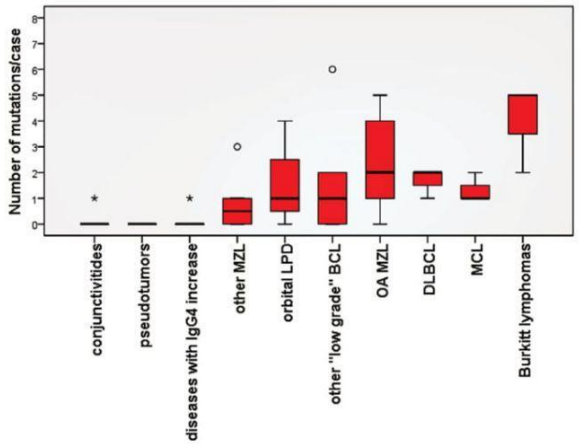

FIGURE 3 Box and whisker plot of the mutational load of the studied entities; the thick black lines within the boxes represent medians; the o and * represent outliers, namely, one chronic conjunctivitis case with a *PTEN* mutation, one *KRAS* mutant juvenile xanthogranuloma that presented as an orbital disease with increased IgG4+ plasma cells, one non-ocular marginal zone B-cell lymphoma (MZL) that relapsed in the ocular adnexa (OA), and one follicular lymphoma (within the group of other "low grade" B-cell lymphomas [BCL]); DLBCL, diffuse large B-cell lymphoma; LPD, lymphoproliferative diseases; MCL, mantle cell lymphoma

nonblastoid B-cell lymphomas in this anatomic region. BL showed the highest mutational load ($P^{Kruskal\text{-}Wallis}$ = .00052; Figure 3).

TNFAIP3 mutations were exclusive to OA-MZL. The highest mutational load among "low grade" B-cell lymphomas (six per case) were observed in the single FL included. One plasmacytoid differentiated MCL showed a *CCND1* mutation on top of the t(11;14) (Figure 2).

A pathogenic nongermline *PTEN* F278 L missense mutation, reported in endometrium carcinoma (https://cancer.sanger.ac.uk/cosmic/mutation/overview?id=96858635), with a variant allelic frequency (VAF) of 19.3% was discovered in one out of 11 (9%) conjunctivitis patients (Figure 2). A *PTEN* S360G missense mutation, referred to as variant of unknown significance (https://www.ncbi.nlm.nih.gov/clinvar/26063487/), was noticed in one case of a severe chronic lympho-follicular conjunctivitis with lympho-epithelial lesions, classified as "OA lymphoid hyperplasia" in a 24-year-old male patient suffering from polyallergy (Figure 2). Both *PTEN* mutant cases underwent reassessment, which disfavored malignant process (polyclonal and free of disease for at least 9 y lasting observational period).

Two additional reactive cases with detectable mutations deserve special attention. One represented a plasma cell-rich, lympho-follicular hyperplasia of the orbit with lympho-epithelial lesions, not fulfilling MZL criteria, classified as "OA lymphoid hyperplasia" in a 47-year-old African female patient, displaying four mutations in three genes (*KMT2D*, *PRDM1*, and *HIST1H2BK* with VAF of 31.4% to 45.7%). On the basis of the different ethnical background of the patient, the absence any reporting on these variants in cancer and their VAF, they were considered of unknown significance/potential germline origin. The case was reassessed and turned out representing severe ulcerating muco-cutaneous leishmaniosis with polyclonal B-cells and plasma cells (Figure 4A).

The second case of an 80-year-old female patient was the only one within the group of diseases with IgG4 increase that showed a pathogenic (activating) *KRAS* G12R mutation with a VAF of 11%. The patient presented with a sclerosing orbital lesion with substantial amounts of plasma cells and more than 40% IgG4+ plasma cells, which allowed a histological diagnosis of probable IgG4-associated fibro-sclerosing disease. Upon reassessment, in step sections nests of foamy histiocytes (making up to 20% of the overall cellularity), and occasional Touton giant cells were observable that forced reconsideration of the initial diagnosis; the changes being integratively consistent with a (juvenile) xanthogranuloma (Figure 4B). Importantly, on the basis of the initial diagnosis, the patient has been treated for half a year with prednisone, which was accompanied by gradual improvement. Upon diagnosis revision, two treatment attempts with the MEK inhibitors trametinib and cobimetinib were performed but had to be promptly tapered because of severe oral aphthosis. Despite short duration, this treatment led to an ongoing radiologic remission.

3.5 | Genetic profiles of relapses

Altogether, four paired primary tumors and their recurrences were available to study clonal evolution. One MZL of the breast spreading to the orbit 15 years later displayed no mutations. Of the three remaining cases (Figure 5), the shortest interval was observed in a nodal MZL of the neck that recurred 15 months later (after chemo-immunotherapy) in the orbit. The other two were OA-MZL that recurred 3 (under a watchful waiting strategy after initial complete surgical removal) and 5 years (after chemo-immunotherapy), respectively, at the primary sites. Interestingly, the former case showed a linear mutational evolution, bearing one mutation at initial presentation (*TBL1XR1*), which was retained and accompanied by additional *HIST1H1C*, *CD58*, and *NOTCH1* mutations on relapse. The second case showed a divergent evolution with four mutations of three genes at initial presentation (*TNFAIP3*, *PDRM1*, and *TBL1XR1*), of which—without the pressure of therapy—only one of the *TNFAIP3* mutations and the *TBL1XR1* mutation were retained. The third case also displayed a divergent evolution with a "trunk" *EP300* mutation, which was accompanied by *BCL7A*, *GNA13*, and *FOXO1* mutations at initial presentation, and two *SOCS1* mutations and a *S1PR2* mutation at the relapse.

4 | DISCUSSION

The aim of our study was to characterize the genetic landscape of OA-MZL in comparison with other types of lymphomas as well as reactive lesions occurring in the same anatomic region. Our results

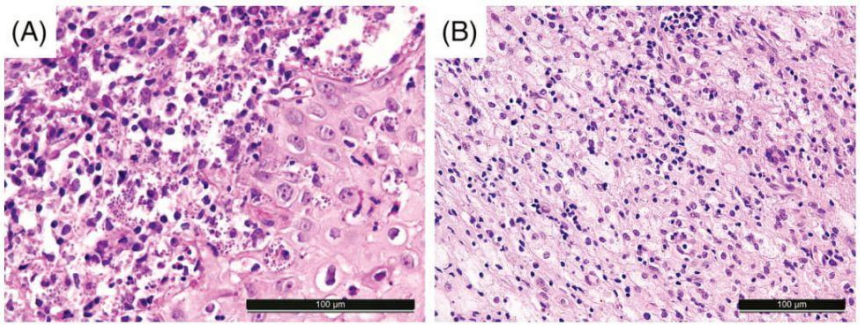

FIGURE 4 A. Histopathology of case OL.LPD1 (ocular adnexal lymphoproliferative disease) that bore three mutations and turned our being—upon revision—a muco-cutaneous Leishmaniosis containing easily identifiable Donovan bodies; original magnification 400×, H&E stain.
B. Histopathology of case IgG4.3 that bore a characteristic *KRAS* G12R mutation and turned our being—upon revision—a juvenile xanthogranuloma containing in addition to groups of IgG4+ plasma cells (not shown), foamy cells and Touton giant cells; original magnification 280×, H&E stain

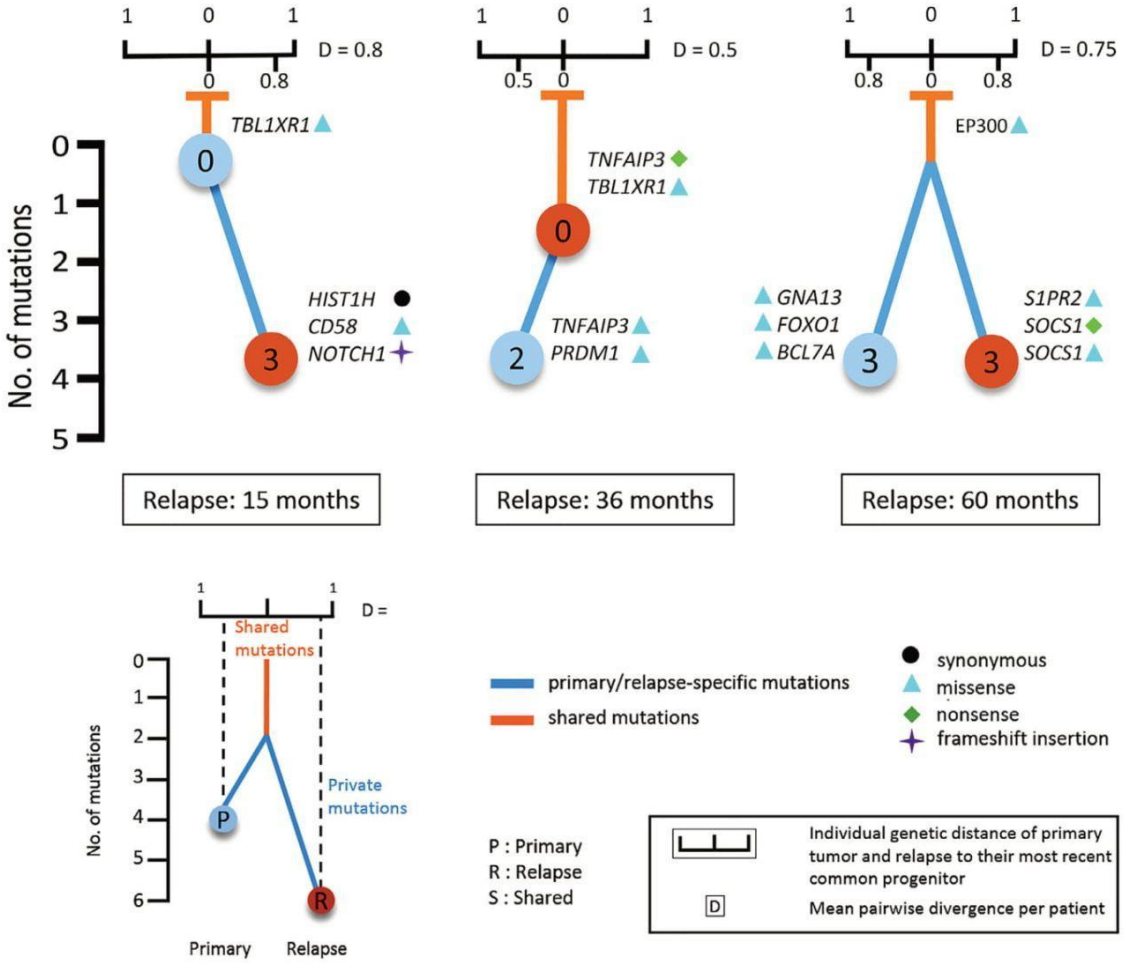

FIGURE 5 Genetic evolution patterns in relapsing ocular adnexal lymphomas. Genetic distances were calculated by the mean pairwise divergence (D) of all mutations between the primary tumor and its relapse. This divergence is scaled between 0 and 1. Thy y-axis displays the cumulative amount of mutations in tumor. The distance of the primary tumor (P, blue) and relapse (R, red) from the trunk (orange) on the x-axis represents the individual genetic dissimilarity to the assumptive common progenitor

partially confirm, sharpen, and considerably extend previous knowledge,[8,9,13-15] and suggest that at least in the area of Basel, OA-MZL are not linked to *Chlamydia spp*. infection, reflecting the considerable geographic variation in that respect.[11,19] The latter finding is supported by our patients' clinical history, showing best treatment responses to local radiotherapy but not to doxycycline. An important and new clinico-pathologic observation, yet on a limited number of cases (N = 26) with the possibility of sample bias, was the rather high incidence of metachronous second lymphoid neoplasms in 10% of the patients, which has been documented for gastric MZL, but not for other MZL.[25]

We confirm, on the basis of observations of a smaller subgroup (N = 25) of study cases with obtainable FISH results, previous observations that OA-MZL do not bear *MALT1* rearrangements.[7] Together with the low frequency and lack of other specific structural chromosomal aberrations in OA-MZL,[2,7,8] this suggests that FISH testing may be of low diagnostic yield.

Our mutational frequencies largely overlap with previous observations,[13,15] but differ from others.[8,14] These discrepancies could be related to population variations and sample size biases that apply to almost all OA-MZL studies including ours, but are most probably linked to differences in the gene panel compositions. For example, one study[14] applied a panel designed for solid tumors and, consequentially, failed to uncover *TNFAIP3* as the most commonly mutant gene in OA-MZL. We aimed to minimize such flaws of targeted sequencing by choosing the until now most comprehensive target enrichment panel covering 146 different genes that was specifically designed for MZL.[24]

Confirming results of other studies[8,13,15] and very recent observations,[9,26] the most frequently (29%) mutated gene (all nonsense or frameshift mutations leading to loss of protein expression) in our OA-MZL collective was *TNFAIP3*, which encodes for A20—a negative regulator of the NF-κB pathway.[27] *TNFAIP3* mutations seem to be quite specific for OA-MZL as exemplified here (no other lymphoma type of this anatomic region displayed *TNFAIP3* mutations) and in a large study of 179 cases, including 20 OA-MZL, in which 32% of the latter bore this mutation compared with only 4% MZL cases of other origin.[26] This specificity confers *TNFAIP3* mutations a diagnostic importance.

Activation of the NF-κB pathway is nearly ubiquitous in OA-MZL with approximately 70% of cases displaying genetic lesions linked to this pathway, as suggested by our and others' results.[8,13,15] A particular new aspect of our study, admittedly substantiated in the study subcohort of NF-κB mutants (N = 22), is the rather "complementing-each-other character" of NF-κB pathway compound mutations, ie, mutation of either *TNFAIP3*, *BCL10*, *MYD88*, *ATM*, *BRAF*, or *NFKBIE* being mutually exclusive.

Although based on a few mutant cases (N = 3), our results point towards the prognostic importance of *BCL10* mutations in OA-MZL. The prognostic significance of BCL10 protein expression has already been noticed,[28] but to our knowledge the present study is the first to suggest a prognostic role of *BCL10* mutations.

An additional relevant observation in the smaller subcohort of respectively mutant instances (N = 13) is the occurrence of nearly mutually exclusive mutations of *KMT2D*, *CREBBP*, *BCL7A*, *DNMT3A*, *EP300*, and *HIST1H1E*-genes encoding for chromatin modifiers in OA-MZL. Only 12% of patients harbored synchronous mutations of NK-κB compounds and of chromatin modifiers and 21% displayed mutations of chromatin modifiers that did not overlap with mutations of NK-κB compounds. One exception to this reciprocity seems to be *TBL1XR1*, the second most commonly mutant gene in OA-MZL, its mutant form being suggested to generally affect both NK-κB[15] and chromatin modification influencing *HDAC3*.[29]

On the basis of our data of reactive lesions and other lymphomas of the orbit, and on previous studies,[14] a conclusion of particular diagnostic importance can be drawn, namely, that OA lymphoid lesions bearing NF-κB compound mutations and/or mutations of acetyltransferase encoding genes, highly likely represent lymphomas. This seems not to apply for *PTEN*, *KMT2D*, *PRDM1*, and *HIST1H2BK* mutations that can also be observed in reactive lesions.

Importantly, mutations of *MYD88*, *BRAF*, and *CREBBP*, and probably *TBL1XR1*, may be actionable, and clinical studies for specific pharmacologic interference are currently been performed in lymphomas.[30-32]

Compared with other studies,[8] we were not able to detect *NOTCH1/2* mutations in OA-MZL. For *NOTCH1*, this might be because of sample size bias of ours since our targeted panel covers all mutant exons of *NOTCH1*. For *NOTCH2*, incomplete coverage can be an additional reason since our panel covers only the most commonly mutant exon 34, and mutations in other exons might have been missed.

Our study allowed to investigate by means of HTS the genetic evolutionary patterns of MZL relapses and suggest, with the caveats of single patient observations, that they basically recapitulate what has been well documented in FL and DLBCL: either (a) linear evolution with early relapse that gained, in our concrete case, an immune escape (*CD58*) and a *NOTCH1* mutation, or (b) divergent evolution with later relapse and single or a few common (trunk) mutation(s) and several specific mutations that are either observed at presentation or at relapse as observable in two study cases. Interestingly, one of the latter cases displayed a mutually exclusive activating mutation of *GNA13* at presentation and an inactivating mutation of *S1PR2* at relapse, both known to have a complementary net effect on downstream activation of the S1PR2/Gα13/AKT signaling axis,[33] and pointing towards the importance of this signaling cascade for lymphomagenesis.

CONFLICT OF INTEREST

The authors have no potential conflicting interest.

ETHICAL BACKGROUND

The study was performed according to the regulations of the safety laws of the canton Basel and the Swiss Federal Act on Research involving Human Beings, and handling with probes was approved by the ethics committee of Northwestern Switzerland (EKNZ 2014-252).

ORCID

Alexandar Tzankov https://orcid.org/0000-0002-1100-3819

REFERENCES

1. Kamal S, Kaliki S. Ocular adnexal lymphoma: clinical presentation, diagnosis, treatment and prognosis. *J Mol Biomark Diagn*. 2016;8:312. https://doi.org/10.4172/2155-9929.1000312.
2. McKelvie PA. Ocular adnexal lymphomas: a review. *Adv Anat Pathol*. 2010;17:251-261. https://doi.org/10.1097/PAP.0b013e3181e4abdb.
3. Moslehi R, Devesa SS, Schairer C, Fraumeni JF. Rapidly increasing incidence of ocular non-Hodgkin lymphoma. *J Natl Cancer Inst*. 2006;98:936-939. https://doi.org/10.1093/jnci/djj248.
4. Sharma T, Kamath M. Diagnosis and management of orbital lymphoma. Eye Net Magazine of the American Academy of Ophthalmology. https://www.aao.org/eyenet/article/diagnosis-management-of-orbital-lymphoma. Published 2015. Accessed August 8, 2019
5. Ponzoni M, Govi S, Licata G, M, et al. A reappraisal of the diagnostic and therapeutic management of uncommon histologies of primary ocular adnexal lymphoma. *Oncologist* 2013;18:876–84. https://doi.org/10.1634/theoncologist.2012-0425
6. Cohen VML. Treatment options for ocular adnexal lymphoma (OAL). *Clin Ophthalmol*. 2009;3:689-692. https://doi.org/10.2147/OPTH.S5828.
7. Bertoni F, Rossi D, Zucca E. Recent advances in understanding the biology of marginal zone lymphoma. *F1000Research*. 2018;7:406. https://doi.org/10.12688/f1000research.13826.1.
8. Johansson P, Klein-Hitpass L, Grabellus F, et al. Recurrent mutations in NF-κB pathway components, *KMT2D*, and *NOTCH1/2* in ocular adnexal MALT-type marginal zone lymphomas. *Oncotarget*. 2016;7:62627-62639. https://doi.org/10.18632/oncotarget.11548.
9. Cascione L, Rinaldi A, Bruscaggin A, et al. Novel insights into the genetics and epigenetics of MALT lymphoma unveiled by next generation sequencing analyses. *Haematologica* 2019;104:e558-e561. https://doi.org/10.3324/haematol.2018.214957
10. Stefanovic A, Lossos IS. Extranodal marginal zone lymphoma of the ocular adnexa. *Blood*. 2009;114:501-510. https://doi.org/10.1182/blood-2008-12-195453.
11. Takada S, Yoshino T, Taniwaki M, et al. Involvement of the chromosomal translocation t(11;18) in some mucosa-associated lymphoid tissue lymphomas and diffuse large B-cell lymphomas of the ocular adnexa evidence from multiplex reverse transcriptase-polymerase chain reaction and fluorescence in situ hybridization on using formalin-fixed, paraffin-embedded specimens. *Mod Pathol*. 2003;16:445-452. https://doi.org/10.1097/01.MP.0000067421.92575.6E.
12. Schiby G, Polak-Charcon S, Mardoukh C, et al. Orbital marginal zone lymphomas: an immunohistochemical, polymerase chain reaction, and fluorescence in situ hybridization study. *Hum Pathol*. 2007;38:435-442. https://doi.org/10.1016/j.humpath.2006.09.007.
13. Yan Q, Wang M, Moody S, et al. Distinct involvement of NF-κB regulators by somatic mutation in ocular adnexal MALT lymphoma. *Br J Haematol*. 2013;160:851-854. https://doi.org/10.1111/bjh.12162.
14. Cani AK, Soliman M, Hovelson DH, et al. Comprehensive genomic profiling of orbital and ocular adnexal lymphomas identifies frequent alterations in MYD88 and chromatin modifiers: new routes to targeted therapies. *Mod Pathol*. 2016;29:685-697. https://doi.org/10.1038/modpathol.2016.79.
15. Jung H, Yoo HY, Ho Lee S, et al. The mutational landscape of ocular marginal zone lymphoma identifies frequent alterations in TNFAIP3 followed by mutations in TBL1XR1 and CREBBP. *Oncotarget*. 2017;8:17038-17049. https://doi.org/10.18632/oncotarget.14928.
16. Novak U, Rinaldi A, Kwee I, et al. The NF-κB negative regulator TNFAIP3 (A20) is inactivated by somatic mutations and genomic deletions in marginal zone lymphomas. *Blood*. 2009;113:4918-4921. https://doi.org/10.1182/blood-2008-08-174110.
17. Honma K, Tsuzuki S, Nakagawa M, Karnan S, Aizawa Y. TNFAIP3 is the target gene of chromosome band 6q23.3-q24.1 loss in ocular adnexal marginal zone B cell lymphoma. *Genes Chromosomes Cancer*. 2008;47:1-7. https://doi.org/10.1002/gcc.20499.
18. Chanudet E, Huang Y, Ichimura K, et al. A20 is targeted by promoter methylation, deletion and inactivating mutation in MALT lymphoma. *Leukemia*. 2010;24:483-487. https://doi.org/10.1038/leu.2009.234.
19. Chanudet E, Zhou Y, Bacon CM, et al. *Chlamydia psittaci* is variably associated with ocular adnexal MALT lymphoma in different geographical regions. *J Pathol*. 2006;209:344-351. https://doi.org/10.1002/path.1984.
20. Liu YC, Ohyashiki JH, Ito Y, Iwaya KI, Serizawa H, Mukai K, Goto H, Usui M, Ohyashiki K Chlamydia psittaci in ocular adnexal lymphoma: Japanese experience. *Leuk Res* 2006;30:1587–1589. https://doi.org/10.1016/J.LEUKRES.2006.01.015.
21. Mollerup S, Mikkelsen LH, Hansen AJ, Heegaard S. High-throughput sequencing reveals no viral pathogens in eight cases of ocular adnexal extranodal marginal zone B-cell lymphoma. *Exp Eye Res*. 2019;185:107677. https://doi.org/10.1016/J.EXER.2019.05.017.
22. van Beers EH, Joosse SA, Ligtenberg MJ, et al. A multiplex PCR predictor for aCGH success of FFPE samples. *Br J Cancer*. 2006;94:333-337. https://doi.org/10.1038/sj.bjc.6602889.
23. Menter T, Dickenmann M, Juskevicius D, Steiger J, Dirnhofer S, Tzankov A. Comprehensive phenotypic characterization of PTLD reveals potential reliance on EBV or NF-κB signalling instead of B-cell receptor signalling. *Hematol Oncol*. 2017;35:187-197. https://doi.org/10.1002/hon.2280.
24. Pillonel V, Juskevicius D, Ng CKY, et al. High-throughput sequencing of nodal marginal zone lymphomas identifies recurrent BRAF mutations. *Leukemia*. 2018;32:2412-2426. https://doi.org/10.1038/s41375-018-0082-4.
25. Tajika M, Matsuo K, Ito H, et al. Risk of second malignancies in patients with gastric marginal zone lymphomas of mucosa associate lymphoid tissue (MALT). *J Gastroenterol*. 2014;49:843-852. https://doi.org/10.1007/s00535-013-0844-8.
26. Moody S, Escudero-Ibarz L, Wang M, et al. Significant association between TNFAIP3 inactivation and biased immunoglobulin heavy chain variable region 4-34 usage in mucosa-associated lymphoid tissue lymphoma. *J Pathol*. 2017;243:3-8. https://doi.org/10.1002/path.4933.
27. Lee EG, Boone DL, Chai S, et al. Failure to regulate TNF-induced NF-κB and cell death responses in A20-deficient mice. *Science*. 2000;289:2350-2354. https://doi.org/10.1126/science.289.5488.2350.
28. Franco R, Camacho FI, Caleo A, et al. Nuclear bcl10 expression characterizes a group of ocular adnexa MALT lymphomas with shorter failure-free survival. *Mod Pathol*. 2006;19:1055-1067. https://doi.org/10.1038/modpathol.3800597.
29. Li JY, Daniels G, Wang J, Zhang X. TBL1XR1 in physiological and pathological states. *Am J Clin Exp Urol* 2015;3:13–23
30. Hiebert SW. Hdac3 as a therapeutic target in Bcl6-dependent lymphoma. http://grantome.com/grant/NIH/R01-CA164605-03. Accessed May 23, 2019
31. Vemurafenib in Treating Patients With Relapsed or Refractory Advanced Solid Tumors, Non-Hodgkin Lymphoma, or Histiocytic Disorders With BRAF V600 Mutations (A Pediatric MATCH Treatment Trial). National Cancer Institute. https://clinicaltrials.gov/ct2/show/NCT03220035. Accessed May 23, 2019
32. Noy A, De Vos S, Thieblemont C, et al. Targeting Bruton tyrosine kinase with ibrutinib in relapsed/refractory marginal zone lymphoma. *Blood*. 2017;129:2224-2232. https://doi.org/10.1182/blood-2016-10-747345.

33. Stelling A, Hashwah H, Bertram K, Manz MG, Tzankov A, Müller A. The tumor suppressive TGF-b/SMAD1/S1PR2 signaling axis is recurrently inactivated in diffuse large B-cell lymphoma. *Blood*. 2018;131:2235-2246. https://doi.org/10.1182/blood-2017-10-810630.

SUPPORTING INFORMATION

Additional supporting information may be found online in the Supporting Information section at the end of this article.

How to cite this article: Vela V, Juskevicius D, Gerlach MM, et al. High throughput sequencing reveals high specificity of *TNFAIP3* mutations in ocular adnexal marginal zone B-cell lymphomas. *Hematological Oncology*. 2020;38:284–292. https://doi.org/10.1002/hon.2718

3.3 Deciphering the genetic landscape of pulmonary lymphomas

Visar Vela, Darius Juskevicius, Spasenija Savic Prince, Gieri Cathomas, Susanne Dertinger, Joachim Diebold, Lukas Bubendorf, Milo Horcic, Gad Singer, Andreas Zettl, Stefan Dirnhofer, Alexandar Tzankov & Thomas Menter

-Research Article-

Published in *Modern Pathology*, 2020

Modern Pathology
https://doi.org/10.1038/s41379-020-00660-2

ARTICLE

Deciphering the genetic landscape of pulmonary lymphomas

Visar Vela[1] · Darius Juskevicius[1] · Spasenija Savic Prince[1] · Gieri Cathomas[2] · Susanne Dertinger[3] · Joachim Diebold[4] · Lukas Bubendorf[1] · Milo Horcic[5] · Gad Singer[6] · Andreas Zettl[7] · Stefan Dirnhofer[1] · Alexandar Tzankov[1] · Thomas Menter[1]

Received: 7 July 2020 / Revised: 7 August 2020 / Accepted: 7 August 2020

Abstract

Pulmonary lymphoid malignancies comprise various entities, 80% of them are pulmonary marginal zone B-cell lymphomas (PMZL). So far, little is known about point mutations in primary pulmonary lymphomas. We characterized the genetic landscape of primary pulmonary lymphomas using a customized high-throughput sequencing gene panel covering 146 genes. Our cohort consisted of 28 PMZL, 14 primary diffuse large B-cell lymphomas (DLBCL) of the lung, 7 lymphomatoid granulomatoses (LyG), 5 mature small B-cell lymphomas and 16 cases of reactive lymphoid lesions. Mutations were detected in 22/28 evaluable PMZL (median 2 mutation/case); 14/14 DLBCL (median 3 mutations/case) and 4/7 LyG (1 mutation/case). PMZL showed higher prevalence for mutations in chromatin modifier-encoding genes (44% of mutant genes), while mutations in genes related to the NF-κB pathway were less common (24% of observed mutations). There was little overlap between mutations in PMZL and DLBCL. *MALT1* rearrangements were more prevalent in PMZL than *BCL10* aberrations, and both were absent in DLBCL. LyG were devoid of gene mutations associated with immune escape. The mutational landscape of PMZL differs from that of extranodal MZL of other locations and also from splenic MZL. Their landscape resembles more that of nodal MZL, which also show a predominance of mutations of chromatin modifiers. The different mutational composition of pulmonary DLBCL compared to PMZL suggests that the former probably do not present transformations. DLBCL bear more mutations/case and immune escape gene mutations compared to LyG, suggesting that EBV infection in LyG may substitute for mutations.

Introduction

Primary lymphomas of the lung are very rare, accounting for only 0.4% of all lymphomas [1]. Pulmonary marginal zone lymphoma (PMZL), derived from bronchus-mucosa associated lymphatic tissue (BALT/MALT), is the most common type (80% of cases), followed by diffuse large B-cell lymphoma (DLBCL) and lymphomatoid granulomatosis (LyG), an Epstein-Barr virus (EBV)-related disorder [2].

PMZL belongs to the group of extranodal marginal zone lymphomas (EMZL). These EMZL are thought to originate from post-germinal center B-cells, which are located in the external part of secondary follicles, in the so-called marginal zone [2, 3]. PMZL presents mostly in the sixth decade of life without sex predilection. In more than half of the cases, it is an incidental finding and patients do not show any symptoms of lymphoma involvement; however, up to 15% of patients suffer from concurrent autoimmune diseases [4]. Generalized disease involving other organs or the bone marrow is seen in about 25% of PMZL patients [5].

These authors contributed equally: Alexandar Tzankov, Thomas Menter

Supplementary information The online version of this article (https://doi.org/10.1038/s41379-020-00660-2) contains supplementary material, which is available to authorized users.

✉ Alexandar Tzankov
alexandar.tzankov@usb.ch

1 Pathology, Institute of Medical Genetics and Pathology, University Hospital Basel, University of Basel, Basel, Switzerland

2 Institute of Pathology, Cantonal Hospital Baselland, Liestal, Switzerland

3 Institute of Pathology, Hospital Feldkirch, Feldkirch, Austria

4 Institute of Pathology, Cantonal Hospital Lucerne, Lucerne, Switzerland

5 Institute for Histologic und Cytologic Diagnostics AG, Aarau, Switzerland

6 Institute of Pathology, Cantonal Hospital Baden, Baden, Switzerland

7 Institute of Pathology, Viollier AG, Allschwil, Switzerland

Table 1 General characteristics of the study collective.

Entity	*N*	Age, median (range)	M: F	Mutational load, median; mean (range)
PMZL	28	72 (25–85)	14: 14	2; 1.7 (0–5)
Lymphomatoid granulomatosis grade 2 ($n = 2$) and grade 3 ($n = 5$)	7	75 (56–94)	6: 1	1; 1.1 (0–3)
Diffuse large B-cell lymphomas	14	80 (65–96)	10: 4	3; 3.8 (1–7)
Mature small B-cell lymphomas	5	76 (42–100)	5: 0	2; 2 (1–3)
-CLL/SLL	2	70 (42–99)		2; 2 (1–3)
-MCL	2	88 (76–100)		2; 2
-FL	1	69		2
Reactive lesions	16	68 (71–95)	10: 6	0; 0.06 (0–1)
-follicular bronchitis	12	67 (56–91)	7: 5	0; 0.08 (0–1)
-lymphocytic interstitial pneumonia	2	89 (81–85)	2: 0	0
-nodular lymphoid hyperplasia	2	53 (21–84)	1: 1	0

EMZL occur most frequently in the stomach (70%), followed by the lung (14%), ocular adnexa (12%), skin (9%) thyroid (4%), and small intestine (1%) [6, 7]. There is evidence that EMZL are associated with chronic antigenic stimulation, either by autoantigens or by foreign pathogens, leading to the accumulation of MALT in respective organs [8]. The mutational landscape of MZL of different origin is variegated: ocular adnexal [9–12], gastric [13], thyroid MZL [14, 15], as well as nodal MZL (NMZL) [16, 17] commonly display somatic mutations in genes encoding for compounds of the NF-κB pathway, chromatin modifier-encoding genes and genes related to the NOTCH pathway. Splenic MZL display mainly *KLF2* mutations [18]. In ocular adnexal MZL, *TNFAIP3* mutations affecting the NF-κB pathway are most prevalent [12]. Cutaneous MZL show recurrent *FAS* alterations [19].

In contrast, PMZL more commonly display structural and/or numeric chromosomal aberrations. Previous FISH studies revealed frequent t(11;18)(q21;q21) and t(14;18)(q32;q21) involving *MALT1*, and rarer t(1;14)(p22;q32) and t(3;14)(p14.1;q32) involving *BCL10* and *FOXP1*, respectively, as well as trisomies 3 and 18 [20–22]. The mutational landscape of PMZL has not been studied at a larger scale so far. Although mutations—in descending order of frequency—of genes encoding for chromatin modifiers (*CREBBP, TET2*), members of the NOTCH- (*TLBXR1, NOTCH1*) and NF-κB signaling pathways (*TNFAIP3, CARD11*) have been previously detected by two research groups [14, 15], the mutational background of other primary lymphomas of the lung has not been addressed yet.

In this study, we aimed to expand the knowledge on the genetic landscape of PMZL as well as to comparatively analyze other lymphomas involving the lungs. We also investigated reactive lesions such as follicular bronchitis and lymphocytic interstitial pneumonia in order to see whether they can qualify as precursors to PMZL.

Materials and methods

Patients

Our study included 70 formalin-fixed, paraffin-embedded (FFPE) tissue samples of different lymphoproliferative disorders of the lung (Tables 1 and S1). Cases were provided by the departments of pathology of the contributing authors and were collected between 2005 and 2019. All cases were reviewed, and diagnosis was verified by TM and AT. The study was performed according to the safety laws of canton Basel and handling was approved by the ethics committee of Northwestern Switzerland (EKNZ 2014–252).

DNA extraction

Genomic DNA was obtained from the samples containing a tumor cell fraction or, in cases of reactive lymphoproliferations, lymphocyte fraction of more than 60% by conventional microscopy enforced by a CD20 staining, except for LyG cases grade 2, in which the region with the highest content of EBV-positive blasts was taken (Table S1). The extraction was performed according standard procedures with the GeneRead^{TM} DNA-FFPE-Kit (Qiagen, Hilden, Germany), which includes uracil–DNA–glycosylase (UDG) to cleave deaminated cytosines (uracils), reducing C → T or G → A mismatches that lead to common artifacts in FFPE material. Genomic DNA was quantified using a Qubit fluorometer (Invitrogen, Eugene, OR, USA).

Immunohistochemistry, fluorescence in situ hybridization, and immunoglobulin heavy chain-gene (*IGH*) clonality analysis

Immunohistochemistry and FISH were performed according to routine standard operation procedures and hybridization

procedures as described elsewhere [23]. For both *BCL10* and *MALT1*, a break apart probe was used (BCL10–20-OR, Empire Genomics, Williamsville, NY, USA; SPEC MALT1, ZytoVision, Bremerhaven, Germany). Only PMZL and DLBCL cases with available material underwent FISH examination. *IGH-BCL2* t(14;18)(q32;q21) and B-cell clonality (monoclonal *IGH* rearrangement) have been sought for by means of PCR and fragment analysis as described before [24].

Targeted HTS with custom lymphoma panel and data analysis

Targeted HTS was performed with the IonTorrent S5XL instrument; target enrichment for library preparation was done with an amplicon-based (AmpliSeq, IonTorrent, Thermo Fisher Scientific, Carlsbad, California) custom lymphoma panel (Table S2), which has been validated and used in earlier studies [12, 17]. All the samples included in this study had a mean coverage depth of ~1900× (range 1000×–6000×). Information for coverage depth, uniformity, and mapping quality are summarized in Table S3. Sequencing reads were aligned to the reference genome hg19 and the variant caller plug-in v5.10 from the IonTorrent software suite (Thermo Fisher Scientific) with default settings for somatic mutation detection was used to identify variants. Variants were annotated with the Single Sample Annotation Workflow of the Ion Reporter and dbNSFP database v3.2. Filtering was done according to criteria listed in Table S4; in short, variants with Phred-based quality lower or equal than 50, strand bias higher or equal to 0.75 were filtered out. Furthermore, we discarded variants below 5% in all entities except LyG (here the threshold was 1% due to scarcity of tumor cells) as potential artifacts and variants with variant allelic frequencies (VAF) higher than 95% as homozygous SNPs. Finally, variants found in assumingly healthy controls datasets (1000 genomes, ExAC) were excluded. Remaining mutations were manually reviewed, by using the IGV viewer to exclude remaining sequencing artifacts. Ensemble MetaLR score combining multiple functional prediction and conservation algorithms was used for *in silico* effect prediction of missense somatic point mutations [25]. Table S1 lists all somatic mutations identified in the study.

Statistical analysis

The distribution of entities according to sex was compared by the χ^2 test. To assess the significance of mutational burden differences between entities, we applied the Kruskal-Wallis test. To assess the discriminating value of the presence of distinct mutations between PMZL and other lymphomas in this anatomic region, the Fisher's exact test was used. Correlations were estimated with the Spearman rank correlation test; only strong correlations with $\rho > 0.3$ were further considered. All statistical calculations including descriptive data analysis were performed with MS Excel, SPSS.25, or R statistical package. Statistical significance threshold of $p < 0.05$ was assumed in all analyses. Whenever applicable, two-sided test were utilized.

Results

Clinico-pathological parameters

All clinical data are shown in Table 1. There were no significant differences regarding age and sex distribution between the different entities. Representative morphological images of PMZL, pulmonary DLBCL and LyG are shown in Fig. 1.

Mutational landscape of PMZL

PMZL had a median of 2 mutations per case (0–5) (Fig. 2; Table 2). The most commonly mutated gene was *KMT2D*

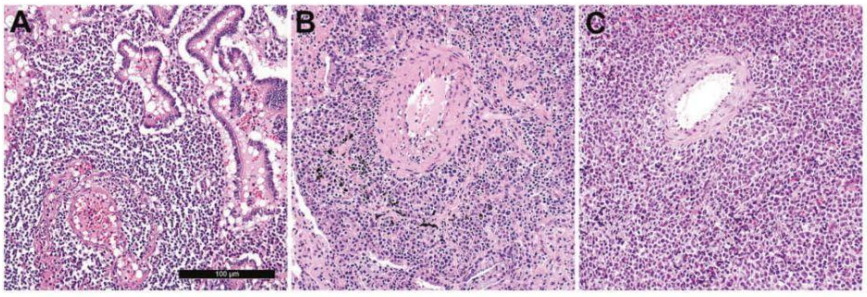

Fig. 1 Morphologic appearances of pulmonary lymphomas. a Pulmonary marginal zone B-cell lymphoma showing infiltrates of small lymphoid cells with lympho-epithelial lesion (central upper part) (hematoxylin and eosin stain (H&E), 200×); **b** Mixed angiocentric infiltrates of larger atypical and small reactive lymphoid cells, and plasma cells, characteristic of lymphomatoid granulomatosis (H&E, 200×). **c** Pulmonary infiltration by sheets of blastoid cells corresponding to diffuse large B-cell lymphoma of the lung (H&E, 200×).

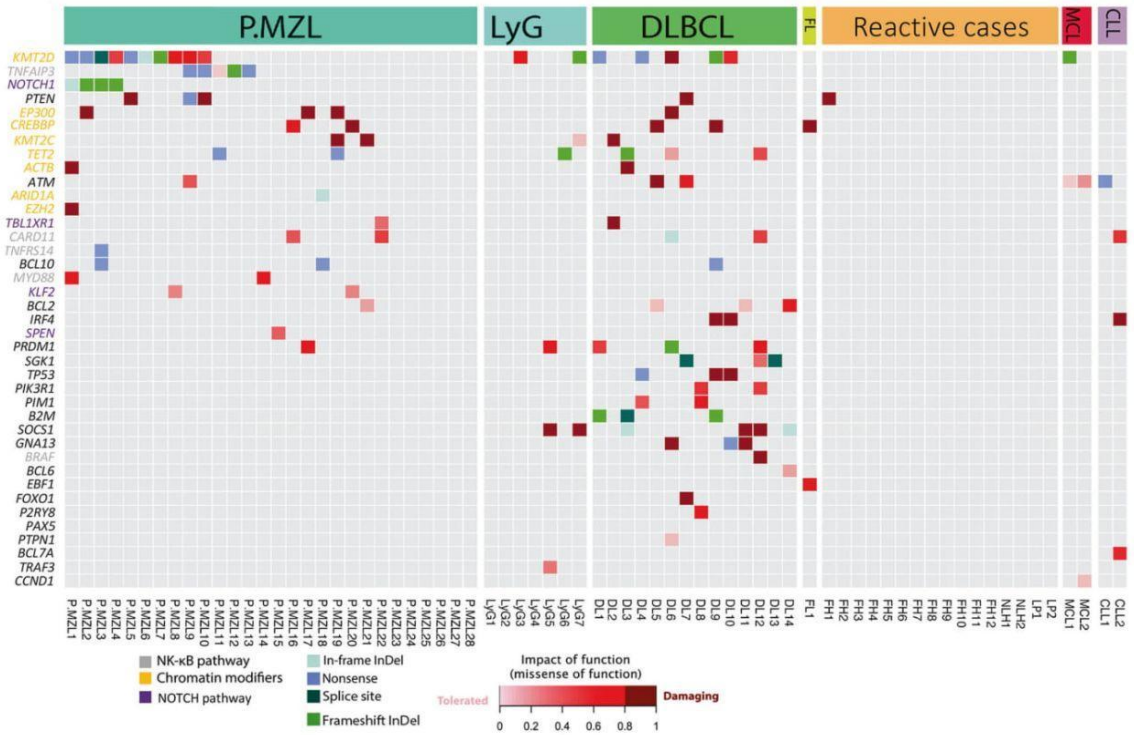

Fig. 2 Heatmap of the mutational analysis. Heatmap plot of somatic mutations in the studied entities showing all non-synonymous variants detected by targeted high-throughput sequencing. Each column represents a case grouped according to the assigned subtype. Each row represents a gene ordered top-down in decreasing order of detection frequency in pulmonary marginal zone B-cell lymphomas. When multiple mutations are present in the same gene, the most damaging mutation is displayed. PMZL pulmonary marginal zone lymphoma, LyG lymphomatoid granulomatosis, DLBCL diffuse large B-cell lymphoma, FL follicular lymphoma, FH follicular hyperplasia, NLH nodular lymphoid hyperplasia, LP lymphocytic interstitial pneumonia, MCL mantle cell lymphoma, CLL chronic lymphocytic leukemia.

(10/28, 36%). Importantly, in PMZL, mutations of other genes encoding for chromatin modifiers (*ARID1A, CREBBP, EP300, KMT2C, TET2*) were observable in nearly mutually exclusive manner to mutant *KMT2D* in additional 6 cases, thus altogether 16/28 (57%) displayed a mutant gene in this group of genes. Mutations of *TNFAIP3*, *NOTCH1, KLF2* and *SPEN* were exclusively seen in PMZL. These mutations as well as mutations of other genes encoding for NF-κB compounds (*BCL10, CARD11, MYD88, TNFRSF14*) were mutually exclusive. Accordingly, *BCL10, MYD88,* and *TNFRSF14* mutations were also mutually exclusive to *MALT1* and *BCL10* rearrangements (Supplementary Fig. 1). Finally, *NOTCH1* and its antagonists *SPEN* and *KLF2* (and *TBL1XR1*) were mutually exclusively mutated. The mutation load of PMZL positively correlated with the Ki67 proliferation rate analyzed by immunohistochemistry (Rho = 0.733, $p < 0.0001$; Supplementary Fig. 2). In comparison to the other studied B-cell lymphomas, mutations of either *TNFAIP3, NOTCH1, SPEN,* or *KLF2* (mutually complementary) were exclusive to PMZL ($p = 0.001$) and found in 12/28 cases.

PMZL and LyG significantly differ from DLBCL of the lung on a genetic basis

DLBCL had a median of 3 mutations per case (1–7) (Fig. 2; Table 2). Mutations of *B2M, BRAF, SGK1, GNA13, TP53* were only seen in the DLBCL cohort ($p = 0.014$), as were e.g. mutations of *PIK3R1* and *PIM1* (yet not statistically significant). Characteristic mutations of PMZL such as *TNFAIP3, NOTCH1, KLF2,* and *SPEN*, were absent from the sub-cohort of DLBCL.

The mutational load of LyG was significantly lower than that of DLBCL (mean 1.1 versus 3.8 mutations/case, $p = 0.002$). Shared mutations were found in *KMT2D*, *PRDM1,* and *SOCS1*, while no mutations in genes related to immune escape, such as *B2M* or *CD58*/*CD274,* could be detected in LyG ($p = 0.014$ for *B2M*). Most mutations in LyG were in genes encoding for epigenetic modifiers (50%). However, one LyG case showed a mutation in *TRAF3*, which encodes for a CD40-signaling protein that interacts with the latent membrane protein 1 (*LMP1*) of EBV.

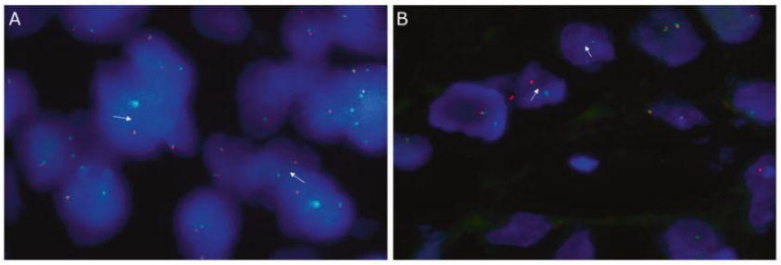

Fig. 3 FISH results. a Break apart probe-based analysis of the *BCL10* locus yielding rearranged (split) signals (arrows) (400×); **b** Break apart analysis of the *MALT1* locus yielding rearranged (split) signals (arrows) (400×).

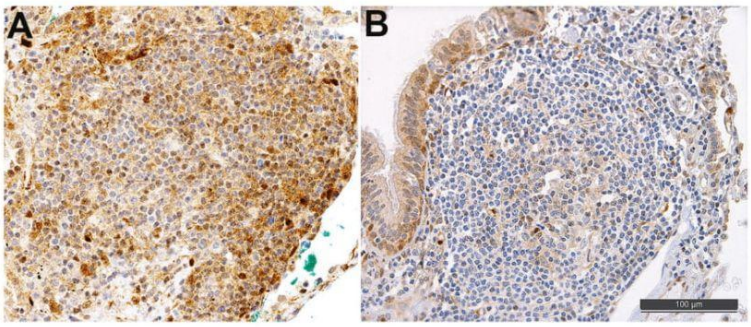

Fig. 4 Follicular bronch(iol)itis with *PTEN* mutation. a Immunohistochemistry showing preserved PTEN-expression in a case of follicular bronch(iol)it is without detectable mutations (immunohistochemistry, 100×). **b** Immunohistochemistry showing loss of PTEN-expression confined to the area of follicular hyperplasia/lymphoid compartment, confirming the functional importance of the *PTEN*-mutation found in the respective case.

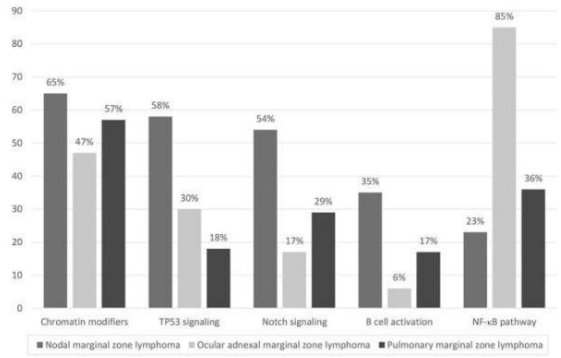

Fig. 5 Genetic landscape of selected extranodal marginal zone B-cell lymphomas according to pathways. Overview of pathways affected by mutations in pulmonary marginal zone lymphomas in comparison to cohorts of nodal marginal zone lymphomas (NMZL) and ocular adnexal marginal zone B-cell lymphomas (OAMZL) analyzed using the same HTS panel. Data of the NMZL and OAMZL cohorts were derived from previous studies of our group [12, 17].

common mutant gene in both PMZL and DLBCL. *KMT2D* mutations are known to be the most frequent mutations in B-cell lymphomas in general and in DLBCL in particular [26]. They are also common in NMZL [16, 17] and gastric MZL [13], while they occur more rarely in other subtypes of EMZL [15]. Other studies of PMZL have also shown both *KMT2D* mutations and mutations of chromatin modifiers in general, but less frequently than in our cohort [14, 15]. In the six cases of our cohort, in which both mutations of chromatin modifier-encoding genes and genes involved in the NOTCH pathway were present, the VAF of the first group was always higher than of the latter (Supplementary Fig. 3). This indicates that mutations in chromatin modifiers occurred before mutations of genes related to the NOTCH pathway. This finding confirms that mutations of chromatin modifiers are an early event in lymphomagenesis also in EMZL as has been shown for FL [27].

The second most commonly mutant gene, *TNFAIP3*, inhibits NF-κB activation by exerting dual ubiquitin-editing functions [28]. Furthermore, it augments molecular pathways including tumor necrosis factor receptor (TNFR) TLR/IL1-R and B-cell receptor (BCR) signaling, which are critical in the development of marginal zone B-cells. Similar to our previous study on ocular adnexal MZL and other lymphoproliferations of the orbit [12], also in this study we found that *TNFAIP3* was not mutated in lymphoproliferations of the lungs other than PMZL.

Mutations affecting the NOTCH pathway including *NOTCH1, SPEN, KLF2,* and *TBL1XR1* were also common in PMZL, but absent in other lymphoproliferations of the

lungs. These genes affect the NOTCH pathway, which is essential for marginal zone B-cell development [29–31]. It has been shown that conditional knock out of Notch2 in mice results in the complete absence of marginal zone B-cells [32] leaving other B-cell subsets unaffected. Except for one *TBL1XR1* mutant case (TBL1XR1 is suspected of playing a minor role in this pathway), NOTCH-pathway related mutations were absent in our limited pulmonary DLBCL cohort. This observation was made in spite of the fact that in *de novo* (nodal) DLBCL, NOTCH-mutations are an integral part of two recently defined genetic subsets (BN2 and N1) [33]. Nevertheless, these observations are in line with our remaining data disfavoring a relationship between PMZL and pulmonary DLBCL. Finally, while *KLF2* is commonly mutated in splenic MZL [18], no other study on PMZL has described mutations in this gene [14, 15].

Interestingly, the mutational load of PMZL correlated with proliferation rate, in line with respect to lymphoma aggressiveness [34]. The mutational load inversely correlated with rearrangements of the *BCL10* or *MALT1* loci. In that context, our observed incidence of these rearrangements and their lack in pulmonary DLBCL were similar to previous reports [20, 35]. These translocations appear to be linked through the roles of *BCL10* and *MALT1* in activating the NF-κB pathway. Indeed, they not only were exclusively detectable in PMZL, thus further strengthening our assumption that pulmonary DLBLC do no not represent transformed PMZL, but were mutually exclusive and – with exception of a *CARD11* mutation—mutually exclusive to presence of mutations of other genes encoding for NF-κB pathway compounds.

As to be expected and in line with previous studies of our group [36], LyG had a significantly lower mutational load than DLBCL. According to our knowledge, this is the first comprehensive analysis of the mutational landscape of LyG so far. Looking at primary EBV-positive DLBCL, another recent study could also show that the mutational profiles of EBV-positive and EBV-negative DLBCL significantly differ [37]. Yet in contrast to this study, most mutations in our LyG cases were observable in epigenetic modifiers while no mutations could be detected in *MYC*, or *RHOA* or components of the NF-κB pathway. In our previous study analyzing EBV-positive DLBCL-type post-transplant lymphoproliferative disorders (PTLD), mutations of *MYC* and components of the NF-κB pathway were seen in two cases each. Independent of the actual mutant genes, studies on EBV-positive B-cell lymphomas, including the current one on LyG, uniformly show that such instances display significantly lower mutational load than DLBCL suggesting that EBV infection may "substitute" for mutations. LyG cases furthermore did not show mutations in genes related to immune escape such as *B2M* or *CD58/CD274;* amplifications of *PDL1* could not be assessed applying our methodology. Interestingly, one iatrogenic immunodeficiency-associated DLBCL case of our pulmonary DLBCL cohort was EBV-positive and did not display mutations in genes related to immune escape as well. These findings are in line with the proposed mechanistic model of EBV-driven lymphomagenesis that preferentially affects immunocompromised patients and/or body niches with decreased immunological control, and do not put tumor (precursor-)cells on pressure to acquire immune escape mutations [38].

Investigating reactive lesions of the lungs, including follicular bronchitis, lymphocytic interstitial pneumonia, and nodular lymphoid hyperplasia, one follicular bronchitis case displayed a known *PTEN* mutation [12]. *In silico* prediction and immunohistochemistry confirmed the potentially damaging effect of this mutation leading to *PTEN* expression loss in the lymphoid compartment. The same mutation was also detected in two other cases of our PMZL cohort. Importantly, within a follow-up period of 12 years this former patient is still alive and without evidence of lymphoma or other tumors. The identical mutation has been observed by us in a case of follicular conjunctivitis [12]. This mutation in both cases is to be considered somatic and not-germline derived due to relatively low VAF and confinement to lymphoid cells based on the immunohistochemical appearance. These two identical observations in extranodal follicular hyperplasias tempt us to speculate whether "clonal lymphopoiesis" exists, and if such *PTEN* mutant subclones may foster follicular hyperplasias in general, and extranodal follicular hyperplasias in particular. At the very least, these observations in reactive lesions underscore once again the fact that detection of mutations outside a proper clinic-pathologic context is of little diagnostic value.

To conclude, this study consolidates our knowledge on the genetic landscape of PMZL. It confirms the hypothesis that EMZL rely on and cluster around different signaling pathways, some of which are characteristic for their primary site of origin. It brings evidence that PMZL and primary pulmonary DLBCL are probably not related, and confirms the tumorigenic role of EBV in LyG, "substituting" for –especially immune escape- gene mutations.

Acknowledgements The authors would like to thank Prof. C. Hamilton for critically proofreading the manuscript. The study has been supported by the Stiftung zur Krebsbekaempfung Zuerich (SKB473).

Compliance with ethical standards

Conflict of interest The authors declare that they have no conflict of interest.

References

1. Ferraro P, Trastek VF, Adlakha H, Deschamps C, Allen MS, Pairolero PC. Primary non-Hodgkin's lymphoma of the lung. Ann Thorac Surg. 2000;69:993–7.
2. Borie R, Wislez M, Antoine M, Cadranel J. Lymphoproliferative disorders of the lung. Respiration. 2017;94:157–75.
3. Bertoni F, Rossi D, Zucca E. Recent advances in understanding the biology of marginal zone lymphoma. F1000Res. 2018;7:406.
4. Borie R, Wislez M, Thabut G, Antoine M, Rabbat A, Couderc L-J, et al. Clinical characteristics and prognostic factors of pulmonary MALT lymphoma. Eur Respir J. 2009;34:1408–16.
5. Nathwani BN, Anderson JR, Armitage JO, Cavalli F, Diebold J, Drachenberg MR, et al. Marginal zone b-cell lymphoma: a clinical comparison of nodal and mucosa-associated lymphoid tissue types. Non-hodgkin's lymphoma classification project. J Clin Oncol. 1999; 17:2486–92.
6. Troppan K, Wenzl K, Neumeister P, Deutsch A. Molecular pathogenesis of MALT lymphoma. Gastroenterol Res Pr. 2015; 2015:1–10.
7. Cook JR, PG Isaacson, A Chott, S Nakamura, HK Müller-Hermelink, NL Harris et al. WHO classification of tumours of haematopoietic and lymphoid tissues, 4th ed. Lyon: International Agency for Research on Cancer; 2017.
8. Schreuder MI, van den Brand M, Hebeda KM, Groenen PJTA, van Krieken JH, Scheijen B. Novel developments in the pathogenesis and diagnosis of extranodal marginal zone lymphoma. J Hematop. 2017;10:91–107.
9. Cani AK, Soliman M, Hovelson DH, Liu C-J, McDaniel AS, Haller MJ, et al. Comprehensive genomic profiling of orbital and ocular adnexal lymphomas identifies frequent alterations in MYD88 and chromatin modifiers: new routes to targeted therapies. Mod Pathol. 2016;29:685–97.
10. Jung H, Yoo HY, Ho Lee S, Shin S, Kim SC, Lee S, et al. The mutational landscape of ocular marginal zone lymphoma identifies frequent alterations in TNFAIP3 followed by mutations in TBL1XR1 and CREBBP. Oncotarget. 2017;8:17038–49.
11. Johansson P, Klein-Hitpass L, Grabellus F, Arnold G, Klapper W, Pförtner R, et al. Recurrent mutations in NF-κB pathway components, KMT2D, and NOTCH1/2 in ocular adnexal MALT-type marginal zone lymphomas. Oncotarget. 2016;7:62627–39.
12. Vela V, Juskevicius D, Gerlach MM, Meyer P, Graber A, Cathomas G, et al. High throughput sequencing reveals high specificity of TNFAIP3 mutations in ocular adnexal marginal zone B-cell lymphomas. Hematol Oncol. 2020;107:2718–31.
13. Hyeon J, Lee B, Shin SH, Yoo HY, Kim SJ, Kim WS, et al. Targeted deep sequencing of gastric marginal zone lymphoma identified alterations of TRAF3 and TNFAIP3 that were mutually exclusive for MALT1 rearrangement. Mod Pathol. 2018;31:1418–28.
14. Moody S, Thompson JS, Chuang S-S, Liu H, Raderer M, Vassiliou G, et al. Novel GPR34 and CCR6 mutation and distinct genetic profiles in MALT lymphomas of different sites. Haematologica. 2018;103:1329–36.
15. Cascione L, Rinaldi A, Bruscaggin A, Tarantelli C, Arribas AJ, Kwee I, et al. Novel insights into the genetics and epigenetics of MALT lymphoma unveiled by next generation sequencing analyses. Haematologica. 2019;104:558–61.
16. Spina V, Khiabanian H, Messina M, Monti S, Cascione L, Bruscaggin A, et al. The genetics of nodal marginal zone lymphoma. Blood. 2016;128:1362–73.
17. Pillonel V, Juskevicius D, Ng CKY, Bodmer A, Zettl A, Jucker D, et al. High-throughput sequencing of nodal marginal zone lymphomas identifies recurrent BRAF mutations. Leukemia. 2018;32:2412–26.
18. Clipson A, Wang M, De Leval L, Ashton-Key M, Wotherspoon A, Vassiliou G, et al. KLF2 mutation is the most frequent somatic change in splenic marginal zone lymphoma and identifies a subset with distinct genotype. Leukemia. 2015;29:1177–85.
19. Maurus K, Appenzeller S, Roth S, Kuper J, Rost S, Meierjohann S, et al. Panel sequencing shows recurrent genetic FAS alterations in primary cutaneous marginal zone lymphoma. J Invest Dermatol. 2018;138:1573–81.
20. Remstein ED, Dogan A, Einerson RR, Paternoster SF, Fink SR, Law M, et al. The incidence and anatomic site specificity of chromosomal translocations in primary extranodal marginal zone B-cell lymphoma of mucosa-associated lymphoid tissue (MALT lymphoma) in North America. Am J Surg Pathol. 2006;30:1546–53.
21. Dierlamm J, Baens M, Wlodarska I, Stefanova-Ouzounova M, Hernandez JM, Hossfeld DK, et al. The apoptosis inhibitor gene API2 and a novel 18q gene, MLT, are recurrently rearranged in the t(11;18)(q21;q21) associated with mucosa-associated lymphoid tissue lymphomas. Blood. 1999;93:3601–9.
22. Willis TG, Jadayel DM, Du M-Q, Peng H, Perry AR, Abdul-Rauf M, et al. Bcl10 Is Involved in t(1;14)(p22;q32) of MALT B cell lymphoma and mutated in multiple tumor types. Cell. 1999;96:35–45.
23. Tzankov A, Xu-Monette ZY, Gerhard M, Visco C, Dirnhofer S, Gisin N, et al. Rearrangements of MYC gene facilitate risk stratification in diffuse large B-cell lymphoma patients treated with rituximab-CHOP. Mod Pathol. 2014;27:958–71.
24. Meier VS, Rufle A, Gudat F. Simultaneous evaluation of T- and B-cell clonality, t(11;14) and t(14;18), in a single reaction by a fourcolor multiplex polymerase chain reaction assay and automated high-resolution fragment analysis: A method for the rapid molecular diagnosis of lymphop. Am J Pathol. 2001;159: 2031–43.
25. Liu X, Wu C, Li C, Boerwinkle E. dbNSFP v3.0: a one-stop database of functional predictions and annotations for human nonsynonymous and splice-site SNVs. Hum Mutat. 2016;37:235–41.
26. Juskevicius D, Jucker D, Klingbiel D, Mamot C, Dirnhofer S, Tzankov A. Mutations of CREBBP and SOCS1 are independent prognostic factors in diffuse large B cell lymphoma: mutational analysis of the SAKK 38/07 prospective clinical trial cohort. J Hematol Oncol. 2017;10:1–10.
27. Green MR. Chromatin modifying gene mutations in follicular lymphoma. Blood. 2018;131:595–604.
28. Heyninck K, Beyaert R. A20 inhibits NF-κB activation by dual ubiquitin-editing functions. Trends Biochem Sci. 2005;30:1–4.
29. Spina V, Rossi D. Molecular pathogenesis of splenic and nodal marginal zone lymphoma. Best Pr Res Clin Haematol. 2017; 30:5–12.
30. Kuroda K, Han H, Tani S, Tanigaki K, Tun T, Furukawa T, et al. Regulation of marginal zone B cell development by MINT, a suppressor of Notch/RBP-J signaling pathway. Immunity. 2003; 18:301–12.
31. Pillai S, Cariappa A. The follicular versus marginal zone B lymphocyte cell fate decision. Nat Rev Immunol. 2009;9:767–77.
32. Saito T, Chiba S, Ichikawa M, Kunisato A, Asai T, Shimizu K, et al. Notch2 is preferentially expressed in mature B cells and indispensable for marginal zone B lineage development. Immunity. 2003;18:675–85.
33. Schmitz R, Wright GW, Huang DW, Johnson CA, Phelan JD, Wang JQ, et al. Genetics and pathogenesis of diffuse large B-cell lymphoma. N. Engl J Med. 2018;378:1396–407.
34. Zhou H, Du X, Zhao T, Ouyang Z, Liu W, Deng M, et al. Distribution and influencing factors of tumor mutational burden in different lymphoma subtypes. J Clin Oncol. 2019;37: e19053–e19053.

35. Zhu Z, Liu W, Mamlouk O, O'Donnell JE, Sen D, Avezbakiyev B. Primary pulmonary diffuse large B cell non-hodgkin's lymphoma: a case report and literature review. Am J Case Rep. 2017; 18:286–90.
36. Menter T, Juskevicius D, Alikian M, Steiger J, Dirnhofer S, Tzankov A, et al. Mutational landscape of B-cell post-transplant lymphoproliferative disorders. Br J Haematol. 2017;178:48–56.
37. Zhou Y, Xu Z, Lin W, Duan Y, Lu C, Liu W, et al. Comprehensive genomic profiling of EBV-positive diffuse large B-cell lymphoma and the expression and clinicopathological correlations of some related genes. Front Oncol. 2019;9:683.
38. Ok CY, Li L, Young KH. EBV-driven B-cell lymphoproliferative disorders: from biology, classification and differential diagnosis to clinical management. Exp Mol Med. 2015;47:e132–e132.

4. DISCUSSION

4.1 The genetic landscape of ocular adnexal marginal zone lymphoma

4.1.1 Frequent *TNFAIP3* alterations in OMZL

The molecular basis and the etiology of OMZL is not fully understood. In our OMZL study, we characterized their genetic landscape and compared them to other types of lymphomas in the same anatomic region. Prior to our work, authors of several studies have discovered that *TNFAIP3* plays an important role in OMZL. Out of a cohort comprising 34 patients, we detected *TNFAIP3* as the most frequently mutated gene. Similar to previous studies, the majority of these mutations were either nonsense or frameshift. *TNFAIP3* is a negative regulator of the NF-κB pathway and inactivates several proteins that are necessary for NF-κB signaling such as NEMO, TRAF6, TAK1 and receptor interacting proteins (RIP) 1 and 2.[175] *TNFAIP3* causes the deactivation of this pathway due to its dual ubiquitin-editing functions.[91] This ubiquitination is reversible and controlled by deubiquitinases. Loss-of-function mutations of *TNFAIP3* that occur in MZL stimulate canonical NF-κB signalling, which reduces apoptosis and cell proliferation.[93,94] We know that the NF-κB pathway plays an important role for memory B-cells leading to a neoplastic transformation and MZL progression.[176] Lee et al.[177] demonstrated that in *TNFAIP3* knockout mice, the NF-κB pathway is activated constitutively, leading to an overproduction of proinflammatory cytokines and severe multi-organ inflammation. The inactivation of *TNFAIP3* is, therefore, one important factor for the pathogenesis of OMZL.

However, these mutations might not be sufficient to initiate the NF-κB pathway signaling activation. MZL development requires other genetic mutations. Furthermore, chronic bacterial infections have been reported and constitutive extrinsic stimulation of the BCR may also activate the NF-κB signaling pathway.[178]

4.1.2 Genetic mutations identified in key biological pathways

One potential reason for OMZL to develop is the occurrence of genetic mutations in the biological pathways such as the NF-κB pathway, NOTCH pathway and chromatin modifier. Sixty-five percent of our studied cohort have genetic mutations related to the NF-κB pathway. These include mutations of genes with "complementing-each-other character" such *BCL10*, *MYD88*, *TBL1XR1*, and other several transcription factors that activate the NF-κB pathway. In our heat map of unsupervised clustering analysis, *TNFAIP3*, *BCL10*, and *MYD88* mutations clustered together exclusively in the MZL cohort (Figure 12), suggesting that these mutations are of diagnostic potential. Furthermore, this heatmap shows us that specific genes in the MZL entity are recurrently mutated and clustered together. Therefore the mutational landscape of MZL differs from other entities in the same anatomic region.

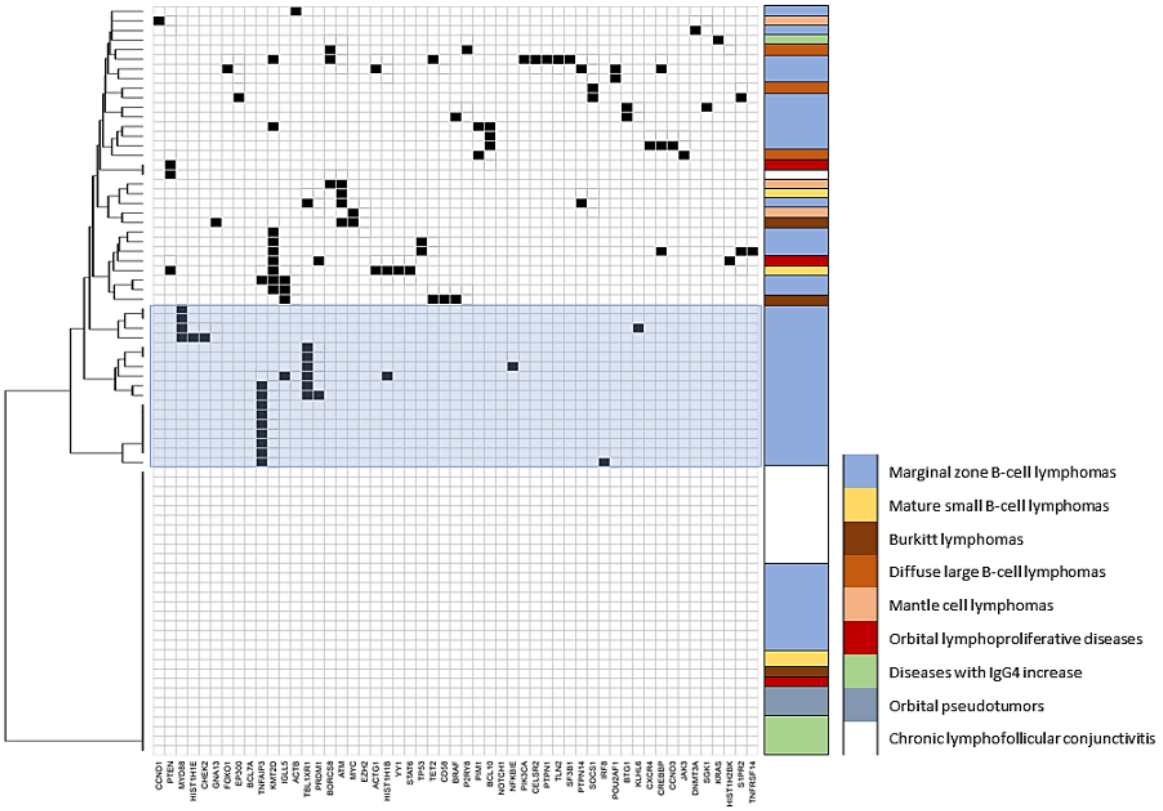

Figure 12. Heatmap of unsupervised clustering analysis. The left-handed dendrogram reflects case clustering.

In comparison, the minority of the cases (38% of the cohort) display mutually exclusive mutations of genes that encode chromatin modifiers such as *KMT2D*, *CREBBP*, *BCL7A*, *DNMT3A*, *EP300*, and *HIST1H1E* genes.

While Johansson et al.[139,179] identified mutations in *NOTCH1* and *NOTCH2* – both of which belong to the NOTCH pathway and are recurrently mutated in several types of B-cell NHL – we could not detect them. For *NOTCH1*, this might be due to sample size bias because our targeted panel covers all mutant exons of *NOTCH1*. For *NOTCH2*, incomplete coverage could be an additional reason because our panel covers only the most commonly mutated exon 34, and mutations in other exons might have been missed.

These findings are in line with our meta analysis. Here we showed that genes in the NF-κB pathway were mainly mutated followed by the mutations in the chromatin modifiers and the NOTCH pathway.

4.1.3 Recurrent *MYD88* and *BCL10* mutations in OMZL

In several OMZL studies, researchers have detected recurrent *MYD88* and *BCL10* mutations.[176,180–182] Several ocular MZL studies show recurrent mutations of *MYD88.* In the study of Cani et al. *MYD88* was the most frequent mutated gene. This adaptor protein binds to the intracellular domains of Toll-like receptors (TLRs) and IL-1 receptor on B cells which stimulates the NF-κB signaling pathway. These reports are supported by the study of Johansson et al.,[139] who observed that patients with *MYD88* mutation have a significantly shorter disease-free survival (DFS) than those without mutations.

Similarly, *BCL10* has been investigated in several OMZL studies. *BCL10* is a positive regulator of lymphocyte proliferation, and is linked to recurrent chromosomal aberrations in MALT lymphomas.[183,184] Upregulation of *BCL10* causes an escape in the upstream B-cell antigen receptor signaling, constitutively activating the NF-κB pathway.[183] Expression of *BCL10* has also presented prognostic significance due to a shorter failure-free survival (FFS) (Figure 13).[185] However, to our knowledge, our study is the first to suggest the prognostic

importance of *BCL10* mutations in OMZL. Moreover, our results are limited by the relatively small number of patients we analysed. Thus, these encouraging findings need to be validated in an independent patient cohort and ideally in the context of a prospective trial of homogeneously treated patients with OMZL.

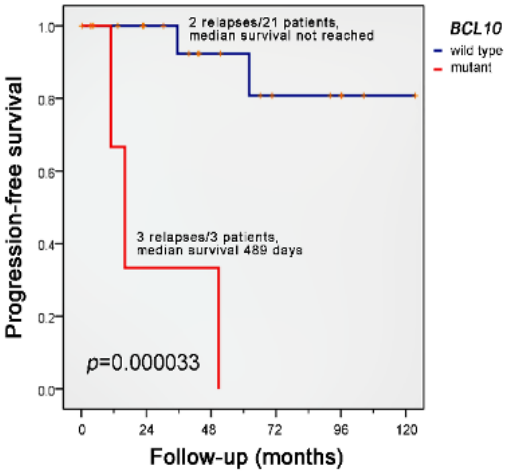

Figure 13. Survival curve estimates of the studied ocular adnexal marginal zone B-cell lymphomas according to *BCL10* mutational status; CTX, chemotherapy, RTX, radiotherapy, W&W, watchful waiting.

4.1.4 Association of *Chlamydia psittaci* infection and OMZL

The role of infectious agents that causes NHL has been a topic for many years. There is the hypothesis that infectious agents may initiate chronic inflammation that leads to B-cell transformation and lymphomagenesis.[186] Besides viruses, bacteria have been shown as carcinogens and tumor promoters. They can take part in tumorigenesis by activating various intracellular signaling pathways, modulate apoptosis and cell proliferation.[186] One potential reason for the etiology of ocular adnexal MZL is the presence of *Chlamydia psittaci*. *C. psittaci* is an obligate intracellular bacterium usually found in animals such as birds and cats and is spread to humans through inhalation of aerosolized bacteria or handling contaminated feathers or fecal matter.[187]

Chlamydia occurs in three forms, the elementary body (EB) - a metabolically inactive infectious form, the reticulate body (RB) - a metabolically active intracellular growth stage,

and the intermediate body (IB). These properties, together with its complex developmental cycle, allows *Chlamydia* to establish persistent infections. In addition, this bacteria can modify its life cycle as a response to a changing environment causing resistance of the infected cell to apoptosis.[188,189] This constant infection leads to cells gradually becoming independent of the involvement in their microenvironment. Chronic stimulation due to *C. psittaci* infection may be favored by molecular mimicry due to its ability to induce immune reactions that cross-react with the host self-antigens, causing failure to eliminate the pathogen and induce lymphomagenesis.[186,189]

Ferreri et al.[190] tested the association of different NHL cohorts with *C. psittaci* infection. While patients with DLBCL displayed a lower infection prevalence, patients with MZL were more commonly infected with *C. psittaci.* These findings suggest the presence of different pathways that lead to lymphomagenesis.[190] In addition, these results present the possibility that *C. psittaci*–positive MZL cases are more likely to undergo transformation to a more aggressive type that is no longer dependent on antigenic stimulation. Beside *C. psittaci*, the presence of other bacteria like *Chlamydia trachomatis* and *Chlamydia pneumoniae* is tested in OMZL, but they turn out negative.[190] However, in our OMZL cohort, all samples tested by polymerase chain reaction (PCR) were negative for *C. psittaci*.

Since both OMZL and *C. psittaci* infection are rare diseases, there is no current universal recommended therapeutic approach. These lesions are often located superficially, indolent, and rarely progress to more malignant types of lymphoma.[186] In a phase II randomized control trials, 65% of the patients experienced regression of lesions after antibiotic therapy with doxycycline.[66]

The involvement of *C. psittaci* infection in OMZL development is noted in only some geographic regions. Earlier studies from Italy show the frequent presence of *C. psittaci* in OMZL. However, succeeding studies present marked variation in the association between the *C. psittaci* infection and OMZL in different geographic regions. This association is prevalent in Italy, Germany, and Korea but relatively uncommon or absent in the United Kingdom, Japan, China, and certain areas of the USA.[191] Therefore, multinational studies have to be conducted to establish or disprove this connection.

4.1.5 OMZL and other histologically related reactive lesions

Lymphoproliferative disorders (LPDs) frequently found in the ocular adnexa include malignant lymphoma and orbital inflammation with lymphoid hyperplasia or infiltration, IgG4-related ophthalmic disease, and IgG4-related orbital disease. Around 24% to 49% of these are LPDs with orbital tumors and simulating lesions. In addition, 53% to 55% of the malignant orbital tumors account for orbital lymphoma. The IgG4-related orbital disease accounts for 61% of benign ocular adnexal LPDs.[192]

Our study characterized ocular adnexal lymphomas and lymphoid lesions of the ocular adnexa by targeted HTS. In one IgG4 patient, we detected a pathogenic *KRAS* G12R mutation. Upon reassessment, the initial diagnosis was corrected to juvenile xanthogranuloma. Further, in a 47-year-old African patient initially classified as OA lymphoid hyperplasia, we detected four mutations in three genes (*KMT2D*, *PRDM1*, and *HIST1H2BK*). When reassessed, the patient actually had mucocutaneous leishmaniosis. From this data of reactive lesions and other lymphomas of the orbit, a conclusion of particular diagnostic importance can be drawn, namely that OA lymphoid lesions bearing mutations of NF-κB components and/or mutations of acetyltransferase-encoding genes are highly likely to represent lymphomas. This seems not to apply to phosphatase and tensin homolog deleted on chromosome 10 (*PTEN*), *KMT2D*, *PRDM1*, and *HIST1H2BK* mutations, all of which can also be observed in reactive lesions. These results point out the need for correct diagnosis.

Immunoglobulin G4-related disease (IgG4-RD) is a systemic disorder characterized by tissue fibrosis and intense lymphoplasmacytic infiltration with IgG4-bearing plasma cells, reactive lymphoid follicles and sclerosing fibrosis that causes progressive organ dysfunction.[193,194] It is an autoimmune disease that can affect nearly any organ. This disease can be hard to diagnose because patients present characteristics that mimic other disorders. Therefore, the diagnosis is based on exclusion criteria, requiring histologic confirmation.[195] To diagnose IgG4-RD, histopathological findings such as dense lymphoplasmacytic infiltration and storiform fibrosis, are utilized including recently proposed diagnostic criteria.[193,196]
Several studies have identified the relationship between IgG4-related disease and OMZL. A link between ocular adnexal IgG4-related disease and EMZL has been proposed, as clinical

manifestations of IgG4-related disease may resemble those of EMZL, and ocular adnexal IgG4-related disease can potentially develop to EMZL. IgG4-positive plasma cells are thought to be a precursor or as a promoter of pathogenesis of some OMZL cases.[194]

Lee et al. analyzed the clinical and pathological characteristics of OMZL and accompanying IgG4-positive cells in 50 patients, and they reported IgG4-positive plasma cell infiltration in 10% of the cases. However, the causal relationship between IgG4-related disease and EMZL remains uncertain, as IgG4-positive lymphomas can develop independently or arise from underlying IgG4-related disease.[193] Tissue biopsy and IgG4 immunostaining are required to diagnose IgG4-positive MALT lymphoma from LPDs.[197] However, it is suggested that IgG4 may be a possible prognostic indicator in OMZL. Large-scale studies have to be conducted to fully investigate the clinical implications of the involvement of IgG4-related disease and EMZL.[193]

It is crucial to discriminate orbital lymphoma from benign ocular adnexal LPDs as it holds different therapeutic implications.[192] For example, orbital lymphoma is responsive to low-dose radiation therapy, whereas benign ocular adnexal LPDs respond well to corticosteroid therapy.[198] Making a differential diagnosis of malignant lymphoma from benign LPDs often is challenging. A high-resolution SNP-A is used to detect extensive genomic alterations and discriminate ocular adnexal lymphomas from benign LPDs, including copy number variations (CNVs) associated with the clinical features and outcome. In ocular adnexal MALT lymphomas, the most frequent CN gain region was trisomy 3, followed by trisomy 18, 6p, and 21q. The most frequent CN loss region was 6q and 9p. On the other hand, copy number variations were not detected in cases with benign LPDs such as IgG4-related ophthalmic disease and reactive lymphoid hyperplasia. This report shows that differences in the chromosomal abnormality patterns may reflect the activity of ocular adnexal LPDs.[192]

4.2 The genetic landscape of pulmonary lymphomas

In our second study, we focused on primary pulmonary lymphomas, which are very rare, and only very little information about point mutations is available in this entity. The most common type of pulmonary lymphoma is PMZL derived from bronchus-mucosa-associated lymphatic tissue (BALT/MALT), followed by DLBCL and LyG, an Epstein–Barr virus (EBV)-related disorder.[199] Researchers have also detected several genetic mutations in PMZL, including in genes that encode chromatin modifiers and members of the NOTCH and NF-κB signalling pathways.[98,122] In our large cohort, we were able to examine the mutational background of PMZL.

To expand the knowledge on the genetic landscape of PMZL, we used our in-house-designed HTS gene panel with 146 genes to study our cohort of 28 patients with PMZL. Based on our genetic landscape of selected EMZL entities, we were able to create an overview of the pathways affected by mutations in PMZL compared with cohorts of NMZL and OMZL. We extracted these data from our previous studies.[92,107]

4.2.1 *KMT2D* is highly mutated in PMZL cases

In our study, we showed that PMZL has distinct mutational and rearrangement patterns. While OMZL showed predominant mutations in the NF-κB signalling pathway, in PMZL, we detected *KMT2D* and other chromatin-modifying genes as the most common mutation in PMZL. These mutations are also common in NMZL[107,136] and GMZL,[116] suggesting the similarity of the genetic landscape between these EMZL entities. *KMT2D* encodes a highly conserved protein that belongs to the SET1 family of histone lysine methyltransferases (KMT), a group of enzymes that catalyse the methylation of lysine 4 on histone H3 (H3K4) associated with transcriptionally active chromatin.[200] Furthermore, *KMT2D* functions as a non-redundant methyltransferase that controls the methylation state of a large number of regions in the mature B-cell compartment.[200] Most *KMT2D* mutations are postulated to generate truncated proteins that are functionally defective due to the loss of the catalytic SET domain.[200] Besides PMZL, this epigenetic regulator is also known to be mutated frequently in

DLBCL.[201] In B lymphocytes, it acts as a tumour suppressor.[202] Alam et al.[203] identified this tumour-suppressive function of *KMT2D* that causes indirect downregulation of glycolytic genes via the super-enhancer activation that enhances *Per2* expression. Thus, these glycolytic pathways can be an effective therapeutic target to prevent the growth of cancer cells.[203]

4.2.2 Genetic mutations in key biological pathways

Mutually exclusive mutations of *NOTCH1*, *SPEN*, *KLF2*, and *TBL1XR1* were found in PMZL but absent in other lymphoproliferations of the lungs. These genes affect the NOTCH pathway and are considered essential for marginal zone B-cell development.[12,132,133] Mutations of chromatin-modifying genes affect 57% of the studied PMZL cases and are mutually exclusive to genes related to the NF-κB signalling cluster that affects 36% of the cases. Moreover, only 29% of all PMZL cases contain mutations affecting genes related to the NOTCH signalling pathways. The variant allelic frequency (VAF) of the mutations of chromatin-modifying genes is always higher than the VAF of the mutations of the genes involved in the NOTCH pathway, indicating that the mutations in chromatin modifiers occurred prior to the mutations of genes involved in the NOTCH pathway. This result confirms that mutations of chromatin modifiers are an early event in lymphomagenesis, as shown in follicular lymphomas (Figure 14).[204]

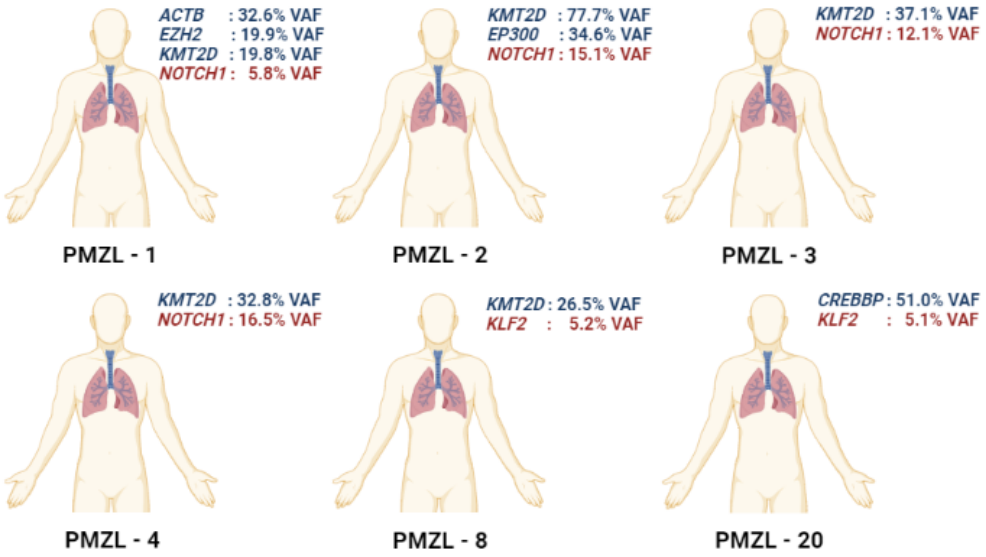

Figure 14. Chromatin modifier versus NOTCH pathway mutation evolution. Comparison of variant allelic frequencies (VAF) between mutation frequencies of epigenetic modifier–encoding genes and Notch-pathway-related genes in six patients with pulmonary marginal zone lymphoma (PMZL). All frequencies are from 5.1% to 77.7%. Each PMZL sample displays higher frequencies in epigenetic-modifier-encoding genes compared with Notch-pathway-related genes. This finding confirms that mutations of chromatin modifiers are an early event in EMZL lymphomagenesis.

4.2.3 Role of PTEN in lymphomas

Surprisingly, after *TP53*, *PTEN* is the second most frequently mutated gene in human cancers.[205] Phosphatase and tensin homolog deleted on chromosome 10 (*PTEN*) is a phosphatase that acts as a tumor suppressor. Furthermore, *PTEN* is a negative regulator of the cell growth and survival signaling pathway.[206] Its protein is present in the cytoplasm and nucleus, which can stabilize chromosomes, participate in DNA repair, and regulate the cell cycle.[206] Interestingly, mice with a B-cell-specific *PTEN* mutation display increased numbers of marginal zone B-cells.[207] So far, *PTEN* mutations have not been reported in reactive lymphoid lesions. Furthermore, these lesions display a very similar clinical appearance to benign neoplastic proliferation. Because of this similarity, a differential diagnosis is, in many cases, troublesome.[208]

In our cohort, one patient with follicular hyperplasia showed the *PTEN* mutation c.834 C>G with a predicted damaging effect. The same mutation was also detected in two other cases of our PMZL cohort. In addition, in our previous ocular adnexal cohort, a chronic conjunctivitis case presented with a pathogenic non-germline *PTEN* F278L mutation, formerly reported in endometrial carcinoma.[209] A patient with severe chronic lympho-follicular conjunctivitis with lympho-epithelial lesions classified as OA lymphoid hyperplasia was found to have a *PTEN* S360G missense mutation, a variant of unknown significance. Both of these cases underwent reassessment that disfavored a malignant process. Immunohistochemistry (Figure 15) confirmed the potentially damaging effect of *PTEN* mutations leading to loss of protein expression in the lymphocytes of the lesion while being retained in the epithelial cells of the lung, suggesting functional relevance of the mutation. Loss-of-function *PTEN* mutations play a critical role in the pathogenesis of human cancers. These genetic alterations have been linked to advanced disease, chemotherapy resistance, and poor survival of patients.[210] This

PTEN alteration is considered to represent a relevant somatic mutation and not a germline variant due to a relatively low VAF and confinement to lymphoid cells. These observations allow us to speculate whether 'clonal lymphopoiesis' exists and if such *PTEN* mutant subclones could foster follicular hyperplasias in general and extranodal follicular hyperplasias in particular.

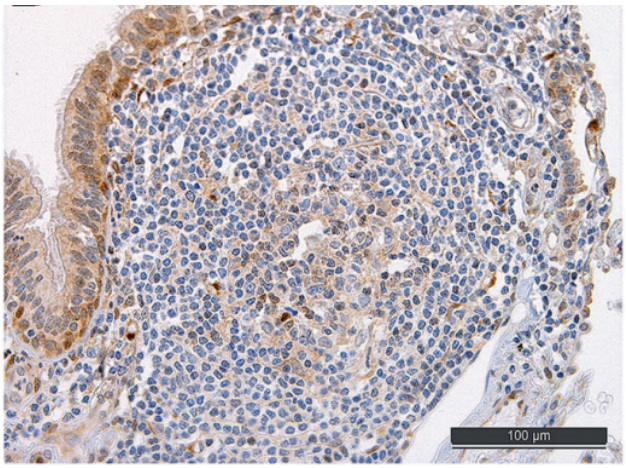

Figure 15. Follicular bronch(iol)itis with PTEN mutation. Immunohistochemistry showing loss of PTEN-expression confined to the area of follicular hyperplasia/lymphoid compartment, confirming the functional importance of the PTEN-mutation found in the respective case.

4.2.4 Significant differences between of PMZL, LyG, and DLBCL

Until today, a lack of molecular data and a low number of specific PMZL cases have limited the in-depth analysis of primary pulmonary lymphomas. PMZL is rather an indolent disease. On the other hand, primary pulmonary DLBCL is much more aggressive and needs aggressive treatment even in the early stage. So far, the diagnosis of primary pulmonary DLBCL is very challenging because of its nonspecific presentation, a phenomenon that often leads to misdiagnosis or delayed diagnosis.[211] With our new data, we were able to compare the genetic landscape between PMZL and primary pulmonary DLBCL. Pulmonary DLBCL is thought to arise by transformation from primary PMZL of MALT.[212] Some of its main characteristics are programmed death receptor-1 (PD-1) overexpression and constitutional JAK–STAT activation.[213] Our immunohistochemistry and FISH results showed that *MALT1* rearrangements were more prevalent in PMZL than *BCL10* aberrations, but neither were found in DLBCL. These findings disprove the assumption that the development of pulmonary

DLBCL and PMZL is related. DLBCL cases that underwent HTS had a median of three mutations per case, while in PMZL, we found two mutations per case. Mutations of *B2M*, *BRAF*, *SGK1*, *GNA13*, and *TP53* were seen exclusively in the DLBCL cohort. Characteristic mutations of PMZL, such as *TNFAIP3*, *NOTCH1*, *KLF2*, and *SPEN*, were not detected in DLBCL. NOTCH-pathway-related mutations were absent in the pulmonary DLBCL cohort. Thus, we were also able to provide genetic evidence that shows the distinction between PMZL and primary DLBCL of the lungs and disfavouring their relationship.

According to our knowledge, this is the first comprehensive analysis of the mutational landscape of LyG. This angio-destructive B-cell lymphoproliferative disorder is associated with vasculitis and various amounts of necrosis that are graded according to the grade of the lesion.[214–216] The vasculitic changes are caused by chemokine-mediated invasion of inflammatory cells responding to EBV infection as an immune response. Furthermore, the differential diagnosis with LYG can be challenging, especially if it involves extranodal sites. Most often, LYG has no clear immunodeficient state that can easily be identified.[217] In the case between LyG and primary pulmonary DLBCL, both express B-cell markers; however, large amounts of necrosis associated with vasculitis favor LyG over DLBCL.[218] We found that nearly all mutations in our LyG cases are epigenetic modifiers, while we found no mutations in the NF-κB pathway. While all three entities PMZL, LyG, and DLBCL, share genetic mutations like *KMT2D*, *KMT2C*, *TET2*, and *PRDM*, LyG lacks mutations associated with immune escape, such as *B2M* or *CD58/CD274*, unlike PMZL and DLBCL (Figure 16). LyG showed recurrent mutations in *TRAF3*, which encodes an important CD40-signalling protein that interacts with LMP1 of EBV. These results confirm the tumorigenic role of EBV infection in LyG, which may substitute for immune escape gene mutations. This may also be a reason why LyG cases show a uniformly lower mutational load than DLBCL. Failure of the immune escape mechanism can lead to EBV-induced B-cell proliferation where carrier B-cells transform from latent to malignant leading to the development of lymphoma. While being latent, EBV-infected resting memory cells evade immune recognition by limiting gene expression.[219] However, complete understanding of the immune characteristics associated with LyG has not been met. Further studies have to be done to come up with a successful course of therapy.

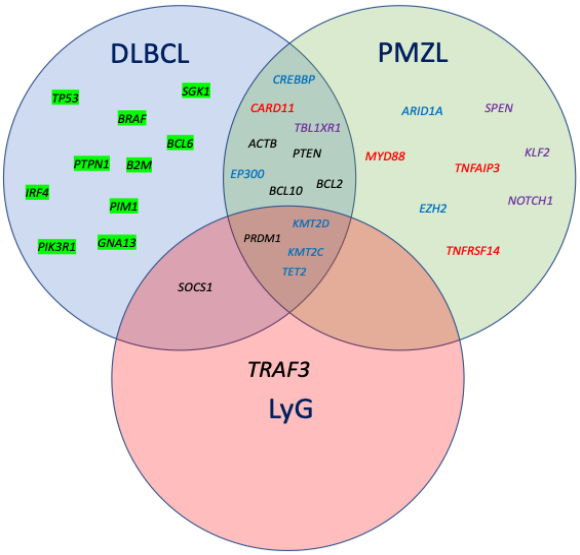

Figure 16. Diffuse large B-cell lymphoma (DLBCL) versus pulmonary marginal zone lymphoma (PMZL) versus lymphomatoid granulomatosis (LyG). A Venn diagram identifying the genetic similarities and differences of three lymphoproliferation of the lung.

A. xylosoxidans is a Gram-negative bacterium closely related to the genus *Bordetella*.[220] This opportunistic and motile bacterium has a low virulence but a high resistance to antibiotics. Beside cystic fibrosis, it is also associated with PMZL. Similarly to *C. psittaci* in OMZL, *A. xylosoxidans* infection also depends on different geographical regions, with high prevalence in Italy and low prevalence in Germany.[71] However, in our study we did not test for the presence and correlation of *A. xylosoxidans* with PMZL.

Furthermore, we showed that PMZL has distinct mutational and rearrangement patterns. This knowledge might help in diagnostically equivocal cases regarding other B-cell lymphomas and reactive lymphoid lesions in the lung.

4.3 The genetic landscape of splenic, nodal, and extranodal marginal zone lymphomas in the dura mater, salivary gland, thyroid, ocular adnexa, lung, stomach and skin

Despite the various extensive efforts to study the genomic landscape of the different MZL entities, there is still a need to define clearly the genetic mutations that will serve as diagnostic borders due to the considerable overlap between these mutations across the various MZL entities. Thus, we created a general overview of the MZL genomic information by performing a meta-analysis of 25 carefully curated MZL studies. The selection includes publications that reported somatic mutations in MZL of various origins and identified variants with consistent and detailed annotations. The selected studies were divided according to the different entities, and duplicates were removed, screened, and filtered using specific inclusion criteria such as diagnosis and read-out methods. Manuscripts and supplementary data were studied to ensure a complete list of variants with appropriate sample information and genetic coordinates. Genomic information was extracted from 1,663 cases and was uniformed to the GRCh38/hg38 genome by applying LiftOver – UCSC Genome Browser.[221] VEP[221] and Annovar software[222] were used to complete the missing information, such as genomic location and reference sequence annotation. The mutation frequency of the different genetic mutations was calculated and compared between the different entities using the two-tailed Fisher's exact test.

4.3.1 Mutational profile of SMZL

SMZL studies[107–110,135,137] showed a higher prevalence of *KLF2* and *NOTCH2* mutations. These genes are physiologically involved in proliferation, homing of B-cells to the spleen, and marginal zone differentiation.[223] *KLF2,* a member of the KLF family of zinc-finger transcription factors, regulates the expression of genes involved in apoptosis and cell trafficking and negatively regulates NF-κB signaling. Mutations in *KLF2* disrupt its nuclear localization signal, suppressing NF-κB induction by upstream signaling pathways, leading to orchestrated NF-κB activation.[110,223] *KLF2* inactivation leads to altered gene expression that favors homing of B-cells to the marginal zone.[110] *NOTCH2* regulates marginal zone

differentiation and homing of B-cells to the splenic marginal zone.[224] *NOTCH2* mutations in SMZL cause truncation of the C-terminal PEST domain, impairing protein degradation and activating NOTCH signaling.[223]

KLF2 mutations also occur in other indolent B-cell tumors, and they cannot be used to diagnose SMZL. On the other hand, *NOTCH2* mutations represent a biomarker specific for SMZL because these mutations are virtually absent in other mature B-cell neoplasia and rare in DLBCL.[138,142,225] *KLF2* and *NOTCH2* mutations are prognostically relevant in SMZL since these mutations become a marker for an inferior outcome.[108–110,138] Therefore patients with *KLF2* and *NOTCH2* mutations are at a higher risk of receiving treatment such as splenectomy.[108] *NOTCH2* upregulation or *KLF2* inactivation may be insufficient as single events for malignant lymphoma transformation, thereby requiring the cooperation of other genetic and cellular events in SMZL development. Transgenic mice that overexpress *NOTCH2* or lack *KLF2* in mature B-cells do not develop lymphoma.[226,227] The potential cell survival advantage due to early *KLF2* mutations allows additional genetic mutations to promote tumorigenesis.[108]

In addition, *TP53* is mutated considerably more often in SMZL. Mutations inactivate *TP53* tumour suppressor function, as well as promote disease progression and high-grade transformation.[110] The presence of *TP53* mutations is linked with poor prognosis and they are an independent marker of short OS.[108] Researchers reported that patients with *TP53* deletions had the shortest survival. All of these indicators allow the consideration of *TP53* mutations as a parameter to ascertain SMZL prognosis.[49]

4.3.2 Mutational profile of NMZL

BRAF is found to be highly mutated in NMZL. BRAF is a serine/threonine kinase commonly activated by a somatic point mutation hotspot V600E which is at the same time the most common mutation in *BRAF*.[124] Mutations in BRAF lead to constitutive activation of kinases. *BRAF i*nteracts with MEK and phosphorylates it which activates the phosphorylation of ERK. This signaling promotes cellular growth and inhibits apoptosis.[228] Pillonel et al.[107] identified for the first time this canonical *BRAF* V600E hotspot mutation in cases with strong IgD

expression from their NMZL study cohort. Therefore it could help to discriminate NMZL from other closely related small B-cell lymphomas. Recurrent *BRAF* mutations in NMZL are of diagnostic importance and a good targeted therapeutic opportunity. The *BRAF* V600E mutation can be identified by immunohistochemistry and is a known target for the *BRAF* kinase inhibitors.[125,126]

Beside *BRAF* mutations *PTPRD* is proposed as a diagnostic biomarker in NMZL. This gene encodes a receptor-type-protein- phosphatase that is expressed in normal germinal center B-cells and is involved in several cell pagrams, including proliferation and cytokine signaling. In our metaanalysis *PTPRD* is mutated in 12% of NMZL.[132] Lesions in *PTPRD* damage the tyrosine phosphatase function of the protein or remove the entire protein. Beside genetic lesions *PTPRD* is also affected in its epigenome by aberrant methylation of the gene promoters that decrease the *PTPRD* expression.[132]

4.3.3 Mutational profile of EMZL entities

The NF-κB inhibitor *TNFAIP3* has been studied extensively and is mutated frequently in EMZL entities such as DMZL[229] and OMZL, [92,98,122,139,148,179] but are rare in GMZL and PMZL. However, the mutational profile of conjunctival and periorbital OMZL cases differs. This phenomenon makes us wonder whether OMZL of different anatomic sub-sites are linked to different aetiologies and should generally be further sub-divided.

Notably, the epigenetic regulator *TET2* is highly mutated in TMZL.[98,122] These loss-of-function mutations result in an inactive protein and a net general hypermethylated state of the cells.[150] *TET2* mutations are commonly seen in myeloid neoplasms and T-cell lymphomas[230] but are generally uncommon in B-cell lymphomas. Thus, *TET2* mutations can be considered specific for TMZL and might be of diagnostic importance that sets TMZL apart from other EMZL entities. Frameshift insertions/deletions make up a high percentage of the *TET2* mutations, making them more commonly observable than other MZL entities and subentities.

Despite only a few studies that have explored *FAS* mutations,[116,229,231] *FAS* turned out to be the most frequently mutated gene in CMZL.[231] *FAS* belongs to the TNFR family. Its mutations affect the death domain, fostering anti-apoptotic properties, leading to disrupted protein function, and empowering cancer cells with survival advantages.[231,232] *FAS* mutations in CMZL are located at splice sites, establishing it as an entity with the highest proportion of splice-site mutations. A *FAS* splice-site mutation renders cells insensitive to *FAS*-mediated apoptotic stimuli.[233] *FAS* is considered specific for this entity, a factor that possibly provides diagnostic importance to help distinguish CMZL from other EMZL entities and pseudolymphoma of the skin.

4.3.4 Preferred signaling pathways

We also analysed signalling pathways to determine whether different MZL entities rely on different intracellular signalling conduits. In most cases, the mutations of the genes related to the NOTCH pathway were rather mutually exclusive to genetic mutations in the NF-κB pathway and chromatin modifiers, while the latter two showed overlap. This mutual exclusivity was most prominently seen in SMZL and OMZL and to a lesser extent in SAMZL and GMZL. While the mutational landscape of MZL derived from the stomach and lung mainly involves chromosomal translocations of the NF-κB pathway, in OMZL, the somatic mutation is the main reason that activates the NF-κB pathway. These findings underline the heterogeneity of MZL. Recognising such mutational distribution patterns could help diagnose MZL in challenging cases and lead to novel, more tailored treatment.

4.3.5 Further implications

Several factors might have affected the outcome of this study. In particular, some entities come with a limited number of patients. The different cohorts were very heterogeneous due to inconsistent clinical data, various sequencing strategies, and different bioinformatic workups. To minimise the effects of these limitations, the published data was homogenised using algorithms and normalised based on reference genome hg38. The nature of the material employed, FF or FFPE tissue, could have affected the study results. However, this might not be a significant factor, as shown by the excellent linear correlation of Pillonel et al.[107,234]

between results obtained on either material for DLBCL. For future MZL studies, these challenges could be reduced if a worldwide protocol would be set regarding sample handling, gathering of clinical data, similar sequencing strategies, and uniform bioinformatic workups.

Information regarding infectious agents such as *H. pylori* in GMZL, *B. burgdorferi* in CMZL, or *C. psittaci* in OMZL has not been provided consistently to address the interrelations between mutational profiles and infectious aetiology. Similarly, no information on autoimmune diseases, especially in SAMZL and TMZL, had been provided in the studies included.

A lot of work still has to be done to define MZL diagnosis clearly and to pave the way for more targeted treatment. For example, chromosomal aberrations linked to MZL include the trisomies of chromosomes 3, 12, and 18, t(11;18)(q21;q21), del(7)(q31), and t(3;14)(p14;q32).[85–87] Chromosomal translocations play a more important role in MZL differentiation and are linked with diagnostic potential.[235] However, due to the restrictions of labour- and material-intensive methodologies such as FISH, no large-scale studies have been conducted to investigate translocations in MZL. For example, FISH results in an OMZL study exhibited low frequency and lack of structural chromosomal aberrations in OMZL, suggesting that FISH may have a low diagnostic yield. New methods such as RNA-based sequencing techniques could be implemented to allow large-scale studies to investigate chromosomal translocations related to MZL.[236]

In addition, despite having a comprehensive target enrichment panel in the PMZL and OMZL studies of Vela et al.,[92,237] the genetic mutations identified are limited to the 146 genes that the panel covers. Several other genetic mutations might have been identified if the researchers used other sequencing methods such as Sanger sequencing, WES, and WGS. Furthermore, the germline controls were missing for the validation of the mutations in the OMZL cohort. The small cohort size did not allow us to have a precise picture of the pathways affected in MZL. Recognising the complete genomic information of the different MZL entities will greatly aid diagnostics, especially in complex cases, and will pave the way for novel, more tailored treatment.

Aside from genetic mutations, other epigenetic mechanisms such as DNA methylation are essential to the malignant progression of lymphomas.[235] DNA methylation contributes to tumour suppressor inactivation and regulates transcription and expression of genes that sustain tumour cell survival and proliferation.[238] Through DNA methylation profiling, Arribas et al.[236] identified two SMZL subtypes with different clinical and genetic features and different degrees of promoter methylation. These clusters are the higher-promoter methylation (High-M) and the lower-promoter methylation (Low-M) cluster. In the High-M cluster, the tumour suppressor genes were methylated and suppressed; thus, it is associated with histologic transformation and a poorer overall survival when compared with the Low-M cluster.[239] A study showed that exposure of SMZL cell lines to demethylating agents caused a partial reversion of the High-M cluster and inhibited proliferation.[239]

Aberrant 5'—C—phosphate—G—3' (CpG) island methylation of tumour suppressor genes, downregulation of *p16/INK4a* expression, and promoter hypermethylation of the *p16/INK4a* and *ECAD* genes are frequent events that characterise extranodal MZL entities.[239–242] OMZL exhibits distinct methylation profiles according to *C. psittaci* infection, and these reflect the response to doxycycline treatment.[243] *ECAD* hypermethylation is closely associated and is significantly higher in *C. psittaci*–positive cases, but promoter hypermethylation status is not correlated with clinical characteristics.[241] Genetic alterations of *p16/INK4a* are associated with lymphoma tumour progression.[244] The *p16/INK4a* promoter gene is partially methylated in *C. psittaci*–negative cases, but hypermethylation is absent in *C. psittaci*–positive cases.[240] The *p16*/*INK4a* and *MAD2* genes are key regulator proteins at the mitotic checkpoint of the cell cycle. The majority of GMZL with *p16*/*INK4a* methylation are negative for t(11;18)(q21;q21) translocation and is *H. pylori*–dependent, while those with *MAD2* methylation frequently express *BCL10* and are known to be independent of *H. pylori* infection.[245] These results may shed light on the mechanisms of bacterium-induced oncogenesis.[239] In addition, methylation of *p16*/*INK4a* followed by methylation of the kinase-inhibitor *p57*/*KIP2* during GMZL tumorigenesis is associated with *H. pylori* infection. Methylation of both of these genes is found to be more frequent in higher-grade lymphoma; thus, it can be said that they contribute to the malignant progression of GMZL.[246] Takino et al.[244] concluded that *p16* methylation might be an early event in EMZL lymphomagenesis and is maintained throughout tumour progression. Associated with methylation of the *p16* gene is the methylation of the candidate

tumour suppressor *p15*/*MTS2* gene. This uncommon selective methylation is specific to T-cell NHL.[247]

In the case of colorectal extranodal MZL, methylation was more frequently observed in cases with advanced disease stages than with earlier stages, with patterns differing by location. These results suggest that methylation profiles define a clinically more aggressive EMZL subgroup and multiclonal origin with multiorgan involvement.[248]

We may conclude that the role of epidemiologic, environmental, and genetic factors must be considered in the aetiology of this disease. These findings would help us better understand MZL biology and disease pathogenesis. Taking note of these methylation changes will help identify prognostic markers and pave the way for novel therapy using demethylating agents to target malignant B-cells and reverse the high-methylation phenotype.[235,238]

5 GENERAL CONCLUSION

Precision medicine strategies, including the new sequencing techniques, will offer us new treatment opportunities in patients with MZL. Our increasing understanding of the cellular and molecular variations in MZL and the development of new biomarkers will lead to successful personalised and tailored MZL therapies.

In this work, I described the genetic landscape of OMZL and PMZL. With our in-house-created sequencing lymphoma panel, we detected *TNFAIP3* as the most mutated gene in OMZL and *KMT2D* in PMZL. With our meta-analysis, we summarised the genetic landscape of SMZL, NMZL, and EMZL. For a better understanding of the molecular pathology in MZL, we compared the three most affected pathways within different entities. While in PMZL and NMZL, chromatin-modifying genes were predominantly mutated, OMZL, DMZL, and GMZL showed recurrent mutations in the NF-κB pathway. Further, with the help of HTS, we distinguished between the different mutational compositions of pulmonary DLBCL and PMZL and showed that the former is not a progression of the latter.

In our two studies, we characterised the mutational landscape of reactive lesions and found *PTEN* to be recurrently mutated in such occasions. Hence, this gene could serve as a biomarker in further validation studies.

All these findings provide a deeper understanding of the pathogenic pathways that are activated in MZL and will help us in the future to find new genetic biomarkers for targeted therapies.

REFERENCES

1 Sriskandarajah P, Dearden CE. Epidemiology and environmental aspects of marginal zone lymphomas. *Best Pract Res Clin Haematol* 2017; **30**: 84–91.

2 Janeway Jr CA, Travers P, Walport M, Shlomchik MJ, Jr CAJ, Travers P *et al. Immunobiology*. 5th ed. Garland Science, 2001.

3 Owen JA, Punt J, Stranford SA. *Kuby Immunology*. Seventh Edition. W.H. Freeman and Company: New York, 2013.

4 Nagasawa T. Microenvironmental niches in the bone marrow required for B-cell development. *Nat Rev Immunol* 2006; **6**: 107–116.

5 Allman D, Li J, Hardy RR. Commitment to the B Lymphoid Lineage Occurs before DH-JH Recombination. *J Exp Med* 1999; **189**: 735–740.

6 Vilagos B, Hoffmann M, Souabni A, Sun Q, Werner B, Medvedovic J *et al.* Essential role of EBF1 in the generation and function of distinct mature B cell types. *J Exp Med* 2012; **209**: 775–792.

7 Oettinger MA, Schatz DG, Gorka C, Baltimore D. RAG-1 and RAG-2, adjacent genes that synergistically activate V(D)J recombination. *Science* 1990; **248**: 1517–1523.

8 Samitas K, Lötvall J, Bossios A. B Cells: From Early Development to Regulating Allergic Diseases. *Arch Immunol Ther Exp (Warsz)* 2010; **58**: 209–225.

9 Bräuninger A, Goossens T, Rajewsky K, Küppers R. Regulation of immunoglobulin light chain gene rearrangements during early B cell development in the human. *Eur J Immunol* 2001; **31**: 3631–3637.

10 Chung JB, Silverman M, Monroe JG. Transitional B cells: step by step towards immune competence. *Trends Immunol* 2003; **24**: 342–348.

11 Mebius RE, Kraal G. Structure and function of the spleen. *Nat Rev Immunol* 2005; **5**: 606–616.

12 Pillai S, Cariappa A. The follicular versus marginal zone B lymphocyte cell fate decision. *Nat*

Rev Immunol 2009; **9**: 767–777.

13 Lucas AH. Immunoglobulin Gene Construction: Human. In: *eLS*. American Cancer Society, 2003 doi:10.1038/npg.els.0001172.

14 Schroeder HW, Cavacini L. Structure and Function of Immunoglobulins. *J Allergy Clin Immunol* 2010; **125**: S41–S52.

15 Ru H, Chambers MG, Fu T-M, Tong AB, Liao M, Wu H. Molecular Mechanism of V(D)J Recombination from Synaptic RAG1-RAG2 Complex Structures. *Cell* 2015; **163**: 1138–1152.

16 Stavnezer J, Schrader CE. Ig heavy chain class switch recombination: mechanism and regulation. *J Immunol Baltim Md 1950* 2014; **193**: 5370–5378.

17 Stavnezer J, Guikema JEJ, Schrader CE. Mechanism and Regulation of Class Switch Recombination. *Annu Rev Immunol* 2008; **26**: 261–292.

18 Lieber MR, Yu K, Raghavan SC. Roles of nonhomologous DNA end joining, V(D)J recombination, and class switch recombination in chromosomal translocations. *DNA Repair* 2006; **5**: 1234–1245.

19 Zouali M, Richard Y. Marginal Zone B-Cells, a Gatekeeper of Innate Immunity. *Front Immunol* 2011; **2**. doi:10.3389/fimmu.2011.00063.

20 Steiniger B, Timphus EM, Barth PJ. The splenic marginal zone in humans and rodents: an enigmatic compartment and its inhabitants. *Histochem Cell Biol* 2006; **126**: 641–648.

21 Martin F, Kearney JF. Marginal-zone B cells. *Nat Rev Immunol* 2002; **2**: 323–335.

22 Bendelac A, Bonneville M, Kearney JF. Autoreactivity by design: innate B and T lymphocytes. *Nat Rev Immunol* 2001; **1**: 177–186.

23 Puga I, Cols M, Barra CM, He B, Cassis L, Gentile M *et al.* B–helper neutrophils stimulate immunoglobulin diversification and production in the marginal zone of the spleen. *Nat Immunol* 2011; **13**: 170–180.

24 Spencer J, Finn T, Pulford KA, Mason DY, Isaacson PG. The human gut contains a novel population of B lymphocytes which resemble marginal zone cells. *Clin Exp Immunol* 1985; **62**: 607–612.

25 Tierens A, Delabie J, Michiels L, Vandenberghe P, De Wolf-Peeters C. Marginal-Zone B Cells in the Human Lymph Node and Spleen Show Somatic Hypermutations and Display Clonal Expansion. *Blood* 1999; **93**: 226–234.

26 Dono M, Zupo S, Leanza N, Melioli G, Fogli M, Melagrana A *et al.* Heterogeneity of Tonsillar Subepithelial B Lymphocytes, the Splenic Marginal Zone Equivalents. *J Immunol* 2000; **164**: 5596–5604.

27 Weill J-C, Weller S, Reynaud C-A. Human Marginal Zone B Cells. *Annu Rev Immunol* 2009; **27**: 267–285.

28 Srivastava B, Quinn WJ, Hazard K, Erikson J, Allman D. Characterization of marginal zone B cell precursors. *J Exp Med* 2005; **202**: 1225–1234.

29 Won W-J, Kearney JF. CD9 Is a Unique Marker for Marginal Zone B Cells, B1 Cells, and Plasma Cells in Mice. *J Immunol* 2002; **168**: 5605–5611.

30 Cerutti A, Cols M, Puga I. Marginal zone B cells: virtues of innatelike antibody-producing lymphocytes. *Nat Rev Immunol* 2013; **13**: 118–132.

31 Attanavanich K, Kearney JF. Marginal Zone, but Not Follicular B Cells, Are Potent Activators of Naive CD4 T Cells | The Journal of Immunology. *J Immunol* 2004; **172**.https://www.jimmunol.org/content/172/2/803.long (accessed 4 Jun2021).

32 Humphrey JH, Grennan D, Sundaram V. The origin of follicular dendritic cells in the mouse and the mechanism of trapping of immune complexes on them. *Eur J Immunol* 1984; **14**: 859–864.

33 Fang Y, Xu C, Fu Y-X, Holers VM, Molina H. Expression of Complement Receptors 1 and 2 on Follicular Dendritic Cells Is Necessary for the Generation of a Strong Antigen-Specific IgG Response. *J Immunol* 1998; **160**: 5273–5279.

34 Kosco-Vilbois MH, Gray D, Scheidegger D, Julius M. Follicular dendritic cells help resting B cells to become effective antigen-presenting cells: induction of B7/BB1 and upregulation of major histocompatibility complex class II molecules. *J Exp Med* 1993; **178**: 2055–2066.

35 Oliver AM, Martin F, Kearney JF. IgMhighCD21high Lymphocytes Enriched in the Splenic Marginal Zone Generate Effector Cells More Rapidly Than the Bulk of Follicular B Cells. *J Immunol* 1999; **162**: 7198–7207.

36 Bialecki E, Paget C, Fontaine J, Capron M, Trottein F, Faveeuw C. Role of Marginal Zone B Lymphocytes in Invariant NKT Cell Activation. *J Immunol* 2009; **182**: 6105–6113.

37 Zucca E, Bertoni F. The spectrum of MALT lymphoma at different sites: biological and therapeutic relevance | Blood | American Society of Hematology. *Ash Publ* 2016; **127**: 2082–2092.

38 Zucca E, Arcaini L, Buske C, Johnson PW, Ponzoni M, Raderer M *et al.* Marginal zone lymphomas: ESMO Clinical Practice Guidelines for diagnosis, treatment and follow-up☆. *Ann Oncol* 2020; **31**: 17–29.

39 Bertoni F, Coiffier B, Salles G, Stathis A, Traverse-Glehen A, Thieblemont C *et al.* MALT Lymphomas: Pathogenesis Can Drive Treatment. *Oncology* 2011; **25**: 1134–1142, 1147.

40 Joshi M, Sheikh H, Abbi K, Long S, Sharma K, Tulchinsky M *et al.* Marginal zone lymphoma: old, new, targeted, and epigenetic therapies. *Ther Adv Hematol* 2012; **3**: 275–290.

41 Swerdlow S, Campo E, Harris N, Jaffe E, Pileri S, Stein H *et al.* (eds.). *WHO Classification of Tumours of Haematopoietic and Lymphoid Tissues*. 4th ed. IARC Press: Lyon, France, 2017https://publications.iarc.fr/Book-And-Report-Series/Who-Classification-Of-Tumours/WHO

-Classification-Of-Tumours-Of-Haematopoietic-And-Lymphoid-Tissues-2017 (accessed 24 Jan2021).

42 Dreyling M, Thieblemont C, Gallamini A, Arcaini L, Campo E, Hermine O *et al.* ESMO Consensus conferences: guidelines on malignant lymphoma. part 2: marginal zone lymphoma, mantle cell lymphoma, peripheral T-cell lymphoma. *Ann Oncol* 2013; **24**: 857–877.

43 Caponetti G, Bagg A. [PDF] Demystifying the diagnosis and classification of lymphoma : a hematologist / oncologist ' s guide to the hematopathologist ' s galaxy | Semantic Scholar. https://www.semanticscholar.org/paper/Demystifying-the-diagnosis-and-classification-of-%3A-Caponetti-Bagg/e05e75d8010193c297da1c0d4a619ffbcd79fed6#citing-papers (accessed 10 Jun2021).

44 Al-Hamadani M, Habermann TM, Cerhan JR, Macon WR, Maurer MJ, Go RS. Non-Hodgkin lymphoma subtype distribution, geodemographic patterns, and survival in the US: A longitudinal analysis of the National Cancer Data Base from 1998 to 2011. *Am J Hematol* 2015; **90**: 790–795.

45 Oscier D, Owen R, Johnson S. Splenic marginal zone lymphoma. *Blood Rev* 2005; **19**: 39–51.

46 Olszewski AJ, Castillo JJ. Survival of patients with marginal zone lymphoma. *Cancer* 2013; **119**: 629–638.

47 Mazloom A, Medeiros LJ, McLaughlin PW, Reed V, Cabanillas FF, Fayad LE *et al.* Marginal zone lymphomas. *Cancer* 2010; **116**: 4291–4298.

48 Matutes E, Oscier D, Montalban C, Berger F, Callet-Bauchu E, Dogan A *et al.* Splenic marginal zone lymphoma proposals for a revision of diagnostic, staging and therapeutic criteria. *Leukemia* 2008; **22**: 487–495.

49 Salido M, Baró C, Oscier D, Stamatopoulos K, Dierlamm J, Matutes E *et al.* Cytogenetic aberrations and their prognostic value in a series of 330 splenic marginal zone B-cell lymphomas: a multicenter study of the Splenic B-Cell Lymphoma Group. *Blood* 2010; **116**: 1479–1488.

50 Zucca E, Stathis A, Bertoni F. The Management of Nongastric MALT Lymphomas. *Cancer Netw* 2014; **28**.https://www.cancernetwork.com/view/management-nongastric-malt-lymphomas (accessed 10 Jun2021).

51 Goda JS, Gospodarowicz M, Pintilie M, Wells W, Hodgson DC, Sun A *et al.* Long-term outcome in localized extranodal mucosa-associated lymphoid tissue lymphomas treated with radiotherapy. *Cancer* 2010; **116**: 3815–3824.

52 A Clinical Evaluation of the International Lymphoma Study Group Classification of Non-Hodgkin's Lymphoma. *Blood* 1997; **89**: 3909–3918.

53 Troppan K, Wenzl K, Neumeister P, Deutsch A. Molecular Pathogenesis of MALT Lymphoma. *Gastroenterol Res Pract* 2015; **2015**. doi:10.1155/2015/102656.

54 Khalil MO, Morton LM, Devesa SS, Check DP, Curtis RE, Weisenburger DD *et al.* Incidence of marginal zone lymphoma in the United States, 2001–2009 with a focus on primary anatomic site. *Br J Haematol* 2014; **165**: 67–77.

55 Doglioni C, Moschini A, Boni M de, Wotherspoon AC, Isaacson PG. High incidence of primary gastric lymphoma in northeastern Italy. *The Lancet* 1992; **339**: 834–835.

56 Cho EY, Han JJ, Ree HJ, Ko YH, Kang Y, Ahn HS *et al.* Clinicopathologic analysis of ocular adnexal lymphomas: Extranodal marginal zone b-cell lymphoma constitutes the vast majority of ocular lymphomas among Koreans and affects younger patients. *Am J Hematol* 2003; **73**: 87–96.

57 Zucca E, Bertoni F, Vannata B, Cavalli F. Emerging Role of Infectious Etiologies in the Pathogenesis of Marginal Zone B-cell Lymphomas. *Clin Cancer Res* 2014; **20**: 5207–5216.

58 Kuo S-H, Cheng A-L. Helicobacter pylori and mucosa-associated lymphoid tissue: what's new. *Hematology* 2013; **2013**: 109–117.

59 Cover TL, Dooley CP, Blaser MJ. Characterization of and human serologic response to proteins in Helicobacter pylori broth culture supernatants with vacuolizing cytotoxin activity. *Infect Immun* 1990; **58**: 603–610.

60 Crabtree JE, Taylor JD, Heatley RV, Shallcross TM, Rathbone BJ, Wyatt JI *et al.* Mucosal IgA recognition of Helicobacter pylori 120 kDa protein, peptic ulceration, and gastric pathology. *The Lancet* 1991; **338**: 332–335.

61 Blaser MJ, Perez-Perez GI, Kleanthous H, Cover TL, Peek RM, Chyou PH *et al.* Infection with Helicobacter pylori Strains Possessing cagA Is Associated with an Increased Risk of Developing Adenocarcinoma of the Stomach. *Cancer Res* 1995; **55**: 2111–2115.

62 Kuo S-H, Chen L-T, Lin C-W, Wu M-S, Hsu P-N, Tsai H-J *et al.* Detection of the Helicobacter pylori CagA protein in gastric mucosa-associated lymphoid tissue lymphoma cells: clinical and biological significance. *Blood Cancer J* 2013; **3**: e125.

63 Yamazaki S, Yamakawa A, Ito Y, Ohtani M, Higashi H, Hatakeyama M *et al.* The CagA Protein of Helicobacter pylori Is Translocated into Epithelial Cells and Binds to SHP-2 in Human Gastric Mucosa. *J Infect Dis* 2003; **187**: 334–337.

64 Mimuro H, Suzuki T, Tanaka J, Asahi M, Haas R, Sasakawa C. Grb2 Is a Key Mediator of Helicobacter pylori CagA Protein Activities. *Mol Cell* 2002; **10**: 745–755.

65 Tsutsumi R, Higashi H, Higuchi M, Okada M, Hatakeyama M. Attenuation of Helicobacter pylori CagA·SHP-2 Signaling by Interaction between CagA and C-terminal Src Kinase *. *J Biol Chem* 2003; **278**: 3664–3670.

66 Ferreri AJM, Govi S, Pasini E, Mappa S, Bertoni F, Zaja F *et al.* Chlamydophila Psittaci Eradication With Doxycycline As First-Line Targeted Therapy for Ocular Adnexae Lymphoma: Final Results of an International Phase II Trial. *J Clin Oncol* 2012; **30**: 2988–2994.

67 Ponzoni M, Ferreri AJM, Guidoboni M, Lettini AA, Cangi MG, Pasini E *et al.* Chlamydia Infection and Lymphomas: Association Beyond Ocular Adnexal Lymphomas Highlighted by Multiple Detection Methods. *Clin Cancer Res* 2008; **14**: 5794–5800.

68 Knittler MR, Sachse K. Chlamydia psittaci: update on an underestimated zoonotic agent. *Pathog Dis* 2015; **73**: 1–15.

69 Ferreri AJM, Govi S, Ponzoni M. Marginal zone lymphomas and infectious agents. *Semin Cancer Biol* 2013; **23**: 431–440.

70 Garbe C, Stein H, Dienemann D, Orfanos CE. Borrelia burgdorferi—associated cutaneous B cell lymphoma: Clinical and immunohistologic characterization of four cases. *J Am Acad Dermatol* 1991; **24**: 584–590.

71 Adam P, Czapiewski P, Colak S, Kosmidis P, Tousseyn T, Sagaert X *et al.* Prevalence of Achromobacter xylosoxidans in pulmonary mucosa-associated lymphoid tissue lymphoma in different regions of Europe. *Br J Haematol* 2014; **164**: 804–810.

72 Suthar AB, Harries AD. A Public Health Approach to Hepatitis C Control in Low- and Middle-Income Countries. *PLOS Med* 03 10, 15; **12**: e1001795.

73 Benova L, Mohamoud YA, Calvert C, Abu-Raddad LJ. Vertical Transmission of Hepatitis C Virus: Systematic Review and Meta-analysis. *Clin Infect Dis Off Publ Infect Dis Soc Am* 2014; **59**: 765–773.

74 Rosa D, Saletti G, De Gregorio E, Zorat F, Comar C, D'Oro U *et al.* Activation of naïve B lymphocytes via CD81, a pathogenetic mechanism for hepatitis C virus-associated B lymphocyte disorders. *Proc Natl Acad Sci U S A* 2005; **102**: 18544–18549.

75 Luppi M, Longo G, Ferrari MG, Ferrara L, Marasca R, Barozzi P *et al.* Additional neoplasms and HCV infection in low-grade lymphoma of MALT type. *Br J Haematol* 1996; **94**: 373–375.

76 Arcaini L, Burcheri S, Rossi A, Paulli M, Bruno R, Passamonti F *et al.* Prevalence of HCV infection in nongastric marginal zone B-cell lymphoma of MALT. *Ann Oncol* 2007; **18**: 346–350.

77 Nocturne G, Mariette X. Sjögren Syndrome-associated lymphomas: an update on pathogenesis and management. *Br J Haematol* 2015; **168**: 317–327.

78 Eguchi K. Apoptosis in Autoimmune Diseases. *Intern Med* 2001; **40**: 275–284.

79 Nakamura H, Kawakami A, Eguchi K. Mechanisms of autoantibody production and the relationship between autoantibodies and the clinical manifestations in Sjögren's syndrome. *Transl Res* 2006; **148**: 281–288.

80 Jeon EJ, Shon HS, Jung ED. Primary Mucosa-Associated Lymphoid Tissue Lymphoma of Thyroid with the Serial Ultrasound Findings. *Case Rep Endocrinol* 2016; **2016**. doi:10.1155/2016/5608518.

81 Sarinah B, Hisham A-N. Primary Lymphoma of the Thyroid: Diagnostic and Therapeutic Considerations. *Asian J Surg* 2010; **33**: 20–24.

82 van den Brand M, van Krieken JHJM. Recognizing nodal marginal zone lymphoma: recent advances and pitfalls. A systematic review. *Haematologica* 2013; **98**: 1003–1013.

83 Rinaldi A, Mian M, Chigrinova E, Arcaini L, Bhagat G, Novak U *et al.* Genome-wide DNA profiling of marginal zone lymphomas identifies subtype-specific lesions with an impact on the clinical outcome. *Blood* 2011; **117**: 1595–1604.

84 Zinzani PL. The many faces of marginal zone lymphoma. *Hematology* 2012; **2012**: 426–432.

85 Boonstra R, Bosga-Bouwer A, van Imhoff GW, Krause V, Palmer M, Coupland RW *et al.* Splenic Marginal Zone Lymphomas Presenting with Splenomegaly and Typical Immunophenotype Are Characterized by Allelic Loss in 7q31–32. *Mod Pathol* 2003; **16**: 1210–1217.

86 Lloret E, Mollejo M, Mateo MS, Villuendas R, Algara P, Martínez P *et al.* Splenic marginal zone lymphoma with increased number of blasts: An aggressive variant? *Hum Pathol* 1999; **30**: 1153–1160.

87 Schreuder MI, van den Brand M, Hebeda KM, Groenen PJTA, van Krieken JH, Scheijen B. Novel developments in the pathogenesis and diagnosis of extranodal marginal zone lymphoma. *J Hematop* 2017; **10**: 91–107.

88 Balaji S, Ahmed M, Lorence E, Yan F, Nomie K, Wang M. NF-κB signaling and its relevance to the treatment of mantle cell lymphoma. *J Hematol OncolJ Hematol Oncol* 2018; **11**. doi:10.1186/s13045-018-0621-5.

89 Du M-Q. MALT lymphoma: A paradigm of NF-κB dysregulation. *Semin Cancer Biol* 2016; **39**: 49–60.

90 Gilmore TD. Introduction to NF- κ B: players, pathways, perspectives. *Oncogene* 2006; **25**: 6680–6684.

91 Brand M van den, Rijntjes J, Hebeda KM, Menting L, Bregitha CV, Stevens WBC *et al.* Recurrent mutations in genes involved in nuclear factor-κB signalling in nodal marginal zone lymphoma—diagnostic and therapeutic implications. *Histopathology* 2017; **70**: 174–184.

92 Vela V, Juskevicius D, Gerlach MM, Meyer P, Graber A, Cathomas G *et al.* High throughput sequencing reveals high specificity of TNFAIP3 mutations in ocular adnexal marginal zone B-cell lymphomas. *Hematol Oncol* 2020; **38**: 284–292.

93 Compagno M, Lim WK, Grunn A, Nandula SV, Brahmachary M, Shen Q *et al.* Mutations of multiple genes cause deregulation of NF-kB in diffuse large B-cell lymphoma. *Nature* 2009; **459**: 717–721.

94 Karin M. Nuclear factor-κB in cancer development and progression. *Nature* 2006; **441**: 431–436.

95 Boone D, Turer E, Lee E, Ahmad R-C, Wheeler M, Tsui C *et al.* The ubiquitin-modifying enzyme A20 is required for termination of Toll-like receptor responses | Nature Immunology. *Nat Immunol* 2004; **5**: 1052–1060.

96 Whiteside ST, Epinat JC, Rice NR, Israël A. I kappa B epsilon, a novel member of the I kappa B family, controls RelA and cRel NF-kappa B activity. *EMBO J* 1997; **16**: 1413–1426.

97 Koh J, Jang I, Choi S, Kim S, Jang I, Ahn HK *et al.* Discovery of Novel Recurrent Mutations and Clinically Meaningful Subgroups in Nodal Marginal Zone Lymphoma. *Cancers* 2020; **12**. doi:10.3390/cancers12061669.

98 Moody S, Thompson JS, Chuang S-S, Liu H, Raderer M, Vassiliou G *et al.* Novel GPR34 and CCR6 mutation and distinct genetic profiles in MALT lymphomas of different sites. *Haematologica* 2018; **103**: 1329–1336.

99 Yoon H-G, Chan DW, Huang Z-Q, Li J, Fondell JD, Qin J *et al.* Purification and functional characterization of the human N-CoR complex: the roles of HDAC3, TBL1 and TBLR1. *EMBO J* 2003; **22**: 1336–1346.

100 Liu F, He Y, Cao Q, Liu N, Zhang W. TBL1XR1 Is Highly Expressed in Gastric Cancer and Predicts Poor Prognosis. *Dis Markers* 2016; **2016**: 2436518.

101 Zhang T, Liu C, Yu Y, Geng J, Meng Q, Xu S *et al.* TBL1XR1 is involved in c-Met-mediated tumorigenesis of human nonsmall cell lung cancer. *Cancer Gene Ther* 2020; **27**: 136–146.

102 Pearson R, Fleetwood J, Eaton S, Crossley M, Bao S. Krüppel-like transcription factors: A functional family. *Int J Biochem Cell Biol* 2008; **40**: 1996–2001.

103 Mahabeleshwar GH, Kawanami D, Sharma N, Takami Y, Zhou G, Shi H *et al.* The Myeloid Transcription Factor KLF2 Regulates the Host Response to Polymicrobial Infection and Endotoxic Shock. *Immunity* 2011; **34**: 715–728.

104 Heo K-S, Chang E, Takei Y, Le N-T, Woo C-H, Sullivan MA *et al.* Phosphorylation of protein inhibitor of activated STAT1 (PIAS1) by MAPK-activated protein kinase-2 (MK2) inhibits endothelial inflammation via increasing both PIAS1 transrepression and SUMO E3 ligase activity. *Arterioscler Thromb Vasc Biol* 2013; **33**: 321–329.

105 Zahlten J, Steinicke R, Opitz B, Eitel J, N'Guessan PD, Vinzing M *et al.* TLR2- and Nucleotide-Binding Oligomerization Domain 2-Dependent Krüppel-Like Factor 2 Expression Downregulates NF-κB–Related Gene Expression. *J Immunol* 2010; **185**: 597–604.

106 Nayak L, Goduni L, Takami Y, Sharma N, Kapil P, Jain MK *et al.* Kruppel-Like Factor 2 Is a Transcriptional Regulator of Chronic and Acute Inflammation. *Am J Pathol* 2013; **182**: 1696–1704.

107 Pillonel V, Juskevicius D, Ng CKY, Bodmer A, Zettl A, Jucker D *et al.* High-throughput sequencing of nodal marginal zone lymphomas identifies recurrent BRAF mutations. *Leukemia*

2018; **32**: 2412–2426.

108 Parry M, Rose-Zerilli MJ, Ljungström V, Gibson J, Wang J, Walewska R *et al.* Genetics and Prognostication in Splenic Marginal Zone Lymphoma: Revelations from Deep Sequencing. *Clin Cancer Res Off J Am Assoc Cancer Res* 2015; **21**: 4174–4183.

109 Piva R, Deaglio S, Famà R, Buonincontri R, Scarfò I, Bruscaggin A *et al.* The Krüppel-like factor 2 transcription factor gene is recurrently mutated in splenic marginal zone lymphoma. *Leukemia* 2015; **29**: 503–507.

110 Clipson A, Wang M, de Leval L, Ashton-Key M, Wotherspoon A, Vassiliou G *et al.* KLF2 mutation is the most frequent somatic change in splenic marginal zone lymphoma and identifies a subset with distinct genotype. *Leukemia* 2015; **29**: 1177–1185.

111 Wu C-J, Ashwell JD. NEMO recognition of ubiquitinated Bcl10 is required for T cell receptor-mediated NF-κB activation. *Proc Natl Acad Sci U S A* 2008; **105**: 3023–3028.

112 Marcus R. Pathogenesis of MALT lymphoma: Implications for risk stratification and therapy. *Leuk Lymphoma* 2007; **48**: 2087–2088.

113 Kingeter LM, Schaefer BC. Malt1 and cIAP2-Malt1 as effectors of NF-κB activation: Kissing cousins or distant relatives? *Cell Signal* 2010; **22**: 9–22.

114 Hamoudi RA, Appert A, Ye H, Ruskone-Fourmestraux A, Streubel B, Chott A *et al.* Differential expression of NF-κB target genes in MALT lymphoma with and without chromosome translocation: insights into molecular mechanism. *Leukemia* 2010; **24**: 1487–1497.

115 Moore CR, Edwards SK, Xie P. Targeting TRAF3 Downstream Signaling Pathways in B cell Neoplasms. *J Cancer Sci Ther* 2015; **7**: 67–74.

116 Hyeon J, Lee B, Shin S-H, Yoo HY, Kim SJ, Kim WS *et al.* Targeted deep sequencing of gastric marginal zone lymphoma identified alterations of TRAF3 and TNFAIP3 that were mutually exclusive for MALT1 rearrangement. *Mod Pathol* 2018; **31**: 1418–1428.

117 Rossi D, Deaglio S, Dominguez-Sola D, Rasi S, Vaisitti T, Agostinelli C *et al.* Alteration of BIRC3 and multiple other NF-κB pathway genes in splenic marginal zone lymphoma. *Blood* 2011; **118**: 4930–4934.

118 Ngo VN, Young RM, Schmitz R, Jhavar S, Xiao W, Lim K-H *et al.* Oncogenically active MYD88 mutations in human lymphoma. *Nature* 2011; **470**: 115–119.

119 Juárez-Salcedo LM, Castillo JJ. Lymphoplasmacytic Lymphoma and Marginal Zone Lymphoma. *Hematol Oncol Clin North Am* 2019; **33**: 639–656.

120 Rossi D. Role of MYD88 in lymphoplasmacytic lymphoma diagnosis and pathogenesis. *Hematology* 2014; **2014**: 113–118.

121 Kotsiou E, Okosun J, Besley C, Iqbal S, Matthews J, Fitzgibbon J *et al.* TNFRSF14 aberrations in follicular lymphoma increase clinically significant allogeneic T-cell responses. *Blood* 2016;

128: 72–81.

122 Cascione L, Rinaldi A, Bruscaggin A, Tarantelli C, Arribas AJ, Kwee I *et al.* Novel insights into the genetics and epigenetics of MALT lymphoma unveiled by next generation sequencing analyses. *Haematologica* 2019; **104**: e558–e561.

123 Mintz MA, Felce JH, Chou MY, Mayya V, Xu Y, Shui J-W *et al.* The HVEM-BTLA Axis Restrains T Cell Help to Germinal Center B Cells and Functions as a Cell-Extrinsic Suppressor in Lymphomagenesis. *Immunity* 2019; **51**: 310-323.e7.

124 Davies H, Bignell GR, Cox C, Stephens P, Edkins S, Clegg S *et al.* Mutations of the BRAF gene in human cancer. *Nature* 2002; **417**: 949–954.

125 Sosman JA, Kim KB, Schuchter L, Gonzalez R, Pavlick AC, Weber JS *et al.* Survival in BRAF V600–Mutant Advanced Melanoma Treated with Vemurafenib. *N Engl J Med* 2012; **366**: 707–714.

126 Tiacci E, Park JH, De Carolis L, Chung SS, Broccoli A, Scott S *et al.* Targeting Mutant BRAF in Relapsed or Refractory Hairy-Cell Leukemia. *N Engl J Med* 2015; **373**: 1733–1747.

127 Suresh S, Irvine A. The NOTCH signaling pathway in normal and malignant blood cell production. *J Cell Commun Signal* 2015; **9**. doi:10.1007/s12079-015-0271-0.

128 Notch Signaling. Cell Signal. Technol. https://www.cellsignal.at/pathways/notch-signaling-pathway (accessed 16 Sep2021).

129 Bray SJ. Notch signalling in context. *Nat Rev Mol Cell Biol* 2016; **17**: 722–735.

130 Komatsu H, Chao MY, Larkins-Ford J, Corkins ME, Somers GA, Tucey T *et al.* OSM-11 Facilitates LIN-12 Notch Signaling during Caenorhabditis elegans Vulval Development. *PLoS Biol* 2008; **6**: e196.

131 Ayaz F, Osborne BA. Non-Canonical Notch Signaling in Cancer and Immunity. *Front Oncol* 2014; **4**. doi:10.3389/fonc.2014.00345.

132 Spina V, Rossi D. Molecular pathogenesis of splenic and nodal marginal zone lymphoma. *Best Pract Res Clin Haematol* 2017; **30**: 5–12.

133 Kuroda K, Han H, Tani S, Tanigaki K, Tun T, Furukawa T *et al.* Regulation of Marginal Zone B Cell Development by MINT, a Suppressor of Notch/RBP-J Signaling Pathway. *Immunity* 2003; **18**: 301–312.

134 Saito T, Chiba S, Ichikawa M, Kunisato A, Asai T, Shimizu K *et al.* Notch2 Is Preferentially Expressed in Mature B Cells and Indispensable for Marginal Zone B Lineage Development. *Immunity* 2003; **18**: 675–685.

135 Jallades L, Baseggio L, Sujobert P, Huet S, Chabane K, Callet-Bauchu E *et al.* Exome sequencing identifies recurrent BCOR alterations and the absence of KLF2, TNFAIP3 and MYD88 mutations in splenic diffuse red pulp small B-cell lymphoma. *Haematologica* 2017;

102: 1758–1766.

136 Spina V, Khiabanian H, Messina M, Monti S, Cascione L, Bruscaggin A *et al.* The genetics of nodal marginal zone lymphoma. *Blood* 2016; **128**: 1362–1373.

137 Campos-Martín Y, Martínez N, Martínez-López A, Cereceda L, Casado F, Algara P *et al.* Clinical and diagnostic relevance of NOTCH2-and KLF2-mutations in splenic marginal zone lymphoma. *Haematologica* 2017; **102**: e310–e312.

138 Kiel MJ, Velusamy T, Betz BL, Zhao L, Weigelin HG, Chiang MY *et al.* Whole-genome sequencing identifies recurrent somatic NOTCH2 mutations in splenic marginal zone lymphoma. *J Exp Med* 2012; **209**: 1553–1565.

139 Johansson P, Klein-Hitpass L, Grabellus F, Arnold G, Klapper W, Pförtner R *et al.* Recurrent mutations in NF-κB pathway components, KMT2D, and NOTCH1/2 in ocular adnexal MALT-type marginal zone lymphomas. *Oncotarget* 2016; **7**: 62627–62639.

140 Li J, Li J, Yang X, Qin H, Zhou P, Liang Y *et al.* The C terminus of MINT forms homodimers and abrogates MINT-mediated transcriptional repression. *Biochim Biophys Acta BBA - Gene Struct Expr* 2005; **1729**: 50–56.

141 VanderWielen BD, Yuan Z, Friedmann DR, Kovall RA. Transcriptional repression in the Notch pathway: thermodynamic characterization of CSL-MINT (Msx2-interacting nuclear target protein) complexes. *J Biol Chem* 2011; **286**: 14892–14902.

142 Rossi D, Trifonov V, Fangazio M, Bruscaggin A, Rasi S, Spina V *et al.* The coding genome of splenic marginal zone lymphoma: activation of NOTCH2 and other pathways regulating marginal zone development. *J Exp Med* 2012; **209**: 1537–1551.

143 Baylin SB, Jones PA. A decade of exploring the cancer epigenome — biological and translational implications. *Nat Rev Cancer* 2011; **11**: 726–734.

144 You JS, Jones PA. Cancer Genetics and Epigenetics: Two Sides of the Same Coin? *Cancer Cell* 2012; **22**: 9–20.

145 Garraway LA, Lander ES. Lessons from the Cancer Genome. *Cell* 2013; **153**: 17–37.

146 Shen H, Laird PW. Interplay Between the Cancer Genome and Epigenome. *Cell* 2013; **153**: 38–55.

147 Phillips T, Shaw K. Chromatin Remodeling in Eukaryotes | Learn Science at Scitable. *Nat Educ*; **1**: 209.

148 Jung H, Yoo HY, Lee SH, Shin S, Kim SC, Lee S *et al.* The mutational landscape of ocular marginal zone lymphoma identifies frequent alterations in TNFAIP3 followed by mutations in TBL1XR1 and CREBBP. *Oncotarget* 2017; **8**: 17038–17049.

149 Fontes JD, Kanazawa S, Jean D, Peterlin BM. Interactions between the Class II Transactivator and CREB Binding Protein Increase Transcription of Major Histocompatibility Complex Class II

Genes. *Mol Cell Biol* 1999; **19**: 941–947.

150 Forbes SA, Beare D, Gunasekaran P, Leung K, Bindal N, Boutselakis H *et al.* COSMIC: exploring the world's knowledge of somatic mutations in human cancer. *Nucleic Acids Res* 2015; **43**: D805–D811.

151 Martínez N, Almaraz C, Vaqué JP, Varela I, Derdak S, Beltran S *et al.* Whole-exome sequencing in splenic marginal zone lymphoma reveals mutations in genes involved in marginal zone differentiation. *Leukemia* 2014; **28**: 1334–1340.

152 Baylin SB, Jones PA. Epigenetic Determinants of Cancer. *Cold Spring Harb Perspect Biol* 2016; **8**: a019505.

153 Mazzaro C, Franzin F, Tulissi P, Pussini E, Crovatto M, Carniello GS *et al.* Regression of monoclonal B-cell expansion in patients affected by mixed cryoglobulinemia responsive to alpha-interferon therapy. *Cancer* 1996; **77**: 2604–2613.

154 Arcaini L, Vallisa D, Merli M. Hematological response to antiviral therapy in 94 patients with indolent B-cell lymphomas associated with hepatitis C virus infection: a study of the Fondazione Italiana Linfomi (FIL). *Ann Oncol* 2011; **22**: 128–129.

155 Zucca E, Conconi A, Martinelli G, Martelli M, Thieblemont C, Johnson PW *et al.* Chlorambucil Plus Rituximab Produces Better Event-Free Survival in Comparison with Chlorambucil Alone in the Treatment of MALT Lymphoma: 5-Year Analysis of the 2-Arms Part of the IELSG-19 Randomized Study. *Blood* 2010; **116**: 432–432.

156 Goteri G, Ranaldi R, Simonetti O, Capretti R, Menzo S, Stramazzotti D *et al.* Clinicopathological features of primary cutaneous B-cell lymphomas from an academic regional hospital in central Italy: No evidence of Borrelia burgdorferi association. *Leuk Lymphoma* 2007; **48**: 2184–2188.

157 Mulligan SP, Matutes E, Dearden C, Catovsky D. Splenic lymphoma with villous lymphocytes: natural history and response to therapy in 50 cases. *Br J Haematol* 1991; **78**: 206–209.

158 Troussard X, Valensi F, Duchayne E, Garand R, Felman P, Tulliez M *et al.* Splenic lymphoma with villous lymphocytes: clinical presentation, biology and prognostic factors in a series of 100 patients. *Br J Haematol* 1996; **93**: 731–736.

159 Thieblemont C, Felman P, Berger F, Dumontet C, Arnaud P, Hequet O *et al.* Treatment of Splenic Marginal Zone B-Cell Lymphoma: An Analysis of 81 Patients. *Clin Lymphoma* 2002; **3**: 41–47.

160 Chacón JI, Mollejo M, Muñoz E, Algara P, Mateo M, Lopez L *et al.* Splenic marginal zone lymphoma: clinical characteristics and prognostic factors in a series of 60 patients. *Blood* 2002; **100**: 1648–1654.

161 Thieblemont C, Berger F, Dumontet C, Moullet I, Bouafia F, Felman P *et al.* Mucosa-associated

lymphoid tissue lymphoma is a disseminated disease in one third of 158 patients analyzed. *Blood* 2000; **95**: 802–806.

162 Radaszkiewicz T, Dragosics B, Bauer P. Gastrointestinal malignant lymphomas of the mucosa-associated lymphoid tissue: factors relevant to prognosis. *Gastroenterology* 1992; **102**: 1628–1638.

163 Zucca E, Conconi A, Pedrinis E, Cortelazzo S, Motta T, Gospodarowicz MK *et al.* Nongastric marginal zone B-cell lymphoma of mucosa-associated lymphoid tissue. *Blood* 2003; **101**: 2489–2495.

164 Qian L, Soderquist C, Schrank-Hacker A, Strauser H, Dupoux V, Tang CN *et al.* Deletion 20q12 is associated with histological transformation of nodal marginal zone lymphoma to diffuse large B-cell lymphoma. *Am J Hematol* 2020; **95**: 238–244.

165 Camacho FI, Mollejo M, Mateo M-S, Algara P, Navas C, Hernández J-M *et al.* Progression to Large B-Cell Lymphoma in Splenic Marginal Zone Lymphoma: A Description of a Series of 12 Cases. *Am J Surg Pathol* 2001; **25**: 1268–1276.

166 Thieblemont C. Clinical Presentation and Management of Marginal Zone Lymphomas. *Hematology* 2005; **2005**: 307–313.

167 Thieblemont C, Bastion Y, Berger F, Rieux C, Salles G, Dumontet C. Mucosa-associated lymphoid tissue gastrointestinal and nongastrointestinal lymphoma behavior: analysis of 108 patients. | Journal of Clinical Oncology. *J Clin Oncol* 1997; **15**: 1624–1630.

168 Ye H, Liu H, Attygalle A, Wotherspoon AC, Nicholson AG, Charlotte F *et al.* Variable frequencies of t(11;18)(q21;q21) in MALT lymphomas of different sites: significant association with CagA strains of H pylori in gastric MALT lymphoma. *Blood* 2003; **102**: 1012–1018.

169 Rollinson S, Levene AP, Mensah FK, Roddam PL, Allan JM, Diss TC *et al.* Gastric marginal zone lymphoma is associated with polymorphisms in genes involved in inflammatory response and antioxidative capacity. *Blood* 2003; **102**: 1007–1011.

170 Liu H, Ye H, Ruskone-Fourmestraux A, De Jong D, Pileri S, Thiede C *et al.* T(11;18) is a marker for all stage gastric MALT lymphomas that will not respond to H. pylori eradication. *Clin Cancer Res Off J Am Assoc Cancer Res* 2002; **122**: 1286–1294.

171 Kuo S-H, Chen L-T, Yeh K-H, Wu M-S, Hsu H-C, Yeh P-Y *et al.* Nuclear Expression of BCL10 or Nuclear Factor Kappa B Predicts Helicobacter pylori–Independent Status of Early-Stage, High-Grade Gastric Mucosa-Associated Lymphoid Tissue Lymphomas | Journal of Clinical Oncology. https://ascopubs.org/doi/10.1200/JCO.2004.10.087?url_ver=Z39.88-2003&rfr_id=ori:rid:crossref.org&rfr_dat=cr_pub%20%200pubmed (accessed 28 Jun2021).

172 Ye H, Gong L, Liu H, Ruskone‐Fourmestraux A, de Jong D, Pileri S *et al.* Strong BCL10

nuclear expression identifies gastric MALT lymphomas that do not respond to H pylori eradication. *Gut* 2006; **55**: 137–138.

173 Sagaert X, de Paepe P, Libbrecht L, Vanhentenrijk V, Verhoef G, Thomas J *et al.* Forkhead Box Protein P1 Expression in Mucosa-Associated Lymphoid Tissue Lymphomas Predicts Poor Prognosis and Transformation to Diffuse Large B-Cell Lymphoma. *J Clin Oncol* 2006; **24**: 2490–2497.

174 Haralambieva E, Adam P, Ventura R, Katzenberger T, Kalla J, Höller S *et al.* Genetic rearrangement of FOXP1 is predominantly detected in a subset of diffuse large B-cell lymphomas with extranodal presentation. *Leukemia* 2006; **20**: 1300–1303.

175 Shembade N, Harhaj EW. Regulation of NF-κB signaling by the A20 deubiquitinase. *Cell Mol Immunol* 2012; **9**: 123–130.

176 Yan Q, Wang M, Moody S, Xue X, Huang Y, Bi Y *et al.* Distinct involvement of NF-κB regulators by somatic mutation in ocular adnexal malt lymphoma. *Br J Haematol* 2013; **160**: 851–854.

177 Lee EG, Boone DL, Chai S, Libby SL, Chien M, Lodolce JP *et al.* Failure to Regulate TNF-Induced NF-κB and Cell Death Responses in A20-Deficient Mice. *Science* 2000; **289**: 2350–2354.

178 Zhu D, Ikpatt OF, Dubovy SR, Lossos C, Natkunam Y, Chapman-Fredricks JR *et al.* Molecular and Genomic Aberrations in Chlamydophila psittaci Negative Ocular Adnexal Marginal Zone Lymphomas. *Am J Hematol* 2013; **88**: 730–735.

179 Johansson P, Klein-Hitpass L, Budeus B, Kuhn M, Lauber C, Seifert M *et al.* Identifying Genetic Lesions in Ocular Adnexal Extranodal Marginal Zone Lymphomas of the MALT Subtype by Whole Genome, Whole Exome and Targeted Sequencing. *Cancers* 2020; **12**. doi:10.3390/cancers12040986.

180 Bi Y, Zeng N, Chanudet E, Huang Y, Hamoudi RA, Liu H *et al.* A20 inactivation in ocular adnexal MALT lymphoma. *Haematologica* 2012; **97**: 926–930.

181 Chanudet E, Huang Y, Ichimura K, Dong G, Hamoudi RA, Radford J *et al.* A20 is targeted by promoter methylation, deletion and inactivating mutation in MALT lymphoma. *Leukemia* 2010; **24**: 483–487.

182 Zhu J, Wei RL, Pi YL, Guo Q. Significance of Bcl10 gene mutations in the clinical diagnosis of MALT-type ocular adnexal lymphoma in the Chinese population. *GMR Genet Mol Res Orig FUNPEC-RP* 2015; **12**: 1194–1204.

183 Ponzoni M, Ferreri AJM. Bacteria associated with marginal zone lymphomas. *Best Pract Res Clin Haematol* 2017; **30**: 32–40.

184 Cerrone M, Collina F, De Chiara A, Corazzelli G, Curcio MP, De Renzo A *et al.* BCL10

expression and localization in ocular adnexa MALT lymphomas: a comparative cytogenetic and immunohistochemical study. *Histol Histopathol* 2014; **29**: 77–87.

185 Franco R, Camacho FI, Caleo A, Staibano S, Bifano D, De Renzo A *et al.* Nuclear bcl10 expression characterizes a group of ocular adnexa MALT lymphomas with shorter failure-free survival. *Mod Pathol* 2006; **19**: 1055–1067.

186 Biernat MM, Wróbel T. Bacterial Infection and Non-Hodgkin B-Cell Lymphoma: Interactions between Pathogen, Host and the Tumor Environment. *Int J Mol Sci* 2021; **22**: 7372.

187 Cerhan JR, Habermann TM. Epidemiology of marginal zone lymphoma. *Ann Lymphoma* 2021; **5**. doi:10.21037/aol-20-28.

188 Sassone M, Ponzoni M, Ferreri AJM. Ocular adnexal marginal zone lymphoma: Clinical presentation, pathogenesis, diagnosis, prognosis, and treatment. *Best Pract Res Clin Haematol* 2017; **30**: 118–130.

189 Collina F, De Chiara A, De Renzo A, De Rosa G, Botti G, Franco R. Chlamydia psittaci in ocular adnexa MALT lymphoma: a possible role in lymphomagenesis and a different geographical distribution. *Infect Agent Cancer* 2012; **7**: 8.

190 Ferreri AJM, Guidoboni M, Ponzoni M, De Conciliis C, Dell'Oro S, Fleischhauer K *et al.* Evidence for an Association Between Chlamydia psittaci and Ocular Adnexal Lymphomas. *JNCI J Natl Cancer Inst* 2004; **96**: 586–594.

191 Decaudin D, Dolcetti R, de Cremoux P, Ponzoni M, Vincent-Salomon A, Doglioni C *et al.* Variable association between Chlamydophila psittaci infection and ocular adnexal lymphomas: methodological biases or true geographical variations? *Anticancer Drugs* 2008; **19**: 761–765.

192 Takahashi H, Usui Y, Ueda S, Yamakawa N, Sato-Otsubo A, Sato Y *et al.* Genome-Wide Analysis of Ocular Adnexal Lymphoproliferative Disorders Using High-Resolution Single Nucleotide Polymorphism Array. *Invest Ophthalmol Vis Sci* 2015; **56**: 4156–4165.

193 Lee MJ, Kim N, Choe J-Y, Khwarg SI, Jeon YK, Choung H-K *et al.* Clinicopathological Analysis of Ocular Adnexal Extranodal Marginal Zone B-Cell Lymphoma with IgG4-Positive Cells. *PLoS ONE* 2015; **10**: e0131458.

194 Annibali O, Sabatino F, Mantelli F, Olimpieri OM, Bonini S, Avvisati G. Review article: Mucosa-associated lymphoid tissue (MALT)-type lymphoma of ocular adnexa. Biology and treatment. *Crit Rev Oncol Hematol* 2016; **100**: 37–45.

195 Chen LYC, Mattman A, Seidman MA, Carruthers MN. IgG4-related disease: what a hematologist needs to know. *Haematologica* 2019; **104**: 444–455.

196 Deshpande V, Zen Y, Chan JK, Yi EE, Sato Y, Yoshino T *et al.* Consensus statement on the pathology of IgG4-related disease. *Mod Pathol* 2012; **25**: 1181–1192.

197 Sohn EJ, Ahn HB, Roh MS, Jung WJ, Ryu WY, Kwon YH. Immunoglobulin G4 (IgG4)-Positive

Ocular Adnexal Mucosa-Associated Lymphoid Tissue Lymphoma and Idiopathic Orbital Inflammation. *Ophthal Plast Reconstr Surg* 2018; **34**: 313–319.

198 Garner A. Orbital lymphoproliferative disorders. *Br J Ophthalmol* 1992; **76**: 47–48.

199 Borie R, Wislez M, Antoine M, Cadranel J. Lymphoproliferative Disorders of the Lung - FullText - Respiration 2017, Vol. 94, No. 2 - Karger Publishers. *Respiration* 2017; **94**: 157–175.

200 Zhang J, Dominguez-Sola D, Hussein S, Lee J-E, Holmes AB, Bansal M *et al.* Disruption of KMT2D perturbs germinal center B cell development and promotes lymphomagenesis. *Nat Med* 2015; **21**: 1190–1198.

201 Juskevicius D, Jucker D, Klingbiel D, Mamot C, Dirnhofer S, Tzankov A. Mutations of CREBBP and SOCS1 are independent prognostic factors in diffuse large B cell lymphoma: mutational analysis of the SAKK 38/07 prospective clinical trial cohort. *J Hematol OncolJ Hematol Oncol* 2017; **10**: 70.

202 Ortega-Molina A, Boss IW, Canela A, Pan H, Jiang Y, Zhao C *et al.* The histone lysine methyltransferase KMT2D sustains a gene expression program that represses B cell lymphoma development. *Nat Med* 2015; **21**: 1199–1208.

203 Alam H, Tang M, Maitituoheti M, Dhar SS, Kumar M, Han CY *et al.* KMT2D deficiency impairs super-enhancers to confer a glycolytic vulnerability in lung cancer. *Cancer Cell* 2020; **37**: 599-617.e7.

204 Green MR. Chromatin modifying gene mutations in follicular lymphoma. *Blood* 2018; **131**: 595–604.

205 Miletic AV, Anzelon-Mills AN, Mills DM, Omori SA, Pedersen IM, Shin D-M *et al.* Coordinate suppression of B cell lymphoma by PTEN and SHIP phosphatases. *J Exp Med* 2010; **207**: 2407–2420.

206 Zhan H, Bai Y, Lv Y, Zhang X, Zhang L, Deng S. Pharmacological mechanism of mylabris in the treatment of leukemia based on bioinformatics and systematic pharmacology. *Bioengineered* 2021; **12**: 3229–3239.

207 Suzuki A, Sasaki T, Mak TW, Nakano T. Functional analysis of the tumour suppressor gene PTEN in murine B cells and keratinocytes. *Biochem Soc Trans* 2004; **32**: 362–365.

208 Naderi NJ, Eshghyar N, Esfehanian H. Reactive lesions of the oral cavity: A retrospective study on 2068 cases. *Dent Res J* 2012; **9**: 251–255.

209 Mutation overview page LAMA5 - p.G1927V (Substitution - Missense). https://cancer.sanger.ac.uk/cosmic/mutation/overview?id=96858635 (accessed 3 Aug2021).

210 Wang X, Cao X, Sun R, Tang C, Tzankov A, Zhang J *et al.* Clinical Significance of PTEN Deletion, Mutation, and Loss of PTEN Expression in De Novo Diffuse Large B-Cell Lymphoma. *Neoplasia N Y N* 2018; **20**: 574–593.

211 Zhu Z, Liu W, Mamlouk O, O'Donnell JE, Sen D, Avezbakiyev B. Primary Pulmonary Diffuse Large B Cell Non-Hodgkin's Lymphoma: A Case Report and Literature Review. *Am J Case Rep* 2017; **18**: 286–290.

212 Cardenas-Garcia J, Talwar A, Shah R, Fein A. Update in primary pulmonary lymphomas. *Curr Opin Pulm Med* 2015; **21**: 333–337.

213 Steidl C, Gascoyne RD. The molecular pathogenesis of primary mediastinal large B-cell lymphoma. *Blood* 2011; **118**: 2659–2669.

214 Weissferdt A. *Diagnostic Thoracic Pathology*. 1st ed. Springer International Publishing, 2020 doi:10.1007/978-3-030-36438-0.

215 Piña-Oviedo S, Weissferdt A, Kalhor N, Moran CA. Primary Pulmonary Lymphomas. *Adv Anat Pathol* 2015; **22**: 355–375.

216 Liebow AA, Carrington CRB, Friedman PJ. Lymphomatoid granulomatosis. *Hum Pathol* 1972; **3**: 457–558.

217 Melani C, Jaffe ES, Wilson WH. Pathobiology and treatment of lymphomatoid granulomatosis, a rare EBV-driven disorder. *Blood* 2020; **135**: 1344–1352.

218 Sanguedolce F, Zanelli M, Zizzo M, Bisagni A, Soriano A, Cocco G *et al.* Primary Pulmonary B-Cell Lymphoma: A Review and Update. *Cancers* 2021; **13**: 415.

219 Dunleavy K, Roschewski M, Wilson WH. Lymphomatoid Granulomatosis and Other Epstein-Barr Virus Associated Lymphoproliferative Processes. *Curr Hematol Malig Rep* 2012; **7**: 208–215.

220 Gross R, Guzman CA, Sebaihia M, Martins dos Santos VA, Pieper DH, Koebnik R *et al.* The missing link: Bordetella petrii is endowed with both the metabolic versatility of environmental bacteria and virulence traits of pathogenic Bordetellae. *BMC Genomics* 2008; **9**: 449.

221 McLaren W, Gil L, Hunt SE, Riat HS, Ritchie GRS, Thormann A *et al.* The Ensembl Variant Effect Predictor. *Genome Biol* 2016; **17**. doi:10.1186/s13059-016-0974-4.

222 Wang K, Li M, Hakonarson H. ANNOVAR: functional annotation of genetic variants from high-throughput sequencing data. *Nucleic Acids Res* 2010; **38**: e164.

223 Arcaini L, Rossi D, Paulli M. Splenic marginal zone lymphoma: from genetics to management. *Blood* 2016; **127**: 2072–2081.

224 Arasu A, Balakrishnan P, Velusamy T. RNA sequencing analyses reveal differentially expressed genes and pathways as Notch2 targets in B-cell lymphoma. *Oncotarget* 2020; **11**: 4527–4540.

225 Lee SY, Kumano K, Nakazaki K, Sanada M, Yamamoto G, Nannya Y *et al.* Gain-of-Function Mutations and Copy Number Increases of Notch2 in Diffuse Large B-Cell Lymphoma. *Blood* 2007; **110**: 695–695.

226 Winkelmann R, Sandrock L, Porstner M, Roth E, Mathews M, Hobeika E *et al.* B cell

homeostasis and plasma cell homing controlled by Krüppel-like factor 2. *Proc Natl Acad Sci U S A* 2011; **108**: 710–715.

227 Hampel F, Ehrenberg S, Hojer C, Draeseke A, Marschall-Schröter G, Kühn R *et al.* CD19-independent instruction of murine marginal zone B-cell development by constitutive Notch2 signaling. *Blood* 2011; **118**: 6321–6331.

228 Sharma A, Trivedi NR, Zimmerman MA, Tuveson DA, Smith CD, Robertson GP. Mutant V599EB-Raf regulates growth and vascular development of malignant melanoma tumors. *Cancer Res* 2005; **65**: 2412–2421.

229 Ganapathi KA, Jobanputra V, Iwamoto F, Jain P, Chen J, Cascione L *et al.* The genetic landscape of dural marginal zone lymphomas. *Oncotarget* 2016; **7**: 43052–43061.

230 Ko M, Huang Y, Jankowska AM, Pape UJ, Tahiliani M, Bandukwala HS *et al.* Impaired hydroxylation of 5-methylcytosine in myeloid cancers with mutant TET2. *Nature* 2010; **468**: 839–843.

231 Maurus K, Appenzeller S, Roth S, Kuper J, Rost S, Meierjohann S *et al.* Panel Sequencing Shows Recurrent Genetic FAS Alterations in Primary Cutaneous Marginal Zone Lymphoma. *J Invest Dermatol* 2018; **138**: 1573–1581.

232 Zhang J, Manley JL. Misregulation of pre-mRNA alternative splicing in cancer. *Cancer Discov* 2013; **3**: 1228–37.

233 Crotty R, Hu K, Stevenson K, Pontius MY, Sohani AR, Ryan RJH *et al.* Simultaneous Identification of Cell of Origin, Translocations, and Hotspot Mutations in Diffuse Large B-Cell Lymphoma Using a Single RNA-Sequencing Assay. *Am J Clin Pathol* 2021; **155**: 748–754.

234 Juskevicius D, Lorber T, Gsponer J, Perrina V, Ruiz C, Stenner-Liewen F *et al.* Distinct genetic evolution patterns of relapsing diffuse large B-cell lymphoma revealed by genome-wide copy number aberration and targeted sequencing analysis. *Leukemia* 2016; **30**: 2385–2395.

235 Ansell SM. DNA methylation in lymphoma: an opportunity? *Blood* 2015; **125**: 1848–1849.

236 Arribas AJ, Rinaldi A, Mensah AA, Kwee I, Cascione L, Robles EF *et al.* DNA methylation profiling identifies two splenic marginal zone lymphoma subgroups with different clinical and genetic features. *Blood* 2015; **125**: 1922–1931.

237 Vela V, Juskevicius D, Prince SS, Cathomas G, Dertinger S, Diebold J *et al.* Deciphering the genetic landscape of pulmonary lymphomas. *Mod Pathol* 2021; **34**: 371–379.

238 Arribas AJ, Bertoni F. Methylation patterns in marginal zone lymphoma. *Best Pract Res Clin Haematol* 2017; **30**: 24–31.

239 Huang Q, Su X, Ai L, Li M, Fan C-Y, Weiss LM. Promoter hypermethylation of multiple genes in primary gastric lymphoma. *Leuk Lymphoma* 2007; **48**: 1988–1996.

240 Carugi A, Onnis A, Antonicelli G, Rossi B, Mannucci S, Luzzi A *et al.* Geographic variation and

environmental conditions as cofactors in Chlamydia psittaci association with ocular adnexal lymphomas: a comparison between Italian and African samples. *Hematol Oncol* 2010; **28**: 20–26.

241 Choung H-K, Kim YA, Lee MJ, Kim N, Khwarg SI. Multigene Methylation Analysis of Ocular Adnexal MALT Lymphoma and Their Relationship to Chlamydophila psittaci Infection and Clinical Characteristics in South Korea. *Invest Ophthalmol Vis Sci* 2012; **53**: 1928–1935.

242 Martinez-Delgado B, Fernandez-Piqueras J, Garcia MJ, Arranz E, Gallego J, Rivas C *et al.* Hypermethylation of a 5′ CpG island of p16 is a frequent event in non-Hodgkin's lymphoma. *Leukemia* 1997; **11**: 425–428.

243 Lee MJ, Min B-J, Choung H-K, Kim N, Kim YA, Khwarg SI. Genome-wide DNA methylation profiles according to Chlamydophila psittaci infection and the response to doxycycline treatment in ocular adnexal lymphoma. *Mol Vis* 2014; **20**: 1037–1047.

244 Takino H, Okabe M, Li C, Ohshima K, Yoshino T, Nakamura S *et al.* p16/INK4a gene methylation is a frequent finding in pulmonary MALT lymphomas at diagnosis. *Mod Pathol* 2005; **18**: 1187–1192.

245 Park S, Kim K-M, Kim JJ, Lee J-H, Rhee J-C, Ko Y-H. Methylation of p16INK4A and Mitotic Arrest Defective Protein 2 (MAD2) Genes in Gastric Marginal-Zone B-Cell Lymphomas. *Acta Haematol* 2008; **120**: 217–224.

246 Min KO, Seo EJ, Kwon HJ, Lee EJ, Kim WI, Kang CS *et al.* Methylation of p16INK4A and p57KIP2 are involved in the development and progression of gastric MALT lymphomas. *Mod Pathol* 2006; **19**: 141–148.

247 Martinez-Delgado B, Robledo M, Arranz E, Osorio A, García MJ, Echezarreta G *et al.* Hypermethylation of p15/ink4b/MTS2 gene is differentially implicated among non-Hodgkin's lymphomas. *Leukemia* 1998; **12**: 937–941.

248 Sinn DH, Kim Y-H, Lee EJ, Ko Y-H, Kim K-M. Methylation and API2/MALT1 fusion in colorectal extranodal marginal zone lymphoma. *Mod Pathol* 2009; **22**: 314–320.

FIGURE INDEX

GLOSSARY

Activation-induced cytidine deaminase (AID). An enzyme that removes an amino group from deoxycytidine, forming deoxyuridine. This is the first step in the processes of both somatic hypermutation and class switch recombination.

Adaptive immunity. Host defenses mediated by B-cells and T-cells following exposure to antigen exhibit specificity, diversity, memory, and self-nonself discrimination.

Antibodies. Immunoglobulin proteins consisting of two identical heavy chains and two identical light chains that recognize a particular epitope on an antigen and facilitates clearance of that antigen. Membrane-bound antibody is expressed by B-cells that have not encountered antigen; secreted antibody is produced by plasma cells. Some antibodies are multiples of the basic four-chain structure.

Antigen. Any substance (usually foreign) that binds specifically to an antibody or a T-cell receptor; often is used as a synonym for immunogen.

Apoptosis. A process often referred to as programmed cell death, where cells initiate a signaling pathway that results in their own demise. Apoptosis requires ATP and is typically dependent on the activation of internal caspases.

Autoimmune diseases. A group of disorders caused by the action of one's own antibodies or T-cells reactive against self-proteins.

B-cell receptor (BCR). Complex comprising a membrane-bound Ig molecule and two associated signal-transducing Ig /Ig molecules.

B-lymphocytes (B-cells). Lymphocytes that mature in the bone marrow and express membrane-bound antibodies. After interacting with antigen, they differentiate into antibody-secreting plasma cells and memory cells.

BAFF. B-cell survival factor; a membrane-bound homolog of tumor necrosis factor, to which mature B-cells bind through the TACI receptor. This interaction activates important transcription factors that promote B-cell survival, maturation, and antibody secretion.

BAFF receptor (BAFFR). Receptor for BAFF, a cytokine belonging to the tumor necrosis factor family that is important in B-cell development and homeostasis.

Benign. Pertaining to a non-malignant form of a neoplasm or a mild form of an illness.

Bone marrow. The living tissue found within the hard exterior of the bone.

Bronchus-associated lymphoid tissue (BALT). Secondary lymphoid microenvironments in the lung mucosa system that support the development of the T- and B-lymphocyte response to antigens that enter the lower respiratory tract. Part of the mucosa-associated lymphoid tissue system (MALT).

Chemokines. Any of several secreted low-molecular-weight cytokines that mediate chemotaxis in particular leukocytes via receptor engagement and that can regulate the expression and/or adhesiveness of leukocyte integrins.

Class. The property of an antibody defined by the nature of its heavy chain (μ, δ, γ, or ε).

Class (isotype) switching. The change in the antibody class that a B-cell produces.

Class II MHC genes. The set of genes that encode class II MHC molecules, which are glycoproteins expressed by only professional antigen-presenting cells.

Class switch recombination (CSR). The generation of antibody genes for heavy chain isotypes other than or by DNA recombination.

Cluster of differentiation (CD). A collection of monoclonal antibodies that all recognize an antigen found on a particular differentiated cell type or types. Each of the antigens recognized by such a collection of antibodies is called a CD marker and is assigned a unique identifying number.

Constant (CL). That part of the light chain that is not variable in sequence.

Constant (C) region. The nearly invariant portion of the Ig molecule that does not contain antigen-binding domains. The sequence of amino acids in the constant region determines the isotype (α, γ, δ, ε, and μ) of heavy chains and the type (κ and λ) of light chains.

Cytokines. Any of numerous secreted, low-molecular-weight proteins that regulate the intensity and duration of the immune response by exerting a variety of effects on lymphocytes and other immune cells that express the appropriate receptor.

Diversity (D) segment. One of the gene segments encoding the Ig heavy chain or the TCR β or δ chains or its protein product.

Downstream. (1) Towards the 3' end of a gene; (2) Further away from the receptor in a signaling cascade.

E2A. A transcription factor required for the expression of the recombination-activating genes (*RAG*) and the expression of the λ5 (lambda 5) component of the pre-B-cell receptor during B-cell development. It is essential for B-cell development.

Early B-cell factor (EBF). A transcription factor that is essential for early B-cell development. It is necessary for the expression of RAG.

Effector cell. Any cell capable of mediating an immune function.

Epitope. The portion of an antigen that is recognized and bound by an antibody or TCR-MHC combination; also called antigenic determinant.

***FAS* (CD95).** A member of the Tumor Necrosis Factor Receptor family. On binding to its ligand, FasL, the Fas-bearing cell will often be induced to commit to an apoptotic program. Occasionally, however, Fas ligation leads to cell proliferation.

Follicles. Microenvironments that specifically support the development of the B-lymphocyte response in lymph nodes, spleen, and other secondary lymphoid tissue. They also become the site of development of the germinal center when a B-cell is successfully activated.

Gene segments. Germ-line gene sequences that are combined with others to make a complete coding sequence; Ig and TCR genes are products of V, D, J gene segments.

Heavy (H) chain. The larger polypeptide of an antibody molecule; it is composed of one variable domain V_H and three or four constant domains (C_H1, C_H2, etc.) There are five major classes of heavy chains in humans (α, γ, δ, ε, and μ), which determine the isotype of an antibody.

Heavy-chain Joining segment (J_H). One of the gene segments encoding the Ig heavy chain or its protein product.

Heavy-chain Variable region. That part of the Ig heavy chain protein that varies from antibody to antibody and is encoded by the V, D, and J gene segments.

Heavy-chain Variable segment (VH). One of the gene segments encoding the Ig heavy chain gene, or its protein product.

Hematopoiesis. The formation and differentiation of blood cells.

Hematopoietic stem cell (HSC). The cell type from which all lineages of blood cells arise.

Heptamer. A conserved set of 7 nucleotides contiguous to each of the V, D, and J gene segments of all Ig and TCR gene segments. It serves as the recognition signal and binding site of the *RAG1/2* protein complex.

Human immunodeficiency virus (HIV). The retrovirus that causes acquired immunodeficiency syndrome (AIDS).

IgD. Ig D. An antibody class that serves importantly as a receptor on naïve B-cells. IgM Immunoglobulin M. An antibody class that serves as a receptor on naïve B-cells.

IgM. is also the first class of antibody to be secreted during the course of an immune response. Secreted IgM exists primarily in pentameric form.

IL-7 receptor. Receptor for the cytokine Interleukin 7, which is important for lymphocyte development.

Immature B-cell. Immature B-cells express a fully-formed IgM receptor on their cell surface. Contact with antigen at this stage of B-cell development results in tolerance induction rather than activation. Immature B-cells express lower levels of IgD and higher levels of IgM than do mature B-cells. They also have lower levels of anti-apoptotic molecules and higher levels of *FAS* than mature B-cells, reflective of their short-half lives.

Immunoglobulin (Ig). Protein consisting of two identical heavy chains and two identical light chains that recognize a particular epitope on an antigen and facilitates clearance of that antigen. There are 5 types: IgA, IgD, IgE, IgG, and IgM. Also called antibody.

Inflammation. Tissue response to infection or damage which serves to eliminate or wall-off the infection or damage; classic signs of acute inflammation are heat, pain, redness, swelling (tumor), and loss of function.

Inhibitor of NF-κB (IκB). A small protein that binds to the transcription factor NF-κB that inhibits its action, in part by retaining it in the cytoplasm.

Innate immunity. Non-antigen-specific host defenses that exist prior to exposure to an antigen and involve anatomic, physiologic, endocytic and phagocytic, anti-microbial, and inflammatory mechanisms, and which exhibit no adaptation or memory characteristics. See also adaptive immunity.

Integrins. A group of heterodimeric cell adhesion molecules (e.g., LFA-1, VLA-4, and Mac-1) present on various leukocytes that bind to Ig-superfamily CAMs (e.g., ICAMs, VCAM-1) on endothelium.

Interferons (IFNs). Several glycoprotein cytokines produced and secreted by certain cells that induce an antiviral state in other cells and also help to regulate the immune response.

Interleukins (ILs). A group of cytokines secreted by leukocytes that primarily affect the growth and differentiation of various hematopoietic and immune system cells.

Invariant NKT (iNKT) cells. A cytotoxic T-cell subset that develops in the thymus and expresses very limited TCR receptor diversity (one specific TCR paired with only a few TCR chains) and recognize lipids associated with CD1, an MHC-like molecule.

Isotype. (1) An antibody class that is determined by the constant-region sequence of the heavy chain. The five human isotypes, designated IgA, IgD, IgE, IgG, and IgM, exhibit structural and functional differences. Also refers to the set of isotypic determinants that is carried by all members of a species. (2) One of the five major kinds of heavy chains in antibody molecules (α, γ, δ, ε, and μ).

Isotype switching. Conversion of one antibody class (isotype) to another resulting from the genetic rearrangement of heavy-chain constant-region genes in B-cells; also called class switching.

IκB kinase (IKK). The enzyme that phosphorylates the inhibitory subunit of the transcription factor NF- B. Phosphorylation of IκB results in its release from the transcription factor and movement of the transcription factor into the nucleus.

J (joining) chain. A polypeptide that links the heavy chains of monomeric units of polymeric IgM and di- or trimeric IgA. The linkage is by disulfide bonds between the J chain and the carboxyl-terminal cysteines of IgM or IgA heavy chains.

J (joining) gene segment. The part of a rearranged Ig or T-cell receptor gene that joins the variable region to the constant region and encodes part of the hypervariable region. There are multiple J gene segments in germ-line DNA, but gene rearrangement leaves only one in each functional rearranged gene.

Janus Activated Kinase (JAK). Kinase that typically transduces a signal from a Type 1 or Type 2 cytokine receptor to a cytoplasmically-located transcription factor belonging to the STAT (Signal Transducer and Activator of Transcription) family. On cytokine binding to the receptor, the JAK kinases are activated and phosphorylate the receptor molecule. This provides docking sites for a pair of STAT molecules which are phosphorylated, dimerize, and translocate to the nucleus to affect their transcriptional programs.

Joining (J) segment. One of the gene segments encoding the Ig heavy or light chain or any of the four TCR chains or its protein product.

Kappa (κ) light chain. One of the two types of Ig light chains that join with heavy chains to form the B-cell receptor and antibody heterodimer. Lambda (λ) is the other type.

Lambda (λ) chain. One of the two types of Ig light chains that join with heavy chains to form the B-cell receptor and antibody heterodimer. Kappa (κ) is the other type.

Late pre-B-cell stage. At the late pre-B-cell stage, the pre-B-cell receptor is lost from the B-cell surface and light chain recombination begins in the genome.

Ligand. A molecule that binds to a receptor.

Light (L) chains. Ig polypeptides of the lambda or kappa type that join with heavy-chain polypeptides to form the antibody heterodimer.

Lipopolysaccharide (LPS). An oligomer of lipid and carbohydrate that constitutes the endotoxin of gram-negative bacteria. LPS acts as a polyclonal activator of murine B-cells, inducing their division and differentiation into antibody-producing plasma cells.

Locus. The specific chromosomal location of a gene.

Lymph node. A small secondary lymphoid organ that contains lymphocytes, macrophages, and dendritic cells and serves as a site for filtration of foreign antigen and for activation and proliferation of lymphocytes.

Lymphocyte. A mononuclear leukocyte that mediates humoral or cell mediated immunity.

Lymphoma. A cancer of lymphoid cells that tends to proliferate as a solid tumor.

Macrophages. Mononuclear phagocytic leukocytes that play roles in adaptive and innate immunity. There are many types of macrophages; some are migratory, whereas others are fixed in tissues.

Major histocompatibility complex (MHC) molecules. Proteins encoded by the major histocompatibility complex and classified as class I, class II, and class III MHC molecules.

Malignant. Refers to cancerous cells capable of uncontrolled growth.

MALT (mucosal-associated lymphoid tissue). Lymphoid cells and tissues organized below the epithelial layer of the body's mucosal surfaces.

Marginal zone. A diffuse region of the spleen, situated on the periphery of the periarteriolar lymphoid sheath (PALS) between the red pulp and white pulp that is rich in B-cells.

Membrane-bound immunoglobulin (mIg). A form of antibody that is bound to a cell as a transmembrane protein. It acts as the antigen-specific receptor of B-cells.

Memory B-cell. An antigen-committed, persistent B-cell. B-cell differentiation results in formation of plasma cells, which secrete antibodies and memory cells, which are involved in the secondary responses.

MYD88. Myeloid differentiation factor 88; adaptor protein that binds to all the IL-1 receptors and all TLRs except *TLR3* and activates downstream signaling.

Necrosis. Morphologic changes that accompany death of individual cells or groups of cells and that release large amounts of intracellular components to the environment, leading to disruption and atrophy of tissue.

Neoplasm. Any new and abnormal growth; a benign or malignant tumor.

Neutrophil. A circulating phagocytic granulocyte involved early in the inflammatory response. It expresses Fc receptors and can participate in antibody-dependent cell-mediated cytotoxicity. Neutrophils are the most numerous white blood cells in the circulation.

NF-κB. An important transcription factor, most often associated with pro-inflammatory responses.

NOTCH. A surface receptor that when bound is cleaved to release a transcriptional regulator that regulates cell fate decisions. *NOTCH* activation is required for T-cell development and determines whether a lymphocyte precursor becomes a B- versus T-cell.

Oncogene, oncogenic. A gene that encodes a protein capable of inducing cellular transformation. Oncogenes derived from viruses are written v-onc; their counterparts (proto-oncogenes) in normal cells are written c-onc.

Pathogen. A disease-causing infectious agent.

Pathogenesis. The means by which disease-causing organisms attack a host.

***PAX5* transcription factor.** A quintessential B-cell transcription factor that controls the expression of many B-cell specific genes.

Periarteriolar lymphoid sheath (PALS). A collar of lymphocytes encasing small arterioles of the spleen.

Peyer's patches. Lymphoid follicles situated along the wall of the small intestine that trap antigens from the gastrointestinal tract and provide sites where B- and T-cells can interact with antigen.

Pre-B-cell checkpoint. Developing B-cells are tested at the pre-B-cell stage to determine whether they can express a functional BCR heavy chain protein, in combination with the VPreB and 5 proteins, to form the pre-B-cell receptor. Those B-cells that fail to form a functional pre-B-cell receptor are eliminated by apoptosis and are referred to as having failed to pass through the pre-B-cell checkpoint.

Pre-B-cell receptor. A complex of the Ig, Ig heterodimer with membrane-bound Ig consisting of the heavy chain bound to the surrogate light chain Vpre-B/ 5.

Pre-T-cell receptor (pre-TCR). A complex of the CD3 group with a structure consisting of the T-cell receptor chain complexed with a 33-kDa glycoprotein called the pre-T chain.

Pre–B-cell (precursor B-cell). The stage of B-cell development that follows the pro-B-cell stage. Pre-B-cells produce cytoplasmic heavy chains, and most display the pre-B-cell receptor.

Pro–B-cell (progenitor B-cell). The earliest distinct cell of the B-cell lineage.

Progenitor cell. A cell that has lost the capacity for self-renewal and is committed to the generation of a particular cell lineage.

***RAG1/2* (recombination-activating genes 1 and 2).** The protein complex of *RAG1* and *RAG2* that catalyzes V(D)J recombination of B- and T-cell receptor genes. These proteins operate in association with a number of other enzymes to bring about the process of recombination, but *RAG1/2*, along with TdT, represent the lymphoid-specific components of the overall enzyme complex.

Receptor. A molecule that specifically binds a ligand.

Recombination signal sequences (RSS). Highly conserved heptamer and nonamer nucleotide sequences that serve as signals for the gene rearrangement process and flank each germ-line V, D, and J segment.

Red pulp. Portion of the spleen consisting of a network of sinusoids populated by macrophages and erythrocytes. It is the site where old and defective red blood cells are destroyed.

Signal joints. In V(D)J gene rearrangement, the nucleotide sequences formed by the union of recombination signal sequences.

Signal Transducer and Activator of Transcription (STAT). Transcription factors that normally reside in the cytoplasm. Phosphorylation of cytokine receptors by Janus Activated Kinases results in the generation of binding sites on those receptors for the STATs, which relocate to the cytoplasmic regions of the receptor and are themselves phosphorylated by JAKs. Phosphorylated STATs dimerize. Phosphorylation and dimerization expose nuclear localization signals, and the STATs move to the nucleus, where they act as transcription factors.

Signaling. Intracellular communication initiated by receptor-ligand interaction.

Spleen. Secondary lymphoid organ where old erythrocytes are destroyed and blood-borne antigens are trapped and presented to lymphocytes in the PALS and marginal zone.

Splenectomy. Surgical removal of the spleen.

Stromal cell. A nonhematopoietic cell that supports the growth and differentiation of hematopoietic cells.

Sub-isotypes. A particular antibody subclass, e.g., IgG1 or IgA2.

Subclasses. Variant sequences of the constant regions of antibodies of the IgG and IgA classes. There are four common variants of IgG and two of IgA in both mice and humans.

Surrogate light chain. The polypeptides Vpre-B and λ5 that associate with heavy chains during the pre-B-cell stage of B-cell development to form the pre-B-cell receptor.

Switch (S) regions. In class switching, DNA sequences located upstream of each C_H segment (except C_δ).

Transformation. Change that a normal cell undergoes as it becomes malignant, normally mediated by DNA alternations; also a permanent, heritable alteration in a cell resulting from the uptake and incorporation of foreign DNA into the genome.

Transgene, transgenic. A cloned foreign gene present in an animal or plant.

Tumor-suppressor genes. Genes that encode products that inhibit excessive cell proliferation or survival. Mutations in these genes are associated with the induction of malignancy.

Ubiquitin. A small signaling peptide that can either tag a protein for destruction by the proteasome, or, under some circumstances, activate that protein.

Upstream. (1) Towards the 5 end of a gene; (2) Closer to the receptor in a signaling cascade.

V (variable) gene segment. The 5' coding portion of rearranged Ig and T-cell receptor genes. There are multiple V gene segments in germ-line DNA, but gene rearrangement leaves only one segment in each functional gene.

V(D)J recombinase. The set of enzymatic activities that collectively bring about the joining of gene segments into a rearranged V(D)J unit.

Variable (V) region. Amino-terminal portions of Ig and T-cell receptor chains that are highly variable and responsible for the antigenic specificity of these molecules.

Variable (V_L). The variable region of an antibody light chain.

Vpre-B. A polypeptide chain that together with λ5 forms the surrogate light chain of the pre-B-cell receptor.

Western blotting. A common technique for detecting a protein in a mixture; the proteins are separated electrophoretically and then transferred to a polymer sheet, which is flooded with radiolabeled or enzyme-conjugated antibody specific for the protein of interest.

White pulp. Portion of the spleen that surrounds the arteries, forming a periarteriolar lymphoid sheath (PALS) populated mainly by T-cells.

LIST OF ABBREVIATIONS

ACVR1/2A/2B	-	Activin A Receptor Type 1/2A/2B
ACVR1B/1C	-	Activin Receptor Type 1B/1C
ACVRL1	-	Activin A Receptor Like Type 1
AID	-	Activation-Induced Cytidine Deaminase
AILD	-	Angioimmunoblastic Lymphadenopathy with Dysproteinemia
AITL	-	Angioimmunoblastic T-cell Lymphoma
AMHR2	-	Anti-Mullerian Hormone Receptor Type 2
ARID1A	-	AT-Rich Interaction Domain 1A
ASM	-	Alpha Smooth Muscle
ATM	-	Ataxia Telangiectasia Mutated
ATP	-	Adenosine triphosphate
B2M	-	Beta 2 Microglobulin
BAFF	-	B-cell Activating Factor
BAFFR	-	B-cell Activating Factor Receptor
BALT/MALT	-	Bronchus-Mucosa Associated Lymphatic Tissue
BCL	-	B-Cell Lymphoma/Leukemia protein
BCR	-	B-Cell Receptor
BL	-	Burkitt Lymphomas
BM	-	Bone Marrow
BMPR2	-	Bone morphogenetic protein receptor type 2
BTLA	-	B and T-cell Lymphocyte Attenuator
CagA	-	Cytotoxin-Associated Gene A
CARD11	-	Caspase Recruitment Domain family member 11
CBL-MZ	-	Conal B-Cell Lymphocytosis of Marginal Zone Origin
CCND1	-	Cyclin D1
CD	-	Cluster of Differentiation
CD10 (CALLA)	-	Common Acute Lymphoblastic Leukemia Antigen
CDH2	-	Cadherin-2
CEBPA	-	CCAAT/Enhancer-Binding Protein, Alpha

CI	-	Confidence Interval
CK1	-	Casein Kinase 1
CLL	-	Chronic Lymphocytic Leukemia
CMZL	-	Cutaneous Marginal Zone Lymphoma
CpG	-	5'—C—phosphate—G—3'
CRBN	-	Cereblon gene
CREBBP	-	Cyclic AMP Response Element Binding - Binding Protein
CSR	-	Class-Switch Recombination
CTX	-	Chemotherapy
CXCL12/13	-	Chemokine (C-X-C motif) Ligand 12/13
DFS	-	Disease-Free Survival
DLBCL	-	Diffuse Large B-Cell Lymphomas
DMZL	-	Dural Marginal Zone Lymphoma
DNA	-	Deoxyribonucleic Acid
DNMT3A	-	DNA (cytosine-5)-methyltransferase 3 ALPHA
DSB	-	Double-Strand Break
EBF1	-	Early B-Cell Factor 1
EBV	-	Epstein-Barr virus
EDTA	-	Ethylenediaminetetraacetic Acid
EMZL	-	Extranodal Marginal Zone Lymphoma
EP300	-	E1A Binding Protein P300
ERK	-	extracellular-signal-regulated kinase
EZH2	-	Enhancer of zeste homolog 2
FF	-	Fresh Frozen
FFPE	-	Formalin-Fixed Paraffin-Embedded
FFS	-	Failure-Free Survival
FISH	-	Fluorescence In Situ Hybridization
FL	-	Follicular Lymphoma
FLT3	-	Fms Like Tyrosine kinase 3
FOXP1/3	-	Forkhead box P1/3
FOXO1	-	Forkhead box protein O1
GEO	-	Gene Expression Omnibus

GMZL	-	Gastric Marginal Zone Lymphoma
GNA13	-	G Protein Subunit Alpha 13
GPR34	-	G-Protein Coupled Receptor 34
H&E	-	Hematoxylin and Eosin
H3K4	-	lysine 4 on histone H3
HCV	-	Hepatitis C virus
HIV	-	Human Immunodeficiency Virus
HD	-	Histidine (H) and/or Aspartate (D)
HDAC3	-	Histone Deacetylase 3
HIST1H2BK	-	Histone H2B type 1-K
HMG1/2	-	High-Mobility Group 1 and 2
HRSCs	-	Hodgkin and Reed-Sternberg cells
HSCs	-	Hematopoietic Stem Cells
HTS	-	High Throughput Sequencing
ICOS	-	Inducible T-cell Costimulator
IDH1/2	-	Isocitrate Dehydrogenase genes 1 and 2
IELSG	-	International Extranodal Lymphoma Study Group
IFN	-	Interferon
Ig	-	Immunoglobulin
IGH/IGHV	-	Immunoglobulin Heavy chain-gene
IGV	-	Integrative Genomics Viewer
IKK	-	IκB kinase
IL-7	-	Interleukin 7
IMiD	-	Immune-Modulatory Drug
iNKT	-	Invariant Natural Killer T
IRF8	-	Interferon Regulatory Factor 8
JAK	-	Janus Activated Kinase
KLF2	-	Krüppel-like Factor 2
KLHL6	-	Kelch Like Family Member 6
KMT	-	histone lysine methyltransferases
KMT2C/D	-	Histone-lysine N-methyltransferase 2C/D
LDH	-	Lactate DeHydrogenase

LMP1	-	Latent Membrane Protein 1
LNs	-	Lymph Nodes
LP	-	Lymphocyte-Predominant
LPD	-	Lymphoproliferative Diseases
LPS	-	Lipopolysaccharide
LR	-	Lymphocyte-Rich
LRP1B	-	Low-density Lipoprotein Receptor Related Protein 1B
LTβ	-	Lymphotoxin B
LyG	-	Lymphomatoid Granulomatosis
MARCO	-	Macrophage Receptor With Collagenous Structure
MALT	-	Mucosa-Associated Lymphoid Tissue
MALT1	-	Mucosa-Associated Lymphoid Tissue Lymphoma Translocation protein 1
MAP3K	-	Mitogen-Activated Protein Kinase Kinase Kinase
MC	-	Mixed Cellularity
MCL	-	Mantle Cell Lymphoma
MDS	-	Myelodysplastic Syndromes
MEK (MAP2K)	-	Mitogen-Activated Protein Kinase Kinase
MHC	-	Major Histocompatibility Complex
MVD	-	Microvessel Density
MWU tests	-	Mann-Whitney tests
MYD88	-	Myeloid Differentiation primary response 88
MZ B-cells	-	Marginal Zone B-cells
MZL	-	Marginal Zone Lymphomas
MZM	-	Marginal Zone Macrophages
NCBI	-	National Center for Biotechnology Information
NFKBIE	-	Nuclear Factor of Kappa light polypeptide gene enhancer in B-cells Inhibitor, Epsilon
NF-κB	-	Nuclear Factor Kappa-light-chain-enhancer of activated B-cells
NHEJ	-	Non-homologous End Joining
NHL	-	Non-Hodgkin Lymphoma
NLH	-	Nodular Lymphoid Hyperplasia

NK	-	Natural Killer
NLPHL	-	Nodular Lymphocyte-Predominant Hodgkin Lymphoma
NMZL	-	Nodal Marginal Zone Lymphoma
NOTCH1/2	-	NOTCH Homolog 1/2
NPM1	-	Nucleophosmin 1
NIK	-	NF-κB-inducing Kinase
NHEJ	-	Non-Homologous End Joining
NS	-	Nodular Sclerosis
OA	-	Ocular Adnexal
OAL	-	Ocular Adnexal Lymphomas
OMZL	-	Ocular Marginal Zone Lymphomas
OS	-	Overall Survival
PALS	-	Periarteriolar Lymphoid Sheath
PAX5	-	Paired Box 5
PCR	-	Polymerase Chain Reaction
PD-1	-	Programmed Death Receptor-1
PD-L1	-	Programmed Death-Ligand 1
PEST	-	proline (P), glutamate (E) or aspartic acid, serine (S), and threonine (T)
PFS	-	Progression-Free Survival
PIK3R1	-	Phosphoinositide-3-Kinase Regulatory subunit 1
PIK3CD	-	Phosphatidylinositol-4,5-Bisphosphate 3-Kinase Catalytic Subunit Delta
PMZL	-	Pulmonary Marginal Zone Lymphoma
PP-DLBCL	-	Primary Pulmonary Diffuse Large B-Cell Lymphoma
PRDM1	-	PR Domain zinc finger protein 1
PS	-	Pathological stage
PT	-	Pseudo Tumors
PTPRD	-	Protein Tyrosine Phosphatase, Receptor type D
PTEN	-	Phosphatase and Tensin
RAG1/2	-	Recombination Activating Gene 1/2
R-CHOP	-	Rituximab-cyclophosphamide-doxorubicin hydrochloride

		(Hydroxydaunorubicin hydrochloride)-vincristine(Oncovin)-prednisone
R-CVP	-	Rituximab-cyclophosphamide-vincristine-prednisone
RHOA	-	Ras homolog gene family member A gene
RNA	-	Ribonucleic acid
RSS	-	Recombination Signal Sequences
RTX	-	Radiotherapy
SAMZL	-	Salivary Marginal Zone Lymphoma
S1PR2	-	Sphingosine-1-phosphate receptor 2
SGK1	-	Serum and Glucocorticoid-regulated Kinase 1
SMAD1	-	SMAD family member 1
SMZL	-	Splenic Marginal Zone Lymphoma
SOCS1	-	Suppressor of Cytokine Signaling 1
SRA	-	Sequence Read Archive
SSB	-	Single-Strand Break
STAT	-	Signal Transducer and Activator of Transcription
SWI/SNF	-	SWItch/Sucrose Non-Fermentable
TAD	-	Transactivation Domain
TBL1XR1	-	Transducin (β)-Like 1 X-linked Receptor 1
TCR	-	Comparative T-cell Receptor
TET2	-	Tet methylcytosine dioxygenase 2
TFHs	-	T Follicular Helper cells
TGF-β	-	Transforming Growth Factor Beta
TGFBR	-	TGF-β Receptors
TGFBR1/3	-	Transforming Growth Factor Beta Receptor 1/3
TGFBRAP1	-	Transforming Growth Factor Beta Receptor Associated Protein 1
TIL	-	Tumor-Infiltrating T-lymphocytes
TLR	-	Toll-Like Receptor
TMZL	-	Thyroid Marginal Zone Lymphoma
TNFAIP3	-	Tumor Necrosis Factor, Alpha-Induced Protein 3
TNFR	-	Tumor Necrosis Factor Receptor

TNFRSF14	-	Tumor Necrosis Factor Receptor Superfamily Member 14
TP53	-	Tumor Protein 53
TRAF	-	TNF Receptor-Associated Factor
UTR	-	Untranslated Region
VAF	-	Variant Allelic Frequency
VEGF	-	Vascular Endothelial Growth Factor
VEGFR	-	Vascular Endothelial Growth Factor Receptor
VEP	-	Variant Effect Predictor
W&W	-	Watchful Waiting
WHO	-	World Health Organization

ACKNOWLEDGEMENTS

I would like to express my deepest thanks to the following people who have made it possible to complete this dissertation. Without them, I would not have made it through my degree!

First and foremost, I am sincerely thankful to Professor Alexandar Tzankov for granting and releasing the necessary monetary funds to help support and accomplish the different research studies conducted. His leadership taught me a lot during these years and helped to value my work, to work precisely and to be focused on my goals. Therefore I grew as a person. I am also grateful for getting the chance to conduct the different research studies and access to use the different laboratories and equipment of our institute.

I want to thank my esteemed supervisor, Darius Juskevicius, for his advice, guidance, and assistance through each stage of the process. He provided insightful comments, suggestions, and critiques under his tutelage, which helped complete this research. Also, I would like to thank my professor, Stefan Dirnhofer, who motivated me constantly to read new journals in lymphoma science. His critical review of my work and, on the other hand, his sports spirit in cycling, volleyball, and triathlon helped me in becoming mentally and physically stronger.

Finally, I would like to extend my sincere thanks to my friends, family, and especially my parents for their unwavering support, strong belief, and extended patience during the times. Your unconditional love has been a great source of motivation to complete this dissertation. A special thanks goes to my grandmother, Shefije Islami. She passed away only vewy days weeks before my defense. You will be missed.

I could not have done this without all of your support, and with that, I am grateful.

Last but not least I want to thank ME for not giving up, pushing and challenging myself in different ways, to create a better future.

CURRICULUM VITAE

Name, First name	: VELA, Visar
Date/Country of Birth	: 1991 / North Macedonia, Tetovë
Nationality	: Swiss
Occupation and Title	: PhD-Student in Genetics & Hematology
Professional Address	: University Hospital Basel Pathology and Genetics Schönbeinstrasse 40 CH-4031 Basel (Switzerland)
Email	: visar.vela@usb.ch
Languages	German Mother tongue Albanian Mother tongue English Fluent French Fluent

GENERAL EDUCATION

2007 – 2012: Matura Kollegium Spiritus Sanctus, Brig Valais

2012 – 2015: Bachelor of Biomedical Science, University of Fribourg

Thesis: ***Effects of Chronic L-arginine Treatment on Monocyte/Macrophage Inflammatory Responses on Glutamine Deprivation Linked to Cardiovascular Disease.*** May 2015, Zhihong Yang

2015 – 2017: Master of Biomedical Science, University of Bern

Thesis: ***Regulatory T cells accumulate in the bone marrow of CML mice and contribute to the disease progression.*** February 2017, Adrian Ochsenbein

2015 – 2021: PhD in Genetics & Hematology, University of Basel

Thesis: ***Analysis of mutational landscape of marginal zone B-cell lymphomas by high throughput sequencing techniques.*** October 2021, Alexandar Tzankov

2020 – 2022: CAS in Labormedizin, University of Zurich

PROFESSIONAL HISTORY

2015: Adolphe Merkle Institute, University of Fribourg; **"Adverse effects of gasoline and diesel car exhaust on lung cells in vitro"**, (2 Months)

2016: University of Fribourg; **"Overcoming the limitations of cancer vaccines by taking advantage of nanoparticle properties"**, (1 Month)

2017 – 2018: Institut für medizinische Mikrobiologie, Universität Zürich; Gen-Banking of Pseudomonas aeruginosa, Whole genome sequencing and FAMH exam, (7 Months)

2018 – 2021: PhD-Student at the University Hospital Basel

CONGRESS

2018: -84th annual congress SGPath, Lugano	Oral presentation
2018: -55th OOG Meeting, London	Oral presentation
2019: -Personalized Oncology, Basel	Visitor
2019: - Joint annual meeting SGPath, Lucerne	Poster presentation
2019: -Seminars in Pathology and Genetics, Basel	Visitor
2021: -EAHAP, Virtual	Poster presentation

PUBLICATIONS

1. **Vela V**, Juskevicius D, Dirnhofer S, Menter T, Tzankov A. Mutational landscape of marginal zone B-cell lymphomas of various origin: organotypic alterations and diagnostic potential for assignment of organ origin. ***Virchows Archiv,*** 2021. DOI:10.1007/s00428-021-03186-3

2. **Vela V**, Juskevicius D, Cathomas G, Dertinger S, Diebold J, Horcic M, Singer G, Zettl A, Dirnhofer S, Menter T, Tzankov A. Deciphering the genetic landscape of pulmonary lymphomas. ***Modern Pathology,*** 34, pages 371–379; 2021. DOI: 10.1038/s41379-020-00660-2

3. **Vela V**, Juskevicius D, Gerlach M, Meyer P, Graber A, Cathomas G, Stefan Dirnhofer S, Tzankov A. High throughput sequencing reveals high specificity of TNFAIP3 mutations in ocular adnexal marginal zone B-cell lymphomas. ***Hematological Oncology,*** 38, pages 284-292; 2020. DOI: 10.1002/hon.2718

4. Brune MM, Stüssi G, Lundberg PP, **Vela V**, Heim D, Manz MG, Haralambieva E, Pabst T, Banz Y, Bargetzi M, Grobholz R, Fehr M, Cogliatti S, Ossenkoppele GJ, Löwenberg B, Rudolf CB, Qiyu Li Q, Passweg J, Mazzuchelli L, Medinger M, Tzankov A. Effects of lenalidomide on the bone marrow microenvironment in acute myeloid leukemia: Translational analysis of the HOVON103 AML/SAKK30/10 Swiss trial cohort. ***Annals of Hematology,*** 100, pages 1169–1179; 2021. DOI: 10.1007/s00277-021-04467-2

5. Gerlach M, Stelling-Germani A, Wu CT, Newrzela S, Döring C, **Vela V**, Müller A, Hartmann S,Tzankov A. SMAD1 promoter hypermethylation and lack of SMAD1 expression in Hodgkin lymphoma: a potential target for hypomethylating drug therapy. ***Haematologica***, 106, pages 619-621; 2021. DOI: 10.3324/haematol.2020.249276

6. Gerlach MM, Darius Juskevicius D, Vela V, Dirnhofer S, Tzankov A. Bone Marrow Infiltration of Angioimmunoblastic T-Cell Lymphoma: Identification and Prognostic Impact of Histologic Patterns and Diagnostic Application of Ancillary Phenotypic and Molecular Analyses. ***Arch Pathol Lab Med***, 144, pages 602-611; 2020. DOI: 10.5858/arpa.2019-0007-OA

APPENDIX

Bone Marrow Infiltration of Angioimmunoblastic T-cell Lymphoma: Identification and Prognostic Impact of Histologic Patterns and Diagnostic Application of Ancillary Phenotypic and Molecular Analyses

Magdalena M. Gerlach, Darius Juskevicius, **Visar Vela**, Stefan Dirnhofer, Alexandar Tzankov

-Research Article-

Published in *Archives of Pathology, and Laboratory Medicine*, 2020

Bone Marrow Infiltration of Angioimmunoblastic T-Cell Lymphoma

Identification and Prognostic Impact of Histologic Patterns and Diagnostic Application of Ancillary Phenotypic and Molecular Analyses

Magdalena M. Gerlach, MD; Darius Juskevicius, PhD; Visar Vela, MSc; Stefan Dirnhofer, MD; Alexandar Tzankov, MD

• ***Context.***—**Angioimmunoblastic T-cell lymphomas originate from T follicular helper cells and express respective markers (BCL6, CD10, CXCL13, ICOS, and PD-1). Although commonly present, bone marrow involvement by angioimmunoblastic T-cell lymphoma can be diagnostically challenging. Additionally, only little is known about the distribution of T follicular helper cells in healthy and reactively changed bone marrows or in samples affected by other lymphomas.**

Objective.—**To establish a diagnostic approach to reliably identify bone marrow infiltration of angioimmunoblastic T-cell lymphoma.**

Design.—**We analyzed the morphologic infiltration pattern and the expression of T follicular helper-cell markers in 42 matched paired lymph node and bone marrow samples and applied comparative clonality testing. Furthermore, we studied the expression of BCL6 and PD-1 in a control cohort of healthy, reactively changed, and otherwise affected bone marrows.**

Results.—**We identified 3 different bone marrow infiltration patterns correlating with overall survival (interstitial/micronodular infiltration with or without eosinophilia and diffuse infiltration with eosinophilia). The matched pairs showed a consistent (co)expression of PD-1 and BCL6 with a generally weaker expression in the bone marrow than in the lymph nodes. Comparative clonality testing was helpful in only a minority of cases. Infiltrates of the most important differential diagnoses contained either PD-1– or BCL6-positive tumor-infiltrating cells, but no coexpressing cells.**

Conclusions.—**Bone marrow infiltration by angioimmunoblastic T-cell lymphoma displays 3 different patterns that correlate with prognosis. BCL6 and PD-1 can be reliably used to identify lymphoma infiltrates and to help rule out several differential diagnoses. Comparative clonality testing rarely provides additional value and cannot replace morphologic and phenotypic analyses.**

(*Arch Pathol Lab Med.* 2020;144:602–611; doi: 10.5858/arpa.2019-0007-OA)

Angioimmunoblastic T-cell lymphoma (AITL) is the most common noncutaneous T-cell neoplasm in the Western world.[1] It is currently defined by the World Health Organization as a neoplasm of mature T follicular helper cells (TFHs) characterized by systemic disease and a polymorphous infiltrate involving lymph nodes (LNs), with a prominent proliferation of high endothelial venules and follicular dendritic cells.[2] Already in 1968, Lennert and Mestdagh[3] suggested that AITL is a supposed special form of Hodgkin lymphoma, accompanied by massive occurrence of epithelial cells in affected LNs, generalized lymphadenopathy, and skin symptoms. In 1974, it was described by Frizzera et al[4] as a "lymphoma-like clinical presentation and a specific histological picture" accompanied by an acute onset of general symptoms; erroneously, it was considered as a nonneoplastic process very similar to graft-versus-host reactions and therefore named *angioimmunoblastic lymphadenopathy with dysproteinemia* (AILD). Shortly thereafter, Lukes and Tindle[5] published their data on a case series of 32 patients, emphasizing the clinical and morphologic resemblance to Hodgkin lymphoma, apart from the absence of diagnostic Reed-Sternberg cells, proposing an underlying hyperproliferation of B cells. Nathwani et al[6] showed that there were no histopathologic features to predict the clinical course of patients with AILD, who later on either did or did not develop what had been called at that time "progression to immunoblastic lymphoma"; they noticed that the most important prognostic factor in either case was achieving complete remission, emphasizing that no sharp line can be drawn between "benign" and "malignant" AILD lesions.[6] On the other side of the Atlantic Ocean, Radaszkiewcz and Lennert[7] published another 50 cases of so-called lymphogranulomatosis X, a term synonymously used for AILD, and elucidated its clinical features, response to treatment, and its prognosis. For the first time, the updated Kiel classification

Accepted for publication July 11, 2019.
Published online September 26, 2019.
From the Institute of Medical Genetics and Pathology, University Hospital Basel, Basel, Switzerland.
The authors have no relevant financial interest in the products or companies described in this article.
Corresponding author: Alexandar Tzankov, MD, Medical Genetics and Pathology, University Hospital Basel, Schoenbeinstr. 40, Basel, BS 4031, Switzerland (email: alexandar.tzankov@usb.ch).

from 1988 subsumed AILD under the low-grade T-cell non-Hodgkin lymphomas and, over time, the concept of AILD was replaced by the term *angioimmunoblastic T-cell lymphoma*.[8]

Today, AITL is recognized as a distinct entity accounting for 1% to 2% of all lymphomas with a slight predominance in male patients.[9,10] It has been convincingly shown that AITL originates from TFHs. Therefore, cases usually express several TFH markers such as B-cell lymphoma 6 (BCL6), cluster of differentiation 10 (CD10), chemokine (C-X-C motif) ligand 13 (CXCL13), inducible T-cell costimulator (ICOS), and programmed death receptor-1 (PD-1).[11–13] AITLs are characterized by an aggressive clinical course with generalized lymphadenopathy and frequent paraneoplastic symptoms, which can only partially be explained by a direct effect of the spreading lymphoma, but must be seen as representing an unrestrained cross-talk between the neoplastic T cells and the host. Fittingly, an expansion of Epstein-Barr virus (EBV)–positive B cells is often found, also playing an important role in the progression of lymphoma.[14,15] Importantly, in patients with bone marrow (BM) involvement, the immunologic symptoms and laboratory findings are more significant than for those without BM infiltration, which may reflect an increased tumor mass in the former.[16]

Although evident in most cases, objectivizing BM involvement by AITL can be diagnostically challenging, especially if there is only subtle tumor spread. Even when taking advantage of the knowledge of AITL's TFH origin and relying on the abovementioned markers, diagnostic uncertainty remains, as those markers are neither specific enough nor expressed as strongly as in the LNs.[16–19] In particular, if a BM biopsy represents the only diagnostic specimen, differential diagnosis of myeloproliferative neoplasms or plasma cell myelomas may be difficult.[16,18] In general, the histomorphologic findings of AITL in the BM were found to differ substantially from those in LNs, especially considering the BM-specific lack of proliferation of follicular dendritic cells, leaving room for misinterpretation ranging from reactive lymphoid proliferation to other lymphomas.[16,19]

Until now, neither a distinct and diagnostically reliable infiltration pattern nor a specific immune phenotype of AITL infiltrating the BM has been recognized, and only few ancillary molecular techniques have been addressed. Finally, only little is known about the TFH marker distribution in the healthy BM and in BM affected by autoimmune disorders and other lymphomas. For this reason, the aim of our study was to analyze the distribution of TFH equivalents in healthy and reactive BM specimens as well as in BM samples with infiltration of B-cell, T-cell, and Hodgkin lymphoma. Furthermore, matching pairs of LN and BM biopsy samples of AITL patients with BM infiltration, with suspected BM involvement, or without morphologically detectable AITL in the BM, were analyzed through the use of immunohistochemistry and molecular techniques.

MATERIALS AND METHODS

The evaluated cases were collected from the archives of the Institute of Pathology at the University Hospital Basel, Switzerland. This study approach was approved by the Ethics Committee of North-Western and Central Switzerland (EKNZ 2014-252). Patients' clinical data were obtained from the electronic medical record system and from the information given by the clinicians.

Table 1. Applied Antibodies, Dilutions, and Incubation Conditions

Antigen	Source	Retrieval, min	Dilution	Incubation, min
BCL6	Ventana 760-4241	CC1 48	Ready to use	20
CD10	Ventana 790-4506	CC1 32	Ready to use	16
CD3	Ventana 790-4341	CC1 32	Ready to use	4
CXCL13	Abcam ab112521	CC1 48	1:100	24
ICOS	Abcam ab105227	CC1 56	1:25	24
PD-1	Ventana 760-4895	CC1 48	Ready to use	12

Abbreviations: BCL6, B-cell lymphoma 6; CD, cluster of differentiation; CXCL13, chemokine (C-X-C motif) ligand 13; ICOS, inducible T-cell costimulator; PD-1, programmed death receptor-1.

Specimens from 37 patients diagnosed with AITL with or without BM involvement were sampled between 2003 and 2018. From a total of 5 patients, matched pairs from 2 different time points were analyzed. Thirty pairs with BM involvement, 9 pairs without BM involvement, and 3 pairs with inconclusive BM findings were studied. The 64 control samples, consisting of healthy (n = 10; individuals donating BM for allogeneous transplantation) or otherwise affected BM samples (n = 54), were from the years 2008–2018. Whenever possible at least 3 cases, with each entity being a potential differential diagnosis to BM infiltration by AITL, were evaluated. All specimens were fixed in 4% formalin and paraffin embedded, and BM biopsy samples were decalcified with ethylenediaminetetraacetic acid (EDTA) as described elsewhere.[20]

Hematoxylin-eosin–stained slides of each sample were reviewed and reclassified, if necessary. All LN and BM samples from patients with BM involvement by AITL were stained for the TFH markers BCL6, CD10, CXCL13, ICOS, and PD-1. Uninvolved BM samples of patients with AITL, as well as the 3 inconclusive cases and the whole control cohort, were stained for cluster of differentiation 3 (CD3) in order to detect all T cells, and for BCL6 and PD-1 to detect TFHs. Details on the applied antibodies, dilutions, as well as retrieval and incubation conditions are given in Table 1. All immunostaining studies were performed on a Roche/Ventana BenchMark Ultra platform (for details see Table 1). Two authors investigated all stained samples.

Single cell positivity was defined as a positive staining in 1% or less of unequivocal tumor cells. The term *dim positive* was used in cases of distinct, but weaker than expected, positivity. Partial positivity refers to obvious and strong positivity in 50% or less of tumor cells. If there was positivity in nontumor cells, a precise assignment (eg, cells arising from myelopoiesis, tumor-infiltrating lymphocytes) was given whenever possible. If discrimination between stained tumor cells or other cells was not possible, a double-staining assay combining BCL6 as a nuclear and PD-1 as a membranocytoplasmatic marker was applied. The presence of EBV in the affected BM samples and the corresponding LNs was assessed by in situ hybridization for EBV-encoded small RNAs in 13 AITL-affected BM-LN pairs.

Comparative T-cell receptor (TCR)–γ clonality testing was performed on genomic DNA extracted from matched LN and BM samples by using next-generation sequencing–based Lymphotrack TCR-γ assay (Invivoscribe), following manufacturer's instructions. BM biopsy samples of 6 AITL patients without morphologically suspected involvement, 2 inconclusive cases, and 8 morphologically affected BM biopsy samples underwent comparative clonality testing. The presence of identical clonal TCR-γ rearrangement in the LN and the matched BM sample was interpreted as evidence of involvement.

In 3 selected cases (cases 7, 14, and 30), the mutational landscape of the affected LN and BM was analyzed by Sanger sequencing or by a customized lymphoma panel, with special attention to AITL-typical mutations in the Ras homolog gene family member A gene (*RHOA*), the Tet methylcytosine dioxygenase 2 gene (*TET2*), the

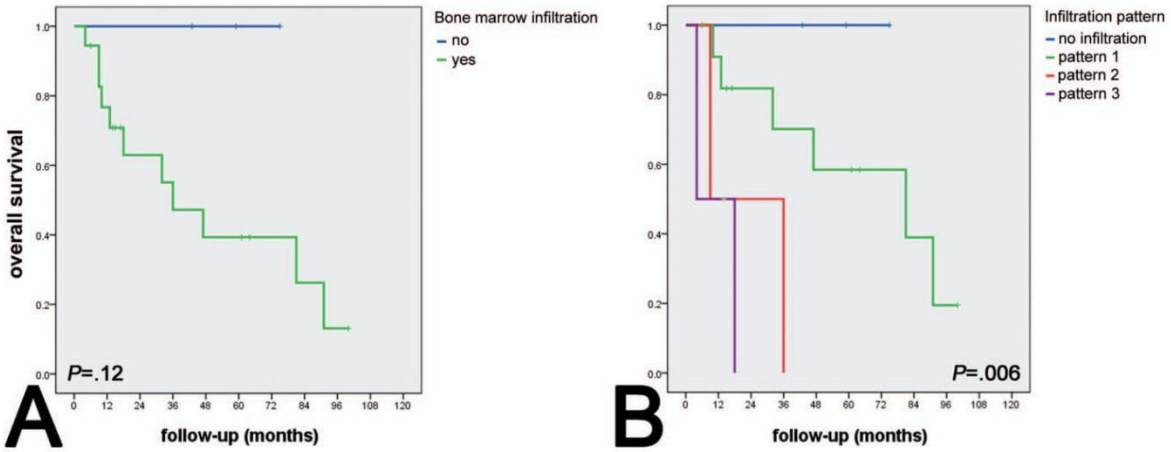

Figure 1. *Overall survival in correlation to bone marrow involvement and infiltration patterns. A, Absence of bone marrow infiltration correlates with longer overall survival. This confirms recently published data by Hong et al,[23] claiming that bone marrow involvement alone is one of the most important prognostic factors in angioimmunoblastic T-cell lymphoma. B, Overall survival highly depends on the different bone marrow infiltration patterns, revealing a better outcome for patients with an interstitial/micronodular involvement in association with eosinophils (pattern 1) than for those with an interstitial/micronodular infiltration without eosinophils (pattern 2) or a diffuse involvement (pattern 3).*

DNA (cytosine-5)-methyltransferase 3A gene (*DNMT3A*), and the isocitrate dehydrogenase genes 1 and 2 (*IDH1/2*), as described previously.[21,22]

Statistical analysis was performed by applying the SPSS version 22 package (IBM, Armonk, New York).

RESULTS

Clinical Data

The available clinical and laboratory data of the patients are summarized in Table 2. Though based on a limited number of retrospective observations, as estimated by the Kaplan-Meier method and the log-rank test, AITL patients with BM involvement had shorter overall survival than patients without BM infiltration (Figure 1, A). However, this result did not reach statistical significance. The only other prognostically relevant factor in our cohort—analogously to what had been noticed more than 4 decades ago[6]—was patients' response to first-line treatment: if a complete remission could be achieved, the overall survival increased significantly.

Morphologic BM Infiltration Patterns

We were able to identify 3 different infiltration patterns of AITL BM spread. Importantly, there was a correlation between the overall survival and these AITL infiltration patterns (Figure 1, B). Most cases, 27 of 30 samples (90%), displayed an interstitial/micronodular infiltration (roughly affecting 5% to 30% of all marrow spaces). In 19 instances, there was an association with eosinophils, reflecting one of AITL's characteristics in the LN (pattern 1). In 8 cases, no eosinophilia was present (pattern 2). Patients with a pattern 1 involvement had longer overall survival than patients without eosinophilia (pattern 2). The remaining 3 of 30 cases (10%) were characterized by a diffuse infiltration, also associated with eosinophilia (pattern 3), and had the shortest overall survival (Figure 1, B; and Figure 2, A through I).

Immunohistochemical Expression of TFH Markers in LN of Patients With AITL (n = 29).—The staining results of the LNs of AITL patients with BM involvement are summarized in Table 3. Any discrepancies in the sum of percentages are due to rounded numbers.

BCL6.—Of 29 LN samples, 20 (69%) expressed BCL6 at least in single cells. Six (21%) were completely negative and 3 (10%) were not evaluable.

CD10.—Expression of CD10 was found in 13 of 29 LN samples (45%). Another 13 samples (45%) tested negatively for this marker and 3 (10%) were not interpretable.

CXCL13.—In 18 of 29 LN samples (62%) there was expression of CXCL13 at least in single cells. Eight samples (26%) were completely negative for this marker, whereas another 3 (10%) were not evaluable.

ICOS.—ICOS was expressed in 23 of 29 cases (79%). Four cases (14%) were completely negative for this marker and 2 (7%) were not interpretable.

PD-1.—Of the 29 LN samples, only 1 (3%) was negative for PD-1, whereas 26 (90 %) expressed this marker. Two samples (7 %) were not analyzable.

Affected BM Biopsy Samples of Patients With AITL (n = 30).—The complete staining results of the AITL-affected BM samples are shown in Table 3 and Figure 3, A through E. Immunohistochemical analysis of the BM samples revealed a more subtle expression of the TFH-typical markers than in the corresponding LN samples. The overall T-cell content and the probable AITL equivalents were evaluated with the help of CD3-stained slides. The staining intensity and the cytomorphology of the positive cells were taken into account (strongly stained small reactive T cells versus more dimly stained, larger AITL cells with irregular nuclei). Any discrepancies in the sum of percentages are due to rounded numbers.

BCL6.—In total, 19 of 29 evaluable BM biopsy samples (66%) expressed BCL6. When compared to the corresponding LN samples, 14 of 30 matched pairs (47%) consistently expressed BCL6 (at least as single cell positivity).

CD10.—Compared to the corresponding LN samples, there were 7 of 30 pairs (23%) showing at least a single tumor cell positivity in both locations. In the BM, the rough

Table 2. Clinicopathologic Characteristics of Patients With Angioimmunoblastic T-Cell Lymphoma[a]

Pair	Age, y/ Sex	Pattern	ECOG Score	Extranodal Sites	B-Symptoms	Skin Involvement	LDH Elevation	Blood Eosinophilia	Hyper-γ-globulinemia	Outcome	Follow-up, mo
1	71/M	2	>1	>1	Yes	Yes	No	Yes	Yes	Deceased	36[b]
2 and 3	72/F	1			Yes					Alive	61
4	78/F	1									
5	60/M	1	≤1	>1	Yes	Yes	Yes	Yes	Yes	Alive	15
6	67/M	2						Yes			
7	67/F	2	≤1	>1	Yes	Yes	Yes	Yes	Yes	Deceased	9[c]
8	46/F	1								Alive	100
9	67/M	3	>1	>1	Yes	Yes	Yes	Yes	Yes	Deceased	4
10	87/M	1	≤1	≤1	Yes	No	Yes	Yes	No	Deceased	13
11	71/M	1		>1	Yes	Yes	Yes	No	Yes		
12	71/M	2	≤1	>1	Yes	No	Yes	No	No	Deceased	9
13	56/M	1								Deceased	91
14	69/F	1									
15	76/M	1									
16 and 17	59/F	1		>1	No		Yes			Deceased	10
18	74/F	3									
19 and 20	77/M	1	>1	>1	Yes	No	Yes	No	No	Alive	17
21	77/F	2		>1	Yes	Yes				Alive	14
22	51/F	1				Yes	Yes				
23	84/F	2						No	No		
24	68/M	1									
25	78/M	1					Yes			Deceased	32
26	57/M	3			Yes					Deceased	18
27	84/M	2		>1				No			
28	49/M	1	≤1	>1	Yes	No	No	No	Yes	Alive	64
29	84/F	1			Yes					Alive	6
30	51/M	1						No			
31	85/M	0									
32	72/M	0									
33	49/M	0			Yes	Yes					59
34	79/F	0			Yes						
35	62/F	1	>1	≤1	No		Yes	Yes	No	Deceased	47
36	81/M	0									
37 and 38	64/F	1	>1		Yes	Yes	No	No	No	Deceased	81
39 and 40	84/M	0			No						43
41	64/F	0	>1	≤1	Yes	Yes	Yes	Yes		Alive	75
42	56/M	0		≤1	Yes	Yes					

Abbreviations: ECOG, Eastern Cooperative Oncology Group; LDH, lactate dehydrogenase.

[a] Matched pairs of individual patients obtained at different time points are shown in the same line. The age of the patients at the time point of the first diagnosis is given. The histologically identified infiltration pattern is displayed: 0, no infiltration; 1, interstitial/micronodular with eosinophils; 2, interstitial/micronodular without eosinophils; 3, diffuse with eosinophils. Clinical information on the patients' ECOG performance score, the number of involved extranodal sites, presence of B-symptoms, and skin involvement are shown next to laboratory data on elevated LDH, eosinophilia in the peripheral blood, and hypergammaglobulinemia. Additionally, there is information about whether the patient died during the follow-up or whether he or she was still alive. The total follow-up in months is given. Empty boxes were used for nonavailable data.

[b] This patient died of therapy-associated acute myelogenous leukemia.

[c] This patient refused treatment.

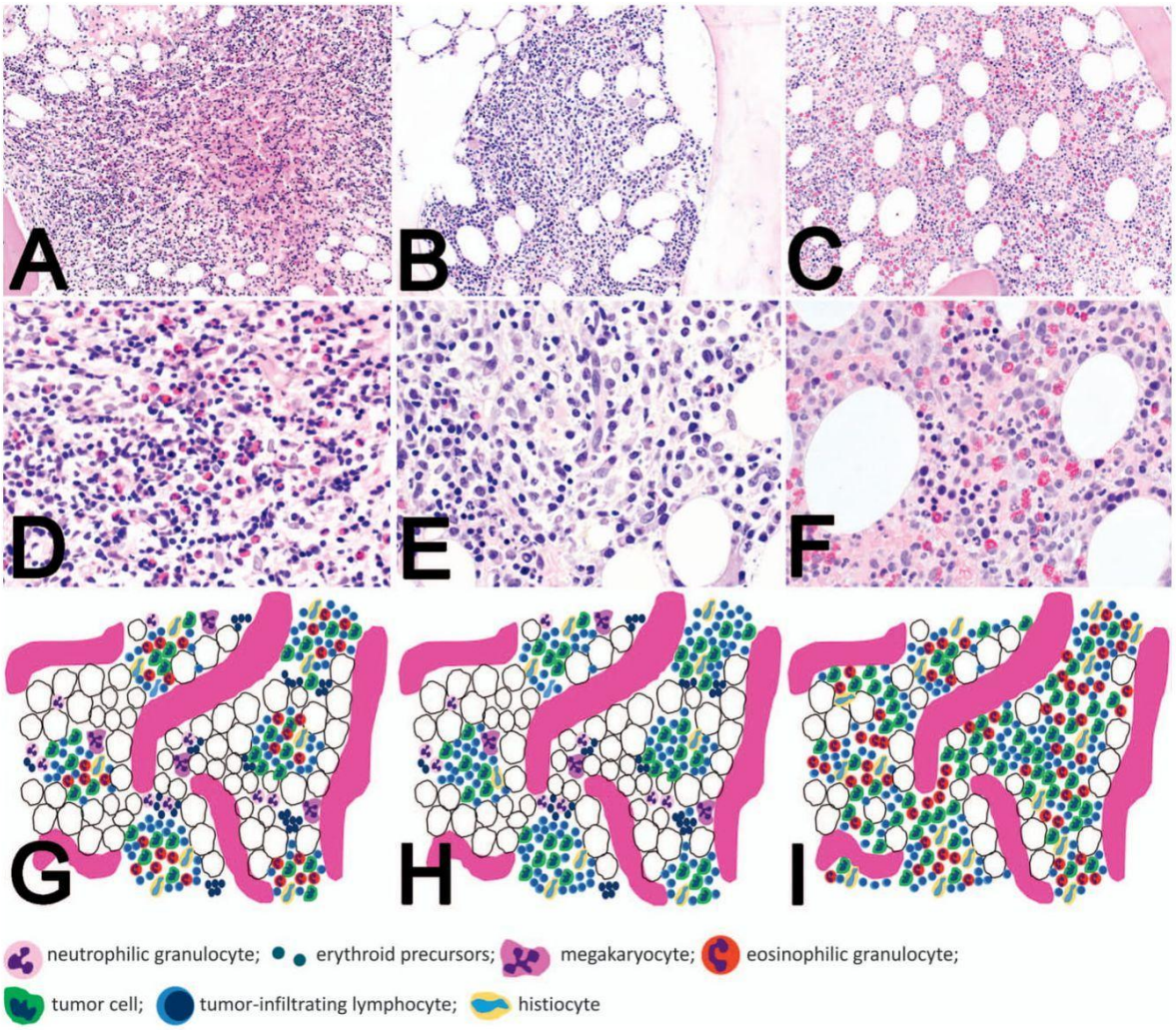

Figure 2. *Different infiltration patterns of angioimmunoblastic T-cell lymphoma (AITL) in the bone marrow. A, D, and G, Nearly two-thirds of the AITL-involved bone marrow samples revealed an interstitial and micronodular infiltration with marked eosinophilia. Lymphomatous micronodule with accompanying eosinophilic granulocytes (A) can be appreciated at a higher magnification (D). The graphic illustration (G) shows micronodular involvement of a bone marrow sample, reflecting a pattern 1 involvement with marked eosinophilia, and consisting, next to eosinophilic granulocytes, of large atypical tumor cells, many tumor-infiltrating lymphocytes, and a few scattered histiocytes. B, E, and H, Eight of 30 samples displayed an interstitial/micronodular involvement, that is, pattern 2 (B), very similar to pattern 1, but without an increase of eosinophilic granulocytes in the infiltrates (E). Graphic illustration is shown in (H). C, F, and I, Three of the affected bone marrow biopsy samples (10%) showed diffuse infiltration (pattern 3) (C) with a subtotal replacement of hematopoiesis (F). Graphic illustration is shown in (I) (hematoxylin-eosin, original magnifications ×50 [A through C] and ×260 [D through F]).*

overlapping of $CD10^+$ and $CD3^+$ cells excluded hematogones.

CXCL13.—Comparing the BM biopsy samples to the matching LN samples, we found only 4 of 30 pairs (13%) expressing CXCL13 in both locations.

ICOS.—When compared to the matching LN samples, there were 4 of 30 pairs (13%) that were positive in both locations.

PD-1.—In total, 29 of 30 BM samples (97%) contained PD-1–positive tumor cells. In comparison to the matching LN samples, there were 26 of 30 positive pairs (87%).

In summary, PD-1 and BCL6 were the most consistently expressed markers (all AITL-affected BM samples expressed either PD-1 or BCL6 or both). Matched pairs showed concordant positivity in 26 of 28 (93%) (PD-1) and 14 of 26 (54%) (BCL6) relevant instances. Fisher exact test showed statistical significance for the results' consistency based on PD-1 staining estimation ($P = .04$), while the next best consistency—yet not statistically significant ($P = .35$)—was suggested for BCL6; all other markers were far below any meaningful significance (data not shown). Therefore, we restricted our analysis of the nonaffected BM and the control

Table 3. Expression of T Follicular Helper Cell Marker in Patients With Angioimmunoblastic T-Cell Lymphoma in Matched Pairs of Lymph Node (LN) and Affected Bone Marrow (BM) Biopsy Samples

	BCL6	CD10	CXCL13	ICOS	PD-1
Positive in LN and BM	14/30 (47%)	7/30 (23%)	4/30 (13%)	4/30 (13%)	26/30 (87%)
Negative in LN and BM	2/30 (7%)	8/30 (27%)	5/30 (17%)	3/30 (10%)	0/30 (0%)
Positive only in LN	6/30 (20%)	5/30 (17%)	13/30 (43%)	17/30 (57%)	1/30 (3%)
Positive only in BM	4/30 (13%)	5/30 (17%)	3/30 (10%)	1/30 (3%)	1/30 (3%)
Not evaluable	4/30 (13%)	5/30 (17%)	5/30 (17%)	5/30 (17%)	2/30 (7%)

Abbreviations: BCL6, B-cell lymphoma 6; CD10, cluster of differentiation 10; CXCL13, chemokine (C-X-C motif) ligand 13; ICOS, inducible T-cell costimulator; PD-1, programmed death receptor-1.

cohort to BCL6, PD-1, and CD3, the latter in order to verify T cells present (as described above) in the BM. Furthermore, BCL6/PD-1 double-staining was performed to address a potential TFH derivation of the respectively stained cells (Figure 3, F).

Nonaffected BM Biopsy Samples of Patients With AITL (n = 9).—In all samples, $CD3^+$ cytologically unremarkable T cells were present. A dim BCL6 positivity was associated with myelopoiesis in 1 of 9 cases (11%). Although this positivity impeded the evaluation of BCL6 staining, morphologic analysis and comparison with the CD3 and the PD-1 staining made a final assignment of the BCL6-positive cells possible. Six cases (66%) displayed complete negativity for BCL6, and in 2 cases (22%) single dim BCL6–positive histiocytes were encountered.

Eight samples (88%) were entirely negative for PD-1 and 1 sample (11%) contained single unremarkable PD-1–positive small lymphocytes. No sample showed coexpression of BCL6 and PD-1 in the same cells.

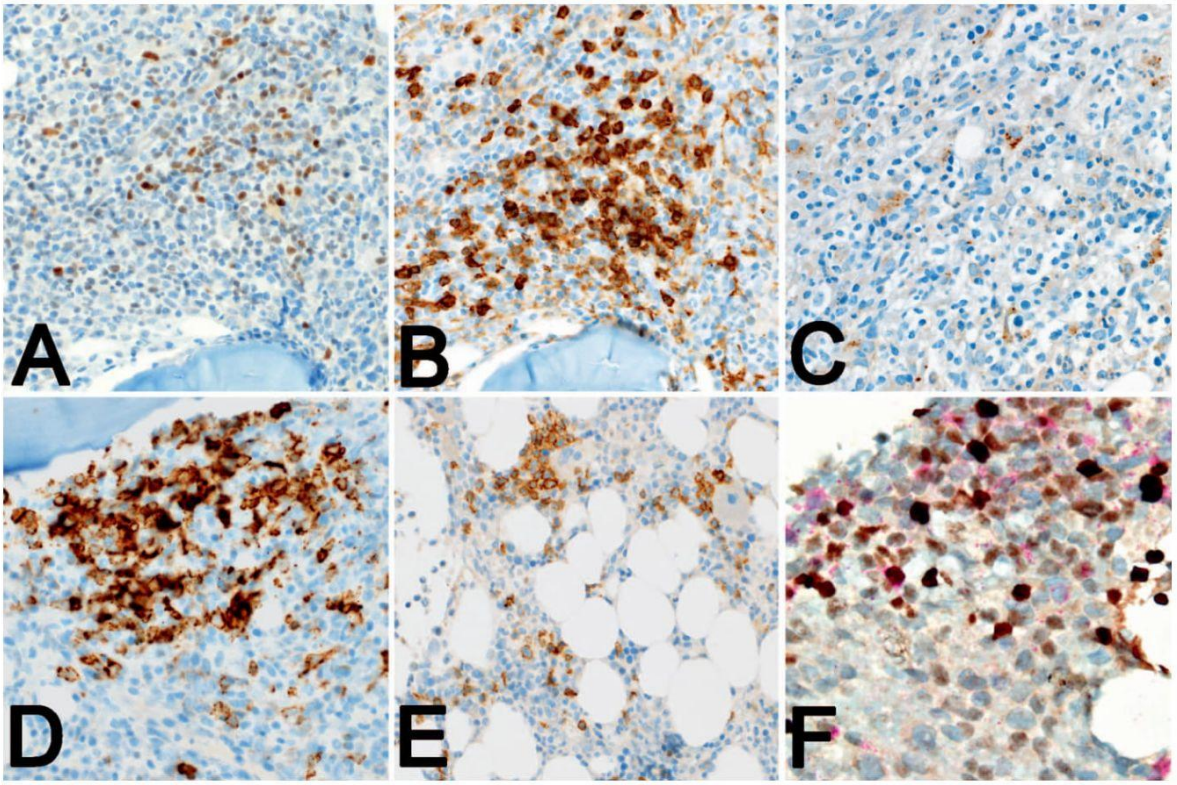

Figure 3. *T follicular helper cell (TFH) marker expression by angioimmunoblastic T-cell lymphoma (AITL) infiltrating the bone marrow. A, Nuclear expression of B-cell lymphoma 6 (BCL6) in the bone marrow was present in more than half of the cases; the interpretation was sometimes impeded by a dim BCL6 expression of myelopoietic cells. B through D, Membranous and cytoplasmatic positivity for cluster of differentiation 10 (CD10) (B), chemokine (C-X-C motif) ligand 13 (CXCL13) (C), and inducible T-cell costimulator (ICOS) (D) that was not consistent between the bone marrow samples and the corresponding lymph nodes in most cases. E, Programmed death receptor-1 (PD-1) was the most reliable marker expressed by AITL infiltrates in the bone marrow. F, BCL6/PD-1 double-staining to verify the TFH derivation of the stained cells, revealing coexpression of both markers in the tumor cells (BCL6 chromogenic detection with immunoperoxidase reaction in brown, PD-1 chromogenic detection by fast red); note several clearly visible tumor cells with cribriform brown nuclei and a small rim of red membranocytoplasmic positivity (original magnifications ×260 [A through E] and ×320 [F]).*

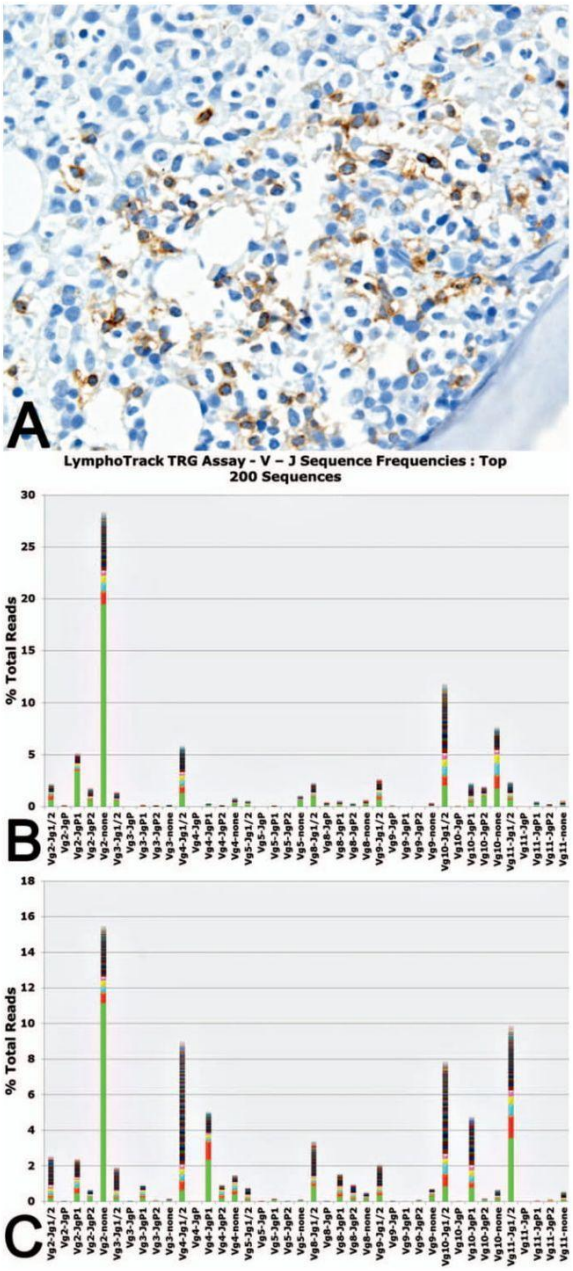

Figure 4. *Phenotype and comparative clonality testing in an inconclusive case. A, Distribution of cluster of differentiation 3 (CD3)–positive T cells (A) in the bone marrow biopsy sample of patient 35, morphologically suggestive of pattern 1 involvement with small nodules composed of larger atypical and weakly CD3⁺ cells, surrounded by unremarkable, small, strongly CD3-expressing reactive T lymphocytes. B-cell lymphoma 6 (BCL6) staining and programmed death receptor-1 (PD-1) staining were negative, most probably owing to loss of antigenicity, and therefore precluding a definitive diagnosis of bone marrow involvement. B and C, Comparative clonality testing yielded useful results, revealing clonally identical T cells in the lymph node (B) and in the bone marrow (C), corroborating the morphologic suspicion of involvement (original magnification ×260 [A]).*

Morphologically Inconclusive BM Biopsy Samples of Patients With AITL (n = 3).—Our cohort contained 3 histologically inconclusive matched pairs from 2 different patients.

The first patient's BM biopsy sample (case 35) showed an interstitial/micronodular infiltrate with marked eosinophilia (pattern 1). CD3 staining revealed small nodules (infiltration volume 7% of the BM biopsy sample) composed of larger atypical and weakly positive CD3 cells, surrounded by unremarkable, strongly CD3-expressing reactive T lymphocytes (Figure 4, A). Interestingly, BCL6 and PD-1 showed negativity, precluding a definitive diagnosis of BM involvement.

The first BM biopsy sample of the second patient (case 37) showed discrete interstitial/micronodular lymphocytosis accompanied by eosinophilic granulocytes, suggestive of pattern 1 involvement. The subsequently performed CD3 staining revealed a few large atypical and weakly positive CD3 tumor cells, surrounded by strongly positive reactive T cells (infiltration volume 2%). PD-1 staining and BCL6 staining were completely negative, also precluding a definitive diagnosis of AITL infiltration. One year later, a second BM staging biopsy sample (case 38) showed the same morphologic and immunophenotypic results, now with an infiltration volume of 5%. Importantly, in this particular case, flow cytometry also did not identify BM lymphoma involvement. Altogether (data not shown), flow cytometry results on BM aspirates were available for 8 cases with histopathologically confirmed BM infiltration by AITL, for which flow cytometry was suggestive of lymphoma only in 2 instances (25%).

EBV Status in Affected BM Samples and in Corresponding LN Samples

There was no link between accompanying EBV-associated lymphoproliferations in the LNs and the presence of EBV-positive cells in the BM as assessed directly by comparing 13 paired samples. Of those, 3 (23%) were EBV-negative and 4 (31%) displayed EBV-positive bona fide B-cell lymphoproliferations both in the AITL-affected BM and LN samples. The remaining 6 (46%) were discordant with EBV-positive compounds in the LNs, but not in the BM ($P = .49$; Fisher exact test). Thus, presence of EBV-positive cells in the BM turned out not to be of diagnostic help for involvement by AITL.

Comparative Clonality Testing Between LN and Corresponding BM

Of all 6 paired samples without BM involvement, interpretable results were obtained in only 1 instance, displaying a polyclonal pattern in the BM, corroborating the diagnosis of an uninvolved staging biopsy.

Both patients with inconclusive morphologic findings yielded useful clonality testing results, showing clonally identical T cells in the LN and in the BM, substantiating the morphologic suspicion (though lacking phenotypic corroboration) of involvement (Figure 4, B and C).

Only 2 of the 8 cases with BM involvement proved to be clonally related, while the others did not yield interpretable results on the LN or on the BM material.

Detection of AITL-Typical Mutations

Molecular workup for mutations was performed in 3 cases (7, 14, and 30); though present in the LN sample of patient

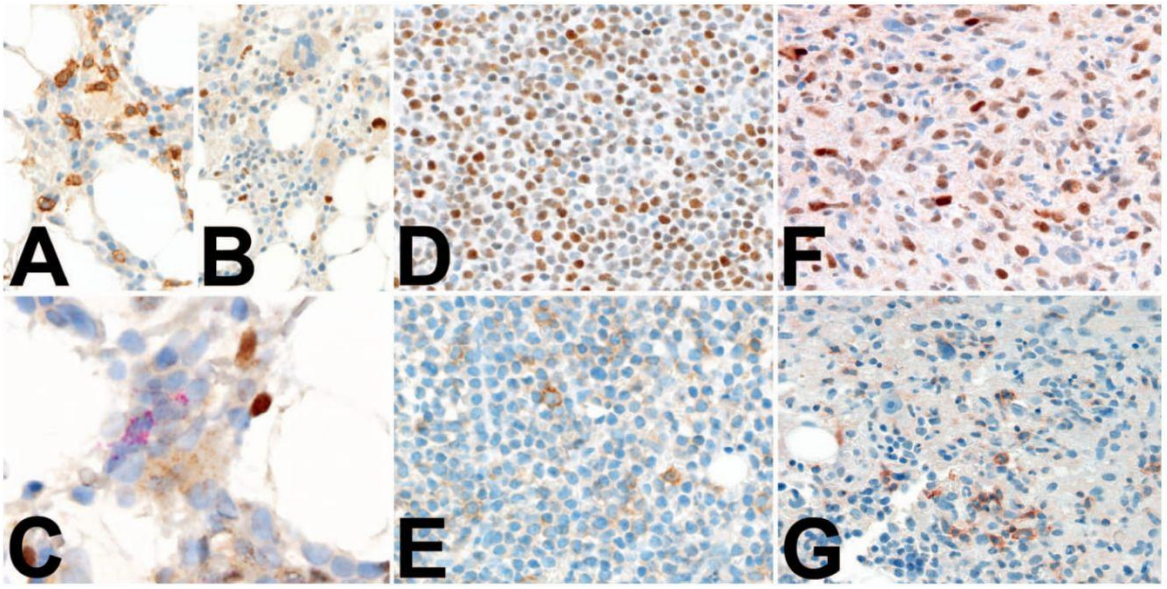

Figure 5. *B-cell lymphoma 6 (BCL6) and programmed death receptor-1 (PD-1) bone marrow expression patterns in relevant differential diagnoses. A, B, and E, Bone marrow sample of toxic myelopathy due to adverse drug effect demonstrates a marked positivity for both PD-1 (A) and BCL6 (B), potentially giving room for diagnostic pitfalls. BCL6/PD-1 double-staining (BCL6 chromogenic detection with immunoperoxidase reaction in brown, PD-1 chromogenic detection by fast red) (E) shows that both markers are expressed in different cell populations, assuming that PD-1 has probably been expressed on exhausted T cells, rather than on T follicular helper-cell equivalents, and BCL6, on myeloid derivatives. C and F, Mycosis fungoïdes involving the bone marrow can occasionally express BCL6 (C) and PD-1 (F). D and G, Classical Hodgkin lymphoma, being one of the most important histomorphologic mimickers of angioimmunoblastic T-cell lymphoma, shows a distinct phenotype allowing a reliable differential diagnosis after careful morphologic evaluation: BCL6 (D) and PD-1 (G) positivity is only present in histiocytes and tumor-infiltrating lymphocytes, respectively, while the Hodgkin and Reed-Sternberg cells (HRSCs) remain completely negative for both markers; note the scattered negative large HRSCs with prominent nucleoli (original magnifications ×260 [A, C, D, F, and G], ×200 [B], and ×400 [E]).*

7, a *RHOA* mutation could not be found in her BM sample because of poor DNA quality. The pathogenic and diagnostically useful *IDH2* mutation (R172W, allelic burden of 8%) was found in the LN of patient 14 but could not be found in the BM. The LN of patient 30 was additionally affected by a marginal zone lymphoma and our customized lymphoma panel revealed only typical mutations of B-cell neoplasms (*CD79A*, *TNFAIP3*, *KMT2D*, *PRDM1*, *HIST1H1C*), but no AITL-typical mutations such as *RHOA*, *TET2*, or *IDH1/2*. Because of no evidence of diagnostically useful mutations for AITL, no molecular analysis of the BM biopsy sample of this case has been performed.

Immunohistochemical Expression of TFH Markers in BM Biopsy Samples From Healthy Individuals and Those Affected by Other Conditions

In healthy individuals (n = 10), dim BCL6 (single cell) positivity was associated with myelopoiesis in 8 cases, and 2 cases were entirely negative. PD-1 expression was found in single small lymphoid cells in 5 samples. The remaining cases were completely negative for PD-1. BM samples of toxic myelopathy (n = 5) due to adverse drug reactions displayed, with the exception of 1 case, neither BCL6- nor PD-1–positive cells. This single case showed a marked positivity for both BCL6 and PD-1 in interstitially distributed myelocytes and reactive T lymphocytes (Figure 5, A and B). Double-staining revealed no coexpression of these markers, assuming that PD-1 has probably been expressed on exhausted T cells rather than on TFH equivalents (Figure 5, C). BM biopsy samples in diverse autoimmune disorders (n = 9) were negative for BCL6, disregarding a dim BCL6 positivity associated with myelopoiesis in 3 cases. PD-1 expression was heterogeneous and ranged from partial positivity in reactive lymphoid aggregates to complete negativity.

BM biopsy samples infiltrated by mantle cell lymphoma (n = 4) exhibited dim to strong BCL6 positivity associated with myelopoiesis in 3 cases and revealed dim BCL6–positive lymphoid infiltrates in 1 case. PD-1 expression was positive in tumor-infiltrating T lymphocytes in 3 cases. BM samples infiltrated by plasma cell myeloma (n = 3) showed irregularly distributed single BCL6-positive cells in 1 case, and PD-1–positive tumor-infiltrating T lymphocytes in 2 cases. BM infiltrated by lymphoplasmacytic lymphoma (n = 3) displayed dim BCL6 positivity in single tumor cells. PD-1 positivity was found in irregularly distributed tumor-infiltrating T lymphocytes. Samples with infiltrates of hairy cell leukemia (n = 3) revealed partial/dim positivity for BCL6 in the lymphoma cells of 2 cases and scattered PD-1–positive single cells, most probably tumor-infiltrating T lymphocytes. Follicular lymphoma (n = 3) infiltrates were, as expected, strongly positive for BCL6 and exhibited a significant amount of PD-1–positive tumor-infiltrating T lymphocytes. Infiltration by Burkitt lymphoma (n = 3) resulted in strong positivity for BCL6 in 2 cases, while staining in the third case failed (most probably because of loss of antigenicity due to the archival nature of the sample). PD-1 showed negativity. Infiltration by diffuse large B-cell lymphoma (n = 3) resulted in positivity for BCL6 in 2 cases.

Those cases also exhibited either single cell or partial positivity for PD-1. One case was completely negative for both markers. BM biopsy samples with T-cell prolymphocytic leukemia (n = 3) displayed a dim BCL6 positivity in single cells, for which a clear distinction between neoplastic T cells and cells arising from myelopoiesis was not possible with certainty. Grouped PD-1–positive cells were found in 1 case, PD-1 single cell expression in another, and 1 sample was negative for PD-1. Samples infiltrated by acute T-lymphoblastic leukemia (n = 3) were partially and dimly positive for BCL6 in 2 cases and contained single PD-1 tumor-infiltrating T lymphocytes in 1 case. Biopsy samples infiltrated by T-cell large granular lymphocytic leukemia (n = 3) featured dim BCL6 positivity associated with myelopoiesis in 2 cases as well as partial positivity of the leukemic infiltrates in 1 case, and all displayed PD-1–positive tumor-infiltrating T lymphocytes. Samples infiltrated by peripheral T-cell lymphoma, not otherwise specified (n = 4), showed negativity for both markers without exception. One of the BM samples infiltrated by mycosis fungoïdes (n = 2) displayed a strong BCL6 and dim PD-1 positivity of the tumor cells, while the other was negative for both markers (Figure 5, D and E). One BM sample infiltrated by a hepatosplenic γδ-T-cell lymphoma (n = 1) was negative for both markers. The BM samples affected by classical Hodgkin lymphoma (n = 3) showed in all instances infiltration by dim BCL6-positive histiocytes. There were also PD-1–positive tumor-infiltrating T lymphocytes detectable in all 3 samples (single cells up to 20% of all cells), while the Hodgkin and Reed-Sternberg cells remained completely negative for both markers (Figure 5, F and G).

DISCUSSION

Nearly 50 years after its first description, diagnosing AITL is still a challenge for clinicians and pathologists. Usually, the initial diagnosis is made by histologic examination of an affected LN, followed by a staging BM biopsy. Evaluating the presence and extent of BM involvement by AITL in staging biopsy samples might be unproblematic when extensive infiltration is present, but it can be more difficult in instances with subtle infiltrates with inconsistent phenotypic and molecular characteristics. Since unspecific systemic symptoms may be present, a BM biopsy can sometimes precede the LN excision or—very rarely in patients with high morbidity—be the only available specimen. Therefore, detailed knowledge of the morphologic, phenotypic, and molecular features, particularly when considering relevant differential diagnoses, is of great importance.

In our cohort of 37 patients with 42 matched pairs of LN and BM samples, we were able to confirm recently published data by Hong et al,[23] showing that BM involvement itself is an independent adverse prognostic risk factor in AITL with respect to overall survival. For that reason, correct staging, even if there are only subtle infiltrates, may be of substantial importance for the individual patient. Yet, the prognostic index of Hong et al[23] (encompassing BM involvement, number of affected extranodal sites, and performance status) was not helpful in our cohort, as most of our patients were classified in the high-risk group, which did not reflect their diverse outcome. Importantly and extending previous knowledge, our study revealed a possible prognostic impact of the exact histologic pattern of BM involvement by AITL. Patients with pattern 1 (interstitial/micronodular in association with eosinophils) had a longer overall survival than patients with infiltration pattern 2 (interstitial/micronodular without marked eosinophilia), and especially pattern 3 (diffuse with eosinophilia). Intriguingly, pattern 1 was not compulsorily associated with eosinophilia in the peripheral blood. While it seems comprehensible that diffuse infiltration of the BM (pattern 3) is associated with advanced disease, we have no explanation for why eosinophilia in the BM was associated with a better prognosis. A possible explanation could be that this pattern may reflect a different, more favorable immunologic response of the patient to the disease or may cause symptoms at an earlier stage. Finally, and as expected, the best prognosticator of outcome in our collective was the achievement of complete remission after induction chemotherapy.

Although the immunohistochemical phenotype of BM infiltration by AITL has been addressed by a few groups, it has never been systematically compared to the phenotype of the corresponding LN or to relevant differential diagnoses. In general, the expression of TFH markers in our AITL cohort was weaker in the BM than the matched LN. On the one hand, this may be related to technical reasons, since we apply less intensive antigenic retrieval protocols with EDTA-decalcified samples to conserve morphologic details and prevent physical destruction of the bony trabeculae–containing biopsy samples after microwaving. On the other hand, this more subtle "TFH signature" of AITL in the BM may be linked to the different microenvironment of the BM (eg, absence of high endothelial venules, LN sinus-lining cells, and follicular dendritic cells). In particular, the absence of follicular dendritic cells may be linked to a weaker expression or loss of CXCL13, CD10, and ICOS by the tumor cells in the BM.[16,19]

Although significantly increased in affected LNs, EBV-positive B cells were not of diagnostic relevance in the AITL-affected BM, which may be explicable by a preferential spread of the tumor, but not of the environmental cells of AITL, to the BM. Additionally, the absence or lower amount of reactivated EBV-positive B cells in the BM is also reflected by the lower proportion of CXCL13-positive cases (62% in LN compared to 13% in BM), as reactivated EBV-positive B cells upregulate CD28 ligand B7 and therefore promote the activation of TFH and CXCL13 production.[24]

Thus, most of the diagnostic reliability was given to PD-1 and BCL6. Importantly, owing to the partial positivity associated with myelopoiesis for BCL6, care has to be taken when evaluating this marker. By assessing double-staining for BCL6/PD-1 (and possibly other combinations such as BCL6/myeloperoxidase), a reliable differentiation between tumor cells and reactively changed lymphocytes or myelopoietic cells is possible and enables identification of even subtle AITL infiltrates.

T-cell receptor clonality testing has become a helpful tool in the diagnosis of AITL.[25] Yet, when applied to BM biopsy samples, clonality testing failed to generate useful results in most of our studied archival cases. Although it might yield more findings when applied to prospective material, the problem of minor tumor cell content scattered in a background of reactive cells may seriously challenge its sensitivity. This may partially be overcome by a targeted search for individual T-cell clones already known from the corresponding LN, yet the specificity and the clinical utility of such an approach remains to be verified. The same applies for the analysis of AITL-typical mutations in the BM.

Aggravatingly, a considerable proportion of these mutations, although being AITL typical in the LN, can be regularly found in clonal hematopoiesis of indeterminate potential and their presence is therefore per se not indicative of BM infiltration by AITL.[26]

Nevertheless, in cases remaining inconclusive after histopathologic analysis based on CD3, PD-1, and BCL6 stains, the evaluation of additional TFH markers (CD10, ICOS, CXCL13) and EBV-encoded small RNAs, as well as the application of molecular testing for T-cell clonality and characteristic mutations of AITL, may still increase the diagnostic yield as exemplified above.

Particular care should be taken when addressing differential diagnoses, especially in cases of "incidental" suspect diagnosis of AITL outside of staging procedures. Notably, reactive BM conditions, for instance toxic myelopathies, can display a substantial BCL6 and PD-1 positivity as shown above (Figure 5, A and B). Apart from the clinical context, application of double-staining for BCL6/PD-1 to demonstrate the coexpression of both markers in specific cellular subpopulations might be helpful in such instances. Importantly, clinicopathologic or morphologic mimickers of AITL—such as plasma cell myelomas, classical Hodgkin lymphomas, and peripheral T-cell lymphomas, not otherwise specified—display a distinct phenotype, allowing a clear-cut differential diagnosis after careful morphologic evaluation of the respectively stained slides. Finally, one should be aware of T-cell lymphoma entities, such as mycosis fungoïdes (and Sézary syndrome), that can coexpress PD-1 and BCL6 and may occasionally be encountered in BM biopsy samples.[27,28]

Taken together, the results of our study point toward the central role of a combined, primarily morphologic and ancillary phenotypic, and—in unequivocal cases—molecular approach to tackle BM infiltration by AITL, taking into consideration a few caveats of reactive and neoplastic conditions that may mimic it. Finally, we corroborate and extend previous results on the important prognostic role of BM involvement by AITL, pointing toward the relevance of systematically obtaining staging biopsy samples for this entity.

References

1. de Leval L, Parrens M, Le Bras F, et al. Angioimmunoblastic T-cell lymphoma is the most common T-cell lymphoma in two distinct French information data sets. *Haematologica*. 2015;100(9):e361–e364.
2. Dogan A, Gaulard P, Jaffe ES, Müller-Hermelink HK, de Leval L. Angioimmunoblastic T-cell lymphoma and other nodal lymphomas of T follicular helper cell origin. In: Swerdlow SH, Harris NL, Jaffe ES, et al, eds. *WHO Classification of Tumours of Haematopoietic and Lymphoid Tissues*. Revised 4th ed. Lyon, France: International Agency for Research on Cancer (IARC); 2017:407–410. *World Health Organization Classification of Tumours*; vol 2.
3. Lennert K, Mestdagh J. Hodgkin's disease with constantly high content of epithelioid cells [in German]. *Virchows Arch A Pathol Pathol Anat*. 1968;344(1):1–20.
4. Frizzera G, Moran EM, Rappaport H. Angio-immunoblastic lymphadenopathy with dysproteinaemia. *Lancet*. 1974;1(7866):1070–1073.
5. Lukes RJ, Tindle BH. Immunoblastic lymphadenopathy: a hyperimmune entity resembling Hodgkin's disease. *N Engl J Med*. 1975;292(1):1–8.
6. Nathwani BN, Rappaport H, Moran EM, Pangalis GA, Kim H. Malignant lymphoma arising in angioimmunoblastic lymphadenopathy. *Cancer*. 1978;41(2):578–606.
7. Radaszkiewicz T, Lennert K. Immunoblastic adenopathy: clinical features, treatment and prognosis (author's transl) [in German]. *Dtsch Med Wochenschr*. 1975;100(21):1157–1163.
8. Stansfeld AG, Diebold J, Noel H, et al. Updated Kiel classification for lymphomas. *Lancet*. 1988;1(8580):292–293.
9. Federico M, Rudiger T, Bellei M, et al. Clinicopathologic characteristics of angioimmunoblastic T-cell lymphoma: analysis of the international peripheral T-cell lymphoma project. *J Clin Oncol*. 2013;31(2):240–246.
10. de Leval L, Gisselbrecht C, Gaulard P. Advances in the understanding and management of angioimmunoblastic T-cell lymphoma. *Br J Haematol*. 2010;148(5):673–689.
11. de Leval L, Rickman DS, Thielen C, et al. The gene expression profile of nodal peripheral T-cell lymphoma demonstrates a molecular link between angioimmunoblastic T-cell lymphoma (AITL) and follicular helper T (TFH) cells. *Blood*. 2007;109(11):4952–4963.
12. Attygalle A, Al-Jehani R, Diss TC, et al. Neoplastic T cells in angioimmunoblastic T-cell lymphoma express CD10. *Blood*. 2002;99(2):627–633.
13. Marafioti T, Paterson JC, Ballabio E, et al. The inducible T-cell co-stimulator molecule is expressed on subsets of T cells and is a new marker of lymphomas of T follicular helper cell-derivation. *Haematologica*. 2010;95(3):432–439.
14. Anagnostopoulos I, Hummel M, Finn T, et al. Heterogeneous Epstein-Barr virus infection patterns in peripheral T-cell lymphoma of angioimmunoblastic lymphadenopathy type. *Blood*. 1992;80(7):1804–1812.
15. Weiss LM, Jaffe ES, Liu XF, Chen YY, Shibata D, Medeiros LJ. Detection and localization of Epstein-Barr viral genomes in angioimmunoblastic lymphadenopathy and angioimmunoblastic lymphadenopathy-like lymphoma. *Blood*. 1992;79(7):1789–1795.
16. Cho YU, Chi HS, Park CJ, Jang S, Seo EJ, Huh J. Distinct features of angioimmunoblastic T-cell lymphoma with bone marrow involvement. *Am J Clin Pathol*. 2009;131(5):640–646.
17. Attygalle AD, Diss TC, Munson P, Isaacson PG, Du MQ, Dogan A. CD10 expression in extranodal dissemination of angioimmunoblastic T-cell lymphoma. *Am J Surg Pathol*. 2004;28(1):54–61.
18. Grogg KL, Morice WG, Macon WR. Spectrum of bone marrow findings in patients with angioimmunoblastic T-cell lymphoma. *Br J Haematol*. 2007;137(5):416–422.
19. Khokhar FA, Payne WD, Talwalkar SS, et al. Angioimmunoblastic T-cell lymphoma in bone marrow: a morphologic and immunophenotypic study. *Hum Pathol*. 2010;41(1):79–87.
20. Torlakovic EE, Brynes RK, Hyjek E, et al. ICSH guidelines for the standardization of bone marrow immunohistochemistry. *Int J Lab Hematol*. 2015;37(4):431–449.
21. Juskevicius D, Lorber T, Gsponer J, et al. Distinct genetic evolution patterns of relapsing diffuse large B-cell lymphoma revealed by genome-wide copy number aberration and targeted sequencing analysis. *Leukemia*. 2016;30(12):2385–2395.
22. Sakata-Yanagimoto M, Enami T, Yoshida K, et al. Somatic RHOA mutation in angioimmunoblastic T cell lymphoma. *Nat Genet*. 2014;46(2):171–175.
23. Hong H, Fang X, Wang Z, et al. Angioimmunoblastic T-cell lymphoma: a prognostic model from a retrospective study. *Leuk Lymphoma*. 2018;59(12):2911–2916.
24. Dunleavy K, Wilson WH. Angioimmunoblastic T-cell lymphoma: immune modulation as a therapeutic strategy. *Leuk Lymphoma*. 2007;48(3):449–451.
25. Zhang D, Saunders CJ, Zhao W, Davis M, Cunningham MT. The clonality of CD3+ CD10+ T cells in angioimmunoblastic T cell lymphoma, B cell lymphoma, and reactive lymphoid hyperplasia. *Am J Hematol*. 2009; 84(9):606–608.
26. Buscarlet M, Provost S, Zada YF, et al. Lineage restriction analyses in CHIP indicate myeloid bias for TET2 and multipotent stem cell origin for DNMT3A. *Blood*. 2018;132(3):277–280.
27. Park JH, Han JH, Kang HY, Lee ES, Kim YC. Expression of follicular helper T-cell markers in primary cutaneous T-cell lymphoma. *Am J Dermatopathol*. 2014;36(6):465–470.
28. Meyerson HJ, Awadallah A, Pavlidakey P, Cooper K, Honda K, Miedler J. Follicular center helper T-cell (TFH) marker positive mycosis fungoides/Sezary syndrome. *Mod Pathol*. 2013;26(1):32–43.

SMAD1 promoter hypermethylation and lack of SMAD1 expression in Hodgkin lymphoma: a potential target for hypomethylating drug therapy

Magdalena M. Gerlach, Anna Stelling-Germani, Cheuk Ting Wu, Sebastian Newrzela, Claudia Döring, **Visar Vela**, Anne Müller, Sylvia Hartmann, Alexandar Tzankov

-Letters to the Editor-
Published in *Haematologica*, 2020

SMAD1 promoter hypermethylation and lack of SMAD1 expression in Hodgkin lymphoma: a potential target for hypomethylating drug therapy

Hodgkin lymphoma (HL) is an immunologically active lymphoid neoplasm composed of a few (usually 1-10%) neoplastic Hodgkin and Reed-Sternberg (HRS) cells or lymphocyte-predominant (LP) cells and >90% non-neoplastic cells, mainly T- and B-lymphocytes, plasma cells, macrophages, eosinophils and fibroblasts. The substantial amount of reactive cells in HL is supposed to be the net effect of a complex signaling network of cytokines and chemokines secreted by either the HRS cells or non-neoplastic cells.[1] One component of this network is transforming growth factor beta (TGF-β), which is produced by HRS cells and cancer-associated fibroblasts. TGF-β unfolds its immunosuppressive impact by stimulating tumor-infiltrating T-lymphocytes (TIL) to differentiate into anergic, tumor-promoting, regulatory T cells (Treg).[2] Additionally, TGF-β inhibits natural killer cells - one of the key components of the innate anticancer immunity.[3] Interestingly and still poorly understood, the HRS cells themselves seem to remain unaffected by the tumor-suppressive properties of TGF-β.[4]

Recent studies on diffuse large B-cell lymphoma (DLBCL) revealed a previously unknown tumor-suppressive signaling axis involving SMAD1 as a downstream messenger of TGF-β.[5] SMAD1 functions as an intracellular signal transducer between extracellular TGF-β and the nucleus, where it modulates the transcription of target genes. This signaling cascade was shown to be recurrently inactivated in DLBCL, mainly by hypermethylation of five promoter regions surrounding the *SMAD1* transcription start site, which finally generates a significant growth advantage for lymphoma cells.[5] In the course of these investigations, we noted that SMAD1 was not expressed in HRS cells of screened HL cases. This led us to hypothesize that the absence of SMAD1 expression in HRS cells may mechanistically be linked to their resistance to the tumor-suppressive effects of TGF-β.[4]

In order to further elucidate this finding, we analyzed 132 well-characterized archival tissue-microarrayed cases,[6] and 11 conventional routine lymphadenectomy specimens from patients suffering from all subtypes of classic HL (77 nodular sclerosis [NS]; 48 mixed cellularity [MC]; 7 lymphocyte-rich [LR]; 5 lymphocyte-depleted; and 6 unclassifiable classic HL) and 14 routine samples from patients suffering from nodular lymphocyte-predominant HL (NLPHL). We analyzed all these instances for immunohistochemical expression of SMAD1. Importantly, to guarantee retained antigenicity, only cases containing (physiologically) SMAD1-positive endothelia were considered. We found that all NLPHL (14/14 cases; 100%) and the great majority of classic HL (138/143 cases; 97%) displayed SMAD1-negative LP and HRS cells, respectively (Figure 1A and B). Single HRS cells stained faintly for SMAD1 in five cases only (2 NS; 2 MC; and 1 LR classic HL). With respect to non-neoplastic cells, 65/143 classic HL (45%) showed moderate (15-49% of TIL) up to abundant (≥50% of TIL) amounts of SMAD1 positive surrounding TIL, thus being potentially susceptible to the suppressive influence of TGF-β (Figure 1A and B); in NLPHL, 11/14 (79%) cases displayed abundant SMAD1-expressing TIL, including TIL involved in rosetting around LP cells (*Online Supplementary Figure S1*). The presence of abundant SMAD1-expressing TIL did not correlate with disease stage, patients' age, gender, presence of B symptoms, association with Epstein-Barr virus (EBV) or outcome, while showing significant correlations with the NS subtype (45/77 NS cases, i.e. 58%, compared to 20/66 non-NS cases, i.e. 30%, P=0.025 χ^2 test) and with the amount of FOXP3-positive Treg (Rho=0.351, P=0.000053 Spearman correlation), which both, in turn, may be directly linked to the effects of TGF-β, promoting sclerosis and a shift towards Treg differentiation.[2] In contrast, surrounding plasma cells seemed to lack SMAD1 expression, potentially rendering them insensitive to the pro-apoptotic and anti-proliferative signals of TGF-β.[7] With regard to plasma cells, this largely fits with the newly described negative prognostic impact of their increased numbers in classic HL.[8]

To strengthen our hypothesis, we investigated the promoter methylation status of the *SMAD1* gene in six different HL cell lines, including one NLPHL cell line (DEV) exactly as described elsewhere.[5] Methylation analysis by bisulfite sequencing was successful for three regions of

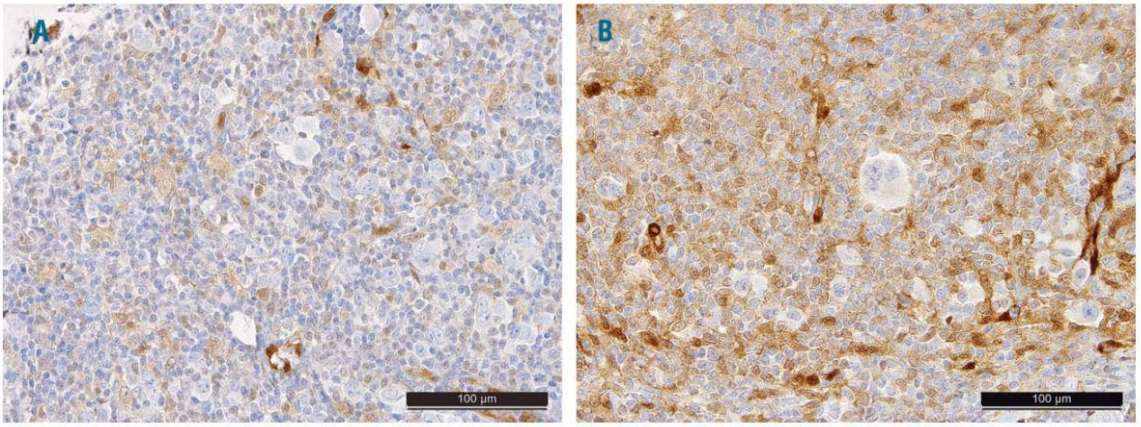

Figure 1. Expression of SMAD1 in classic Hodgkin lymphoma. (A) Tissue microarrayed archival mixed cellularity classic Hodgkin lymphoma with moderate numbers of SMAD1-positive tumor-infiltrating lymphocytes (TIL) and a few strongly staining endothelia. Note that all Hodgkin and Reed-Sternberg (HRS) cells are negative. (B) Diagnostic lymphadenectomy of a nodular sclerosis cHL with abundant SMAD1-positive TIL and a few strongly staining endothelia. Note that all HRS cells are negative. Immunoperoxidase staining, original magnification 400x.

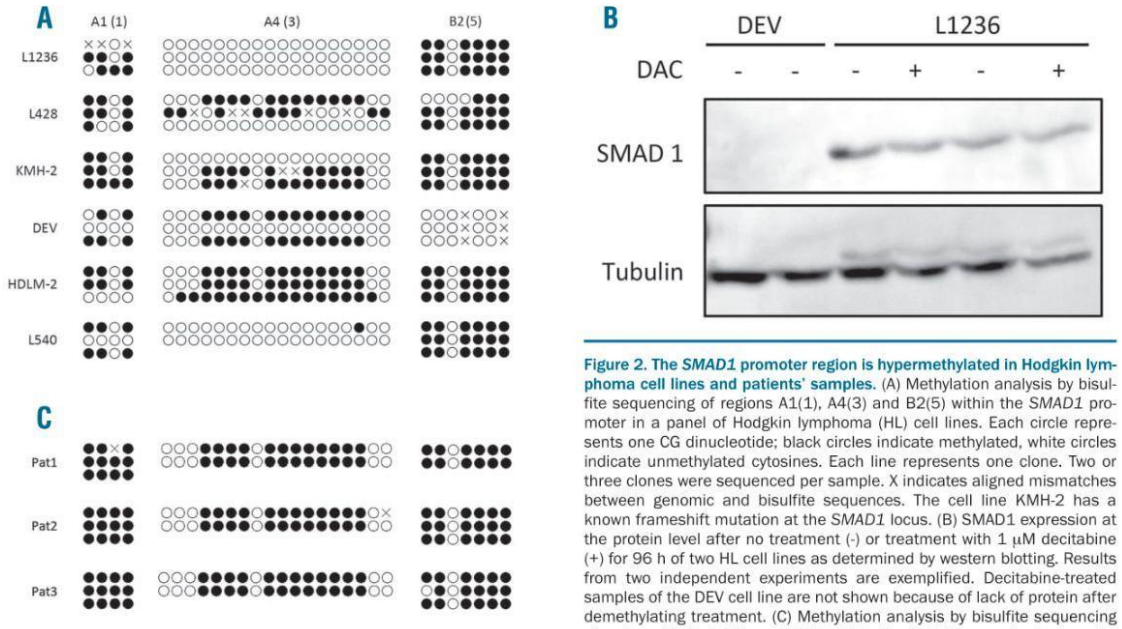

Figure 2. The *SMAD1* promoter region is hypermethylated in Hodgkin lymphoma cell lines and patients' samples. (A) Methylation analysis by bisulfite sequencing of regions A1(1), A4(3) and B2(5) within the *SMAD1* promoter in a panel of Hodgkin lymphoma (HL) cell lines. Each circle represents one CG dinucleotide; black circles indicate methylated, white circles indicate unmethylated cytosines. Each line represents one clone. Two or three clones were sequenced per sample. X indicates aligned mismatches between genomic and bisulfite sequences. The cell line KMH-2 has a known frameshift mutation at the *SMAD1* locus. (B) SMAD1 expression at the protein level after no treatment (-) or treatment with 1 μM decitabine (+) for 96 h of two HL cell lines as determined by western blotting. Results from two independent experiments are exemplified. Decitabine-treated samples of the DEV cell line are not shown because of lack of protein after demethylating treatment. (C) Methylation analysis by bisulfite sequencing of regions A1(1), A4(3) and B2(5) within the *SMAD1* promoter in samples from three patients with classic HL. Each circle represents one CG dinucleotide; black circles indicate methylated, white circles indicate unmethylated cytosines. Each line represents one clone. Two or three clones were sequenced per sample. X indicates aligned mismatches between genomic and bisulfite sequences.

the *SMAD1* promoter and yielded four hypermethylated cell lines (L428, KMH-2, DEV, HDLM-2), that differed substantially, particularly regarding their methylation of region A4(3), from cell lines showing no evidence of promoter hypermethylation (L1236, L540) (Figure 2A). Importantly, KMH-2 is known to be *SMAD1* p.ADTP220fs mutant (*https://portals.broadinstitute.org/ccle/page?cell_line=KMH2_haematopoietic_and_lymphoid_tissue*), which additionally points towards a potential role of this gene silencing in lymphomagenesis.

The impact of the promoter methylation status of *SMAD1* on protein expression was further addressed by western blot analysis, comparing one hypermethylated cell line (DEV) with a cell line without hypermethylation (L1236). Concordantly, the expression of SMAD1 differed clearly, without detectable protein in the DEV cell line (Figure 2B). When treated with the DNA methyltransferase inhibitor decitabine, which reverses, among others, the hypermethylation of *SMAD1* promoters, the SMAD1-negative cell line DEV died immediately after exposure. As expected, the expression of SMAD1 was not affected by treatment in the L1236 cell line, which is not hypermethylated.

To obtain further clinical evidence, the promoter methylation status of *SMAD1* was assessed in samples from three patients with classic HL. To do this, we used our newly developed, flow sorting-assisted technique for HRS cell enrichment from formalin-fixed and paraffin-embedded tissues, allowing for targeted genetic analysis of DNA isolated from classic HL tumor cells.[9] In this collective, not only the A4(3) promoter region of *SMAD1*, but also the A1(1) region was substantially hypermethylated (Figure 2C). Furthermore, *SMAD1* promoter hypermethylation was identified in sorted tumor-infiltrating plasma cells, fitting with the immunohistochemically noted lack of SMAD1 in plasma cells.

Although risk-adjusted standard treatment of HL is successful in over 90% of patients, relapses after salvage therapy and refractory cases represent oncological challenges and run an unfavorable clinical course with limited therapeutic options. In this context, demethylating agents such as decitabine and azacytidine may be of potential therapeutic interest and have already shown promising effects. At clinically relevant concentrations, decitabine has been documented to inhibit the growth of classic HL cell lines *in vitro* and a single case observation of regressing relapsed classic HL as an unexpected "side effect" of azacytidine has been reported in a patient suffering from concomitant myelodysplastic syndrome.[10,11] Decitabine and azacytidine inhibit DNA methyltransferases, and thereby reverse promoter hypermethylation of *SMAD1*.[12] Importantly, promising results with decitabine were also obtained in DLBCL cell lines lacking SMAD1 expression due to promoter hypermethylation.[5] Four days of treatment were sufficient to restore *SMAD1* transcription and protein expression in a subset of initially SMAD1-negative DLBCL cell lines, an effect corroborated by observations in a patient-derived xenograft DLBCL mouse model with proven *SMAD1* promoter hypermethylation.[5] Analogous to this, we treated the SMAD1-negative HL cell line DEV with decitabine. The cells died immediately after exposure, possibly due to marked responsiveness to decitabine.

Since therapeutic reversion of *SMAD1* promoter hypermethylation would be of potential relevance only in the presence of TGF-β receptors (TGFBR), we analyzed publically available (Gene Expression Omnibus [GEO] accession n. GSE12453) and our own (GEO accession n. GSE147387) gene expression data from primary HRS and LP cells and cell lines to estimate whether HRS and LP

cells express TGFBR and associated proteins (ACVR1, ACVR1B, ACVR1C, ACVR2A, ACVR2B, ACVRL1, AMHR2, BMPR2, TGFBR1, TGFBR2, TGFBR3, TGFBRAP1). The classic HL cell line KMH-2 contained relevant transcript levels of all TGFBR types, HDLM-2 expressed TGFBR1 and TGFBR3, and the NLPHL cell line DEV expressed TGFBR1; the classic HL cell lines L1236 and L428 exhibited TGBRAP1 transcripts. In all these cell lines SMAD1 transcripts were decreased.

In summary, our data suggest a likely important, not yet described role of *SMAD1* hypermethylation in HL, potentially causing an imbalance of TGF-β signaling axis responses in involved tissues. SMAD1 has been demonstrated to be part of the TGF-β-mediated anti-proliferative pathway in different B-cell lymphomas. Intriguingly, lymphomas with mutated or knocked-out *SMAD1* were protected from the tumor-suppressive effects of TGF-β.[13]

Lack of SMAD1 expression in HRS and LP cells due to promoter hypermethylation or gene mutation may analogously contribute to their resistance towards the pro-apoptotic and anti-proliferative effects of TGF-β, despite the presence of TGFBR transcripts. This hypothesis is further supported by observations in EBV-positive classic HL, in which decreased SMAD2 levels due to EBNA1-mediated increased protein turnover[14] disable TGF-β signaling, being congruent with our data regarding SMAD1 downregulation in HRS cells.

In contrast, retained SMAD1 expression in surrounding TIL may contribute to immune escape, as intact TGF-β signaling promotes T-cell differentiation into tumor-supporting Treg,[2] which is reflected by the observed correlation between higher numbers of FOXP3-positive Treg and expression of SMAD1 in TIL. The tumor-suppressive effects of TGF-β on TIL have recently been challenged by a promising clinical study in which the infusion of TGF-β-insensitive T cells was successfully used in patients with EBV-positive relapsed classic HL.[15]

Our data suggest a possible rationale for the application of a more tailored treatment with hypomethylating agents in HL, which may be worth of prospective investigations, as agents such as decitabine have already shown promising results in *SMAD1* hypermethylated DLBCL[5] and in classic HL cell lines.[10]

Magdalena M. Gerlach,[1] Anna Stelling-Germani,[2] Cheuk Ting Wu,[2] Sebastian Newrzela,[3] Claudia Döring,[3] Visar Vela,[1] Anne Müller,[2] Sylvia Hartmann[3] and Alexandar Tzankov[1]

[1]Institute of Medical Genetics and Pathology, University of Basel, Basel, Switzerland; [2]Institute of Molecular Cancer Research, University of Zurich, Zurich, Switzerland and [3]Institute of Pathology, Department of Pathology, Goethe University Frankfurt on Main, Germany

Correspondence:
ALEXANDAR TZANKOV - alexandar.tzankov@usb.ch

doi:10.3324/haematol.2020.249276

Disclosures: no conflicts of interests to disclose.

Contributions: MMG wrote the manuscript and evaluated the histology and immunohistochemical stains; AS-G supervised the SMAD1 promoter methylation assessment, performed cell line viability experiments, corrected the manuscript and wrote the legend to Figure 2; CTW assessed SMAD1 promoter methylation; SN provided gene expression data of Hodgkin lymphoma cell lines; CD provided and analyzed gene expression data of Hodgkin lymphoma cell lines; VV enriched Hodgkin and Reed-Sternberg cells from archived clinical samples and isolated DNA from them; AM supervised SMAD1 promoter methylation assessment; SH provided cell lines; AT designed the study, supervised histopathological assessment, performed statistics, analyzed gene expression data of Hodgkin lymphoma cell lines, partially wrote and completely edited the manuscript

Funding: this study was supported by the Swiss National Science Foundation.

References

1. Poppema S. Immunobiology and pathophysiology of Hodgkin lymphomas. Hematology Am Soc Hematol Educ Program. 2005:231-238.
2. Liu Y, Zhang P, Li J, Kulkarni AB, Perruche S, Chen W. A critical function for TGF-beta signaling in the development of natural CD4+CD25+Foxp3+ regulatory T cells. Nat Immunol. 2008; 9(6):632-640.
3. Chiu J, Ernst DM, Keating A. Acquired natural killer cell dysfunction in the tumor microenvironment of classic Hodgkin lymphoma. Front Immunol. 2018;9:267.
4. Menter T, Tzankov A. Lymphomas and their microenvironment: a multifaceted relationship. Pathobiology. 2019;86(5-6):225-236.
5. Stelling A, Wu CT, Bertram K, et al. Pharmacological DNA demethylation restores SMAD1 expression and tumor suppressive signaling in diffuse large B-cell lymphoma. Blood Adv. 2019;3(20):3020-3032.
6. Tzankov A, Matter MS, Dirnhofer S. Refined prognostic role of CD68-positive tumor macrophages in the context of the cellular micromilieu of classical Hodgkin lymphoma. Pathobiology. 2010;77(6):301-308.
7. Lebman DA, Edmiston JS. The role of TGF-beta in growth, differentiation, and maturation of B lymphocytes. Microbes Infect. 1999;1(15):1297-1304.
8. Gholiha AR, Hollander P, Hedstrom G, et al. High tumour plasma cell infiltration reflects an important microenvironmental component in classic Hodgkin lymphoma linked to presence of B-symptoms. Br J Haematol. 2019;184(2):192-201.
9. Juskevicius D, Jucker D, Dietsche T, et al. Novel cell enrichment technique for robust genetic analysis of archival classical Hodgkin lymphoma tissues. Lab Invest. 2018;98(11):1487-1499.
10. Swerev TM, Wirth T, Ushmorov A. Activation of oncogenic pathways in classical Hodgkin lymphoma by decitabine: a rationale for combination with small molecular weight inhibitors. Int J Oncol. 2017;50(2):555-566.
11. D'Alò F, Leone G, Hohaus S, et al. Response to 5-azacytidine in a patient with relapsed Hodgkin lymphoma and a therapy-related myelodysplastic syndrome. Br J Haematol. 2011;154(1):141-143.
12. Foulks JM, Parnell KM, Nix RN, et al. Epigenetic drug discovery: targeting DNA methyltransferases. J Biomol Screen. 2012;17(1):2-17.
13. Munoz O, Fend F, de Beaumont R, Husson H, Astier A, Freedman AS. TGFbeta-mediated activation of Smad1 in B-cell non-Hodgkin's lymphoma and effect on cell proliferation. Leukemia. 2004;18(12):2015-2025.
14. Wood VH, O'Neil JD, Wei W, Stewart SE, Dawson CW, Young LS. Epstein-Barr virus-encoded EBNA1 regulates cellular gene transcription and modulates the STAT1 and TGFbeta signaling pathways. Oncogene. 2007;26(28):4135-4147.
15. Bollard CM, Tripic T, Cruz CR, Dotti G, Gottschalk S, Torrano V. Tumor-specific T cells engineered to overcome tumor immune evasion induce clinical responses in patients with relapsed Hodgkin lymphoma. J Clin Oncol. 2018;36(11):1128-1139.

Effects of lenalidomide on the bone marrow microenvironment in acute myeloid leukemia: Translational analysis of the HOVON103 AML/SAKK30/10 Swiss trial cohort

Magdalena M. Brune, Georg Stüssi, Pontus Lundberg, **Visar Vela**, Dominik Heim, Markus G. Manz, Eugenia Haralambieva, Thomas Pabst, Yara Banz, Mario Bargetzi, Rainer Grobholz, Martin Fehr, Sergio Cogliatti, Gert J. Ossenkoppele, Bob Löwenberg, Christina Biaggi Rudolf, Qiyu Li, Jakob Passweg, Luca Mazzuchelli, Michael Medinger, Alexandar Tzankov, on behalf of the Dutch-Belgian Hemato-Oncology Cooperative Group (HOVON) and Swiss Group for Clinical Cancer Research (SAKK)

-Original Article-

Published in *Annals of Hematology*, 2021

Annals of Hematology
https://doi.org/10.1007/s00277-021-04467-2

ORIGINAL ARTICLE

Effects of lenalidomide on the bone marrow microenvironment in acute myeloid leukemia: Translational analysis of the HOVON103 AML/SAKK30/10 Swiss trial cohort

Magdalena M. Brune[1] · Georg Stüssi[2] · Pontus Lundberg[3] · Visar Vela[1] · Dominik Heim[3] · Markus G. Manz[4] · Eugenia Haralambieva[5] · Thomas Pabst[6] · Yara Banz[7] · Mario Bargetzi[8] · Rainer Grobholz[9] · Martin Fehr[10] · Sergio Cogliatti[11] · Gert J. Ossenkoppele[12] · Bob Löwenberg[13] · Christina Biaggi Rudolf[14] · Qiyu Li[14] · Jakob Passweg[3] · Luca Mazzuchelli[15] · Michael Medinger[3,16] · Alexandar Tzankov[1] · on behalf of the Dutch-Belgian Hemato-Oncology Cooperative Group (HOVON) and Swiss Group for Clinical Cancer Research (SAKK)

Received: 13 October 2020 / Accepted: 18 February 2021

Abstract

This translational study aimed at gaining insight into the effects of lenalidomide in acute myeloid leukemia (AML). Forty-one AML patients aged 66 or older of the Swiss cohort of the HOVON-103 AML/SAKK30/10 study were included. After randomization, they received standard induction chemotherapy with or without lenalidomide. Bone marrow biopsies at diagnosis and before the 2nd induction cycle were obtained to assess the therapeutic impact on leukemic blasts and microenvironment. Increased bone marrow angiogenesis, as assessed by microvessel density (MVD), was found at AML diagnosis and differed significantly between the WHO categories. Morphological analysis revealed a higher initial MVD in AML with myelodysplasia-related changes (AML-MRC) and a more substantial decrease of microvascularization after lenalidomide exposure. A slight increase of T-bet-positive TH1-equivalents was identifiable under lenalidomide. In the subgroup of patients with AML-MRC, the progression-free survival differed between the two treatment regimens, showing a potential but not significant benefit of lenalidomide. We found no correlation between the cereblon genotype (the target of lenalidomide) and treatment response or

Michael Medinger and Alexandar Tzankov contributed equally to this work.

✉ Michael Medinger
michael.medinger@usb.ch

✉ Alexandar Tzankov
alexandar.tzankov@usb.ch

[1] Institute of Medical Genetics and Pathology, University Hospital Basel, Schoenbeinstrasse 40, 4031 Basel, Switzerland

[2] Oncological Institute of Italian Switzerland, Via Ospedale, 6500 Bellinzona, Switzerland

[3] Division of Hematology, Department of Medicine, University Hospital Basel, Petersgraben 4, 4031 Basel, Switzerland

[4] Department of Medical Oncology and Hematology, University and University Hospital Zurich, Raemistrasse 100, 8091 Zurich, Switzerland

[5] Institute of Pathology and Molecular Pathology, University Hospital Zurich, Schmelzbergstrasse 12, 8091 Zürich, Switzerland

[6] Department of Medical Oncology, Inselspital, University Hospital and University of Bern, 3010 Bern, Switzerland

[7] Institute of Pathology, University of Bern, Murtenstrasse 31, 3008 Bern, Switzerland

[8] Clinic for Oncology, Hematology and Transfusion Medicine, Cantonal Hospital Aarau AG, Tellstrasse 25, 5001 Aarau, Switzerland

[9] Institute of Pathology, Cantonal Hospital Aarau AG, Tellstrasse 25, 5001 Aarau, Switzerland

[10] Clinic for Medical Oncology and Hematology, Cantonal Hospital St. Gallen, Rorschacher Strasse 95, 9007 St. Gallen, Switzerland

[11] Institute of Pathology, Cantonal Hospital St. Gallen, Rorschacher Strasse 95, 9007 St. Gallen, Switzerland

[12] Department of Hematology, Amsterdam University Medical Center, Cancer Center Amsterdam, VU University Medical Center, De Boelelaan 1118, 1182 Amsterdam, DB, Netherlands

[13] Department of Hematology, Erasmus University Rotterdam, Dr. Molewaterplein 50, 3000 Rotterdam, CA, Netherlands

[14] Swiss Group for Clinical Cancer Research (SAKK), Coordinating Center, Effingerstrasse 33, CH-3008 Bern, Switzerland

[15] Cantonal Institute of Pathology, Via Selva 24, 6601 Locarno, Switzerland

[16] Division of Internal Medicine, Department of Medicine, University Hospital Basel, Petersgraben 4, 4031 Basel, Switzerland

prognosis. In conclusion, addition of lenalidomide may be beneficial to elderly patients suffering from AML-MRC, where it leads to a reduction of microvascularization and, probably, to an intensified specific T cell-driven anti-leukemic response.

Keywords Acute myeloid leukemia · Bone marrow microenvironment · Cereblon · Lenalidomide · Microvessel density · T cells

Introduction

Most individuals with acute myeloid leukemia (AML) are older than 65 years upon diagnosis [1]. As the incidence of unfavorable genetic alterations increases with age, the prognosis of AML in the elderly is dismal and associated with the worst median overall survival (OS) of all cancers in this age group with nearly 80% of the patients died after 1 year [1, 2]. Aggravatingly, chemotherapeutic treatment remains challenging due to the rising incidence of comorbidities and the poorer performance status of aged individuals. Although the development of less toxic and more effective treatment options is of utter interest, only modest progress has been achieved in clinical outcomes of elderly AML patients in the last decade.

Based on its clinical activity in related disorders such as myelodysplastic syndromes (MDS) and other hematologic malignancies including multiple myeloma and follicular lymphoma [3–5], the orally active immune-modulatory drug (IMiD) lenalidomide gathered attention as a novel antineoplastic agent for the treatment of AML. Lenalidomide targets the omnipresent E3 ubiquitin ligase complex cereblon [6], which mediates its effects on tumor cells and non-neoplastic cells of the tumor microenvironment [7]. Lenalidomide activates cereblon's ligase activity leading to faster degradation of the transcription factors Ikaros and Aiolos, which play an important role in the regulation of B- and T cell development [7], and the casein kinase 1A1 (CK1alpha), which is a negative regulator of p53 [8]. CK1alpha is encoded by the *CSNK1A1* gene, which can be deleted or mutated in del(5q) MDS. In murine models, haploinsufficiency of this gene leads to hematopoietic stem cell expansion, whereas a complete loss induces stem cell apoptosis by activation of p53, explaining at least partially the effect of lenalidomide in del(5q) MDS [9]. In analogy, *Csnk1a1* knockdown in AML cell lines increases p53 activity and myeloid differentiation and results in selective elimination of leukemic cells [10].

Furthermore, autoubiquitination (and thus degradation) of wild-type cereblon is prevented by lenalidomide. In net terms, lenalidomide has anti-proliferative effects particularly on malignant B-cells and stimulating effects on by-stander T cells and natural killer (NK) cells, while promoting the production of anti-inflammatory cytokines [7]. Next to this antineoplastic and immune-modulatory effect, lenalidomide impairs the secretion of the vascular endothelial growth factor (VEGF) in the bone marrow stroma, eventually influencing vessel density and other microenvironmental changes [11]. Recently, the HOVON/SAKK study group published their data of the HOVON103 AML/SAKK 30/10 trial on the addition of lenalidomide to standard intensive treatment in elderly patients with AML and high-risk MDS [12]. Unfortunately, the study failed to show a clear benefit for those patients receiving additional lenalidomide, putting it in line with many other surveys performed in the setting of AML in the elderly. Here, we present a translational research analysis of the study encompassing patients of the Swiss study cohort, for whom bone marrow biopsies at study inclusion and—for the majority of individuals—before the 2nd induction cycle were available. Our results suggest that addition of lenalidomide to induction chemotherapy may be beneficial to elderly patients suffering from AML with myelodysplasia-related changes (AML-MRC).

Materials and methods

Patient cohort and treatment

Forty-one patients of the Swiss cohort of HOVON103 AML/SAKK 30/10 trial were included in this translational research study, of whom 20 were male and 21 female (Table 1). They were all previously untreated, aged ≥ 66, had a WHO performance score of ≤ 2, and a morphologically confirmed diagnosis of de novo AML. Patients with acute promyelocytic leukemia were not included. The patients' mean age at first diagnosis was 69 years (range 66 to 76). Clinical outcome parameters for this study were progression-free survival (PFS) and overall survival (OS). For further details, we refer to the HOVON/SAKK study group publication on the clinical trial [12]. This study was approved by the ethics committee of Northwestern Switzerland (EKNZ BASEC 2016-01218).

To morphologically assess the therapeutic impact on blasts and microenvironment, bone marrow biopsies were gained at the time-point of diagnosis and, whenever possible, before the beginning of the 2nd induction cycle.

Karyotypes were classified according to Grimwade et al. [13] into three prognostically relevant groups (favorable, intermediate, adverse). Considering morphological and genetical criteria, patients were subgrouped into different diagnostic categories, according to the current WHO classification of tumors of hematopoietic and lymphoid tissues [14].

Table 1 Patients' characteristics and responses to treatment

	Standard treatment (n = 19): n(%)	With lenalidomide (n = 22): n(%)
Sex		
• Male	10 (52.6%)	10 (45.5%)
• Female	9 (47.4%)	12 (54.5%)
Dose of lenalidomide		
• 15 mg	NA	1 (4.5%)
• 20 mg	NA	21 (95.5%)
WHO classification of AML		
• AML NOS	10 (52.6%)	11 (50.0%)
• AML mutations	6 (31.6%)	4 (18.2%)
• AML specific translocations	2 (10.5%)	0 (0.0%)
• AML MRC	1 (5.3%)	7 (31.8%)
Age at registration (years)		
• 66–70	13 (68.4%)	20 (90.9%)
• 71–76	6 (31.6%)	2 (9.1%)
Karyotype according to Grimwade		
• Favorable	2 (10.5%)	0 (0.0%)
• Intermediate	15 (78.9%)	15 (68.2%)
• Adverse	0 (0.0%)	5 (22.7%)
• Missing	2 (10.5%)	2 (9.1%)
Best response after cycle 1		
• CR	11 (57.9%)	11 (50.0%)
• CRi	0 (0.0%)	4 (18.2%)
• PR	3 (15.8%)	0 (0.0%)
• RD	3 (15.8%)	6 (27.3%)
• Death in aplasia	0 (0.0%)	1 (4.5%)
• Death of indeterminate cause	2 (10.5%)	0 (0.0%)
Did patient start cycle 2?		
• No	4 (21.1%)	8 (36.4%)
• Yes	15 (78.9%)	14 (63.6%)
Best response after cycle 2 (only for patients started cycle 2)		
• CR	12	8
• CRi	1	3
• PR	1	1
• RD	1	0
• death in aplasia	0	1
• death of indeterminate cause	0	1

NA, not applicable; *NOS*, not otherwise specified; *MRC*, myelodysplasia-related changes; *CR*, complete remission; *CRi*, CR with incomplete hematologic recovery; *PR*, partial remission; *RD*, refractory disease

As described in more detail by Ossenkoppele et al. [12], the patients randomly received either a standard remission induction regimen with or without lenalidomide. Of our cohort, 19 patients were assigned to the standard treatment arm (daunorubicin 45 mg/m^2 days 1–3 and cytarabine 200 mg/m^2 days 1–7 in cycle I; and cytarabine 1000 mg/m^2 q 12 h days 1–6 in cycle II), and 22 patients additionally received lenalidomide at an assigned dose level (10 to 20 mg/day orally, days 1–21 of each cycle) (Table 1).

Morphological, immunohistochemical, and molecular work-up of bone marrow biopsies

Bone marrow biopsies at the time-point of diagnosis were available in 39/41 cases. A second bone marrow biopsy, which was obtained before the 2nd induction cycle, was available in 28/41 cases. The specimens were fixed in 4% formalin and paraffin-embedded, followed by decalcification with ethylenediaminetetraacetic acid (EDTA) [15]. Hematoxylin-and-

eosin- (H&E) and Gömöri-stained slides were reviewed, and the presence and amount of leukemic blasts, myelodysplasia-related changes, and the degree of myelofibrosis [16] were assessed. Immunohistochemistry was performed using the automated staining system Benchmark XT (Roche/Ventana Medical Systems, Tucson, USA). To evaluate microvessels, CD34 staining was performed and scored as described [17], and in cases with excessive amounts of CD34 positive blasts hampering quantification, supplemented by a CD31 staining. Stem cell niches were quantified using a nestin staining as previously shown [18]. Blast quantification was based on morphological analysis of the H&E slides corroborated by CD34 staining, if expressed by the tumor cells, and correlated with the blast counts assessed on aspiration smears. Erythropoiesis was investigated with the help of E-cadherin. Characterization and quantification of B-, T-, NK- cells, and monocytes were performed utilizing antibodies against CD3, CD4, CD8, CD20, CD56, CD57, FoxP3, granzyme B, PD1, PD-L1, TIA1, and T-bet as described [19, 20]. Lenalidomide's target cereblon has also been stained for and was assessed depending on its intensity: a quality score from 0 (negative) to 3 (strong, unequivocal positivity) has been assigned. To highlight vascular endothelial growth factor (VEGF) and -receptor (VEGFR) expression alterations, stainings for VEGF and VEGFR2 were performed [17]. Antibody sources, dilutions, incubation, and retrieval conditions as well as cutoff scores are displayed in Table 2. Two authors (MMB and AT) investigated all stained slides, and reproducibility was estimated applying the Cronbach's Alpha method.

Cereblon genotyping

DNA was extracted from 34 available bone marrow biopsies at the time of first diagnosis using the GeneReadTM DNA-FFPE-Kit (Qiagen, Hilden, Germany) according to the manufacturer's protocol. Fifty nanograms of the extracted DNA was used to determine the rs1672753 (A/G) polymorphism located in the 5′ UTR of *CRBN*. Genotyping was performed using the Biorad QX200 digital PCR platform (Bio-Rad, Berkeley, CA, USA).

Statistical analysis

All statistical analyses were performed with the IBM SPSS 25.0 (IBM, Armonk, New York) and R version 3.5.3. The degree of inter-observer consensus was evaluated by interclass correlation coefficients, using reliability Cronbach's Alpha analysis, α values > 0.75 indicating a good agreement [21]. Comparisons were performed using the Kruskal–Wallis- or the Mann–Whitney U (MWU)–tests. Wilcoxon signed rank test was used to compare numeric variables between pre- and post-treatment. To investigate the correlation between two markers, Spearman rank correlation coefficient (ρ) was estimated; only the estimated $\rho > 0.40$ were further considered. The 95% confidence interval (CI) of ρ was based on bootstrap method. Progression-free survival (PFS) was defined as the time from registration until relapse or death, whichever occurred earlier. Overall survival (OS) was defined as time from registration until death. These time-to-event endpoints were analyzed using 50 ng Kaplan-Meier estimate, and 95% CI of its median was based on log transformation. Generally, log rank test was used to compare time-to-event endpoints between groups. However, if a small group (group size ≤ 2) was involved, permutation test was used. Cox proportional hazards regression model was used to investigate the association between time-to-event endpoints and continuous variables. If the distribution of continuous variable is not symmetric, it will be log transformed before modelling. P values < 0.05 were considered as significant. Two-sided tests were used throughout. All results were not corrected for multiple testing.

Results

Patient cohort and treatment

Patients' baseline characteristics are shown in Table 1. Regarding the karyotype analysis according to Grimwade, two patients were categorized as having a favorable karyotype, five patients had a karyotype with adverse prognostic impact and the karyotype of 30 patients was classified as intermediate; in 4 patients, this information was missing. Patients were assigned to the treatment arms irrespective of their karyotype. Due to the random distribution, all patients with a favorable karyotype were allocated in the standard treatment arm, whereas all patients with an unfavorable karyotype received additional lenalidomide. The 30 patients with intermediate karyotype were distributed equally between both treatment groups.

According to the WHO classification 2017, 21 patients were categorized as AML, not otherwise specified (NOS) (AML, NOS). Of these, ten received standard treatment and eleven additional lenalidomide. AML with defining mutations (*NPM1*, *FLT3*, or *CEBPA)* applied to 10 patients, of whom 4 received lenalidomide and 6 did not. Specific translocations or inversions were found in another 2 patients [inv(16) or t(16;16)], who were assigned to the category AML with defining translocations; both patients underwent standard treatment. The AML category with myelodysplasia-related changes (AML-MRC), either histomorphologically or genetically, applied to 8 patients; 7 of them were treated with additional lenalidomide and only one with the standard regimen (Table 1).

Table 2 Antibodies applied and cut-off scores

Antibody	Source and clone or ID	Dilution	Scoring/counting
Cereblon	Celgene Corporation	1:400	Moderate to strong expression in > 50% of tumor cells
CD3	Ventana 790-4341	Ready to use	Any lymphocyte, finally scored as % positive cells/all cells
CD4	Cell Marque SP35	1:100	Any lymphocyte, finally scored as % positive cells/all cells
CD8	DAKO C8/144B	1:400	Any lymphocyte, finally scored as % positive cells/all cells
CD20	Ventana QBEnd/10	Ready to use	Any lymphocyte, finally scored as % positive cells/all cells
CD31	Ventana 760-4378	rReady to use	Any lymphocyte, finally scored as % positive cells/all cells
CD34	Ventana 790-2927	Ready to use	Any microvessel and any blast, finally scored as $N^{micorvessels}/mm^2$ or % positive blasts/all cells
CD56	Ventana 790-4465	Ready to use	Any lymphocyte, finally scored as % positive cells/all cells
CD57	Ventana 760-2626.	Ready to use	Any lymphocyte, finally scored as % positive cells/all cells
E-cadherin	Ventana EP700Y	Ready to use	Any erythropoietic cells, finally scored as % positive cells/all cells
FoxP3	Abcam mAbcam 22510	1:50	Any lymphocyte, finally scored as % positive cells/all cells
Granzyme B	Novocastra 11F1	1:100	Any lymphocyte, finally scored as % positive cells/all cells
Nestin	AbD Serotec 10C2	1:200	Any perivascular niche (either single cells or clusters of up to three cells), finally scored as N^{niches}/mm^2
PD1	Cell Marque NAT105	1:50	Any lymphocyte, finally scored as % positive cells/all cells
PDL1	Cell signaling E1L3N	1:50	Single+ cells, 1–5% + cells, or > 5% + mononuclear cells
T-bet	Abcam ab154200	1:100	Any lymphocyte, finally scored as % positive cells/all cells
TIA1	Biocare CM130C	1:25	Any lymphocyte, finally scored as % positive cells/all cells
VEGF	DAKO VG1	1:40 *	Moderate to strong expression in > 50% of tumor cells
VEGFR2	Neomarkers RB-10453-P1	1:10 *	Moderate to strong expression in > 50% of tumor cells

In all instances except for *, in which high pH buffers have been applied, respectively, antigen retrieval was based on lower pH buffers and microwaving

Morphological, immunohistochemical, and molecular work-up of pre- and post-treatment bone marrow biopsies

Internal consistency analysis regarding evaluation of the immunohistochemical markers yielded good or excellent results for myelofibrosis, nestin niches, CD34-positive blast counts, and counting of granzyme B, T-bet, FoxP3, CD3, CD4, CD8, and E-cadherin positive cells. Acceptable results were obtained for the analysis of microvessel density, PD-L1, CD20, and CD57. The reproducibility of PD1 was estimated as questionable and was poor for TIA1, and therefore no further analyses linked to this latter marker were done. CD56 staining never yielded positive cells, except for osteoblasts.

All applied immunohistochemical markers were analyzed regarding their distribution among the individual WHO categories, their prognostic impact, and under consideration of the administered therapy (Fig. 1 and Supplementary Table 1). Here, only potentially relevant results are described.

Blasts

Irrespectively of the therapeutic regimes, the amount of blasts significantly decreased after treatment: from 45.4% (± 26.7) to 9.2% (± 21.7) in the standard arm vs. 51.9% (± 25.0) to 17.0% (± 20.8) in the lenalidomide arm (p = 0.001 and 0.004, respectively), (Supplementary Figure 1A-D; Fig. 2a–d); without significant difference of the drops between both treatment arms. With the decrease of blasts, morphological regeneration of the bone marrow with relative increase of adipocytes was detectible (Supplementary Figure 1A-B; Fig. 2a, b). When comparing both treatment regimens with respect to the WHO category, addition of lenalidomide was associated with a more substantial decrease of blasts, particularly in patients with AML with defining mutations (66.7% ± 14.5) compared to standard treatment (24% ± 20.2; p = 0.034), while in all other subgroups it was comparable between both treatment arms.

Microvessel density

Previously, we could show that the bone marrow microvessel density (MVD; given per mm^2), is significantly higher in newly diagnosed AML compared to healthy control individuals [22]. The current study furthermore showed a significant difference between the MVD of the various AML WHO categories (p = 0.011), being highest in AML-MRC (Fig. 2c)

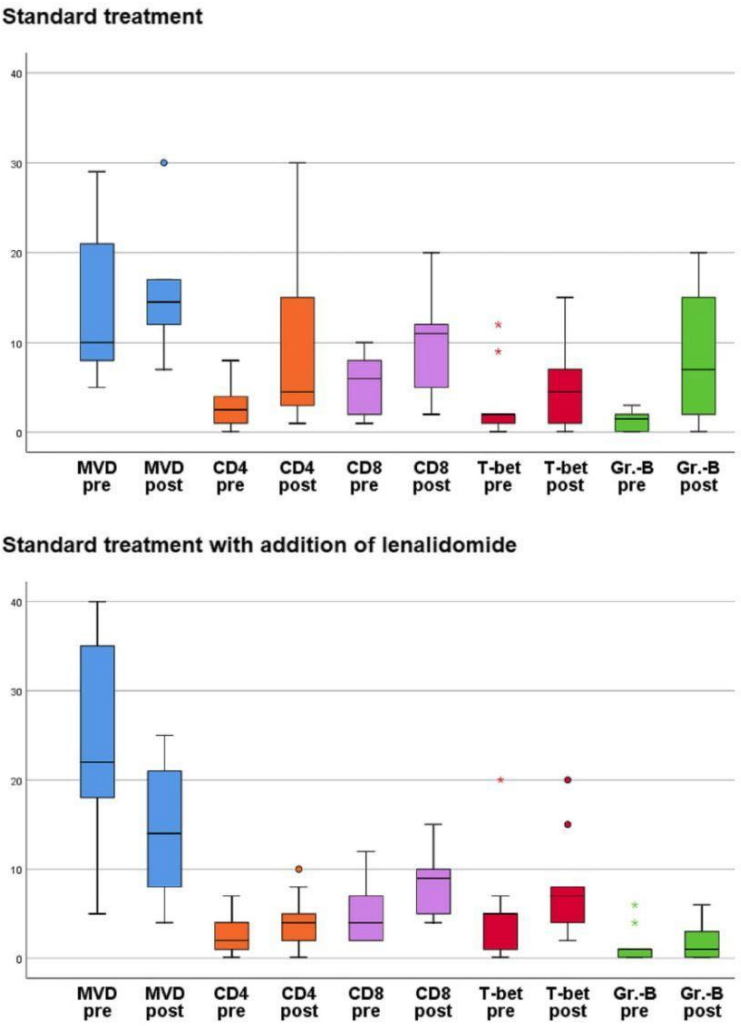

Fig. 1 Boxplot diagram visualizing quantitative changes of microvessel density (MVD) and selected studied T cell populations in acute myeloid leukemia treated by either standard chemotherapy (upper) or standard chemotherapy and additional lenalidomide (lower); boxes are color coded according to variables and pairwise grouped before (pre) and after (post) treatment. Note the considerably more pronounced decrease of MVD and the more limited increase of T cells under lenalidomide with the exception of the T-bet-positive subpopulation that seems to more stringently increase with addition of lenalidomide

(mean 28 ± 6.8; versus 14.9 ± 10.6 in AML, NOS (Supplementary Figure 1C), versus 24 ± 10.7 in AML with defining mutations, versus 9.5 ± 2.1 in AML with defining translocations). The same was true for the drop of MVD after treatment (p = 0.001), showing the most prominent decrease in the WHO category AML-MRC (Fig. 2d) (mean drop 19.5 ± 17.7; versus 9.0 ± 11.6 in AML with defining mutations, versus increases in AML, NOS with 2.5 ± 9.3 (Supplementary Figure 1D) and in one evaluable AML with defining translocations with 41.0). Due to an asymmetric distribution of AML-MRC cases among the two treatment arms (i.e., most cases being treated with additional lenalidomide), the initial MVD was higher in the lenalidomide treated group (24.9 ± 11.4 versus 14.5 ± 8.5; p = 0.011) and – accordingly— under standard treatment microvessels increased from 14.5 ± 8.5 to 17.2 ± 12, in contrast to a reduction from 24.9 ± 11.4 to 12.8 ± 6.7 under additional lenalidomide (p = 0.041) (Fig. 1).

Stem cell niches

The amount of nestin-positive stem cell niches was not modified under treatment, but their increased presence in the initial biopsy seemed to possibly correlate with an adverse prognosis regarding OS (hazard ratio: 1.75, 95% CI: 0.94–3.27; p = 0.076).

Erythropoiesis

Erythropoiesis (assessed by E-cadherin) increased in both treatment arms, which was slightly more prominent with the addition of lenalidomide (4.1 % versus 9.1 %; p = 0.12).

with respect to T cell subpopulations, T-bet-positive T-helper 1 cells seemed to slightly increase under addition of lenalidomide compared to the standard treatment ($p = 0.063$; Fig. 1, Fig. 2g–h, Supplementary Figure 1G-H). In contrast, amounts of FoxP3-positive regulatory T cells were not influenced by either treatment arm. The same was observed for CD57-positive T-large granular lymphocyte-equivalents. Remarkably, the proportion of granzyme-B-positive cells—either representing non activated (since TIA1-negative) cytotoxic T-cells or NK-cells—significantly increased under the standard regimen (6.5% ± 6.9 vs. 0.7% ± 4.6 under addition of lenalidomide, $p = 0.019$; Fig. 1). The increase of PD-1-positive T-cells was not significant in neither treatment arm, but it was slightly less pronounced under lenalidomide (0.2% ± 0.9) compared to the standard treatment (0.9% ± 1.0; $p = 0.19$).

Cereblon

Strong expression of cereblon in the leukemic blasts (Fig. 3) was not linked to unfavorable OS (hazard ratio: 1.18, 95% CI: 0.85–1.65; $p = 0.328$).

Correlation analysis

The presence of T-bet-positive cells correlated with the presence of CD8-positive cells ($p = 0.00004$; $\rho = 0.61$, 95% CI 0.32–0.79), CD4-positive cells ($p = 0.00007$; $\rho = 0.59$, 95% CI 0.37-0.74), CD57-positive cells ($p = 0.001$; $\rho = 0.51$, 95% CI 0.21–0.71), and the expression of VEGFR2 ($p = 0.002$; $\rho = 0.48$, 95% CI 0.14-0.69). In turn, the expression of VEGFR2 correlated with the grade of myelofibrosis (p = 0.001; ρ = 0.53, 95% CI 0.25-0.71) and the presence of nestin-positive stem cell niches (p = 0.001; ρ = 0.53, 95% CI 0.22-0.74). Additionally, CD4-positive cells correlated with the presence of granzyme-B-positive cells ($p = 0.001$; $\rho = 0.55$, 95% CI 0.25–0.74).

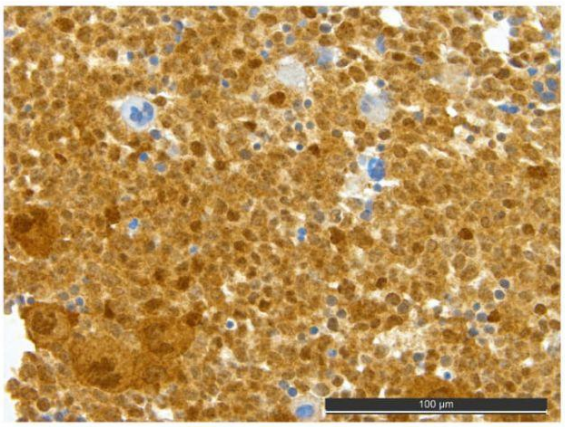

Fig. 3. Cereblon staining of the same patient as in Fig. 2 from the time-point of initial diagnosis showing a distinct strong expression of lenalidomide's target cereblon in all leukemic blasts and dysplastic megakaryocytes. Note: cereblon-negative residual erythropoiesis and isolated unremarkable megakaryocytes

Genotype analysis of CRBN

Whether *CRBN* was homozygous wild type (26 instances) or contained variant alleles (8 instances), did not have an impact on the treatment effect or the prognosis, irrespective of the therapy applied.

Outcome

The median OS of the cohort was 18.5 months (95% CI 8.–46.8, 30 events) and the median PFS 8.9 months (95% CI 6.4–17.1, 34 events). Neither the OS, nor the PFS differed significantly between the two treatment arms, in accordance with the results of Ossenkoppele et al. (12). Neither age nor gender were relevant for clinical outcome. PFS was significantly influenced by the karyotype ($p = 0.012$) and highly significantly by the WHO category ($p = 0.0061$), being shortest in AML-MRC. In this category, the median PFS differed between the patient, who received standard treatment (0.4 months), and the remaining patients receiving additional lenalidomide (2.6 months; $p = 0.25$), yet this did not reach statistical significance. As expected, the karyotype ($p = 0.0042$) and the WHO category ($p = 0.0030$) had a significant impact on the OS. Neither the amounts nor the dynamics of the various studied T cell subpopulations correlated with prognosis.

Discussion

Despite extensive research efforts, the prognosis of AML—especially in the elderly—remains poor. Therefore, more effective and better tolerable therapeutic strategies are of urgent need. Lenalidomide, an immune-modulatory drug already successfully implemented in other hematological malignancies associated with intrinsic dysfunction of the bone marrow, gathered attention as a potentially effective drug in AML. Indeed, in an AML murine model, immune-modulatory drugs were shown to hamper leukemia progression in vivo and to induce enhanced allogenic NK-cell activity [23].

In this translational research study of the Swiss cohort of HOVON103 AML/SAKK30/10, we were able to show perceptible differences in the outcome of AML-MRC patients: those with additional lenalidomide treatment had a longer PFS compared to the AML-MRC patients treated with chemotherapy alone. Unfortunately, a statistical significance was not reached due to the low case numbers and the unfavorable random distribution of patients between both treatment arms (only one patient received standard chemotherapy and 7

patients received additional lenalidomide). Nevertheless, patients with AML-MRC had a significantly higher bone marrow MVD compared to other AML categories and the most prominent lenalidomide-induced decrease of microvessels. Since it is known that a high bone marrow MVD is associated with a poor prognosis and that the reduction of microvessels correlates with treatment response [24, 25], we hypothesize that this particular patient subgroup, i.e., AML-MRC, might profit from the antiangiogenic effects of lenalidomide. Consistently, AML blasts are known to depend on the presence of nestin-positive stem cell niches [26], the density of which in turn correlated with the expression of the neovascularization-promoting VEGFR2 in our cohort. In general, myeloid malignancies such as AML can remodel stem cell niches to support malignant growth and to sustain stemness [27, 28]. Concordantly, in our study, therapy-induced blast reduction was not reflected by numeric changes of nestin-positive stem cell niches, yet an increased presence of such niches was linked to adverse outcome with respect to OS. If these niches represent a treatment-refractory place of retreat of leukemic blasts remains to be determined.

At least in our study, the effect of lenalidomide in AML-MRC was independent of the presence of del(5q), which has been linked to a better susceptibility to lenalidomide treatment in MDS [29]: the only patient of our cohort, who displayed del(5q) (in the context of a complex karyotype) and fulfilled the criteria of AML-MRC, received standard therapy. Irrespectively of the AML category, subtle treatment-induced changes in the composition of T cell subpopulations were observed, although the total number of T cells did not significantly differ between pre- and post-treatment biopsies. Under lenalidomide, the amount of T-bet-positive T cells more consistently increased, which might be interpreted as a sign of increased T cell driven immune response against the tumor cells. Indeed, the transcription factor T-bet has been found to be one of the key players in the induction of leukemia-reactive T-cells, and lower T-bet expression rates have been linked to poor immune responses and disease progressions [30, 31]. Correspondingly, the presence of T-bet-positive cells correlated, among others, with the presence of CD8-positive cytotoxic T cell-equivalents and CD57-positive large granular lymphocyte-equivalents.

The low PD-1-positive T cell count in all our samples fits to the fact that immune-checkpoint inhibitor treatment failed to achieve a major breakthrough in AML. This may be linked to a lower immunogenic potential compared to solid tumors such as melanoma or non-small cell lung cancer or due to genuine impairment of the antigen processing machinery in AML [32]. Nonetheless, we found a slight increase of PD-1-positive T cells in the bone marrow biopsies after treatment, indicative for a growing T cell exhaustion and enhanced inhibition of anti-tumor immune response. Although not significant, this effect seemed to be less pronounced under lenalidomide, which leads us to hypothesize, that lenalidomide—as an IMiD—may support some anti-leukemic immune responses. This is in accordance with observations in other hematologic malignancies such as multiple myeloma, in which lenalidomide significantly reduces PD-1 surface expression on T cells and enhances the anti-tumor response [33]. Additionally, lenalidomide was noticed to counteract the negative impact of PD-1-positive cells in follicular lymphoma patients, potentially due to its stimulating effect on the immune response [4].

The presence of cytotoxic, granzyme-B-positive T cells differed between various AML categories of our study collective, being highest in AML-MRC. This observation is supported by recently published data, demonstrating an association between cell-intrinsic genetic alterations in AML and the amount of cytotoxic lymphocytes, suggesting that AML-MRC may be more immunogenic. Indeed, genetic alterations linked with poor prognosis [*TP53*, del(5q), complex karyotypes] and being more frequently encountered in AML-MRC, as well as AML-MRC per se were found to be associated with higher T cell induced cytolytic activity [34].

Significant decrease of leukemic blasts under treatment was observed in both arms. With respect to the AML-categories, a more substantial blast drop under lenalidomide was noticed in AML with defining mutations, despite the fact that the presence of driver mutations such as *FLT3* and *NPM1* has been linked to low cytolytic activity of the tumor microenvironment [34]. If this effect is linked to the immune modulatory or other functions of lenalidomide and if it is reproducible in other AML collectives, remains to be determined [35].

Strong expression of lenalidomide's target cereblon in the leukemic blasts was rather associated with an unfavorable OS, which has also been documented for gastric marginal zone lymphomas [36], but has until now not been addressed in myeloid neoplasms and may deserve attention in larger studies. Interestingly, all of the described effects were independent from the genotype of the cereblon gene (*CRBN*), which is in line with data from other IMiDs [23].

Our study has several shortcomings. We were not able to investigate the bone marrow samples of all patients included in the HOVON103 AML/SAKK 30/10 study due to lacking material and therefore the sample size is very limited. Due to the random distribution of cases, there was an imbalance of the assigned treatment arms among the AML categories. Finally, the observed beneficial effect of the addition of lenalidomide was present only in a subgroup of patients, i.e., AML-MRC, which although being a WHO category, is yet a post-hoc subcohort from the perspective of the initial clinical trial design [12].

Observable on a small number of patients, addition of lenalidomide led to a perceptible but not significant increase of PFS in patients with AML-MRC, a category characterized by a poor prognosis and often complex karyotypes. Our

findings are in keeping with encouraging results in the literature, showing on the one hand a direct anti-leukemic effect of lenalidomide, and, on the other hand, an important immune-activating impact on the tumor microenvironment. We think that our observations also highlight the importance of taking the WHO defined subentities into consideration when designing clinical trials in AML.

Supplementary Information The online version contains supplementary material available at https://doi.org/10.1007/s00277-021-04467-2.

Code availability All statistical analyses were performed with the IBM SPSS 25.0 (IBM, Armonk, New York) and R version 3.5.3.

Author contribution MMB, MM, and AT wrote the manuscript. GS, MM, and AT designed the study. MMB, VV, and AT performed immunohistochemical analyses. PL performed cereblon genotyping. AT, MMB, and QL performed statistical analyses. GS, GJO, and BL were the principal investigators on behalf of the Swiss Group for Clinical Cancer Research (SAKK) and the Dutch-Belgian Hemato-Oncology Cooperative Group (HOVON). MMB, AT, EG, YB, RG, SC, and LM primarily analyzed the cases and provided the specimens for immunohistochemical analyses. GS, MM, DH, MGM, TP, MB, MF, and JP provided and analyzed the clinical data. CBR supported the organization of the study. All authors read and approved the final manuscript.

Funding The study was supported by a grant from the Stiftung zur Krebsbekämpfung Zürich (grant no. 398) to MM. The study was supported by the SAKK (Swiss Group for Clinical Cancer Research).

Data availability The datasets generated during and/or analyzed during the current study are available from the corresponding author on reasonable request.

Declarations

Ethics approval This study was approved by the ethics committee of Northwestern Switzerland (EKNZ BASEC 2016-01218).

Consent to participate Informed consent was obtained from all individual participants included in the study.

Consent for publication All of the authors have agreed with the publication.

Conflict of interest The authors declare no competing interests.

References

1. Shallis RM, Wang R, Davidoff A, Ma X, Zeidan AM (2019) Epidemiology of acute myeloid leukemia: recent progress and enduring challenges. Blood Rev 36:70–87. https://doi.org/10.1016/j.blre.2019.04.005
2. Ossenkoppele G, Löwenberg B (2015) How I treat the older patient with acute myeloid leukemia. Blood 125:767–774. https://doi.org/10.1182/blood-2014-08-551499
3. Freedman A, Jacobsen E (2020) Follicular lymphoma: 2020 update on diagnosis and management. Am J Hematol 95:316–327. https://doi.org/10.1002/ajh.25696
4. Menter T, Tzankov A, Zucca E, Kimby E, Hultdin M, Sundström C, Beiske K, Cogliatti S, Banz Y, Cathomas G, Karjalainen-Lindsberg ML, Grobholz R, Mazzucchelli L, Sander B, Hawle H, Hayoz S, Dirnhofer S (2020) Prognostic implications of the microenvironment for follicular lymphoma under immunomodulation therapy. Br J Haematol 189:707–717. https://doi.org/10.1111/bjh.16414
5. Platzbecker U (2019) Treatment of MDS. Blood 133:1096–1107. https://doi.org/10.1182/blood-2018-10-844696
6. Lopez-Girona A, Mendy D, Ito T et al (2012) Cereblon is a direct protein target for immunomodulatory and antiproliferative activities of lenalidomide and pomalidomide. Leukemia 26:2326–2335. https://doi.org/10.1038/leu.2012.119 Erratum in: Leukemia. 2012 26:2445
7. Gribben JG, Fowler N, Morschhauser F (2015) Mechanisms of action of lenalidomide in B cell non-Hodgkin lymphoma. J Clin Oncol 33:2803–2811. https://doi.org/10.1200/JCO.2014.59.5363
8. Krönke J, Fink EC, Hollenbach PW, MacBeth KJ, Hurst SN, Udeshi ND, Chamberlain PP, Mani DR, Man HW, Gandhi AK, Svinkina T, Schneider RK, McConkey M, Järås M, Griffiths E, Wetzler M, Bullinger L, Cathers BE, Carr SA, Chopra R, Ebert BL (2015) Lenalidomide induces ubiquitination and degradation of CK1α in del(5q) MDS. Nature 523:183–188. https://doi.org/10.1038/nature14610
9. Schneider RK, Ademà V, Heckl D, Järås M, Mallo M, Lord AM, Chu LP, McConkey ME, Kramann R, Mullally A, Bejar R, Solé F, Ebert BL (2014) Role of casein kinase 1A1 in the biology and targeted therapy of del(5q) MDS. Cancer Cell 26:509–520. https://doi.org/10.1016/j.ccr.2014.08.001
10. Järås M, Miller PG, Chu LP, Puram RV, Fink EC, Schneider RK, al-Shahrour F, Peña P, Breyfogle LJ, Hartwell KA, McConkey ME, Cowley GS, Root DE, Kharas MG, Mullally A, Ebert BL (2014) Csnk1a1 inhibition has p53-dependent therapeutic efficacy in acute myeloid leukemia. J Exp Med 211:605–612. https://doi.org/10.1084/jem.20131033
11. Vallet S, Palumbo A, Raje N, Boccadoro M, Anderson KC (2008) Thalidomide and lenalidomide: Mechanism-based potential drug combinations. Leuk Lymphoma 49:1238–1245. https://doi.org/10.1080/10428190802005191
12. Ossenkoppele GJ, Breems DA, Stuessi G et al (2020) Lenalidomide added to standard intensive treatment for older patients with AML and high-risk MDS. Leukemia 34:1751–1759. https://doi.org/10.1038/s41375-020-0725-0
13. Grimwade D, Hills RK, Moorman AV, Walker H, Chatters S, Goldstone AH, Wheatley K, Harrison CJ, Burnett AK, on behalf of the National Cancer Research Institute Adult Leukaemia Working Group (2010) Refinement of cytogenetic classification in acute myeloid leukemia: determination of prognostic significance of rare recurring chromosomal abnormalities among 5876 younger adult patients treated in the United Kingdom Medical Research Council trials. Blood 116:354–365. https://doi.org/10.1182/blood-2009-11-254441

14. Swerdlow SH, Harris NL, Jaffe ES et al (2017) WHO classification of tumours of haematopoietic and lymphoid tissues. International Agency for Research on Cancer (IARC), Lyon
15. Torlakovic EE, Brynes RK, Hyjek E, Lee SH, Kreipe H, Kremer M, McKenna R, Sadahira Y, Tzankov A, Reis M, Porwit A, the International Council for Standardization in Haematology (2015) ICSH guidelines for the standardization of bone marrow immunohistochemistry. Int J Lab Hematol 37:431–449. https://doi.org/10.1111/ijlh.12365
16. Thiele J, Kvasnicka HM, Facchetti F, Franco V, van der Walt J, Orazi A (2005) European consensus on grading bone marrow fibrosis and assessment of cellularity. Haematologica 90:1128–1132
17. Medinger M, Skoda R, Gratwohl A, Theocharides A, Buser A, Heim D, Dirnhofer S, Tichelli A, Tzankov A (2009) Angiogenesis and vascular endothelial growth factor-/receptor expression in myeloproliferative neoplasms: correlation with clinical parameters and JAK2-V617F mutational status. Br J Haematol 146:150–157. https://doi.org/10.1111/j.1365-2141.2009.07726.x
18. Medinger M, Krenger W, Jakab A, Halter J, Buser A, Bucher C, Passweg J, Tzankov A (2015) Numerical impairment of nestin(+) bone marrow niches in acute GvHD after allogeneic hematopoietic stem cell transplantation for AML. Bone Marrow Transplant 50:1453–1458. https://doi.org/10.1038/bmt.2015.189
19. Menter T, Kuzmanic B, Bucher C, Medinger M, Halter J, Dirnhofer S, Tzankov A (2018) Beneficial role of increased FOXP3^{+} regulatory T-cells in acute myeloid leukaemia therapy response. Br J Haematol 182:581–583. https://doi.org/10.1111/bjh.14819
20. Sterlacci W, Fiegl M, Juskevicius D, Tzankov A (2020) Cluster analysis according to immunohistochemistry is a robust tool for non-small cell lung cancer and reveals a distinct, immune signature-defined subgroup. Appl Immunohistochem Mol Morphol. 28:274–283. https://doi.org/10.1097/PAI.0000000000000751
21. Tzankov A, Zlobec I, Went P, Robl H, Hoeller S, Dirnhofer S (2010) Prognostic immunophenotypic biomarker studies in diffuse large B cell lymphoma with special emphasis on rational determination of cut-off scores. Leuk Lymphoma. 51:199–212. https://doi.org/10.3109/10428190903370338
22. Medinger M, Tichelli A, Bucher C, Halter J, Dirnhofer S, Rovo A, Passweg J, Tzankov A (2013) GVHD after allogeneic haematopoietic SCT for AML: angiogenesis, vascular endothelial growth factor and VEGF receptor expression in the BM. Bone Marrow Transplant 48:715–721. https://doi.org/10.1038/bmt.2012.200
23. Le Roy A, Prébet T, Castellano R et al (2018) Immunomodulatory drugs exert anti-leukemia effects in acute myeloid leukemia by direct and immunostimulatory activities. Front Immunol 9:977. https://doi.org/10.3389/fimmu.2018.00977
24. Rabitsch W, Sperr WR, Lechner K, Chott A, Prinz E, Valent P, Kalhs P (2004) Bone marrow microvessel density and its prognostic significance in AML. Leuk Lymphoma 45:1369–1373. https://doi.org/10.1080/10428190410001663707
25. Padró T, Ruiz S, Bieker R et al (2000) Increased angiogenesis in the bone marrow of patients with acute myeloid leukemia. Blood 95:2637–2644
26. Forte D, García-Fernández M, Sánchez-Aguilera A et al (2020) Bone marrow mesenchymal stem cells support acute myeloid leukemia bioenergetics and enhance antioxidant defense and escape from chemotherapy. Cell Metab 32:829–843.e9. https://doi.org/10.1016/j.cmet.2020.09.001
27. Baryawno N, Przybylski D, Kowalczyk MS et al (2019) A cellular taxonomy of the bone marrow stroma in homeostasis and leukemia. Cell 177:1915–1932.e16. https://doi.org/10.1016/j.cell.2019.04.040
28. Duarte D, Hawkins ED, Akinduro O et al (2018) Inhibition of endosteal vascular niche remodeling rescues hematopoietic stem cell loss in AML. Cell Stem Cell 22:64–77.e6. https://doi.org/10.1016/j.stem.2017.11.006
29. Adès L, Boehrer S, Prebet T, Beyne-Rauzy O, Legros L, Ravoet C, Dreyfus F, Stamatoullas A, Pierre Chaury M, Delaunay J, Laurent G, Vey N, Burcheri S, Mbida RM, Hoarau N, Gardin C, Fenaux P (2009) Efficacy and safety of lenalidomide in intermediate-2 or high-risk myelodysplastic syndromes with 5q deletion: results of a phase 2 study. Blood 113:3947–3952. https://doi.org/10.1182/blood-2008-08-175778
30. Berrien-Elliott MM, Yuan J, Swier LE, Jackson SR, Chen CL, Donlin MJ, Teague RM (2015) Checkpoint blockade immunotherapy relies on T-bet but not Eomes to induce effector function in tumor-infiltrating CD8^{+} T cells. Cancer Immunol Res 3:116–124. https://doi.org/10.1158/2326-6066.CIR-14-0159
31. Jia B, Zhao C, Rakszawski KL, Claxton DF, Ehmann WC, Rybka WB, Mineishi S, Wang M, Shike H, Bayerl MG, Sivik JM, Schell TD, Drabick JJ, Hohl RJ, Zheng H (2019) Eomes^{+}T-bet^{low} CD8^{+} T cells are functionally impaired and are associated with poor clinical outcome in patients with acute myeloid leukemia. Cancer Res 79:1635–1645. https://doi.org/10.1158/0008-5472.CAN-18-3107
32. Stahl M, Goldberg AD (2019) Immune checkpoint inhibitors in acute myeloid leukemia: novel combinations and therapeutic Targets. Curr Oncol Rep 21:37. https://doi.org/10.1007/s11912-019-0781-7
33. Görgün G, Samur MK, Cowens KB, Paula S, Bianchi G, Anderson JE, White RE, Singh A, Ohguchi H, Suzuki R, Kikuchi S, Harada T, Hideshima T, Tai YT, Laubach JP, Raje N, Magrangeas F, Minvielle S, Avet-Loiseau H, Munshi NC, Dorfman DM, Richardson PG, Anderson KC (2015) Lenalidomide enhances immune checkpoint blockade-induced immune response in multiple myeloma. Clin Cancer Res 21:4607–4618. https://doi.org/10.1158/1078-0432.CCR-15-0200
34. Dufva O, Pölönen P, Brück O et al (2020) Immunogenomic landscape of hematological malignancies. Cancer Cell 38:380–399.e13. https://doi.org/10.1016/j.ccell.2020.06.002
35. Wei A, Tan P, Perruzza S, Govindaraj C, Fleming S, McManus J, Avery S, Patil S, Stevenson W, Plebanski M, Spencer A (2015) Maintenance lenalidomide in combination with 5-azacitidine as post-remission therapy for acute myeloid leukaemia. Br J Haematol 169:199–210. https://doi.org/10.1111/bjh.13281
36. Kiesewetter B, Simonitsch-Klupp I, Kornauth C, Dolak W, Lukas J, Mayerhoefer ME, Raderer M (2018) Immunohistochemical expression of cereblon and MUM1 as potential predictive markers of response to lenalidomide in extranodal marginal zone B cell lymphoma of the mucosa-associated lymphoid tissue (MALT lymphoma). Hematol Oncol. 36:62–67. https://doi.org/10.1002/hon.2472